AN ABSTRACT OF THE THESIS OF

Steven C. Lovejoy for the degree of Master of Science in Mechanical Engineering presented on June 16, 1989.

Title: Design and Analysis of a High Speed Dynamic Tow Carriage

Redacted for Privacy

Abstract approved: _____
C.E. Smith

A need exists to develop a high speed dynamic tow carriage used to motivate hydrodynamic specimens through a fluid environment. It is desired to simulate high Reynolds number unsteady flow about the specimen by towing the specimen through the fluid. The fluid environment is to be provided by the existing uni-directional wave tank at O.H. Hinsdale Wave Research Laboratory at Oregon State University. This paper is both a feasibility study and a conceptual design of the dynamic tow carriage.

The first part of this paper develops a first order theoretical model of the dynamic tow carriage. The model has four main components, 1) the carriage/specimen model, 2) the wire rope model, 3) the idler pulley model, and 4) the driver pulley model. The carriage/specimen is modeled as a large point mass with viscous damping. Power is input to the driver pulley which transfers the power to the wire rope. The wire rope is modeled as linear springs with discretized mass and structural damping. The wire rope then transfers power to the carriage/specimen to propel it along the length of the wave tank.

The second half of this paper develops a conceptual design of the system. Theoretical results from the system model are interpreted and used for design parameters for each component of the real system. The carriage/specimen structure is a 5.5 m long 3.7 m wide light weight yet rigid space frame made of aluminum tubing. This component was designed using finite element techniques for both a static and vibrational analysis. The carriage is supported and guided by rigid linear motion bearings that nearly span the length of the wave tank. Power is supplied by a 400 kW hydrostatic drive to a 1.5 m diameter driver drum with enough stored cable to pull the carriage through 60 m oscillations.

The analysis and design suggest that the 1000 Kg carriage/specimen structure can be driven to velocities exceeding 17 m/s and accelerations on the order of gravity. For cylindrical tow specimens having a length of 3.4 m and a diameter ranging from 2 to 600 mm a maximum Reynolds number equal to 4×10^6 and Kuelegan Carpenter parameter equal to 8×10^3 appear feasible.

Design and Analysis of a High Speed Dynamic Tow Carriage

by

Steve C. Lovejoy

A THESIS

submitted to

Oregon State University

in partial fulfillment of
the requirements for the
degree of

Master of Science

Completed June 16, 1989
Commencement June, 1990

APPROVED:

Redacted for Privacy

Professor of Mechanical Engineering in charge of major

Redacted for Privacy

Head of Department of Mechanical Engineering

Redacted for Privacy

Dean of Graduate School

Date thesis is presented: June 16th, 1989

Typed by the author for: Steven C. Lovejoy

Acknowledgement

I would like to thank Prof. Charles Sollitt for his enduring support and enthusiasm. I also greatly appreciate the infinite patience and wisdom of Cheryl Zedwick and Laurie Broderick.

TABLE OF CONTENTS

TABLE OF CONTENTS (Cont)

LIST OF FIGURES

LIST OF FIGURES (Continued)

LIST OF FIGURES (Continued)

LIST OF TABLES

LIST OF APPENDICES FIGURES

LIST OF SYMBOLS

Symbol	Description
a	Numeric constant
A	Square matrix Section (2.2)
A	Reference area Sections (2.3-3.1)
b	Numeric constant Sections (2.2-2.3)
b	Length Section (3.1)
B	Column matrix
c	Numeric constant Section (2.3)
c	Damping coefficient equations (3.1.7,3.1.9,3.1.11,3.1.12)
c	Chord length when associated with airfoils
c_c	Damping coefficient of wire rope model
c_{eff}	Damping coefficient of carriae/speciman model
c_x	Critical damping coefficient
c_δ	Damping coefficient of idler pulley model
c_θ	Rotational damping coefficient
C	Drag coefficient Section (2.3)
C	Basic dynamic load rating Section (5.2)
C_d	Non-linear drag coefficient
C_i	Inertial coefficient
d	Diameter
D	Diameter
DF	Drag force
DF_{max}	Maximum drag force per cycle
DOF	Degree of Freedom
e	Exponential function
E	Modulus of elasticity
E_v	Bulk modulus of elasticity
EM	Effective mass
F	Force
F_D	Drag force
F_i	Inertial force
F_{R1-2}	Reaction forces
F_{s2}	Static preload force
F_x	Force in X-direction
F_y	Force in Y-direction
F_z	Force in Z-direction
F_{1-9}	Nodal forces
H_s	Static tension in cable
i	Square root of -1
I	Rotational moment of inertia
I_1	Rotational inertia of driver pulley model
$I_{1\ 1}$	Maximum area inertia
I_2	Rotational inertia of idler pulley model
$I_{2\ 2}$	Minimum area inertia
IF	Inertial force
IF_{max}	Maximum inertial force per cycle
J	Polar moment of inertia

LIST OF SYMBOLS (continued)

Symbol	Description
k	Spring constant
k_c	Spring constant of wire rope model
k_v	Virtual spring constant
k_6	Spring constant of idler pulley model
$\mathbf{K}$	Stiffness matrix
l	Stroke length of hydraulic cylinder
l_s	Average stroke length
L_{hs}	Half span of cable Equation (3.1.1)
L	Length Equations (3.1.3,3.1.4)
L_c	Length of circular cylinder Figure (3.1.10)
L_N	Nominal bearing life Section (5.2)
Lh	Service life time of bearing
m	Mass
m_c	Mass of wire rope model
m_s	Structural mass of carriage
m_T	Total mass of carriage/specimen model
m_6	Mass of idler pulley model
M	Moment
$\mathbf{M}$	Mass matrix
M_A	Bearing moment
M_B	Bearing moment
M_C	Bearing moment
M_X	Moment in X-direction
M_Y	Moment in Y-direction
M_Z	Moment in Z-direction
n	Index
n_1	Strokes per minute
P	Instantaneous power Section (2.3)
P	Bearing load Section (5.2)
P_{ave}	Average power per cycle
P_D	Power due to drag
P_{max}	Maximum power per cycle
PF	Participation factor
r	Inner radius
R	Outer radius
R_1	Radius of driver pulley model
R_2	Radius of idler pulley model
sby	Stress due to bending in y-direction
sbz	Stress due to bending in z-direction
sdir	Stress due to axial loading
sig1	Maximum stress
sig3	Minimum stress
t	Time Chapter (2)
t_h	Thickness Chapter (3)
T	Drive torque Section (2.2)
T_D	Drive torque
T_M	Motor torque
T_{Max}	Maximum torque
U	Displacement function

LIST OF SYMBOLS (continued)

Symbol	Description
U_o	Displacement amplitude
V	Velocity Chapter (2-4)
V_r	Volume displacement per revolution
V_{max}	Maximum velocity per cycle
w	Unit weight
W	Width
x	Displacement
$\dot{x}$	Velocity
$\ddot{x}$	Acceleration
X_{1-11}	Nodal displacements
$\dot{X}_{1-11}$	Nodal velocities
$\ddot{X}_{1-11}$	Nodal accelerations
δ	Log decrement
Δ	Used as a prefix to denote a change
η	Efficiency factor
θ_1	Displacement of driver pulley model
θ_2	Displacement of idler pulley model
$\dot{\theta}_1$	Velocity of driver pulley model
$\dot{\theta}_2$	Velocity of idler pulley model
$\ddot{\theta}_1$	Acceleration of driver pulley model
$\ddot{\theta}_2$	Acceleration of idler pulley model
μ	Friction factor
ξ	Damping ratio
ρ	Density
ρ_{steel}	Density of steel
σ	Pressure
Σ	Summation
τ	Period
τ_d	Damped natural period
τ_{res}	Resonant period
τ_{ud}	Undamped natural period
ϕ	Phase angle
ϕ_T	Drive torque phase angle
ϕ_1	Driver pulley displacement phase angle
ω	Angular frequency
ω_{ud}	Undamped natural frequency
$\forall$	Displaced volume

Design and Analysis of a High Speed Dynamic Tow Carriage

1.0 Introduction

1.1 Background

Wave loads on ocean and coastal structures may be physically modeled in three ways:

1) fix a model structure in a wave basin and propagate scaled waves past the model

2) fix a model in a U-tube and simulate the wave kinematics with unsteady U-tube oscillations

3) attach the model to a towing device and move the model through still water at the same relative motion as a wave would establish between a fixed structure and a wave induced velocity field.

The first method best reproduces pressure gradients and free surface effects in addition to modeling depth dependent kinematic and dynamic gradients. The second method simulates local loads at any depth but distorts pressure gradients, does not reproduce free surface conditions and cannot simulate random wave loading. The third method does not reproduce the superimposed wave kinematic and dynamic gradients but can be designed and operated to reproduce local relative kinematics exactly and can simulate random as well as periodic motion. Because local kinematics are essential for drag and inertial loading, the third method is the better approximation to the first method.

Wave loads are known to be Reynolds number dependent, i.e., drag and inertial loads scale differently in different models. Most offshore

Wave loads are known to be Reynolds number dependent, i.e., drag and inertial loads scale differently in different models. Most offshore structures are fabricated from cylindrical components. Generally, cylindrical drag coefficients attain a relative minimum and inertial coefficients attain a relative maximum at Reynolds numbers near 5×10^5, as shown in Figs. 1.1 and 1.2. Steady flow results (Roshko, Fig. 1.1) suggests that drag coefficients may become constant beyond the super critical range of Reynolds numbers at approximately 3×10^6. It is to be concluded that simulated wave loads must observe Reynolds similarity for prototype Reynolds numbers less than or equal to 3×10^6.

Typical prototype ocean design conditions involve structure members on the order of 10 ft. in diameter and velocities on the order of 10 ft/sec yielding Reynolds numbers in excess of 10^7. It is clear that large scale facilities are required to simulate these wave conditions.

The O.H. Hinsdale Wave Research Laboratory at Oregon State University is the largest research quality wave testing environment in the United States. Reynolds numbers on the order of 5×10^5 can be simulated in this laboratory with water depths to 11.5 ft and breaking wave heights to 5.0 ft. In the Netherlands and West Germany, two laboratories can produce waves approximately 25 % larger than at OSU. In order to generate waves at Reynolds numbers approaching 5×10^6, the OSU facility size would need to be increased by a factor of 4.64. Costs increase with the square to cube of the size, depending upon whether the basin is proportionately scaled. Accordingly, constructing a laboratory to achieve wave scales at Reynolds numbers approaching 5 x

10^6, would require investments at 21.5 to 100 times the cost of the OSU facility. In today's dollars, this would amount to an investment between 64 and 300 million USA dollars. The alternative to constructing a wave laboratory is to simulate large Reynolds number waveloading with a dynamic tow carriage. As will be shown in this research study, a feasible dynamic tow carriage can be constructed to achieve Reynolds numbers greater than 3×10^6 at a cost of much less than one million USA dollars. It is clear that economic incentives exist to pursue this method of waveload simulation.

1.2 Purpose

The purpose of this research study is to demonstrate that a dynamic tow carriage is feasible and to develop a conceptual design. The function of the design is to illustrate the feasibility analysis and is not necessarily a final design for the optimum dynamic tow carriage.

The conceptual design consists of a lightweight yet rigid space frame used to support a hydrodynamic tow specimen. The frame or carriage is rigidly supported by high speed, low friction linear motion bearings that allow the carriage and specimen to move along the length of the wave channel. The carriage/specimen is propelled by a cable/pulley/drum reeving which in turn is powered by a hydrostatic drive system. A mathematical model of the tow carriage system predicts the carriage and specimen can be driven to speeds in excess of 55 ft/sec and accelerations of 1 g over a 200 ft stroke. With cylindrical test specimens having a length of 11 ft and diameter ranging from 1 in to 2 ft Reynolds numbers near 4×10^6

and Keulegan Carpenter parameters in excess of 8×10^3 appear feasible.

1.3 Scope

This study is divided into five main sections:

1) development of a mathematical model to characterize tow carriage system behavior

2) application of the model to evaluate alternative carriage system components

3) developement and application of a dynamic structural analysis of alternative tow carriage frames

4) sizing and specifying all system components

5) summary of the major components of a feasible tow carriage system.

The mathematical model of the dynamic tow carriage system is a first order representation of the real system. The carriage and specimen are modeled by a large point mass allowed one degree of freedom with linear drag forces and added mass associated with the submerged tow specimen. The cable is modeled by series connected descretized mass with linear springs and dashpots. Driver and idler pulleys are modeled as frictionless circular cylinders with mass and rotational inertia.

System parameter response and sensitivity are analyzed to select the appropriate values for a numerical simulation of system operation. Output performance parameters such as forces, power, and resonance are interpreted to select conceptual design components.

The carriage structure is designed using a finite element model for both static and vibrational analyses. The hydrostatic drive is

designed to provide a broad power range accommodating both high load\low speed and low load\high speed operating conditions. The carriage guide rails are selected to provide very rigid support with low friction.

The final design consists of a 11 ft by 18 ft aluminum tow carriage weighing 2,200 lbs with a load capacity of over 11,000 lbs. The specimen and supporting carriage ride on linear motion bearings which span either side of the wave channel. The cable attaches to one side of the carriage and is spooled on a driver drum with three idler pulleys in series to complete the continuous cable loop. A 700 hp electric motor supplies power to a two pump, four motor hydrostatic drive which powers the driver drum. The major tow carriage system components are identified in Fig. 1.3.

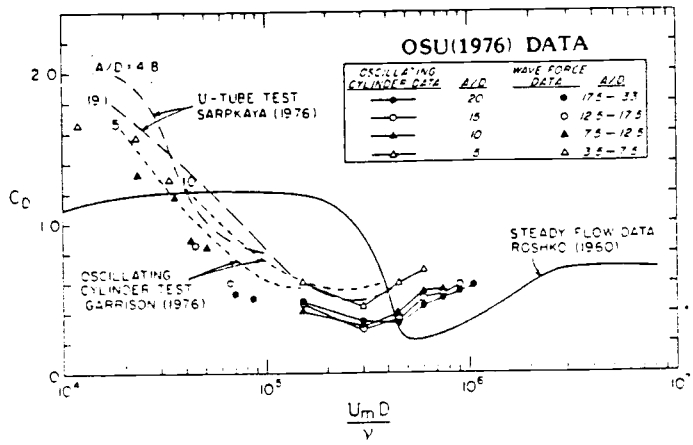

Drag coefficient vs. Reynolds Number for Free Stream Flow condition. (e/D = 6 for oscillating cylinder data and e/D = 3 for wave force data.) Yamamoto & Nath, 1976.

Figure 1.1 Drag coefficient

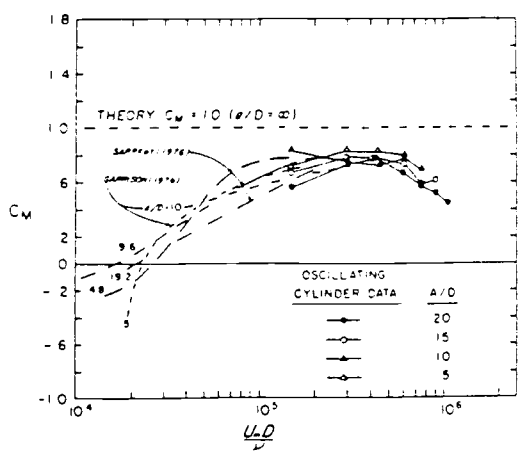

Added Mass coefficient vs. Reynolds Number for Free Stream Flow condition. Yamamoto & Nath, 1976.

Figure 1.2 Added mass

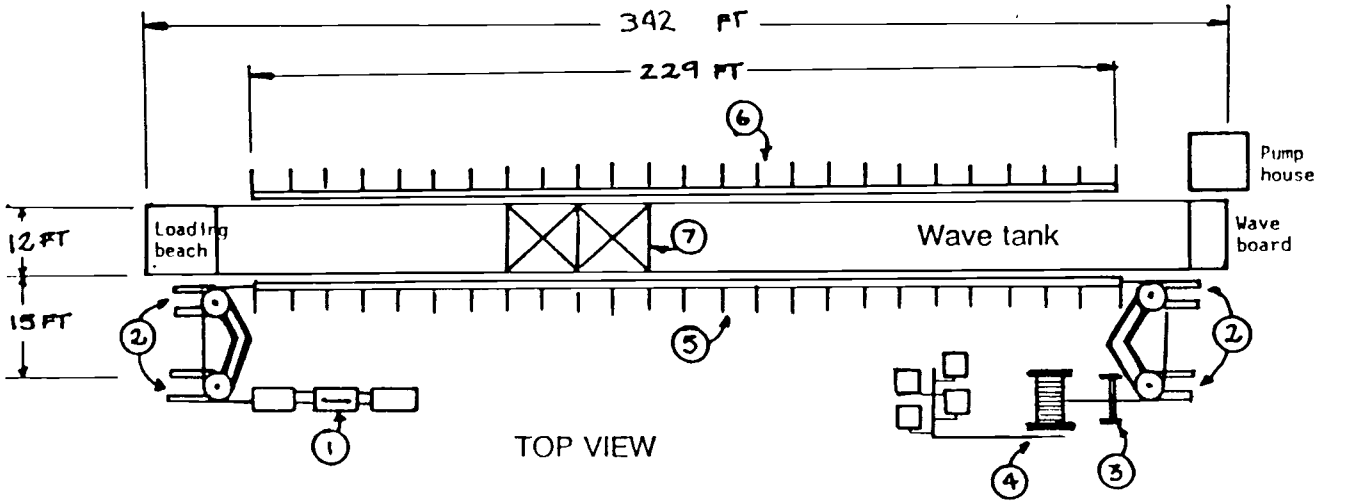

① Primary idler pulley

② Secondary idler pulley

③ Driver cable guide

④ Driver drum & drive train

⑤ Carriage bearing structure with cable way

⑥ Carriage bearing structure

⑦ Tow carriage structure

Figure 1.3 System layout

2.0 Tow Carriage System Analysis

2.1 System Model

The mathematical representation of the dynamic tow carriage is a nine degree of freedom (DOF) system composed of seven point masses coupled by linear springs with viscous structural damping and two rotational DOF with viscous damping and inertia; see Fig. (2.1.1). The system can be divided into four basic components 1) the carriage/specimen model, 2) the wire rope model, 3) the driver pulley model, and 4) the idler pulley model.

1) Carriage/Specimen Model: The carriage with attached tow specimen is modeled as a large point mass. It has one translational DOF and viscous damping associated with a velocity referenced to a fixed inertial reference frame; see Fig. (2.1.2). Because the specimen experiences non-linear turbulent damping an equivalent linear damping coefficient is calculated, based on average power absorption/dissipation per period. Refer to Section (2.3) for a derivation. This damping coefficient is used in force calculations that are 180 degrees out of phase with the carriage/specimen velocity. It is assumed that the drag force of the tow specimen is much larger than any bearing friction associated with the carriage travel and therefore bearing friction is neglected.

The mass of the carriage/specimen is the sum of the structural mass of the carriage, the nodal wire rope mass near the carriage/specimen and the added mass of the tow specimen interaction with the water in the wave channel. The added mass changes with

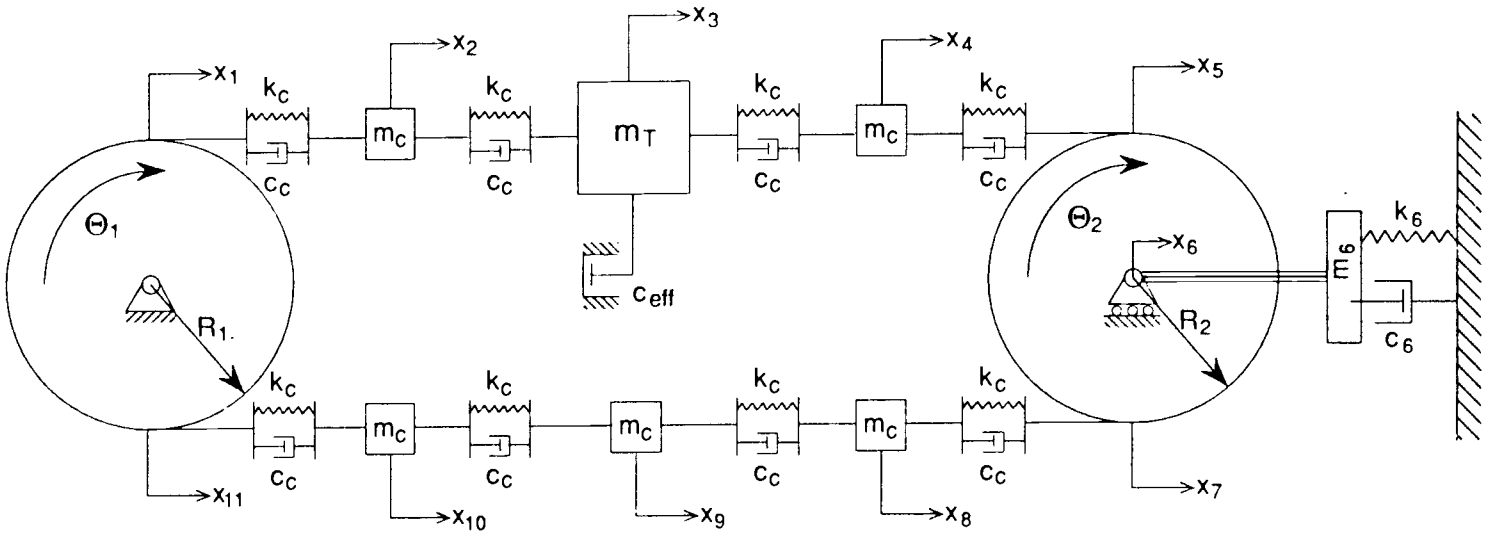

Figure 2.1.1 System model

specimen geometry, therefore the total mass of the carriage/specimen varies with tow specimen geometry. Refer to Section (2.3) for a derivation. The total mass is used for force calculations 180 degrees out of phase with the carriage/specimen acceleration. In addition to drag and inertial forces the carriage/specimen is subjected to wire rope forces that provide the primary tow motion.

2) Wire Rope Model: The wire rope model is discretized into six nodal point masses with six translational DOF; see Fig.(2.1.3). The point masses are coupled by a spring that generates forces linearly proportional to the difference in linked nodal displacement relative to one another. A viscous damper also couples the masses that generates forces linearly proportional to the difference in linked nodal velocities relative to one another. These couplings model structural stiffness and damping of the wire rope respectively. The wire rope model has three components on the upper and lower sides of the system model.

3) Driver Pulley Model: The driver pulley is modeled as a circular cylinder with one rotational DOF about the axis; see Fig. (2.1.4). It is assumed that the wire rope forces act in plane and in line with the wire rope nodal displacements. The rotational inertia is calculated as if the cylinder is hollow with a finite thickness; see Section (3.1). The bearings are assumed frictionless and therefore no rotational damping is considered. A driving torque is imposed about the axis of rotation and is forced to have a sinusoidal temporal dependence.

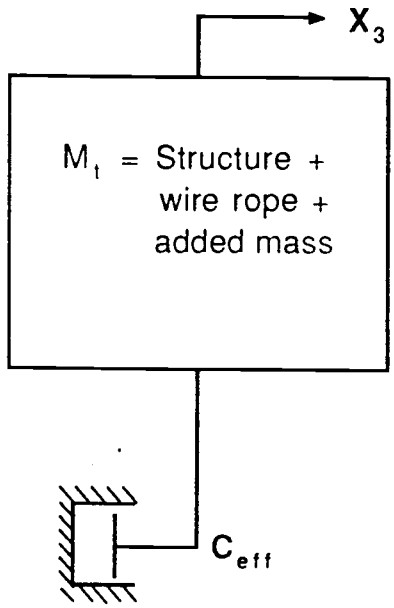

Figure 2.1.2 Carriage/specimen model

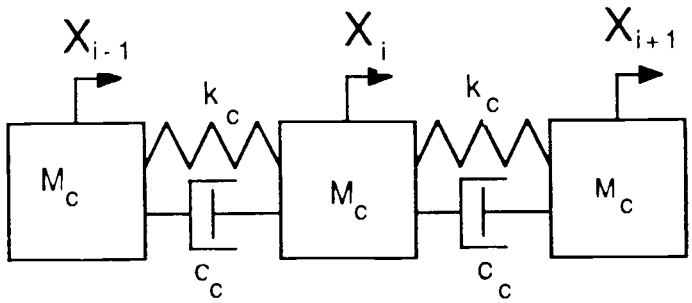

Figure 2.1.3 Wire rope model

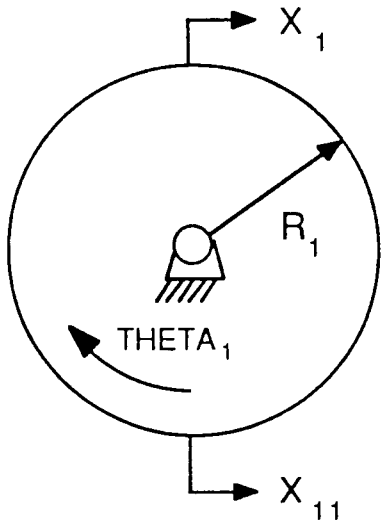

Figure 2.1.4 Driver pulley model

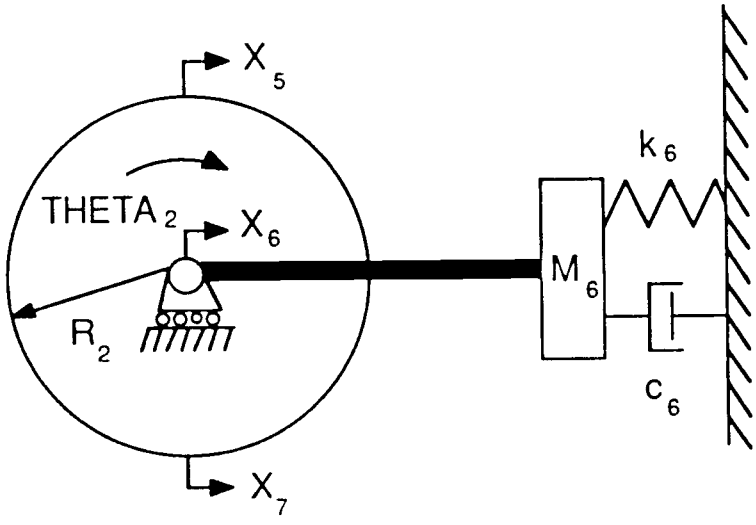

Figure 2.1.5 Idler pulley model

4) Idler Pulley Model: The idler pulley is modeled as a circular cylinder with one rotational DOF about its axis and one translational DOF which allows translation of the rotational axis in line with the linked wire rope displacements; see Fig. (2.1.5). Rotational viscous damping is used to model braking if necessary. This damping produces torque 180 degree. out of phase with the angular velocity and is linearly proportional to the angular velocity. Rotational inertia is calculated similarly to the driver pulley.

The structural mass, stiffness, and damping of the translational DOF is modeled similarly to the wire rope model but with the spring and damper coupling the pulley mass to a fixed wall. It is assumed that the wire rope forces act in plane and in line with wire rope nodal displacements.

2.2 System Equations

Coupling the four sub-models together provides a set of equations to describe the total carriage system as follows. Referring to the free body diagram (FBD) of the driver pulley, Fig. (2.2.1), there is one rotational DOF, θ_1 and two translational DOF , x_1 and x_{11}. The forces acting on the body are the two wire rope forces F_1 and F_8 and the reaction force F_{R1}. The upper wire rope force F_1 can be expressed in terms of the nodal displacements and velocities of nodes 1 and 2 as

$$F_1=k_c(X_1-X_2)+c_c(\dot{X}_1-\dot{X}_2) \qquad (2.2.1a)$$

where k_c and c_c are the linear stiffness and damping coefficients of the wire rope model. Similarly the lower wire rope force F_8 can be expressed in terms of the nodal displacements and velocities of nodes 11 and 10 as

$$F_9=k_c(X_{11}-X_{10})+c_c(\dot{X}_{11}-\dot{X}_{10}) \tag{2.2.1b}$$

If the driver pulley is assumed radially rigid one can make the kinematic observation that relates x_1 and x_{11} to θ_1 as follows

$$X_1=\theta_1 R_1 \tag{2.2.2a}$$

$$\dot{X}_1=\dot{\theta}_1 R_1 \tag{2.2.2b}$$

$$X_{11}=-\dot{\theta}_1 R_1 \tag{2.2.3a}$$

$$\dot{X}_{11}=-\dot{\theta}_1 R_1 \tag{2.2.3b}$$

Substituting Equations 2.2.2 and 2.2.3 into Equation 2.2.1 yields

$$F_1=k_c(\theta_1 R_1-X_2)+c_c(\dot{\theta}_1 R_1-\dot{X}_2) \tag{2.2.4a}$$

and

$$F_9=k_c(-\theta_1 R_1-X_{10})+c_c(-\dot{\theta}_1 R_1-\dot{X}_{10}) \tag{2.2.4b}$$

Summing moments about the axis of rotation and using Newton's Second Law of Motion for rotation yields

$$\sum M=T+F_9 R_1-F_1 R_1=I_1\ddot{\theta}_1 \tag{2.2.5a}$$

where T is the imposed driving torque that motivates the system and I_1 is the rotational inertia of the driver pulley.

Substituting Equation 2.2.4a into Equation 2.2.5a we have

$$\sum M = T + [k_c(-\theta_1 R_1 - X_{10}) + c_c(-\dot{\theta}_1 R_1 - \dot{X}_{10})]R_1 - [k_c(\theta_1 R_1 - X_2) + c_c(\dot{\theta}_1 R_1 - \dot{X}_2)]R_1 = I_1\ddot{\theta} \tag{2.2.5b}$$

Moving to node 2 it appears from the FBD, Fig. (2.2.2), there is one translational DOF at the point mass m_c labeled x_2 and two wire rope forces F_1 and F_2. Applying Newton's Second Law for translation,

$$\sum F = F_1 - F_2 = m_c\ddot{X}_2 \tag{2.2.6a}$$

where m_c is the lumped mass of the wire rope model between x_1 and x_2. Substituting the force expressions in terms of the nodal kinematics into Equation 2.2.6a yields

$$\sum F = k_c(\theta_1 R_1 - X_2) + c_c(\dot{\theta}_1 R_1 - \dot{X}_2) - k_c(X_2 - X_3) - c_c(\dot{X}_2 - \dot{X}_3) = m_c\ddot{X}_2 \tag{2.2.6b}$$

Node 3 is a descretization of the carriage/specimen model plus the adjacent wire rope model. It is seen from the FBD, Fig. (2.2.3), there is one translational DOF x_3 with two wire rope forces F_2 and F_3 plus a drag force F_d. The drag force is linear with carriage/specimen velocity relative to a fixed reference frame. The mass of node three is the sum of the carriage structural mass, the local wire rope mass, and the added mass of the tow specimen. Both the linearized drag coefficient and the added mass of the tow specimen are developed in Section (2.4). The drag force can be expressed as

$$F_D = C_{eff}\dot{X}_3 \tag{2.2.7}$$

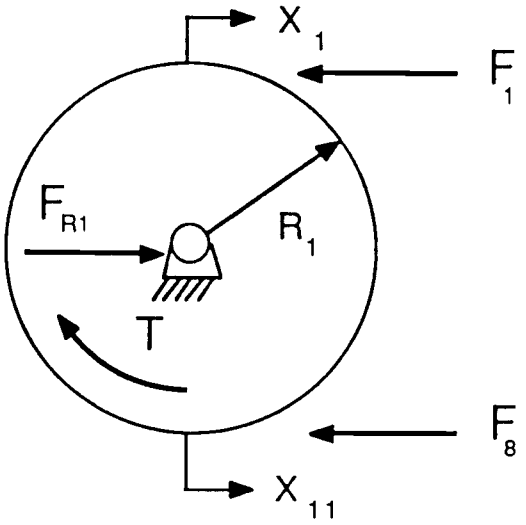

Figure 2.2.1 FBD of driver pulley model

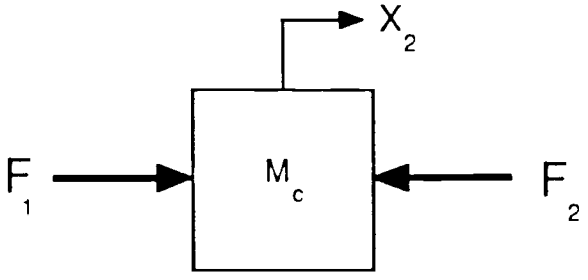

Figure 2.2.2 FBD of node 2

where C_{eff} is the linearized drag coefficient. Applying Newtons Second Law for translation,

$$\sum F = F_2 - F_3 - F_D = m_T \ddot{X}_3 \tag{2.2.8a}$$

where m_T is the sum of the three mass terms described above. Substituting the expressions for the wire rope forces F_2 and F_3 and the drag force F_D yields

$$\sum F = k_c(X_2 - X_3) + c_c(\dot{X}_2 - \dot{X}_3) - k_c(X_3 - X_4) - c_c(\dot{X}_3 - \dot{X}_4) - C_{eff}\dot{X}_3 = m_T \ddot{X}3 \tag{2.2.8b}$$

Instead of developing an equation of motion for node 4 next it is advantageous to first analyze the idler pulley model and then examine node 4. From the FBD of the idler pulley model, Fig. (2.2.4), one finds one rotational DOF θ_2 and three translational DOF x_4, x_6, x_7. This is similar to the driver pulley model but contains one more translational DOF namely x_6. In the real system a pre-load on the wire rope is needed for stability and as a means of absorbing energy. By allowing the axis of the idler pulley to translate as shown, stiffness and damping can be added to provide pre-load and energy absorption respectively.

The forces acting on the idler pulley model are the two wire rope forces F_4 and F_5 plus the reaction force at node six F_{R2}. The reaction force F_{R2} is modeled in a similar manner to the wire rope forces but the reference node is fixed to an inertial reference frame instead of another translational DOF. Thus the reaction force can be expressed as

$$F_{R2}=k_6X_6+c_6\dot{X}_6 \tag{2.2.9}$$

The translational DOF x_6 allows a summation of forces as well as a summation of moments about the axis of rotation. Applying Newtons Second Law for translation yields

$$\sum F=F_4+F_5-F_{R2}=m_6\ddot{X}_6 \tag{2.2.10a}$$

where m_6 is the lumped mass of the idler pulley. Substituting the expressions for the wire rope forces F_4 and F_5 and the reaction force F_{R2} yields

$$\sum F=k_c(X_4-X_5)+c_c(\dot{X}_4-\dot{X}_5)-k_c(X_8-X_7)+c_c(\dot{X}_8-\dot{X}_7)-k_6X_6-c_6\dot{X}_6$$
$$=m_6\ddot{X}_6 \tag{2.2.10b}$$

Assuming the idler pulley radially rigid, one can make the kinematic observation relating nodes x_5 and x_7 to x_6 and θ_2 as follows.

$$X_5=\theta_2R_2+X_6 \tag{2.2.11a}$$

$$\dot{X}_5=\dot{\theta}_2R_2+\dot{X}_6 \tag{2.2.11b}$$

$$X_7=X_6-\theta_2R_2 \tag{2.2.12a}$$

$$\dot{X}_7=\dot{X}_6-\dot{\theta}_2R_2 \tag{2.2.12b}$$

Substituting Equations 2.2.11 and 2.2.12 into Equation 2.2.10b yields

$$\sum F=k_c(X_4-\theta_2R_2-X_6)+c_c(\dot{X}_4-\dot{\theta}_2R_2-\dot{X}_6)+k_c(X_8-X_6+\theta_2R_2)+c_c(\dot{X}_8-\dot{X}_6+\dot{\theta}_2R_2)-k_6X_6-$$
$$c_6\dot{X}_6=m_6\ddot{X}_6 \tag{2.2.10c}$$

Applying Newton's Second Law for rotation yields

$$\sum M = F_4 R_4 - F_5 R_2 = I_2 \ddot{\theta}_2 \tag{2.2.13a}$$

Substituting Equations 2.2.11 and 2.2.12 into Equation 2.2.13a yields

$$\sum M = [k_c(X_4 - \theta_2 R_2 - X_6) + c_c(\dot{X}_4 - \dot{\theta}_2 R_2 - \dot{X}_6)]R_2 - [k_c(X_8 - X_6 + \theta_2 R_2) + c_c(\dot{X}_8 + \dot{X}_6 + \dot{\theta}_2 R_2)]R_2 - \dot{\theta}_2 c_\theta = I_2 \ddot{\theta}_2 \tag{2.2.13b}$$

where I_2 is the rotational inertia of the idler pulley.

With the kinematic relationships expressing the motion of node 5 and 7 in terms of x_6 and θ_2,one can better analyze node 4. Examining the FBD, Fig. (2.2.5), reveals one translational DOF x_4 with two wire rope forces F_3 and F_4. Applying Newtons Second Law for translation yields

$$\sum F = F_4 - F_5 = m_c \ddot{X}_4 \tag{2.2.14a}$$

Substituting the expressions for the wire rope forces yields

$$\sum F = k_c(X_3 - X_4) + c_c(\dot{X}_3 - \dot{X}_4) - k_c(X_4 - X_5) - c_c(\dot{X}_4 -_5) = m_c \ddot{X}_4 \tag{2.2.14b}$$

The kinematic dependence on node 5 can now be eliminated by substituting Equations 2.2.11 into Equation 2.2.14b yielding

$$\sum F = k_c(X_3 - X_4) + c_c(\dot{X}_3 - \dot{X}_4) - k_c(X_4 - \theta_2 R_2 - X_6) - c_c(\dot{X}_4 - \dot{\theta}_2 R_2 - \dot{X}_6) = m_c \ddot{X}_4 \tag{2.2.14c}$$

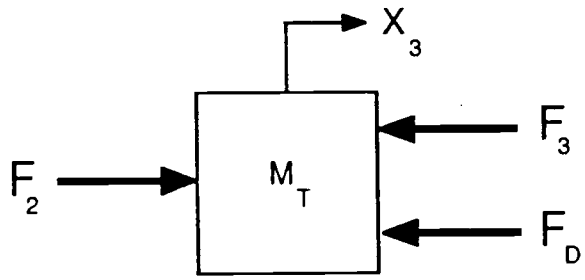

Figure 2.2.3 FBD of node 3

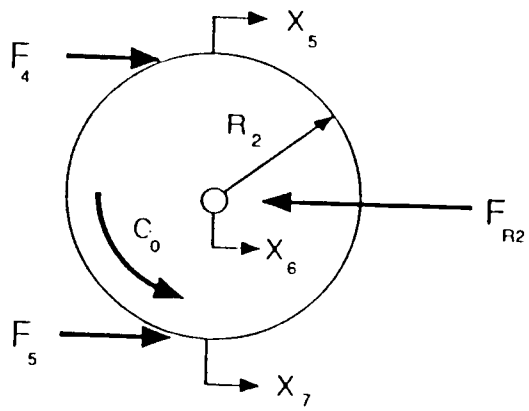

Figure 2.2.4 FBD of idler pulley model

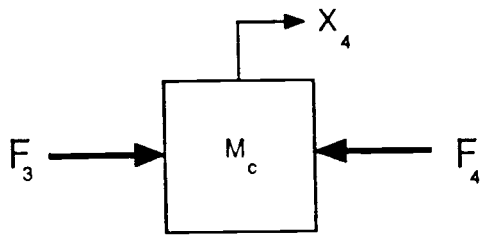

Figure 2.2.5 FBD of node 4

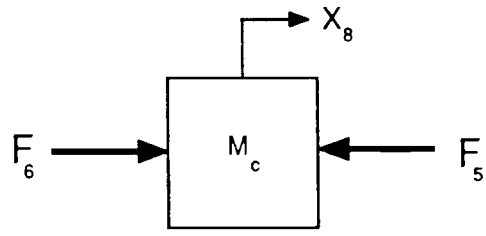

Figure 2.2.6 FBD of node 8

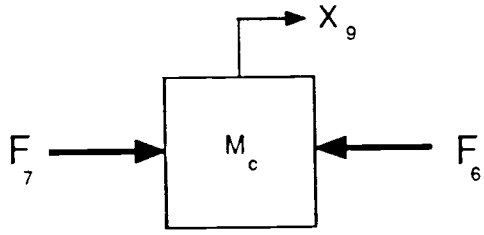

Figure 2.2.7 FBD of node 9

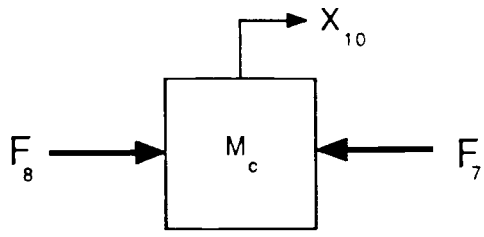

Figure 2.2.8 FBD of node 10

Moving to node 8 it is seen from the FBD, Fig. (2.2.6), there is one translational DOF x_8 and two wire rope forces F_5 and F_6. Applying Newtons Second Law and substituting Equations 2.2.11c and 2.2.11d for x_7 and $\dot{x}_7$ respectively yields

$$\sum F=k_c(X_9-X_8)+c_c(\dot{X}_9-\dot{X}_8)-k_c(X_8-X_6+\theta_2R_2)-c_c(\dot{X}_8-\dot{X}_6+\dot{\theta}_2R_2)=m_c\ddot{X}_8 \qquad (2.2.15)$$

From the FBD of node 9, Fig. (2.2.7), one finds x_9 to be the single translational DOF with wire rope forces F_6 and F_7. Newtons Second Law yields

$$\sum F=k_c(X_{10}-X_9)+c_c(\dot{X}_{10}-\dot{X}_9)-k_c(X_9-X_8)-c_c(\dot{X}_9-\dot{X}_8)=m_c\ddot{X}_9 \qquad (2.2.16)$$

Similarly the FBD of node 10, Fig. (2.2.8), yields

$$\sum F=k_c(X_{11}-X_{10})+c_c(\dot{X}_{11}-\dot{X}_{10})-k_c(X_{10}-X_9)-c_c(\dot{X}_{10}-\dot{X}_9)=m_c\ddot{X}_{10} \qquad (2.2.17a)$$

Eliminating the kinematic dependence on node 11 by substituting Equations 2.2.3a and 2.2.3b for x_{11} and $\dot{x}_{11}$ respectively yields

$$\sum F=k_c(-\theta_1R_1-X_{10})+c_c(-\dot{\theta}_1R_1-\dot{X}_{10})-k_c(X_{10}-X_9)-c_c(\dot{X}_{10}-\dot{X}_9)=m_c\ddot{X}_{10} \qquad (2.2.17b)$$

The equations of motion developed to this point may be summarized as follows:

A moment balance on the driver pulley yielded:

$$T-\theta_1(2R_1^2k_c)-\dot{\theta}_1(2R_1^2c_c)-\ddot{\theta}_1(I_1)+X_2(R_1k_c)+\dot{X}_2(R_1c_c)-X_{10}(R_1k_c)=0 \tag{2.2.5b}$$

A force balance on node 2 yielded:

$$\theta_1(k_cR_1)+\dot{\theta}_1(c_cR_1)-X_2(2k_c)-\dot{X}_2(2c_c)-\ddot{X}(m_c)+X_3(k_c)+\dot{X}_3(c_c)=0 \tag{2.2.6b}$$

A force balance on node 3 yielded:

$$X_2(k_c)+\dot{X}_2(c_c)-X_3(2k_c)-\dot{X}_3(2c_c+c_{eff})-\ddot{X}(m_T)+X_4(k_c)+\dot{X}_4(c_c)=0 \tag{2.2.8b}$$

A force balance on the idler pulley yielded:

$$X_4(k_c)+\dot{X}(c_c)-X_6(2k_c+k_6)-\dot{X}_6(2c_c+c_6)-\ddot{X}(m_6)+X_8(k_c)+\dot{X}_8(c_c)=0 \tag{2.2.10c}$$

A moment balance on the idler pulley yielded:

$$X_4(R_2k_c)+\dot{X}(R_2c_c)-\theta_2(2R_2^2k_c)-\dot{\theta}_2(2R_2^2c_c+c_\theta)-\ddot{\theta}_2(I_2)-X_8(R_2k_c)-\dot{X}_8(R_2c_c)=0 \tag{2.2.13b}$$

A force balance on node 4 yielded:

$$X_3(k_c)+\dot{X}(c_c)-X_4(2k_c)-\dot{X}_4(2c_c)-\ddot{X}_4(m_c)+X_6(k_c)+\dot{X}_6(c_c)+\theta_2(k_cR_2)+\dot{\theta}_2(c_cR_2)=0 \tag{2.2.14c}$$

A force balance on node 8 yielded:

$$X_6(k_c)+\dot{X}_6(c_c)-\theta_2(k_cR_2)-\dot{\theta}_2(c_cR_2)-X_8(2k_c)-\dot{X}(2c_c)-\ddot{X}_8(m_c)+X_9(k_c)+\dot{X}(c_c)=0 \tag{2.2.15}$$

A force balance on node 9 yielded:

$$X_8(k_c)+\dot{X}_8(c_c)-X_9(2k_c)-\dot{X}_9(2c_c)-\ddot{X}(m_c)+X_{10}(k_c)+\dot{X}_{10}(c_c)=0 \tag{2.2.16}$$

A force balance on node 10 yielded:

$$X_9(k_c)+\dot{X}_9(c_c)-X_{10}(2k_c)-\dot{X}(2c_c)-\ddot{X}_{10}(m_c)-\theta_1(k_cR_1)-\dot{\theta}_1(c_cR_1)=0 \tag{2.2.17b}$$

Examining these equations reveals every bracketed quantity is a constant physical parameter of the system, which leaves one unknown torque, nine unknown displacements, nine unknown velocities, and nine unknown accelerations for a total of 28 unknowns with only nine equations. All of the equations are linear and coupled, and a displacement function can be specified for one DOF in such a manner that the velocity and acceleration can be expressed in terms of the displacement.Due to the linearity of the system all other DOF will have kinematics of the same form as the specified DOF.

One convenient form is to specify a simple harmonic displacement of the form

$$x=Xe^{i\omega t} \tag{2.2.18}$$

where x is the displacement function with a displacement phasor

$$X=a+ib \tag{2.2.19}$$

where a and b are real coefficients and i is equal to the square root of -1. Equation (2.2.19) contains both magnitude and phase information for the displacement function, Equation (2.2.18), which oscillates simple harmonically in time at an angular frequency ω. The amplitude of the displacement is the magnitude or modulus of the displacement phasor and can be expressed as

$$|X|=\mathrm{SQRT}(a^2+b^2) \tag{2.2.20}$$

The phase angle or argument of the displacement phasor can be expressed as

$$\phi=\mathrm{ARCTAN}(b/a) \tag{2.2.21}$$

Using this form of the displacement function the velocity function can be found by taking the time rate of change of displacement yielding:

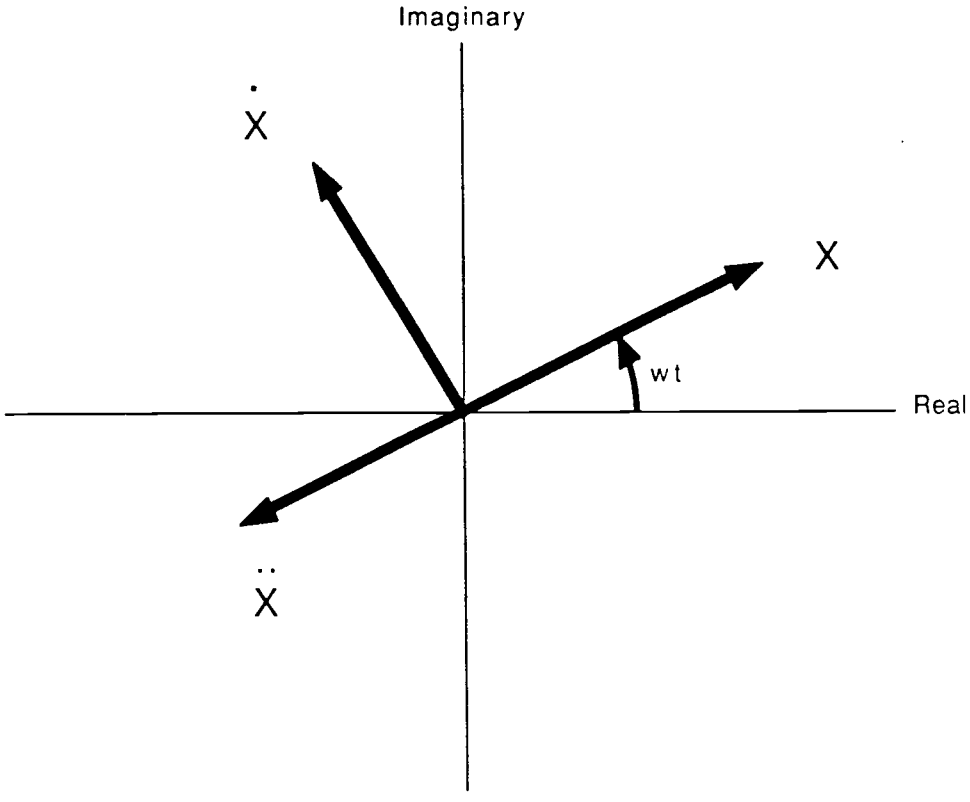

Figure 2.2.9 Phasor diagram of kinematic response

$$\dot{X}=i\omega Xe^{i\omega t} \tag{2.2.22}$$

Note that the velocity oscillates at the same angular frequency and its phasor is expressed as $i\omega X$. Similarly the acceleration function can be found by taking the time rate of change of velocity yielding:

$$\ddot{X}=-\omega^2 Xe^{i\omega t} \tag{2.2.23}$$

Again note that the acceleration oscillates at the same angular frequency as the displacement and its phasor is expressed as $-\omega^2 X$.

To see the phase relationship between the kinematic functions it is useful to use a phasor diagram as shown in Fig. (2.2.9). At time t the displacement phasor is at an angle ωt from the real axis. The velocity phasor leads the displacement by 90 degrees making an angle of ωt+90 degrees from the real axis. The acceleration phasor leads the displacement by 180 degrees and makes an angle of ωt+180 degrees from the real axis.

This form of displacement function is unique in the sense that the velocity and acceleration functions, as well as higher order derivatives, can be expressed in terms of the displacement function itself. Thus by specifying a displacement function of the form of Equation (2.2.18) for a particular DOF we are really specifying the complete kinematics of that DOF. In fact because the equations are linear and coupled we are really specifying the form of the kinematics for the whole system. If all kinematics are simple harmonic we can also

expect the driving torque and other dynamics to be simple harmonic as well.

This approach is convenient for reducing the number of unknown variables in the system, as will be shown,and it is also appropriate to the nature of the tow carriage use. Tow specimens will be tested with both simple harmonic and random kinematics to simulate monochromatic and random waves.Random kinematics can be modeled as the superposition of many simple harmonic signals.

Using the kinematic form expressed in Equations (2.2.18), (2.2.22), and (2.2.23) and substituting into the equations of motion previously developed for the system model, Equation (2.2.5b) yields:

$$\theta_1(-2k_cR_1^2+\omega^2I_1-i2\omega c_cR_1^2)+X_2(k_cR_1+i\omega c_cR_1)+X_{10}(-k_cR_1-i\omega c_cR_1)\ +T=0 \tag{2.2.24}$$

Equation (2.2.6b) becomes:

$$X_1(k_cR_1+i\omega c_cR_1)+X_2(-2k_c+m_c\omega^2-i2c_c\omega)+X_3(k_c+ic_c\omega)=0 \tag{2.2.25}$$

Equation (2.2.8b) becomes:

$$X_2(k_c+i\omega c_c)+X_4(k_c+i\omega c_c)+X_3(-2k_c+\omega^2m_T-i\omega(2c_c+c_{eff}))=0 \tag{2.2.26}$$

Equation (2.2.10c) becomes:

$$X_4(k_c+i\omega c_c)+X_6(-2k_c-k_6+\omega^2m_6-i\omega(2c_c+c_6))+X_8(k_c+i\omega c_c)=0 \tag{2.2.27}$$

Equation (2.2.13b) becomes:

$$X_4(k_cR_2+i\omega c_cR_2)+\theta_2(-2k_cR_2^2+I_2\omega^2-i\omega(2c_cR_2+c_\theta))+X_8(-k_cR_2-i\omega c_cR_2)=0 \quad (2.2.28)$$

Equation (2.2.14c) becomes:

$$X_4(-2k_c+\omega^2m_c-i2c_c\omega)+\theta_2(k_cR_2+i\omega R_2c_c)+X_6(k_c+i\omega c_c)+X_3(k_c+i\omega c_c)=0 \quad (2.2.29)$$

Equation (2.2.15) becomes:

$$\theta_2(-k_cR_2+i\omega c_cR_2)+X_6(k_c+i\omega c_c)+X_8(-2k_c+\omega^2m_c-i2\omega c_c)+X_9(k_c+i\omega c_c) \quad (2.2.30)$$

Equation (2.2.16) becomes:

$$X_8(k_c+i\omega c_c)+X_9(-2k_c+\omega^2m_c-i2\omega c_c)+X_{10}(k_c+i\omega c_c)=0 \quad (2.2.31)$$

And (Equation) 2.2.17b becomes:

$$\theta_1(-k_cR_1-i\omega c_cR_1)+X_9(k_c+i\omega c_c)+X_{10}(-2k_c+\omega^2m_c-i2\omega c_c)=0 \quad (2.2.32)$$

Thus by specifying the form of the kinematics to be simple harmonic the 28 unknown variables of the system model have been reduced to nine unknown displacements and one unknown torque for the nine equations. To solve this linear system we must specify either one of the displacement phasors or the torque phasor as well as the angular

frequency reducing the number of unknowns to nine. It seems logical to prescribe the desired kinematics of the carriage/specimen variable X_3 and solve for the remaining kinematics and dynamics that would be necessary to generate the desired X_3.

As previously stated to fully prescribe the kinematics of the carriage/specimen variable both frequency and phasor must be given. The phase information embedded in the displacement phasor specifies the position of the variable at time zero,i.e., the initial condition. By setting the initial phase of the carriage/specimen displacement to 0 degrees the displacement will be at the maximum real value at time zero with the velocity at the maximum imaginary value or zero on the real axis and the acceleration will be at the maximum negative value on the real axis. Fig. (2.2.10) shows the kinematic relationships for a displacement phase angle of zero at various positions in time. Since the response is temporal and quasi-steady state the phase angle of the specified displacement is arbitrary and can be set to equal to zero for convenience. With this selection all other phase angles can be conveniently referenced to the carriage/specimen displacement.

As a result of the kinematic form being specified as simple harmonic, the eight unknown displacement functions and unknown torque function have been reduced to unknown phasors. With this simple harmonic motion the system model has been reduced to nine linear coupled equations with nine unknown phasors and can be solved using complex linear mathematics. To due this it is necessary to write the equations in matrix form. The given displacement phasor X_3 can be separated from the other variables and transformed into the matrix form

$$[A]\{X\}=\{B\}$$

where the square matrix [A] contains the coefficients of the unknown column matrix {X} and set equal to the known column matrix {B}. Both the [A] matrix and the {B} matrix contain the given frequency of oscillation ω as can be seen in Fig. (2.2.11). Thus the unknown phasors of the {X} matrix can be solved for by the equation

$$\{X\}=[A]^{-1}\{B\}$$

given the physical parameters of the system as well as the displacement phasor and frequency of x_3. This is done by the Fortran program Towplot which is documented in Appendix (A).

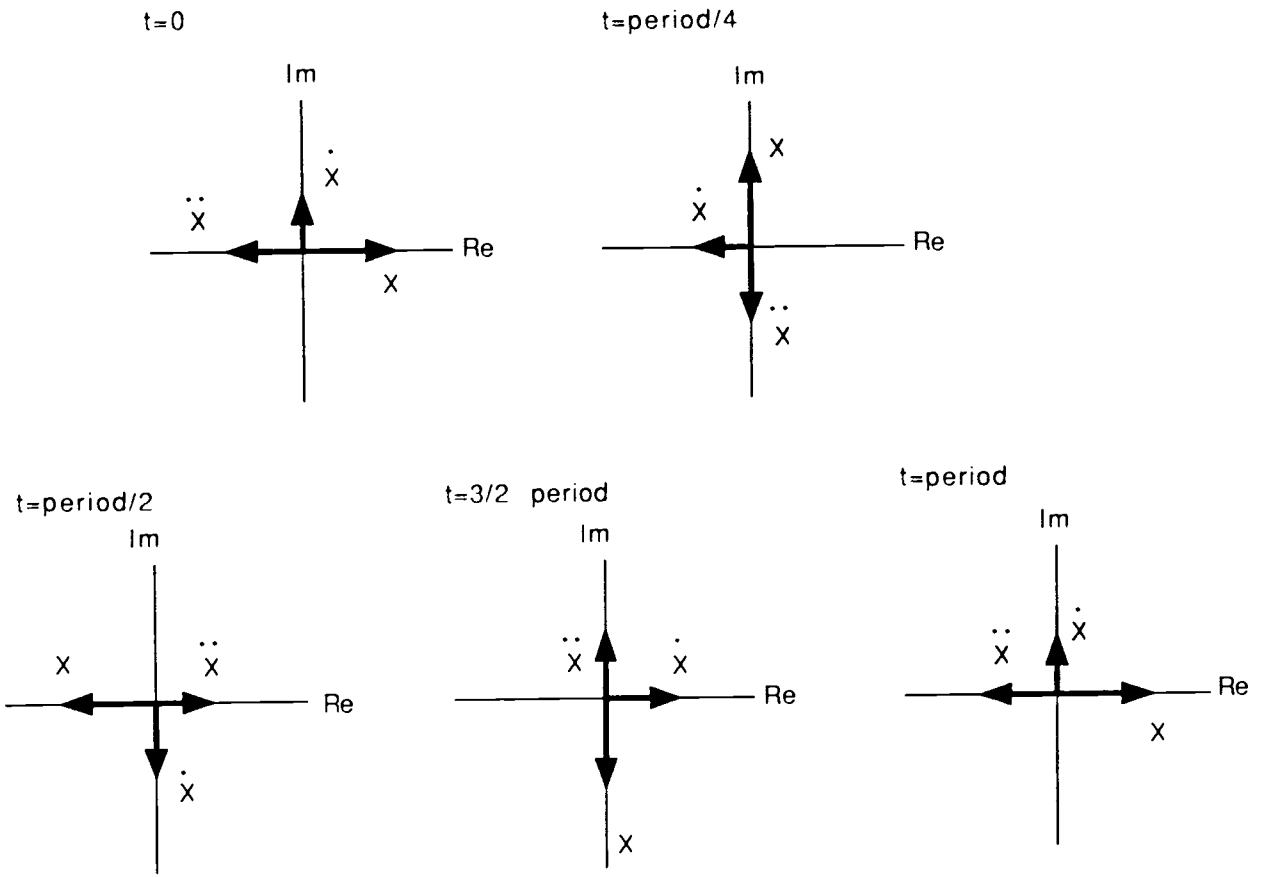

Figure 2.2.10 Kinematic phasors at various positions of the cycle

Eq. #	Θ_1	X_2	X_4	Θ_2	X_6	X_8	X_9	X_{10}	T			
2.2.32	$-k_c R_1 - i\omega c_c R_1$						$k_c + i\omega c_c$	$-2k_c + \omega^2 m_c - i2\omega c_c$		Θ_1		
2.2.25	$k_c R_1 + i\omega c_c R_1$	$-2k_c + \omega^2 m_c - i2\omega c_c$								X_2		$(-k_c - c_c\omega)X_3$
2.2.26		$k_c + i\omega c_c$	$k_c + i\omega c_c$							X_4		$(2k_c - \omega^2 m_T + i\omega(2c_c + c_{eff})X_3$
2.2.29			$-2k_c + \omega^2 m_c - i2\omega c_c$	$k_c R_2 + i\omega c_c R_2$	$k_c + i\omega c_c$					Θ_2		$(-k_c - ic_c\omega)X_3$
2.2.27			$k_c + i\omega c_c$		$-2k_c - k_6 + \omega^2 m_6 - i\omega(C_c + C_6)$	$k_c + i\omega c_c$				X_6	$=$	
2.2.28			$k_c R_2 + i\omega c_c R_2$	$-2k_c R_2^2 + \omega^2 I_2 - i\omega(2C_c R_2 + C_{t4})$		$-k_c R_2 - i\omega c_c R_2$				X_8		
2.2.30				$-k_c R_2 - i\omega c_c R_2$	$k_c + i\omega c_c$	$-2k_c + \omega^2 m_c - i2\omega c_c$	$k_c + i\omega c_c$			X_9		
2.2.31						$k_c + i\omega c_c$	$-2k_c + \omega^2 m_c - i2\omega c_c$	$k_c + i\omega c_c$		X_{10}		
2.2.24	$-2k_c R_1^2 + \omega^2 I_1 - i2\omega c_c R_1^2$	$k_c R_1 + i\omega c_c R_1$						$-k_c R_1 - i\omega c_c R_1$	1	T		

Figure 2.2.11 Matrix representation of system equations

2.3 System Dynamics

2.3.1 Carriage/Specimen Forces

There are three forces which act on the carriage/specimen model as previously discussed in Section (2.2): 1) the drag force which produces forces 180 degrees out of phase with the carriage/specimen velocity ,2) the inertial force which produces forces 180 degrees out of phase with the carriage/specimen acceleration , and 3) the wire rope force which provides motivation. The wire rope forces were discussed in detail in Section (2.2) and will not be expanded on here.

1) Carriage/specimen drag force: The drag force on the carriage/specimen is due to the interaction of the tow specimen with the water in the wave tank. To describe the drag force in terms of the carriage/specimen kinematics we can use the familiar turbulent drag equation

$$F_d=1/2\ \rho C_d A V|V| \tag{2.3.1}$$

where ρ is the mass density of the fluid, C_d is the experimentally determined drag coefficient, A is the reference frontal area used to measure the drag coefficient, and V is the velocity of the specimen relative to the still fluid.

The solution technique for the system of equations requires that all equations be linear. Since the drag force on the tow specimen is proportional to the square of the velocity it must be linearized. Noting that the solution of the system model is quasi-steady an

equivalent linear drag force can be developed that will give the same power or energy dissipation/absorption over one tow cycle or period. To do this we must first equate the non-linear drag force to another non-linear drag force of the form

$$F_d = 1/2\ \rho CAVV_{max} \tag{2.3.2}$$

where C is a drag coefficient based on the reference area A and V_{max} is the maximum velocity of the kinematic cycle. The energy dissipated or absorbed over one cycle can be expressed as the time integral of power

$$\text{Energy} = \int_t^{t+\tau} F_d \bullet V\ dt \tag{2.3.3}$$

where τ is the period of the cycle. Substituting Equation (2.3.1) for F_d into Equation (2.3.3) yields

$$\text{Energy} = \int_t^{t+\tau} 1/2\ \rho C_d AV|V| \bullet V\ dt \tag{2.3.4}$$

Substituting Equation (2.3.2) for F_d into Equation (2.3.3) yields

$$\text{Energy} = \int_t^{t+\tau} 1/2\ \rho CAV_{max} V \bullet V\ dt \tag{2.3.5}$$

Equating energy ,Equations (2.3.4) and (2.3.5) yields

$$\text{Energy} = \int_t^{t+\tau} 1/2 \rho C_d AV|V| \bullet V\ dt = \int_t^{t+\tau} 1/2 \rho CAV_{max} V \bullet V\ dt \tag{2.3.6}$$

With the drag force always being in line with the velocity the dot product can be dropped yielding

$$\text{Energy} = \int_t^{t+\tau} 1/2\rho A C_d |V|^3 \, dt = \int_t^{t+\tau} 1/2\rho A C V_{max} V^2 \, dt \qquad (2.3.7)$$

This is a statement of Lorentz's condition of equivalent work, (Dean and Dalrymple, 1984).

From Section (2.2) we found the velocity could be expressed as

$$V = V_{max} e^{i\omega t} = V_{max}[\cos(\omega t) + i\sin(\omega t)] \qquad (2.3.8)$$

with real component

$$Re\{V\} = V_{max} \cos(\omega t) \qquad (2.3.9)$$

Substituting Equation (2.3.9) into Equation (2.3.7) yields

$$\text{Energy} = \int_t^{t+\tau} 1/2\rho C_d V_{max}{}^3 |\cos|^3(\omega t) \, dt = \int_t^{t+\tau} 1/2\rho A C V_{max}{}^3 \cos^2(\rho t) \, dt \qquad (2.3.10)$$

Cancelling like terms yields

$$C_d \int_t^{t+\tau} \cos^3(\omega t) \, dt = C \int_t^{t+\tau} \cos^2(\omega t) \, dt \qquad (2.3.11)$$

Substituting for the integrals in Equation (2.3.11) yields

$$C_d/3[(2+\cos^3(\omega t))\sin(\omega t)]_t^{t+\tau} =$$
$$C[2\omega t+\sin(2\omega t)]_t^{t+\tau} \qquad (2.3.12)$$

Evaluate the integral over one half wave period where both sin and cos are positive. The results are symmetric over the other half period and will simply produce a multiplier of two on both sides of the equation. Letting

$$t= -\pi/2$$

and

$$t+\tau= \pi/2$$

Evaluating Equation (2.3.12) yields

$$C= 8/3\pi\ C_d \qquad (2.3.13)$$

We seek a linear drag force of the form

$$F_d=C_{eff}V \qquad (2.3.14)$$

where C_{eff} is the equivalent linear coefficient for energy dissipation/absorption over one kinematic cycle. Equating Equation (2.3.14) and Equation (2.3.2)

$$F_d=C_{eff}V=1/2\ \rho CAV_{max}V$$

which reduces to

$$C_{eff}=1/2\ \rho CAV_{max} \tag{2.3.15}$$

Substituting Equation (2.3.13) for C into Equation (2.3.15) yields

$$C_{eff}=4/3\pi\ \rho C_d AV_{max} \tag{2.3.16}$$

The velocity of interest is that of the carriage/specimen model and from Section (2.2) can be expressed as

$$V_{max}=\omega|X_3| \tag{2.3.17}$$

where $|X_3|$ is the magnitude of the carriage/specimen displacement amplitude and ω is the angular frequency of oscillation. Substituting Equation (2.3.17) into Equation (2.3.16) yields

$$C_{eff}=4/3\pi\ \rho C_d A\omega|X_3|. \tag{2.3.18}$$

The drag force of the specimen has been linearized by equating energy dissipation/absorption over one kinematic cycle of oscillation and is expressed in terms of the tow specimen kinematics, geometry, fluid density, and experimental drag coefficient.

2) Carriage/specimen inertial force: The second force acting on the carriage/specimen is the inertial force F_i. This quantity is used in force calculations that are 180 degrees out of phase with the

acceleration. The inertial force is linearly proportional to the acceleration and can be expressed as

$$F_i = m_T \ddot{X} \tag{2.3.19}$$

where m_T is the effective mass of the carriage/specimen model. The effective mass is composed of three components, 1) the lumped mass of the wire rope near the carriage, 2) the structural mass of the carriage and tow specimen, and 3) the added mass of the tow specimen interacting with the water in the wave tank. The first two components are straight forward and will not receive any more detail in this Section. The actual values used for these and other parameters are discussed in Section (2.4). The added mass term of the specimen is the result of accelerating a body in a still fluid and can be expressed as

$$F_{is} = \rho \forall C_i \ddot{X} \tag{2.3.20}$$

where ρ is the mass density of the fluid, $\forall$ is the displaced volume of the fluid by the body, C_i is the analytically determined added mass coefficient, and $\ddot{X}$ is the acceleration of the body. The total effective mass of the carriage/specimen model can now be expressed as

$$m_T = m_c + m_s + \rho \forall C_i \tag{2.3.21}$$

where m_c is the lumped wire rope mass and m_s is the structural mass of the carriage and tow specimen.

2.3.2 Power Calculations

To quantify the power requirements of the system four different expressions for power are investigated ,1) the instantaneous power based on the linearized drag force, 2) the average power based on the linearized drag force, 3) peak power based on the linearized drag force ,and 4) peak power based on the non-linear drag force.

1) Instantaneous power based on the linearized drag force: Power by definition can be expressed as the product of the real part of the drive torque and the real part of the angular velocity of the drive torque as specified in Equation (2.3.22).

$$P=Re\{T_D\}*Re\{\dot{\theta}\} \tag{2.3.22}$$

Power is introduced into the system at the drive pulley where the solution of the system equations yields the drive torque

$$T_D=|T_D|e^{i(\omega t+\phi T)} \tag{2.3.23}$$

where $|T_D|$ is the magnitude of the torque phasor given by Equation (2.2.20) and ϕ_T is the phase angle of the drive torque phasor given by Equation (2.2.21). The angular velocity of the driver pulley can be expressed as

$$\dot{\theta}_1=i\omega|\theta_1|e^{i(\omega t+\phi 1)} \tag{2.3.24}$$

where $|\theta_1|$ is the magnitude of the rotational phasor θ_1 and ϕ_1 is the phase angle. Both drive torque and angular velocity can be expanded in terms of their real and imaginary parts as follows:

$$T_D=|T_D|[\cos(\omega t+\phi_T)+i\sin(\omega t+\phi_T)] \tag{2.3.25}$$

and

$$\dot{\theta}_1=i\omega|\theta_1|[\cos(\omega t+\phi_1)+i\sin(\omega t+\phi_1)] \tag{2.3.26}$$

From Equation (2.3.25) the real part of the drive torque can be expressed as

$$Re\{T_D\}=|T_D|\cos(\omega t+\phi_T) \tag{2.3.27}$$

and the real part of the angular velocity can be found from Equation (2.3.26) as

$$Re\{\dot{\theta}\}=-\omega|\theta_1|\sin(\omega t+\phi_1) \tag{2.3.28}$$

The instantaneous power can be found by substituting Equations (2.3.27) and (2.3.28) into Equation (2.3.22).

$$P=-\omega|T_D||\theta_1|\sin(\omega t+\phi_1)\ \cos(\omega t+\phi_T) \tag{2.3.29}$$

Using the trigonometric identity

$$\sin(ax+b)\ \cos(ax+c) = 1/2[\sin(2ax+b+c)+\sin(a-b)] \tag{2.3.30}$$

the instantaneous power can be expressed as :

$$P=-1/2\omega|T_D||\theta_1|[\sin(2\omega t+\phi_1+\phi_T)+\sin(\phi_1-\phi_T)] \tag{2.3.31}$$

Since the torque and the angular velocity are calculated using the linearized drag coefficient, Equation (2.3.31) is also based on the linearized drag coefficient and approximates the required power. Note that a positive value of power implies energy is being input into the system and conversely a negative value implies energy being extracted form the system.

2) Average power based on the linearized drag force: the average power can be found by integrating Equation (2.3.31) over one wave period which is identical to setting the temporal component of the instantaneous power,Equation (2.3.31), to zero yielding:

$$P_{ave}= -1/2\ \omega|T_D||\theta_1|\sin(\phi_1-\phi_T) \tag{2.3.32}$$

Note that in order to have a positive value for average power, which must be the case, the difference in phase angles $\phi_1-\phi_T$ must be negative. Since the drag force was linearized by equating average power for linear and non-linear drag forces the average power expression should more closely approximate the actual power requirements of the system than the other expressions for power.

3) Maximum instantaneous power based on the linearized drag force: To find the maximum power required per cycle an examination of the response of Equation (2.3.31) will give some insight; see Fig. (2.3.1). The instantaneous power oscillates about the average value given by Equation (2.3.32) at angular frequency 2ω. The maximum value occurs when the temporal component is equal to -1. Thus the maximum instantaneous power based on the linearized drag force can be expressed as :

$$P_{max} = -1/2\ \omega|T_D||\theta_1|[\sin(\phi_1-\phi_T)-1] \qquad (2.3.33)$$

4) Maximum power based on the non-linear drag force: The fourth expression for power that is of interest is that due solely to the drag force of the specimen. Instead of expressing power as the product of torque and angular velocity it can be represented as the product of force and velocity, specifically

$$P=F_d\dot{X}$$

where F_d is the drag force on the specimen being towed at velocity $\dot{X}$. Substituting the non-linear drag force, Equation (2.3.21), for F_d in terms of the carriage/specimen displacement yields:

$$P_d=1/2\ \rho C_d A|\omega X_3|^3 \qquad (2.3.34)$$

Given the specified kinematics of the carriage/specimen the maximum power due to drag can be calculated with Equation (2.3.34) and used for comparison to Equation (2.3.33). Unlike Equation (2.3.33), Equation (2.3.34) does not account for power due to inertial forces. For a kinematic specification that produces a drag dominated power, Equation (2.3.34) will give a better indication of the peak power required.

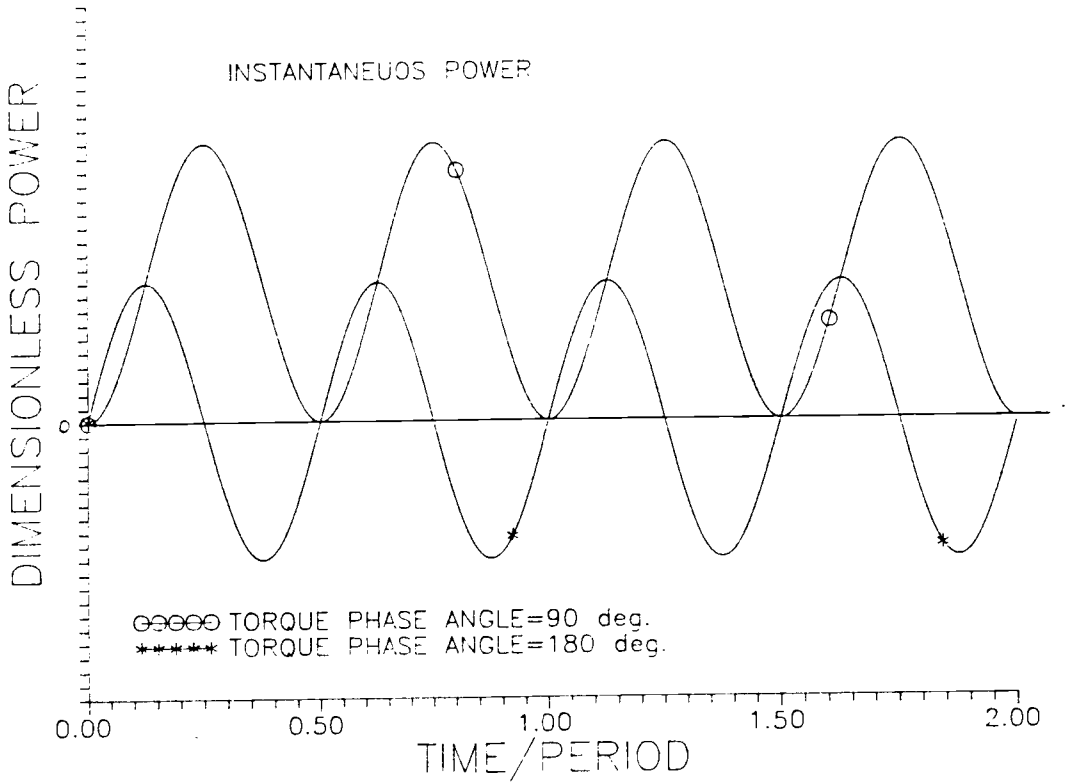

Figure 2.3.1 Instantaneous power requirement response

3.0 Tow Carriage System Behavior

3.1 Parameter Quantification

The physical parameters of the system must be quantified in order to evaluate results of the dynamic tow carriage mathematical model. A summary of these parameters can be seen in Table (3.1.1). These parameters are listed in four categories, each corresponding to the particular sub-model they belong to, i.e., wire rope, driver pulley, idler pulley, and carriage/specimen models.

Wire rope model parameters: There are three physical parameters that describe the wire rope model, 1) the lumped mass m_c, 2) the linear spring constant k_c, and 3) the linear damping coefficient c_c. In order to quantify these parameters a particular wire rope must be selected. The major performance criteria for selecting a wire rope are 1) the strand configuration, 2) the ultimate strength, 3) the stiffness, and 3) the unit mass.

The strand configuration or lay determines the ropes resistance to abrasion and bending stresses. A lay that has good abrasion resistance will in general have poor resistance to bending stresses as can be seen in Fig. (3.1.1), (Bethlehem Steel, 1985). Bending stresses will dominate over abrasion for this application and a 6x19s class wire rope was selected with 19 outside wires per strand. This selection is adequate for this primary analysis but may need refinement as the design progresses. The manufactures properties for this class of wire rope can be seen in Tables (3.1.2) and (3.1.3), (Bethlehem Steel, 1985).

Table 3.1.1 Physical parameters of the tow carriage model.

Parameter	Sub-model	Description	Status	Dimensions
m_c	Wire rope	Lumped mass	Fixed	M
k_c	Wire rope	Spring constant	Fixed	F/L
c_c	Wire rope	Damping coefficient	Fixed	M/T
R_1	Driver pulley	Radius	Fixed	L
I_1	Driver pulley	Rotational inertia	Fixed	$M\text{-}L^2$
R_2	Idler pulley	Radius	Fixed	L
I_2	Idler pulley	Rotational inertia	Fixed	$M\text{-}L^2$
m_6	Idler pulley	Lumped mass	Fixed	M
k_6	Idler pulley	Spring constant	Fixed	F/L
c_6	Idler pulley	Damping coefficient	Fixed	M/T
c_θ	Idler pulley	Damping coefficient	Fixed	$M\text{-}L^2/T$
c_{eff}	Carriage	Damping coefficient	Variable	M/T
m_T	Carriage	Lumped mass	Variable	M

Best scan available. Text on original is blurry.

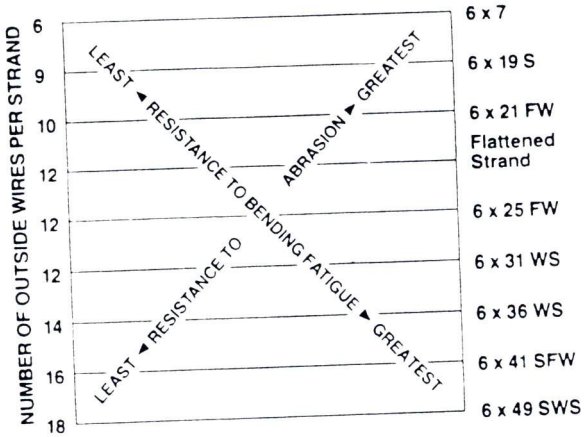

The wire rope industry refers to this as the X-chart. It serves to illustrate the inverse relationship between abrasion resistance and resistance to bending fatigue in a representative number of the most widely used wire ropes.

Figure 3.1.1 X-chart for wire rope lay selection.

Table 3.1.2 Wire rope mass and strength.

6 x 19 CLASS WIRE ROPE

Purple Plus or Purple Grade

Regular or Lang Lay IWRC or Fiber Core

Technical data for the following constructions in the 6 x 19 Class are listed below.

6 x 19 Seale • 6 x 19 Warrington • 6 x 21 filler wire Type U •
6 x 21 Seale • 6 x 25 filler wire Type W •
6 x 26 Type A

Rope Diam in	Approx Weight per ft lb		Breaking Strength tons of 2000 lb*			
			Purple Plus		Purple Grade	
	Fiber Core	IWRC	Fiber Core**	IWRC	Fiber Core	IWRC
¼	0.105	0.116	3.02	3.40	2.74	2.94
5/16	.164	.180	4.69	5.27	4.26	4.58
⅜	.236	.260	6.71	7.55	6.10	6.56
7/16	.32	.35	9.09	10.2	8.27	8.89
½	.42	.46	11.8	13.3	10.7	11.5
9/16	.53	.59	14.9	16.8	13.5	14.5
⅝	.66	.72	18.3	20.6	16.7	17.9
¾	.95	1.04	26.2	29.4	23.8	25.6
⅞	1.29	1.42	35.4	39.8	32.2	34.6
1	1.68	1.85	46.0	51.7	41.8	44.9
1⅛	2.13	2.34	57.9	65.0	52.6	56.5
1¼	2.63	2.89	71.0	79.9	64.6	69.4
1⅜	3.18	3.50	85.4	96.0	77.7	83.5
1½	3.78	4.16	101	114	92	98.9
1⅝	4.44	1.88	118	132	107	115
1¾	5.15	5.67	136	153	124	133
1⅞	5.91	6.50	155	174	141	152
2	6.72	7.39	176	198	160	172
2⅛	7.59	8.35	197	221	179	192
2¼	8.51	9.36	220	247	200	215
2⅜	9.48	10.4	244	274	222	239
2½	10.5	11.6	269	302	244	262
2¾	12.7	14.0	321	361	292	314

*When ropes are zinc coated, deduct 10 per cent from bright rope strengths shown.
**Purple Plus ropes with fiber cores usually have higher breaking strengths than Purple Grade IWRC ropes, but are no substitute for them because of the many other factors to be considered in operating ropes.

6 x 21 filler wire Type U rope with IWRC and lang lay

6 x 21 Seale with IWRC

6 x 19 Seale with IWRC

6 x 19 Warrington with fiber core

Table 3.1.3 Wire rope modulus of elasticity.

Table 16 Approximate Modulus of Elasticity
(Pounds per square inch)

Rope Classification	Zero through 20% Loading	21% to 65% Loading
6 x 7 with fiber core	11,700,000	13,000,000
6 x 19 with fiber core	10,800,000	12,000,000
6 x 37 with fiber core	9,900,000	11,000,000
8 x 19 with fiber core	8,100,000	9,000,000
6 x 19 with IWRC	13,500,000	15,000,000
6 x 37 with IWRC	12,600,000	14,000,000

*Applicable to new rope, i.e., not previously loaded.

The ultimate strength needed can be estimated from the maximum load the wire rope is expected to experience multiplied by an appropriate factor of safety. The maximum wire rope load is the sum of the maximum dynamic load plus the static preload. The maximum dynamic load can be found in Table (3.2.2) as approximately 50 kN (11.2 kips). The static preload is needed to minimize the dynamic vertical deflection of the wire rope termed " cable whip". The vertical deflection can be roughly estimated by a static analysis as follows. The static tension H_s required to have a vertical deflection or sag h can be expressed as

$$H_s = wL_{hs}^2/2h \qquad (3.1.1)$$

where L_{hs} and w are the half span and unit weight of the wire rope respectively (Baumeister, et al., 1978). The cable guides, Section (5.2), are designed for 0.152 m (6 in.) of sag and the cable span can be estimated as one half the distance between the secondary idler pulley , 41.91 m (137.5 ft.) plus a carriage stroke of 30 m (98.4 ft.) giving a maximum span of 71.91 m (236 ft.) with half span 35.96 m (118 ft.). For the 0.035 m (1 3/8 in.) diameter wire rope in Table (3.1.2) the unit weight is 5.22 Kg/m (3.5 lb./ft.). Substituting these values into Equation (3.1.1) yields a static preload of 216.6 kN (48.7 kips). Adding the maximum dynamic load yields a maximum rope loading of 266.6 kN (60 kips). Selecting the 0.035 m (1 3/8 in.) IWRC Purple Plus wire rope will give a total safety factor of 3.2 and a dynamic safety factor of 11.8. Thus with a static preload of 216.6 kN (48.7 kips) a dynamic

load of 587 kN (132 kips) would be needed to break the rope, 11.8 times the maximum design dynamic load.

The third consideration for selecting a wire rope is the stiffness. The spring forces generated by the wire rope model are of the form

$$F=k_c\Delta x \tag{3.1.2}$$

where k_c is the linear spring rate and Δx is the difference in linked nodal displacements. Using the familiar formula for the length wise deflection of a slender rod

$$\Delta x=FL/EA \tag{3.1.3}$$

where F is the longitudinal force acting on the free end of the fixed rod of length L, cross Sectional area A and modulus of elasticity E. Substituting Equation (3.1.3) into Equation (3.1.2) and solving for k_c yields

$$k_c=EA/L \tag{3.1.4}$$

The appropriate length is the total span between the driver pulley and primary idler pulley 99.06 m (325 ft.) divided by the number of spring models on the upper or lower span, which is four, giving a length of 24.76 m (81.25 ft.). The area A of the wire rope can be approximated as

$$A=\pi d^2/4 \tag{3.1.5}$$

where d is the nominal diameter of the wire rope. The modulus of elasticity E can be found from Table (3.1.3). The sensitivity of the system to wire rope stiffness can be seen in Fig. (3.1.2) which varies the diameter and hence k_c as calculated by Equation (3.1.4) for 6x19s class wire rope using a modulus of elasticity of 93.07 GPa (13.5 E6 psi). Increasing the diameter increases the wire rope mass as well as stiffness. This increased mass does not affect the fundamental resonance frequency or period of the system appreciably but will produce a significant increase in inertial loading. As implied above, the decrease in fundamental period with cable diameter is due to the increased stiffness with limited gains using a wire rope diameter greater then 0.035 m (1 3/8 in.), which is the selected diameter for the model.

The lumped mass m_c of the wire rope model is calculated by discretizing the total span between the driver and primary idler pulley into the three mass nodes on either the upper or lower span of the system model. The appropriate length is thus 99.06 m (325 ft.) or 33.02 m (108.3 ft.) per node. The lumped mass is the length per node multiplied by the unit mass of the wire rope as taken from Table (3.1.2). A summary of the discretized stiffness and mass of the wire rope model is shown for various diameters in Table (3.1.4).

The last wire rope model parameter to be quantified is the damping coefficient c_c. From Section (2.2) we found the damping of the wire rope model produced forces of the form

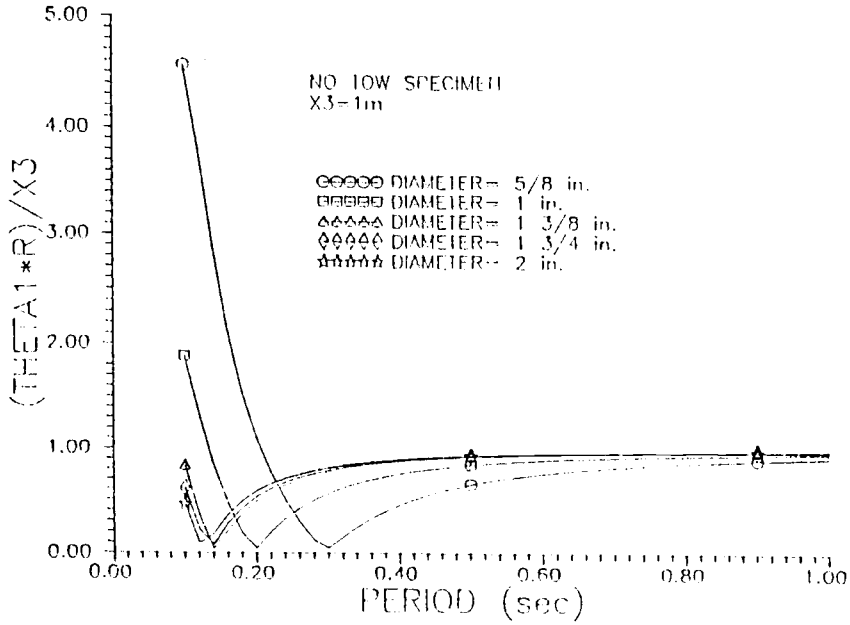

Figure 3.1.2 System sensitvity to wire rope size.

Table 3.1.4 Stiffness and mass values for wire rope model.

Diameter (cm.:in.)	Modulus (Gpa)	k_c (N/m)	m_c (Kg)
1.59 : 5/8	93.08	7.439E5	35.4
2.54 : 1	93.08	1.904E6	91.0
3.49 : 1 3/8	93.08	3.600E6	172
4.44 : 1 3/4	93.08	5.832E6	279
5.08 : 2	93.08	7.612E6	363

$$F_c=c_c(\dot{X}_i-\dot{X}_{i+1}) \tag{3.1.6}$$

where $\dot{X}_i-\dot{X}_{i+1}$ is the difference in linked nodal velocities. By making the substitution

$$\dot{X}=\dot{X}_i-\dot{X}_{i+1}$$

the wire rope model can be reduced to the single DOF system as seen in Figure (3.1.3).

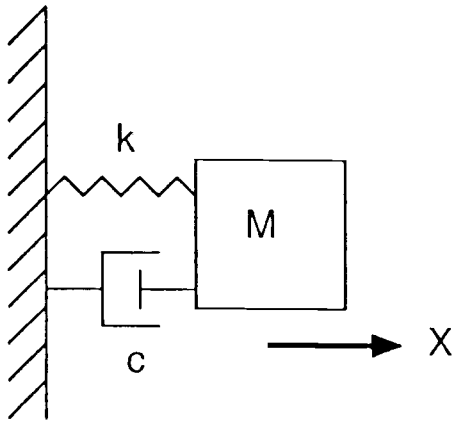

Figure 3.1.3 Reduced wire rope model.

The familiar Equation of motion for this system is given by Equation (3.1.7).

$$m\ddot{X}+c\dot{X}+kX=0 \tag{3.1.7}$$

The critical damping for the system is given by Equation (3.1.8) (Baumeister, et al.).

$$c_x = 2*SQRT(km) \tag{3.1.8}$$

The damping ratio ξ is defined as the ratio of actual damping c to critical damping c_x given by Equation (3.1.9).

$$\xi = c/c_x \tag{3.1.9}$$

One method of quantifying the amount of damping present in an oscillatory system is to measure the rate of decay of free oscillations as shown in Fig. (3.1.4).

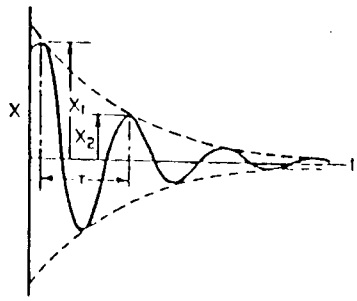

Figure 3.1.4 Response of linear damped free vibration.

This can be expressed by the logarithmic decrement, δ, which is defined as the natural logarithm of the ratio of two successive amplitudes as

$$\delta = \ln(x_i/x_{i+1}) = 2\pi\xi/SQRT(1-\xi^2) \simeq 2\pi\xi$$

which when solved for ξ yields Equation (3.1.10)

$$\xi = \delta/2\pi \tag{3.1.10}$$

Solving Equation (3.1.9) for c yields

$$c=\xi c_x$$

and substituting Equation (3.1.10) for ξ yields

$$c=\delta c_x/2\pi \tag{3.1.11}$$

Substitution of Equation (3.1.8) into Equation (3.1.11) yields

$$c=\delta \text{ SQRT}(km)/\pi \tag{3.1.12}$$

Thus Equation (3.1.12) expresses the actual damping in terms of the representative mass and stiffness and the measured log decrement. For this analysis the representative mass is the structural mass of the carriage/specimen and cable and the representative spring constant can be calculated by discretizing the span of wire rope between the carriage and driver pulley into a single spring. As previously stated the structural mass of the carriage is 1068 Kg. (2350 lb.) and the appropriate cable length is 49.5 m (162.4 ft.) giving a spring rate of 1.8E6 N/m (1.2E5 lb/ft.) for the selected wire rope.

Ramberg and Griffen, (1977), measured the log decrement of 5/8 in. (0.016 m) diameter double armor steel cable as a function of tension in the cable as seen in Fig. (3.1.5). The numbers in the bracket below the data points represent the amplitude of vertical vibration cable diameters. It was concluded that the log decrement and hence damping

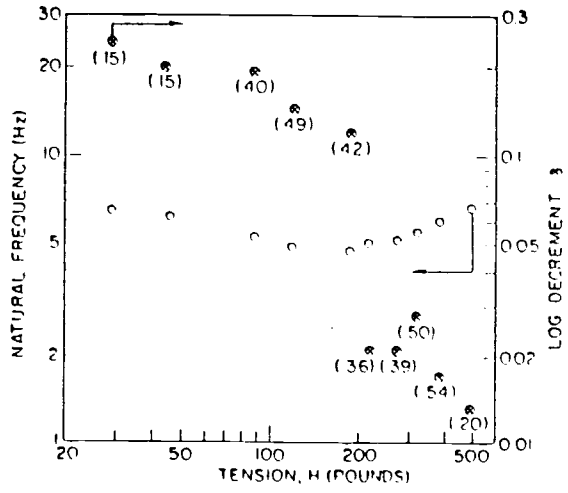

Figure 3.1.5 Log decrement of wire rope versus tension

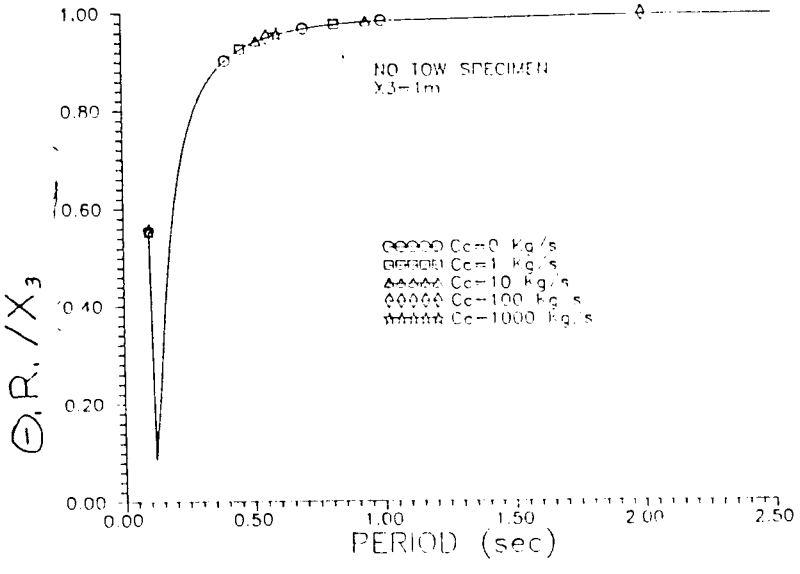

Figure 3.1.6 System sensitivity to cable damping

decreased with cable tension. The maximum tension that data was collected at was 500 lbs which yielded a value for δ on the order of 0.01. Using this value in Equation (3.1.12) with the mass and stiffness discussed above yields a damping coefficient of 135 Kg/s (297 lb/s).

This estimate of the damping present in the wire rope used for this particular model is obviously very approximate. None the less it seems reasonable to assume this value is within four or five orders of magnitude of the real value. The sensitivity of the model to wire rope damping is very small as can be seen in Fig. (3.1.6). In fact no significant difference can seen in fundamental resonance when the cable damping is varied over five orders of magnitude for a 0.035 m (1 3/8 in.) diameter wire rope. If the cable damping did affect the system response significantly it would imply that a significant amount of cable deflection was occurring which would be unacceptable. Thus when a properly selected wire rope is used the internal damping can be neglected for this first order analysis. For completeness, the value of 135 Kg/s is used in the model.

Driver pulley model parameters: There are two physical parameters that describe the driver pulley model are the radius and rotational inertia of the pulley. Both of these parameters must be selected to best represent the real system geometry which differs slightly from the model. As can be seen in Fig. (3.1.7) the layout design of the dynamic tow carriage has the driver pulley conceptualized as a drum with several wrappings of wire rope, component (4). The wire rope also partially wraps around two secondary idler pulleys, components (2) ,

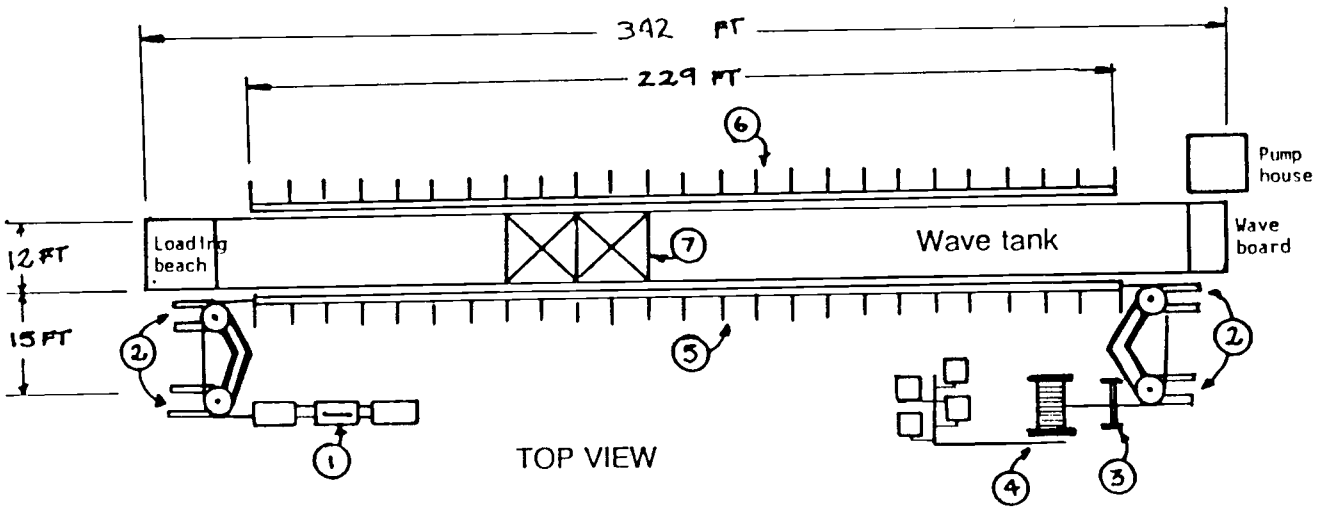

① Primary idler pulley

② Secondary idler pulley

③ Driver cable guide

④ Driver drum & drive train

⑤ Carriage bearing structure with cable way

⑥ Carriage bearing structure

⑦ Tow carriage structure

Figure 3.1.7 Layout drawing of dynamic tow carriage system

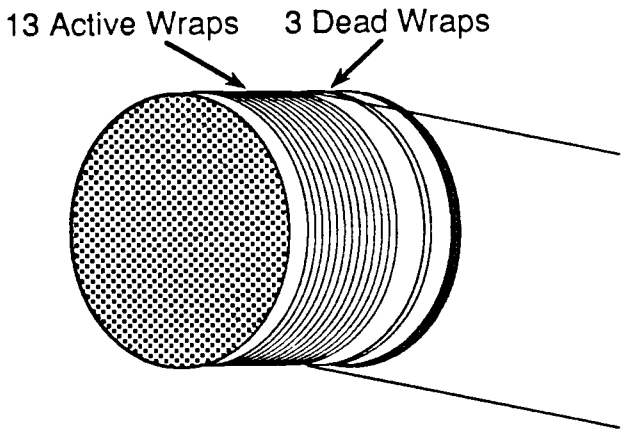

Figure 3.1.8 Driver drum with cable wrap

before spanning the existing wave channel and partially wrapping around two more secondary idler pulley and then wrapping around the primary idler pulley, component (1). In order to properly quantify the rotational inertia of the driver pulley model the inertial contributions of both the driver drum and the first two secondary idler pulleys must be considered. Table (3.1.5) is a summary of the components, equations, and parameters used to model the driver pulley. The following discussion explains the equations and values expressed in Table (3.1.5).

The radius of the driver drum was selected by considering the geometry of the existing wave channel and the minimum radius of curvature suggested for the selected rope by the manufacturer. From Table (3.1.5), (Bethlehem Steel, 1978) the minimum drum diameter D to rope diameter d ratio is 34 for a 6x19 S wire rope and the suggested ratio is 51. These ratios are suggested by the manufacturer to minimize bending stresses in the wire rope. A ratio of 43 was selected after considering the geometry of the existing wave channel. With a wire rope diameter of 0.035 m (1 3/8 in.) the corresponding drum diameter is 1.5 m (59 in.) with a radius of 0.75 m (29.5 in.).

The rotational inertia of the driver drum can be estimated by modeling the drum as a hollow cylinder of width W, outside radius R, and inside radius r. The outside radius has already been specified as 0.75 m. The inside radius was selected as 0.7405 m to give a wall thickness of 9.5 mm (3/8 in.). The actual thickness to be used in construction is unknown at this stage of the design so the value used is an estimate.

The width is calculated by considering the wire rope diameter and the number of wraps around the drum. The maximum carriage travel is expected to be 60 m (196.9 ft.) peak to peak which implies 60 m of active cable must be stored on the drum. Dividing the active length by the circumference of the drum yields 12.7 or 13 wraps around the driver drum. Adding three dead wraps for safety yields a total of 16 wraps; see Fig. (3.1.8). Sixteen cable diameters of 0.035 m equates to a width of 0.56 m (22 in.). Allowing an extra 10% of free width on either side of the wrapping gives a total width of 0.67 m (26.3 in.).

With the pertinent dimensions of the driver drum defined, the rotational inertia can be calculated by Equation (3.1.13)

$$I = \frac{M}{12(3R^2+3r^2+w^2)} (3R^2+3r^2+W^2) \qquad (3.1.13)$$

where the mass of the cylinder is given by Equation (3.1.14).

$$\text{mass} = (\pi/4)\ (R^2-r^2)\rho_{steel} \qquad (3.1.14)$$

Using the previously defined dimensions in Equations (3.1.14) and (3.1.13) yields a mass and inertia of 234 Kg (515 lb.) and 73.7 Kg-m^2 (1745 lb.-ft^2) respectively. The added mass of the wire rope windings can be estimated by multiplying the linear length and unit mass of the wire rope on the drum which yields 394 Kg (867 lb.) of wire rope. The added rotational inertia can be estimated by Equation (3.1.13) using

a mass of 394 Kg ,width of 0.56 m, inside radius of 0.75 m , and outside radius of 0.785 m yielding 90.3 Kg-m^2 (2138 lb.-ft.^{2}).

The secondary idler pulleys are modeled as steel rings with a outside radius of 0.75 m ,inside radius of 0.67 m and thickness of 0.07 m. Again these values are for estimation of the rotational inertia only and do not imply final dimensions. Equations (3.1.15) and (3.1.16) are used to calculate the mass and inertia of each ring respectively.

$$\text{mass} = \pi t \rho_{steel}(R^2-r^2) \tag{3.1.15}$$

$$I = (\text{mass}/2)(R^2-r^2) \tag{3.1.16}$$

Each ring has a mass of 196 Kg (431 lb.) and inertia of 11.1 Kg-m^2 (263 lb.-ft^2.). Each secondary idler pulley has two rings and there are two pulleys in the vicinity of the driver drum for a total of four rings having a rotational inertia of 44.4 Kg-m^2 (1051 lb-ft^2.). When added to the inertia of the drum and wrapped cable, the driver pulley model has a total rotational inertia I_1 of 208.5 Kg-m^2 (4937 lb-ft^2.).

Idler pulley model parameters: The idler pulley model has six physical parameters that describe its role in the system model, 1) the radius R_2, 2) the rotational inertia I_2, 3) The dynamic mass m_6, 4) the spring constant k_6 , 5) the translational damping coefficient c_6, and 6) the rotational damping coefficient c_θ. Referring to Fig. (3.1.7) there are two secondary idler pulleys in the vicinity of the primary idler pulley. The rotational inertia of the idler pulley model must include both primary and secondary idler pulley contributions. Table (3.1.7)

Table 3.1.5 Summary of driver pulley rotational inertia calculation.

Part desription	Parameters	Equations	Value
Driver drum	R:outside radius r:inside radius W:width ρ_{steel}:unit mass of steel	$mass=\pi/4\ (R^2-r^2)\rho_{steel}$ $I_{D1}=mass/12\ (3R^2+3r^2+W^2)$	R=0.75m r=0.7405m W=0.67m $\rho_{steel}=7833Kg/m^3$ mass=234Kg $I_{D1}=73.7Kg\text{-}m^2$
Wire rope wrapping	R:outside radius r:inside radius W:width L:length of rope m:unit mass of rope	mass=Lm $I_{D2}=mass/12\ (3R^2+3r^2+W^2)$	R=0.785m r=0.75m W=0.56m L=75.4m m=5.22Kg/m mass=394Kg $I_{D2}=90.3Kg\text{-}m^2$
Secondary idler ring	R:outside radius r:inside radius t:thickness	$mass=\pi t\rho_{steel}(R^2-r^2)$ $I_{D3}=mass/2\ (R^2-r^2)$	R=0.75m r=0.67m t=0.07m mass=196Kg $I_{D3}=11.1Kg\text{-}m^2$
Driver pulley inertia		$I_1=I_{D1}+I_{D2}+4I_{D3}$	$I_1=208.5Kg\text{-}m^2$

presents a summary of the components, equations, and parameters used for the model.

The primary idler pulley is modeled as a circular ring identical to the secondary pulley. The radius R_2 was chosen to be the same as the driver pulley. The total rotational inertia is the sum of the contributions from the primary idler ring and four secondary idler rings giving a total inertia of 55.5 Kg-m^2 (1314 lb-ft^2.).

In the real system the primary idler pulley is attached to two rigidly supported hydraulic cylinders which provide the static preload on the wire rope. Assuming the support structure to be infinitely rigid these cylinders will control the spring rate k_6 and translational damping c_6. In order to parameterize these two physical parameters the hydraulic cylinders must first be sized. Fig. (3.1.9) shows a FBD of the cylinders of length l and diameter d. The travel of the free end is X_6 being loaded by the force F. The force F is the sum of the maximum dynamic cable load F_{R2} plus twice the static preload F_{s2}. From the cable parameterization F_{r2} and F_{s2} were found to be 49.8 kN (11.2 kips) and 216.7 kN (48.7 kips) respectively giving a total load F of 483.2 kN (108.6 kips). The required cross Sectional area of both cylinders can be calculated by Equation (3.1.17) where σ is the hydraulic pressure in the cylinders.

$$\text{Area}=F/\sigma \tag{3.1.17}$$

Table 3.1.6 Drum to cable diameter ratios

Proper Sheave and Drum Sizes

Construction	Suggested D/d* ratio	Minimum D/d* ratio
6 x 7	72	42
19 x 7 or 18 x 7 Rotation Resistant	51	34
6 x 19 Seale	51	34
6 x 27 H flattened strand	45	30
6 x 31 V flattened strand	45	30
6 x 21 filler wire	45	30
6 x 25 filler wire	39	26
6 x 31 Warrington Seale	39	26
6 x 36 Warrington Seale	35	23
8 x 19 Seale	41	27
8 x 25 filler wire	32	21
6 x 41 Warrington Seale	32	21
6 x 42 filler	21	14

*D = tread diameter of sheave d = nominal diameter of rope

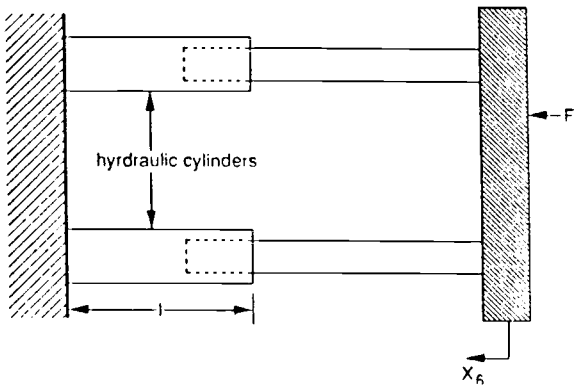

Figure 3.1.9 FBD of hydraulic cylinders

With a hydraulic pressure of 24.13 MPa (3500 psi), 0.020 m^2 (31.03 $in.^2$) total cylinder area is needed. This can be achieved by two 0.112 m (4.44 in.) diameter cylinders. An active cylinder length of 0.61 m (24 in.) was chosen to compensate for cable stretch. The spring rate of the combined cylinders can be estimated by Equation (3.1.18) (See Appendix D for derivation) where E_v is the bulk modulus of elasticity of the hydraulic fluid and F_{S2} is the static preload on the wire rope.

$$k_6=2F_{S2}E_v/\sigma l \qquad (3.1.18)$$

With a static preload of 216.7 kN, a bulk modulus of 1.303 GPa, hydraulic pressure of 24.13 MPa, and length of 0.61 m Equation (3.1.18) yields a stiffness of 38.5E6 N/m. This predicts an extremely rigid connection and thus the idler pulley will experience very small deflection in the model simulation. Small deflections will cause low velocities for the frequency range of interest and thus the translational damping will have a negligible influence on the model

Table 3.1.7 Summary of idler pulley model parameter quantification.

Parameter	Description	Equations	Value
R_2	Primary idler ring	$mass=\pi\rho_{steel}t(R^2-r^2)$	R=0.75m r=0.67m t=0.07m
I_2		$I_{P1}=mass/2\ (R^2-r^2)$	mass=196Kg $I_{P2}=11.1Kg\text{-}m^2$
m_6	Secondary idler ring	$mass=\pi\rho_{steel}t(R^2-r^2)$	R=0.75m r=0.67m t=0.07m
		$I_{P2}=mass/2\ (R^2-r^2)$	mass=196Kg $I_{P2}=11.1Kg\text{-}m^2$
	Total inertia of idler	$I_2=I_{P1}+4I_{P2}$	$I_2=55.5Kg\text{-}m^2$
	Lumped mass of idler	m_6=mass of primary ring	$m_6=196Kg$
k_6	Hydraulic cylinders	$k_6=2F_{S2}E_v/\sigma l$	$F_{S2}=216.7kN$ $E_v=1.303GPa$ $\sigma=24.13MPa$ $l=0.61m$ $k_6=38.4E6N/M$
c_6	Damping of cylinders	N/A	$c_6=0Kg/s$
c_θ	Brake damping	N/A	$c_\theta=0Kg\text{-}m^2/s$

simulation so it can be neglected. The rotational damping coefficient c_θ was installed in the system to model braking if needed. At this stage of the analysis there is no need for braking of the idler pulley and thus c_θ was set equal to zero.

Carriage/specimen model parameters: Two physical parameters are needed for the carriage/specimen model, the linearized drag coefficient c_{eff} and the total mass m_t. As seen in Fig. 3.1.10, the tow specimen is modeled as a horizontal circular cylinder supported by two vertical and one horizontal shrouded strut. The struts are cylinders that have a symmetric airfoil cross Section. The circular cylinder is characterized by the length L and diameter d.

The diameter is a system variable and the length is fixed at 3.05 m (10 ft.) which is slightly short of 3.66 (12 ft.) internal width of the existing wave tank. The drag of the circular cylinder is proportional to the frontal area and drag coefficient as discussed in Section (2.3). The value of the drag coefficient used was 0.7 which applies to Reynolds numbers above 1E6, (Gerhart and Gross, 1985). The frontal area is the product of length and diameter and therefore is a system variable. The vertical struts have a chord length c of 1 m (39.4 in.), a maximum thickness t of 0.127 m (5 in.), and a wetted length b of 3.05 m (10)ft. These dimensions were selected for structural and fluid flow performance as discussed in Chapter (4). From Fig. (3.1.11) (Hoerner, 1965) the drag coefficient, based on strut area bxc is 0.08 for a thickness ratio of 13% and Reynolds number similar to that used for the circular cylinder. The horizontal strut has chord length c of

1 m , a thickness t of 0.076 m (3 in.), and a wetted length of 3.05 m. From figure (3.1.11) the drag coefficient is 0.07 for a thickness ratio of 7%.

From Equation (2.3.18) c_{eff} is found to be a function of a drag coefficient C_d and an area A. A sum of the product C_dA from each of the three components contributing to the drag can be used in Equation (2.3.18). This sum will contain the variable diameter d of the tow specimen cylinder. Table (3.1.7) shows a summary of models, equations, and values used to parameterize c_{eff}.

The mass m_t is the sum of the wire rope model mass in the vicinity of the carriage m_c, the structural mass of the carriage m_s, and the added mass of the tow specimen interaction with the fluid. From the parameterization of the wire rope model the mass m_c was found to be 172 Kg . The structural mass of the carriage can be found in Appendix (C) as 1068 Kg. The added mass of the tow specimen is the product of displaced volume of the tow specimen, the added mass coefficient, and the density of the fluid. Since the volume is a function of the diameter the added mass is also a system variable. The added mass coefficient for a circular cylinder is 1.0 (Sarpkaya and Isaacson, 1987). The added mass of the struts interaction with the fluid is not accounted for in this analysis. Table (3.1.8) shows a summary of the mass calculation.

Table 3.1.8 Summary of carriage/specimen model parameter quantification.

Parameter	Model description	Equations	Value
c_{eff}	Tow Specimen:circular cylinder	$A_1=LD$ $Vol.=\pi/4\ D^2L$ $C_{d1}=0.7$ $C_i=2.0$	D=variable L=3.05m
	Vertical support:airfoil cylinder Thickness ratio=t/c	$A_2=cb$ $C_{d2}=0.08$	c=1m t/c=13% b=3.05m $A_2=3.05m^2$
	Horizontal support:airfoil cylinder b=3.05m	$A_3=cb$ $C_{d3}=0.07$	c=1m t/c=8% $A_3=3.05m^2$
	Total Drag:specimen+supports	$c_{eff}=4/3\pi\ \rho_w\omega X_3^*$ $(C_{d1}A_1+2C_{d2}A_2+C_{d3}A_3)$	$\rho_w=1000Kg/m^3$ ω, X_3, A_1=variable
m_T	Total mass is sum of local cable mass, structural mass, and added mass of specimen.	$m_T=m_c+m_s+C_i\rho_w Vol$	$m_c=172Kg$ $m_s=1068Kg$ Vol=variable

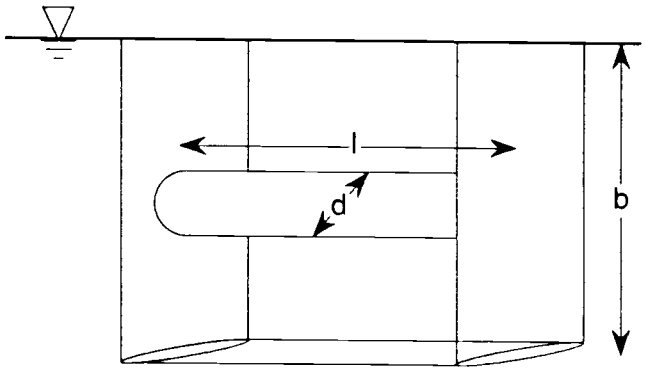

Figure 3.1.10 Tow specimen with supports.

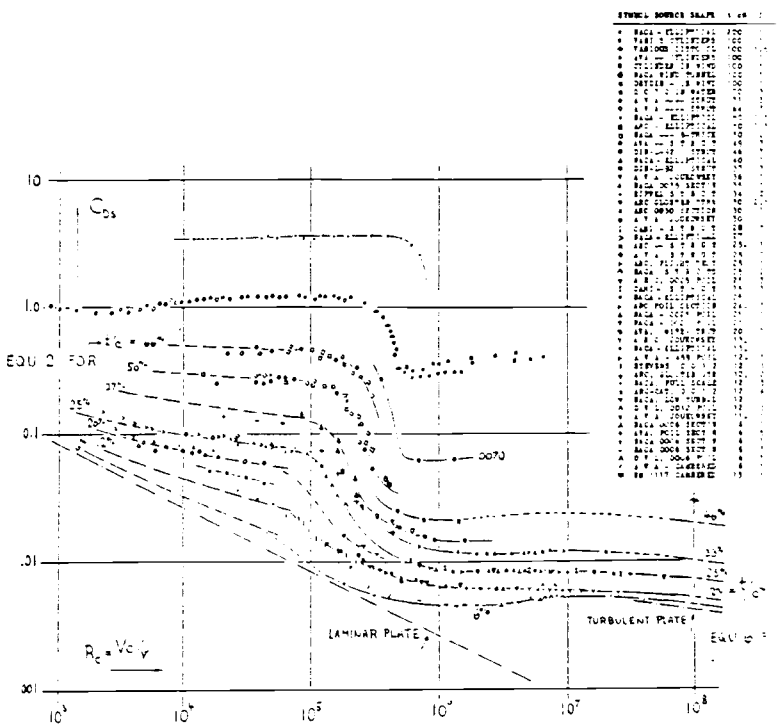

Figure 3.1.11 Drag coefficient of airfoil Sections.

Best scan available. Original is blurry.

3.2. Applications of the System Model

With the physical parameters of the system model quantified the performance can now be investigated. The input variables of the system are the modulus of the carriage/specimen displacement function X_3, the angular frequency of oscillation ω, and the tow specimen cylinder diameter d. For the driving frequency range of interest it is convenient to express the oscillation frequency in terms of the period τ which is given by Equation (3.2.0.1).

$$\tau=2\pi/\omega \tag{3.2.0.1}$$

The performance is presented as plots of the specific performance parameters of interest versus driving period. Each plot has a fixed tow specimen diameter with a family of response curves for various displacement modulus or half strokes. The period is varied from 0.1 seconds to 30 seconds with enough data points in between to generate a smooth curve. The half strokes are plotted for 1,5,10,20,and 30 meters for the specified period range. These families of curves are plotted for tow specimen cylinder diameters of 0.0,0.0254,0.0762,0.1524,0.3048,and 0.6096 meters which corresponds to 0,1,3,6,12,and 24 inches. The performance parameters of interest can be classified as either kinematic or dynamic and are summarized in Table (3.2.0.1).

Table (3.2.0.1) Summary of Performance Parameters

Classification	Parameter	Description
Kinematic	$\theta_1 R_1/X_3$	Maximum angular displacement per cycle of driver pulley non-dimensionalized with carriage displacement.
	ϕ_1	Phase angle of driver pulley displacement relative to carriage displacement phase.
Dynamic	DF_{max}	Maximum drag force per cycle of the towspecimen and supports as computed with the linearized drag force equation.
	IF_{max}	Maximum inertial force per cycle of the carriage structure and tow specimen.
	Force Ratio	DF_{max}/IF_{max}
	T_D	Maximum drive torque per cycle.
	ϕ_T	Drive torque phase angle relative to the carriage displacement phase.
	P_{max}	Maximum power required per cycle based on the linearized drag force.
	P_{ave}	Average power required per cycle based on the linearized drag force.
	Pratio	The ratio of the maximum non-linearized to linearized power per cycle.

3.2.1 Kinematics

With the carriage/specimen kinematics specified as input the best means of investigating the response of the system is to examine the driver pulley response. This response can be represented by the ratio of driver pulley displacement modulus to carriage/specimen displacement modulus. Thus any variation in the response curve reflects a variation of the driver pulley displacement relative to the carriage/specimen displacement. For driving periods that produce a steady state response this ratio is expected to be near unity implying small wire rope deflection between the driver pulley and carriage/specimen model. Fig. (3.2.1.1) shows this response for six tow specimen cylinder diameters. As the ratio becomes smaller than unity the driver pulley is required to go through a smaller displacement to move the carriage/specimen, which implies the wire rope model between the driver and carriage is experiencing stretch release and the remaining rope is stretching. In the real system the driver pulley motion will be specified and the carriage will follow. Operating in the period range where the displacement ratio is less then unity would result in a magnification of the carriage/specimen motion. This magnification continues to increase as the driving period decreases until a peak is reached at the resonant period.

The resonant period depicted in Fig. (3.2.1.1) , is the fundamental resonant period. Other resonant periods exist theoretically at lower periods for each DOF of the system model. In the real system there are an infinite number of DOF's and therefore an infinite number of resonant periods. For this system the fundamental resonant period will

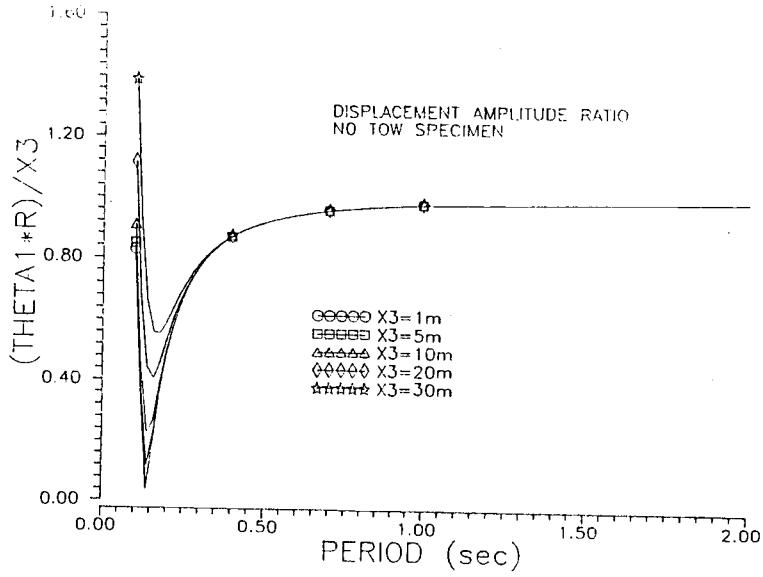

Figure 3.2.1.1a Displacement amplitude ratio response

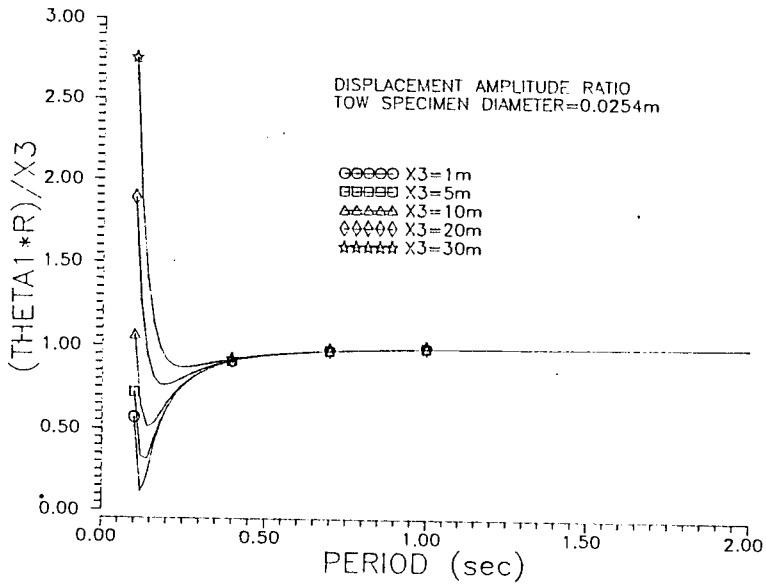

Figure 3.2.1.1b Displacement amplitude ratio response

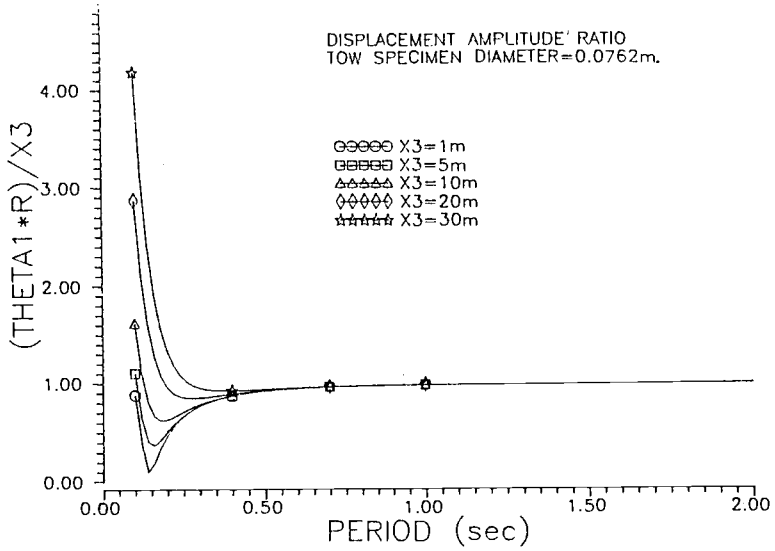

Figure 3.2.1.1c Displacement amplitude ratio response

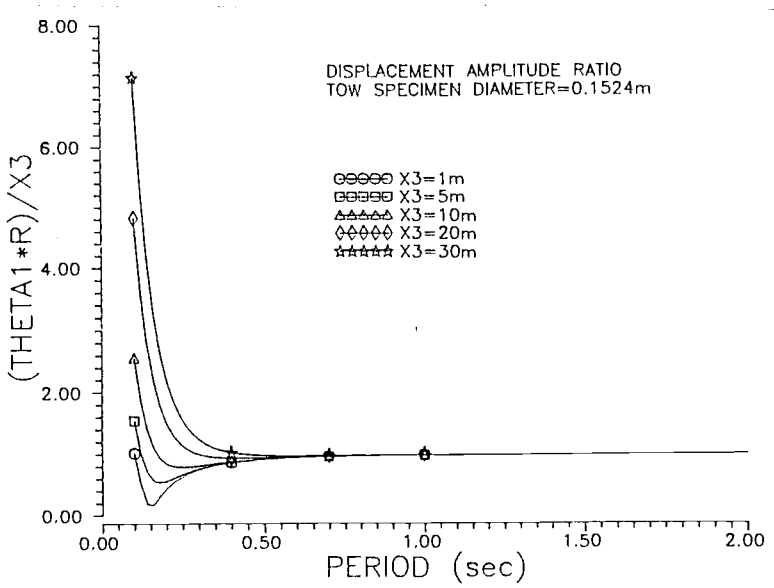

Figure 3.2.1.1d Displacement amplitude ratio response

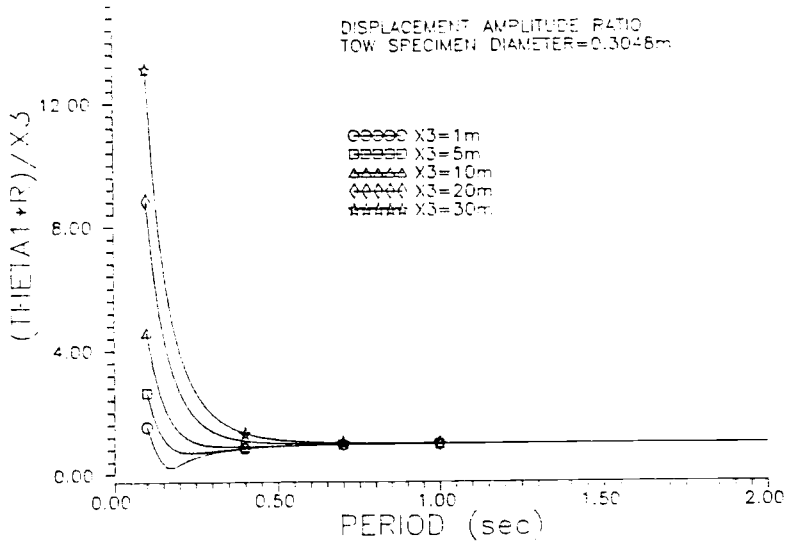

Figure 3.2.1.1e Displacement amplitude ratio response

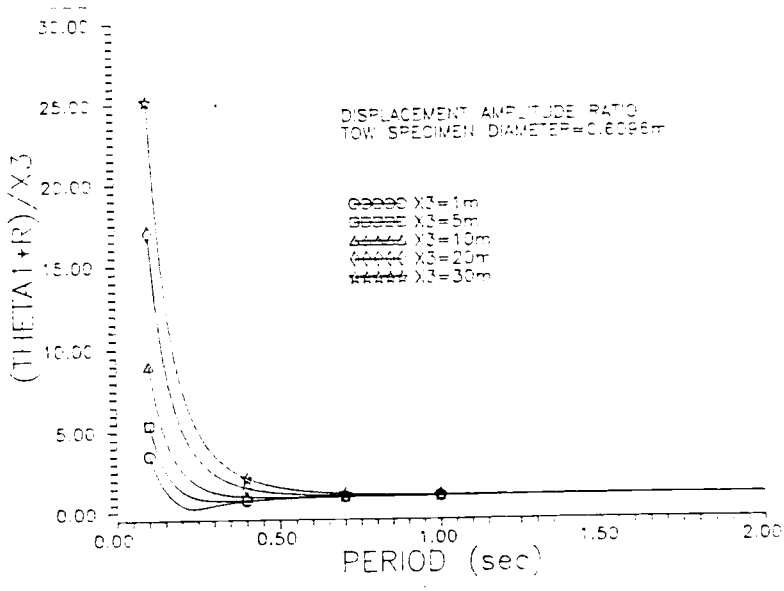

Figure 3.2.1.1f Displacement amplitude ratio response

produce the greatest magnification. The fundamental resonance must be completely avoided in the real system or severe damage could result to both the tow carriage system and the existing wave channel. For the given operating period range the only way to avoid this condition is to drive the system at periods greater then the resonant period. For this reason the shorter resonant periods are not plotted here but are calculated and discussed in Section (3.3).

The fundamental resonant period ranges from approximately 0.15 seconds with no tow specimen to 0.25 seconds with the 0.6096 m diameter tow specimen. Equation (3.2.1.2) gives the resonant period for an undamped one DOF system. Since the carriage/specimen mass dominates the other masses of the system and damping has only a second order effect on resonance this equation can approximate the fundamental resonant period. Using the structural mass of the carriage for m and the linear spring rate of the wire rope model Equation (3.2.1.2) predicts a fundamental resonant period of 0.12 seconds. This value is in good agreement with the damped responses in Fig. (3.2.1.1).

$$\tau_{res} \simeq 2\pi \mathrm{SQRT}(m/k) \qquad (3.2.1.2)$$

The stiffness k is a constant and the mass m varies with specimen size. This would indicate a slight increase in the resonant period as the specimen diameter increased . This trend is present in the response curves of Fig. (3.2.1.1).

The amount of magnification at resonance is a function of the damping present in the system, specifically the damping associated

with the carriage/specimen model c_{eff}. Larger damping reduces the magnification of the carriage/specimen motion. The damping coefficient c_{eff} increases with both specimen diameter and tow velocity as discussed in Section (2.3). For a given diameter the peak velocity of the specimen increases with half stroke X_3 thus increasing the damping with reduced magnification.

For a given half stroke X_3 the damping increases with tow specimen diameter. This can be seen in the response by decreasing magnification at resonance. In fact for diameters 0.0254 m and greater no magnification occurs at resonance. This can be interpreted as the wire rope model between the driver pulley and the carriage stretching which causes large displacement of the driver relative to the carriage.

The phase angle of the driver pulley displacement relative to the carriage/specimen displacement can be seen in Fig. (3.2.1.2). For periods much greater then resonance the driver is in phase , zero phase angle, with the carriage and damping has a very small effect on the response. As the period of oscillation decreases and approaches resonance the phase angle or difference approaches 90 degrees. The damping of the system affects the approach to resonance. Small damping maintains a near zero phase angle right up to resonance and then increases rapidly where as large damping produces a phase angle that reaches the resonant value more uniformly. At resonance the amount of damping present has no effect on the phase angle. For periods shorter then resonance the damping again plays a significant role in determining the phase angle with small damping approaching a maximum of 180 degrees and large damping increasing just over 90 degrees.

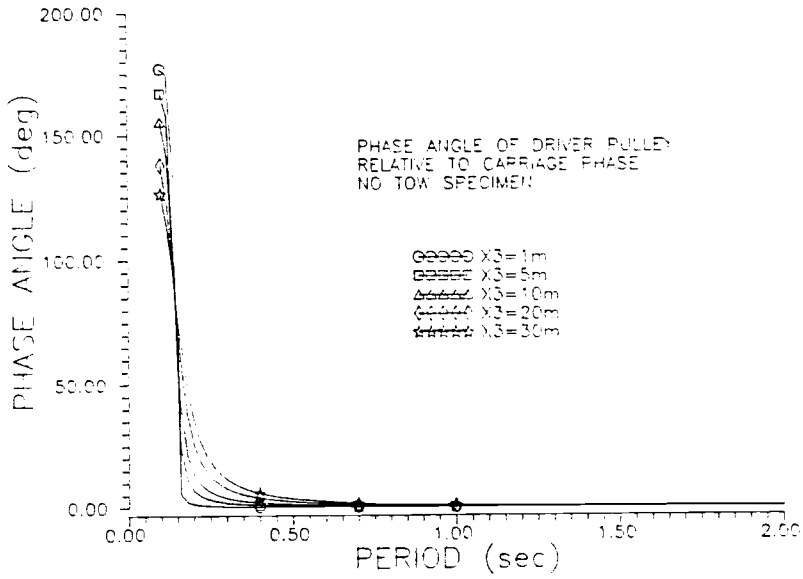

Figure 3.2.1.2a Driver phase response

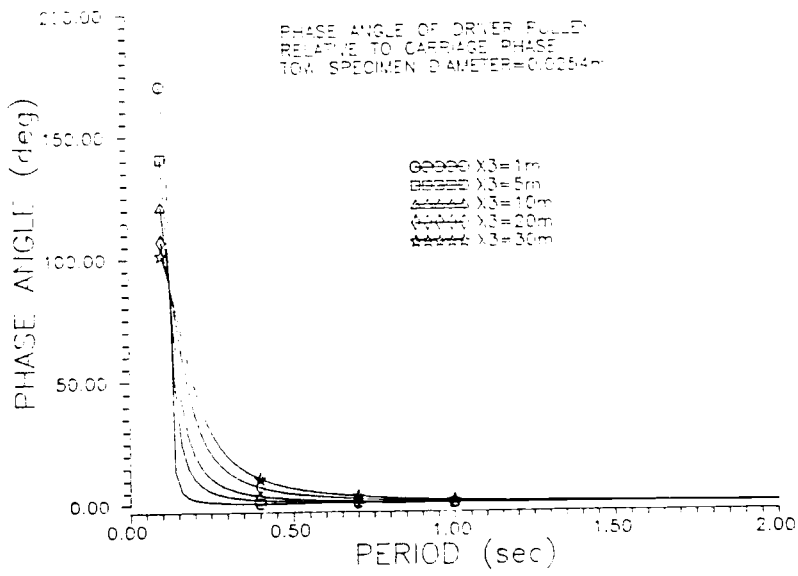

Figure 3.2.1.2b Driver phase response

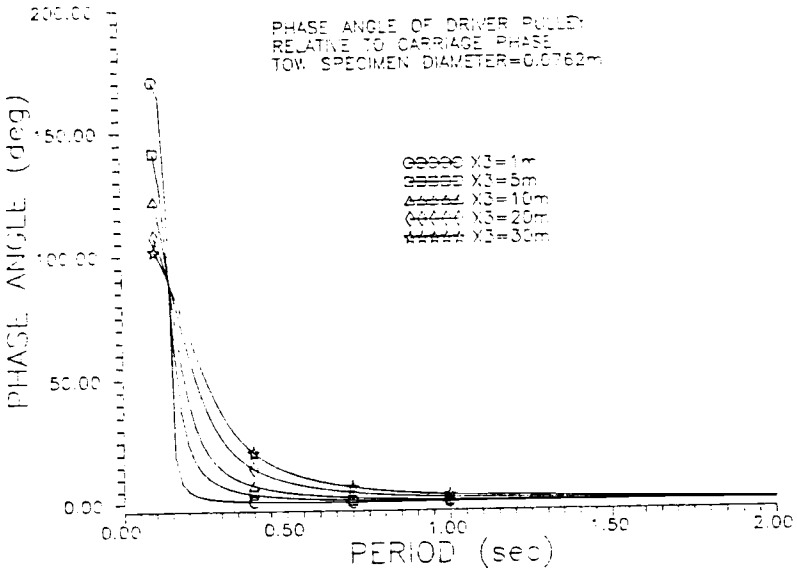

Figure 3.2.1.2c Driver phase response

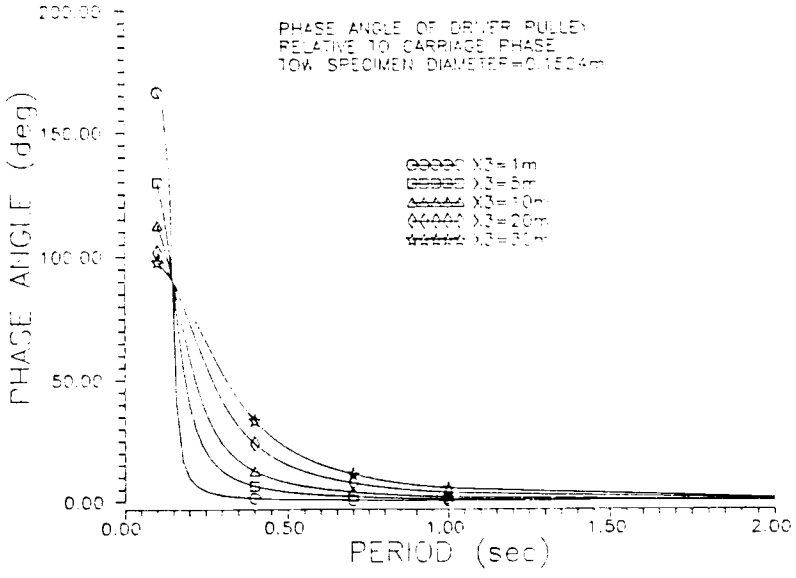

Figure 3.2.1.2d Driver phase response

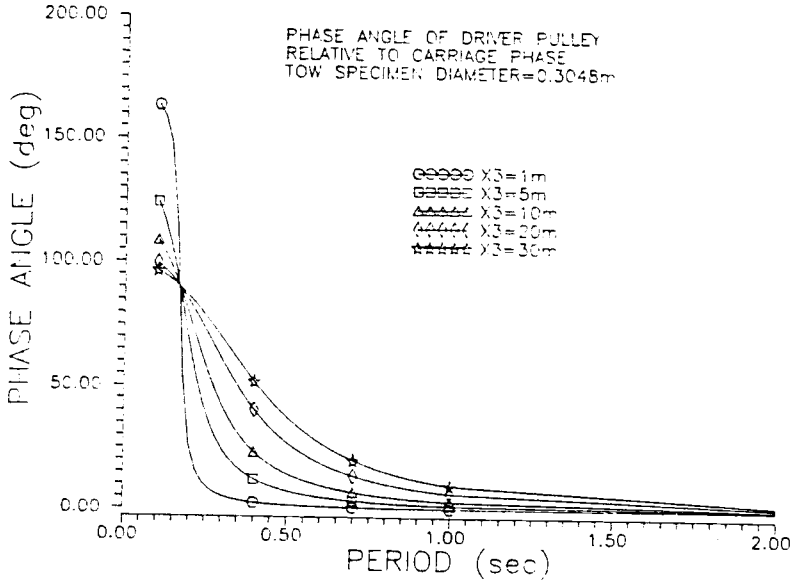

Figure 3.2.1.2e Driver phase response

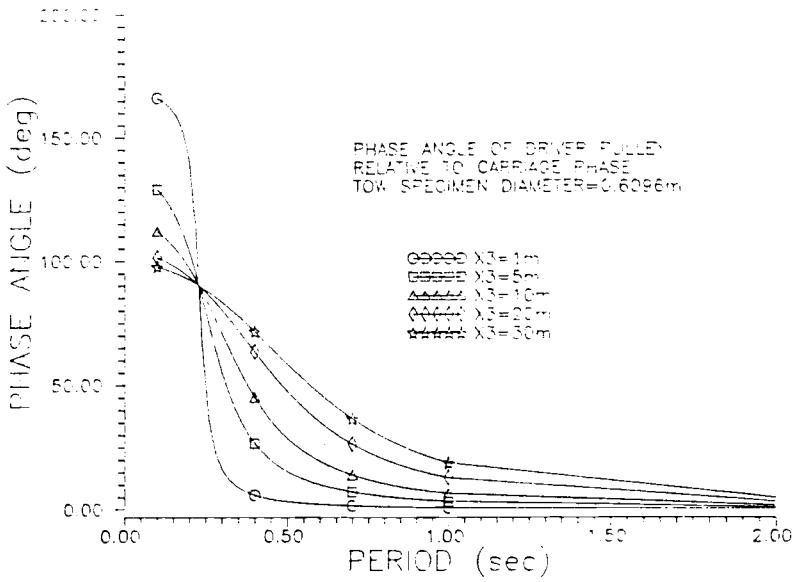

Figure 3.2.1.2f Driver phase response

Similar to the displacement modulus the phase angle response behaves like a single DOF system for periods greater than the fundamental resonance and for shorter periods the other DOF's become significant.

3.2.2 Dynamics

The linearized drag force of the tow specimen and supports can be seen in Fig. (3.2.2.1). Each family of curves responds inversely proportional to the square of the period approaching zero drag force at long periods and infinity as the period approaches resonance. The drag force is proportional to the velocity squared which is equal to $(\omega X_3)^2$. For the simulation with no tow specimen the cycle half stroke length X_3 has a small effect on drag for the larger periods with increasing significance as the period becomes shorter. This drag is due solely to the supports of the tow specimen. For larger tow specimens the half stroke length plays a stronger role in the drag for the entire range of periods.

The inertial force of the carriage/specimen model can be seen in Fig. (3.2.2.2). This response is similar to the linearized drag force and is inversely proportional to the square of the period. The inertial force is proportional to acceleration which is equal to $\omega^2 X_3$. The inertial force is not as sensitive to carriage half stroke as the drag force for the period range plotted because the inertial force is linearly proportional to X_3 while the drag force is proportional to the square of X_3. The inertial force family of curves for no tow specimen is due solely to the structural mass of the carriage. Increasing the

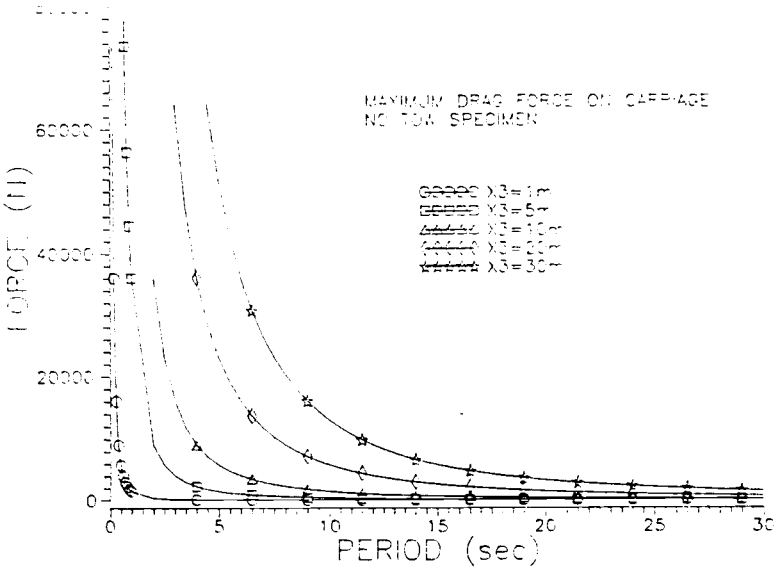

Figure 3.2.2.1a Drag force response

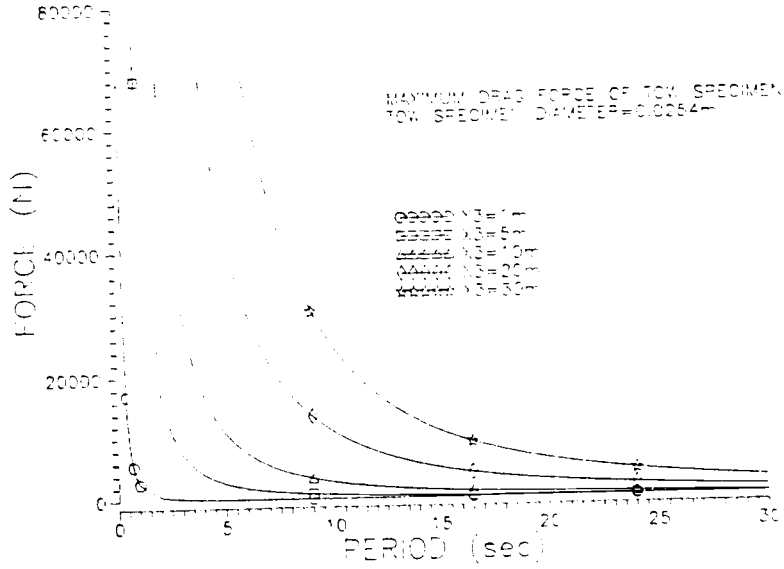

Figure 3.2.2.1b Drag force response

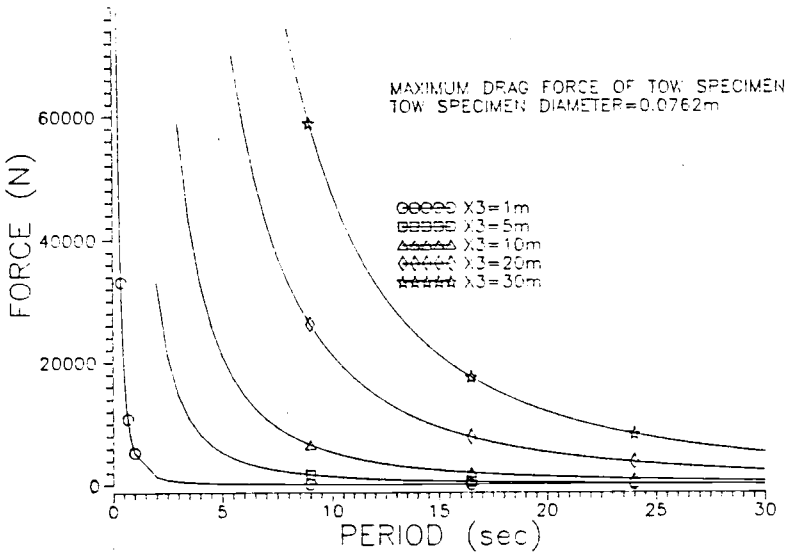

Figure 3.2.2.1c Drag force response

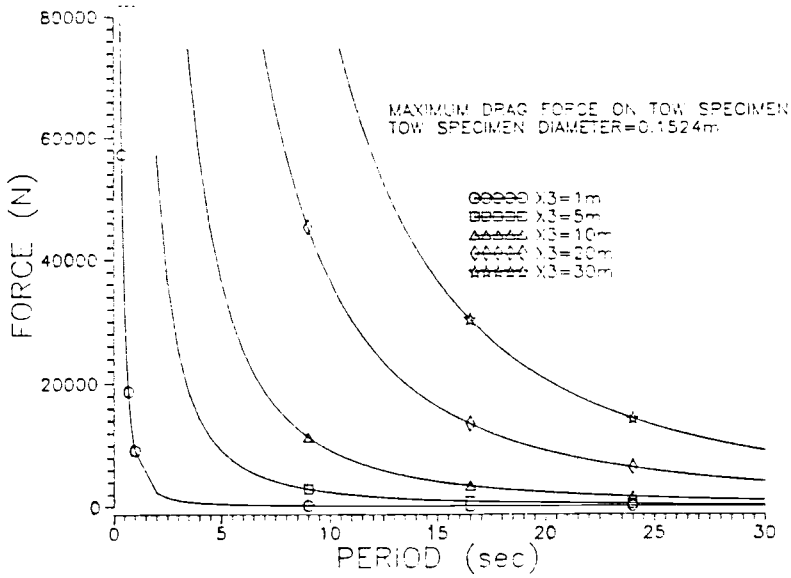

Figure 3.2.2.1d Drag force response

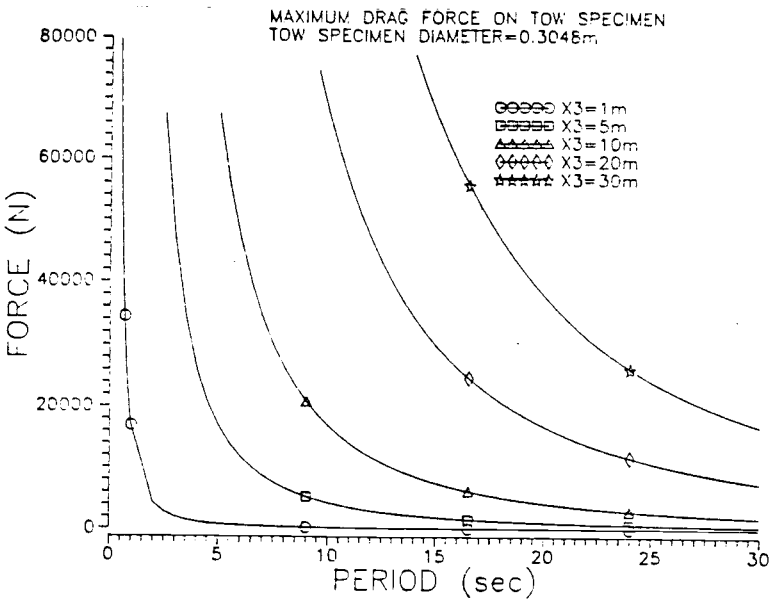

Figure 3.2.2.1e Drag force response

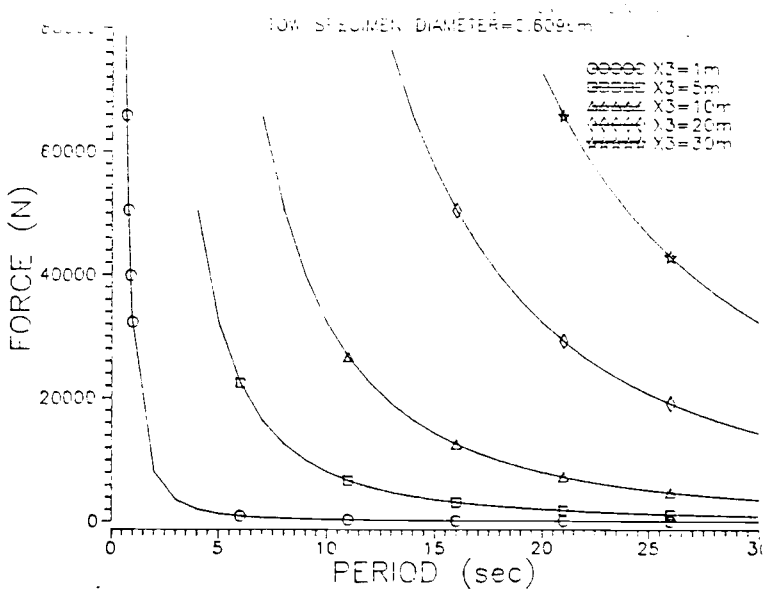

Figure 3.2.2.1f Drag force response

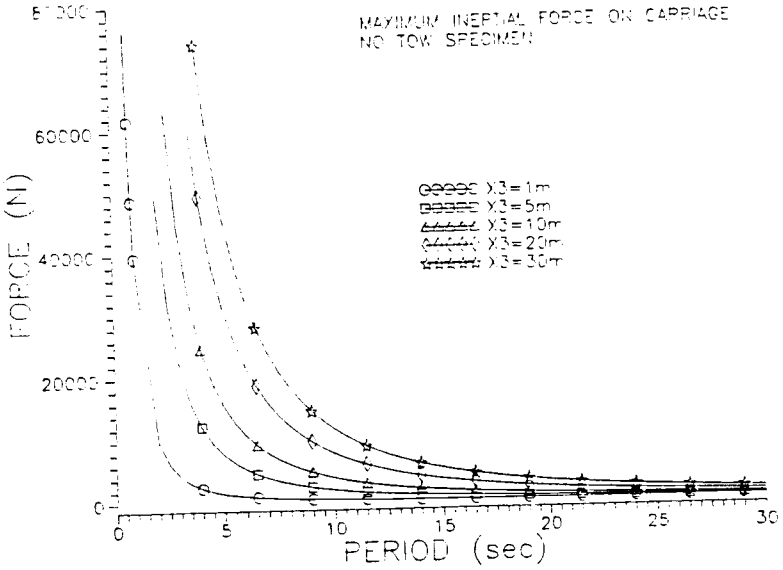

Figure 3.2.2.2a Inertial force response

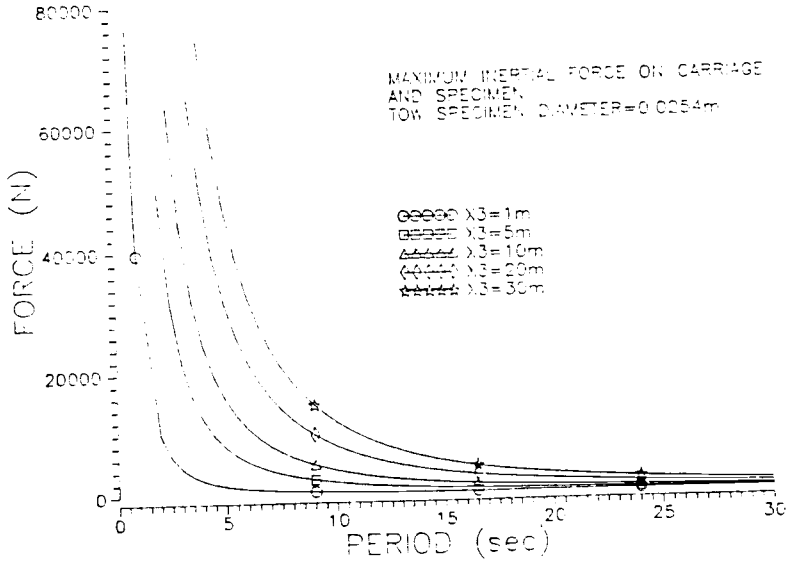

Figure 3.2.2.2b Inertial force response

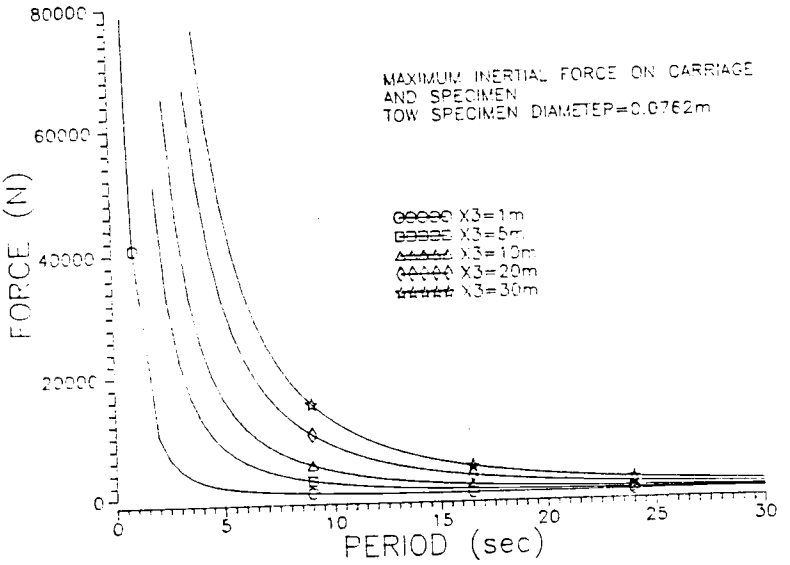

Figure 3.2.2.2c Inertial force response

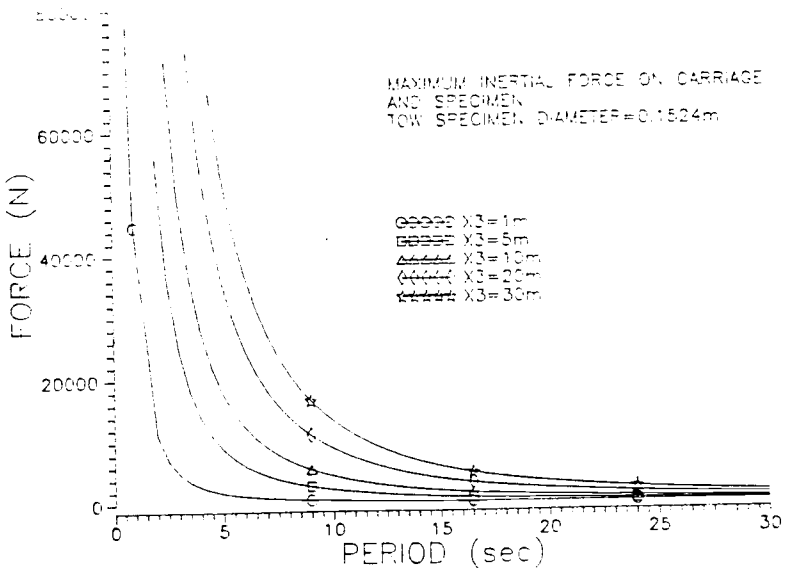

Figure 3.2.2.2d Inertial force response

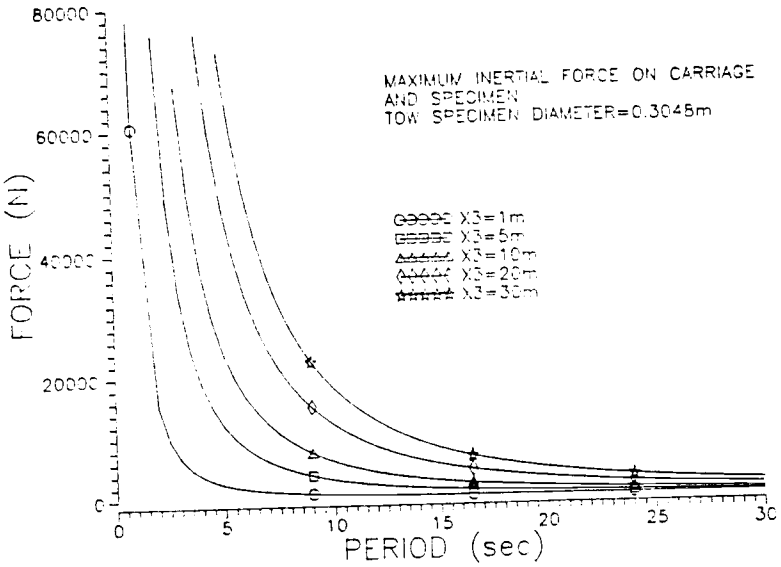

Figure 3.2.2.2e Inertial force response

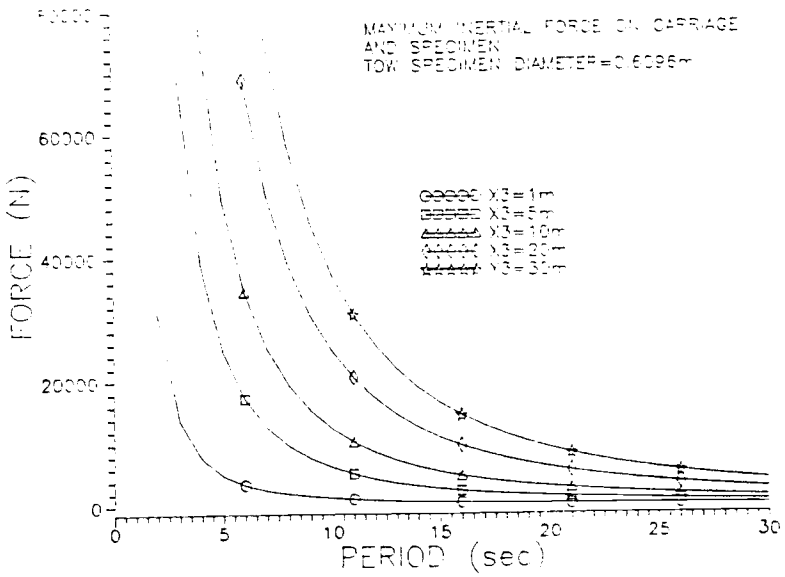

Figure 3.2.2.2f Inertial force response

tow specimen diameter increases the inertial force due to the added mass effect of the specimen interaction with the fluid.

The ratio of the linearized drag force to inertial force can be seen in Fig. (3.2.2.3) This ratio gives insight into which force is dominant for a particular simulation. With no tow specimen the system is inertially dominant for all but the 30 m half stroke implying that the inertial force of the carriage structure is larger than the drag due the specimen supports. As the tow specimen diameter is increased both the inertial and drag forces increase but the system becomes predominantly drag dominate for the larger half strokes. The response is a straight line because both forces have equal dependance on the period and only differ by a constant coefficient. The ratio of the coefficients is equal to the force ratio. The drag force coefficient is proportional to the frontal area of the tow specimen and hence the diameter. The inertial force is proportional to the volume of the tow specimen and hence the square of the diameter. The inertial force will thus dominate when the specimen diameter is significantly increased. This can be seen by comparing the force ratio of the 0.3048 m and 0.6096 m diameter simulations. The later simulation shows a slight decrease in the force ratio for a given half stroke. Note that for the cylinder diameters of interest the drag force is generally dominant.

The drive torque required to propel the carriage/specimen model at the specified kinematics is plotted in Fig. (3.2.2.4). Since the drive torque is a linear combination of both the drag and inertial forces of the system it also is inversely proportional to the square of the period. Similar to the drag and inertial forces, the drive

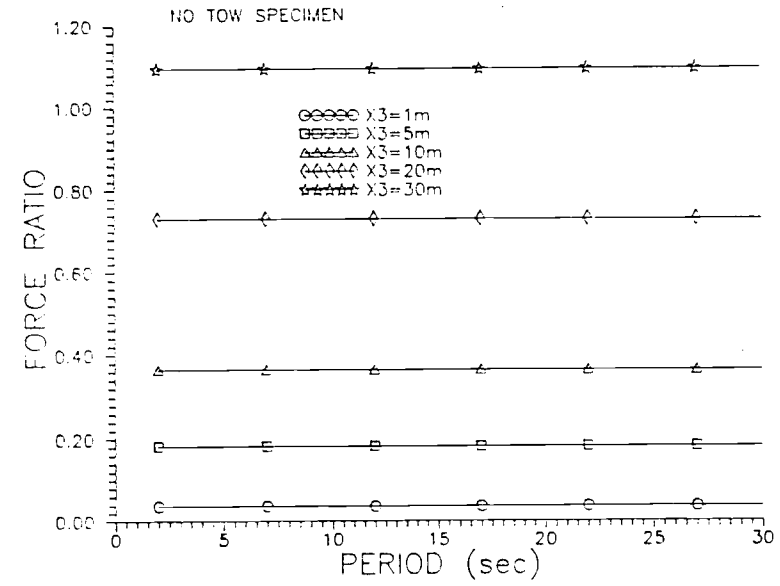

Figure 3.2.2.3a Force ratio response

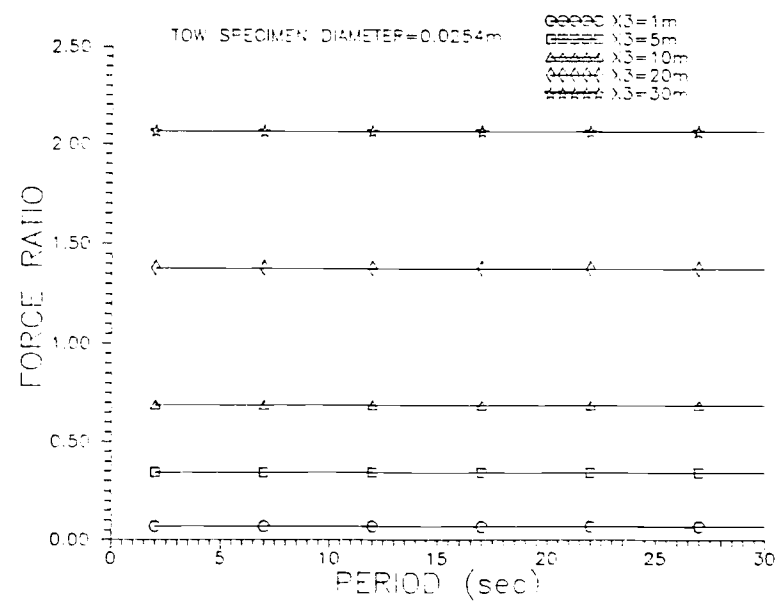

Figure 3.2.2.3b Force ratio response

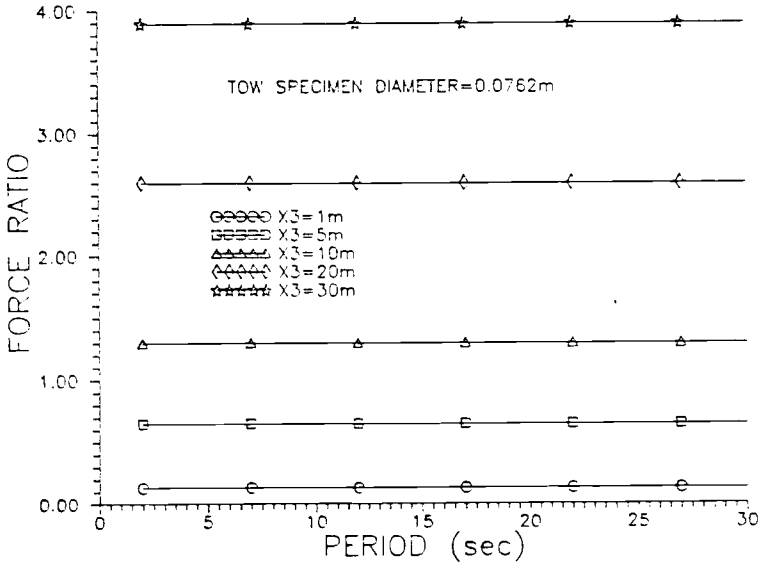

Figure 3.2.2.3c Force ratio response

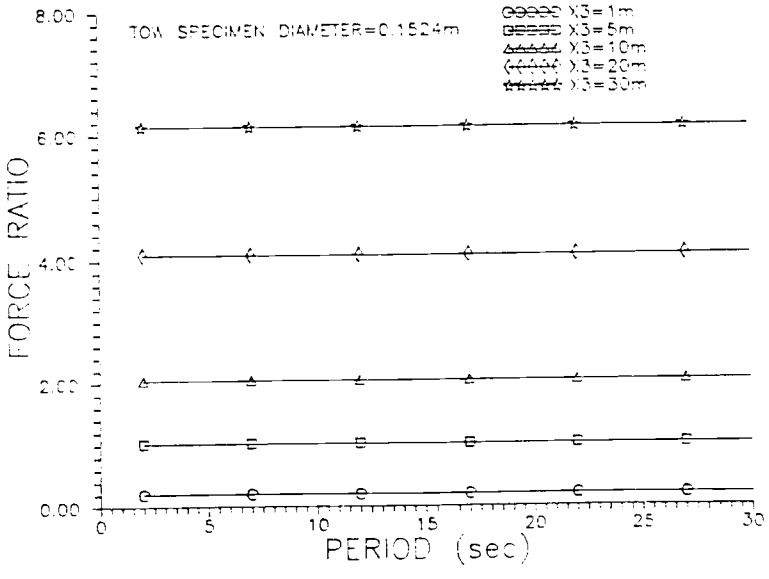

Figure 3.2.2.3d Force ratio response

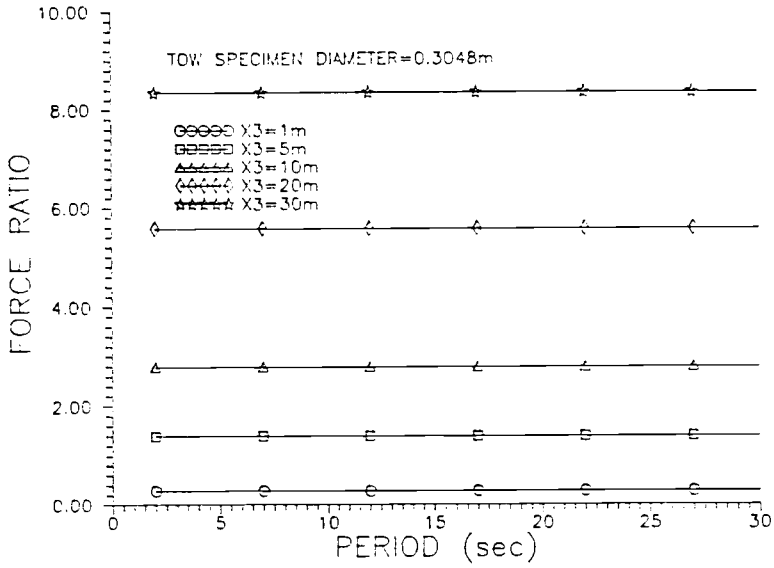

Figure 3.2.2.3e Force ratio response

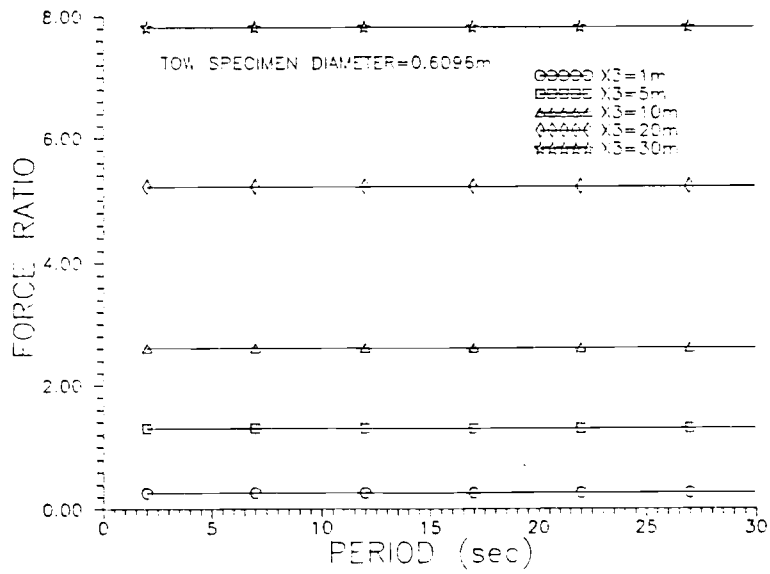

Figure 3.2.2.3f Force ratio response

torque also increases with both the carriage half stroke and tow specimen cylinder diameter.

The phase angle of the drive torque relative to the carriage/specimen displacement is plotted in Fig. (3.2.2.5). This phase angle is quite linear and constant for periods greater than resonance. As resonance is approached the phase angle abruptly reaches 180 degrees and then drops. The steady state value depends on the dominant force of the system. For inertially dominant simulations the torque phase angle is near 180 degrees out of phase with the carriage/specimen displacement. This corresponds to acceleration being 180 degrees out of phase with displacement. As the simulation becomes more drag dominant at larger tow specimen diameters, the torque phase angle approaches 90 degrees with a minimum of 100 degrees for the diameter range plotted. This corresponds to the velocity being 90 degrees out of phase with displacement.

The average power required based on the linearized drag force is plotted in Fig. (3.2.2.6). This power is calculated from Equation (2.3.32). From the response of the driver pulley phase angle ϕ_1, previously discussed, the phase angle was found to be very near zero except at resonance. Since the real system is not going to be operated near resonance the corresponding resonant power requirement is not of interest. Noting that ϕ_1 can be set equal to zero in Equation (2.3.32) which when expressed in terms of the driving period, reduces to

$$P_{ave}=\pi/\tau \ |T_D||\theta_1|\sin(\phi_T) \qquad (3.2.2.1)$$

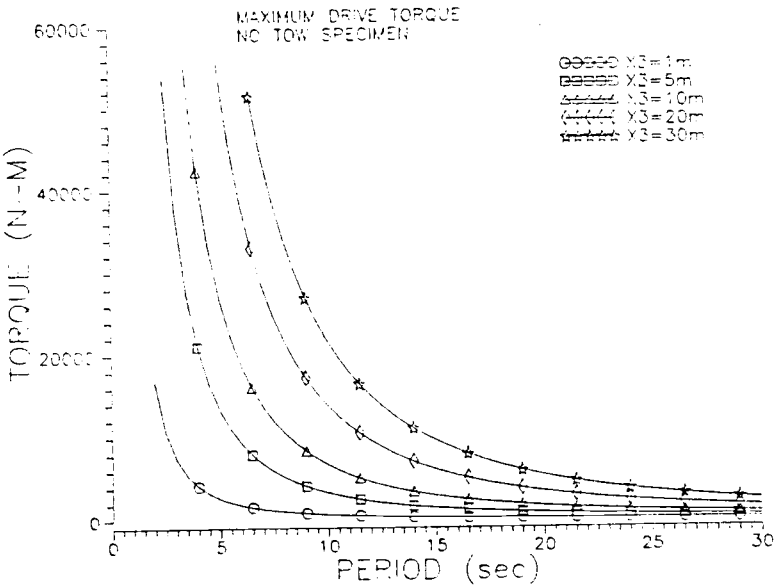

Figure 3.2.2.4a Drive torque response

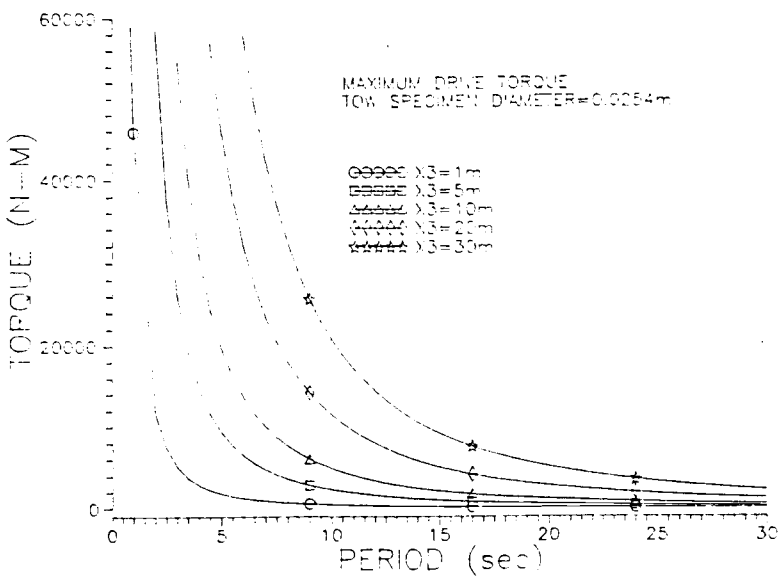

Figure 3.2.2.4b Drive torque response

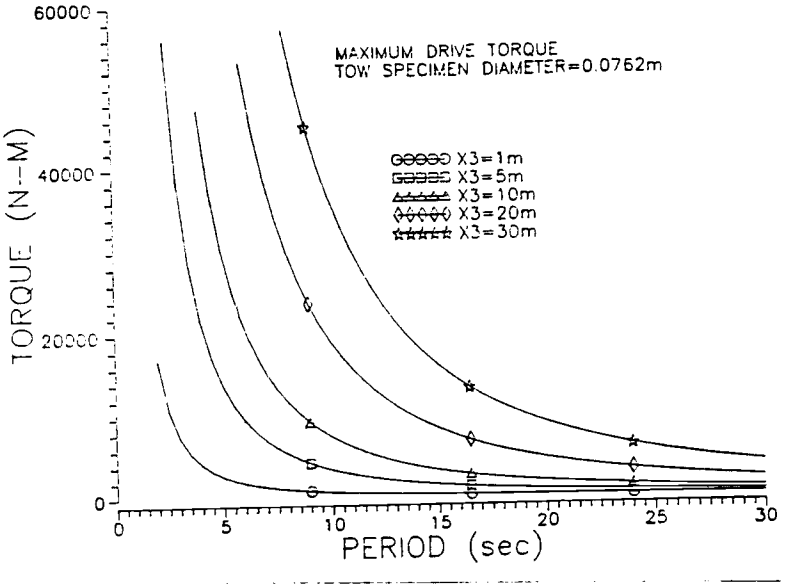

Figure 3.2.2.4c Drive torque response

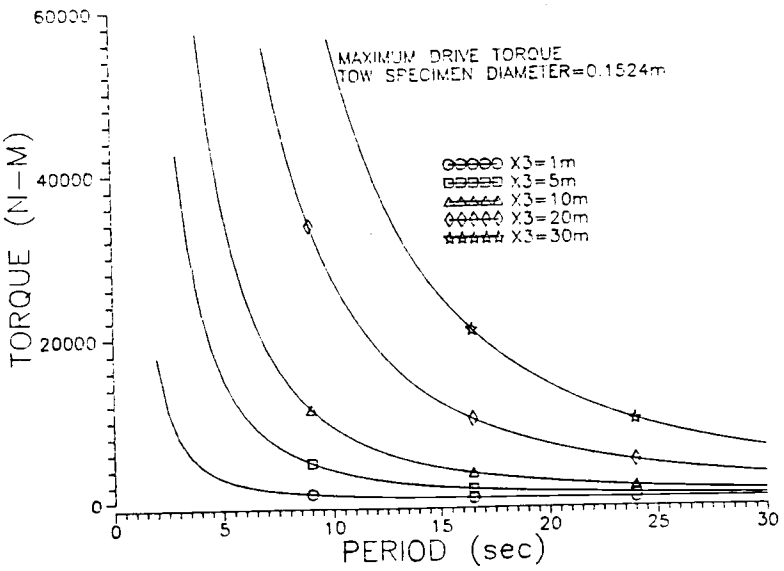

Figure 3.2.2.4d Drive torque response

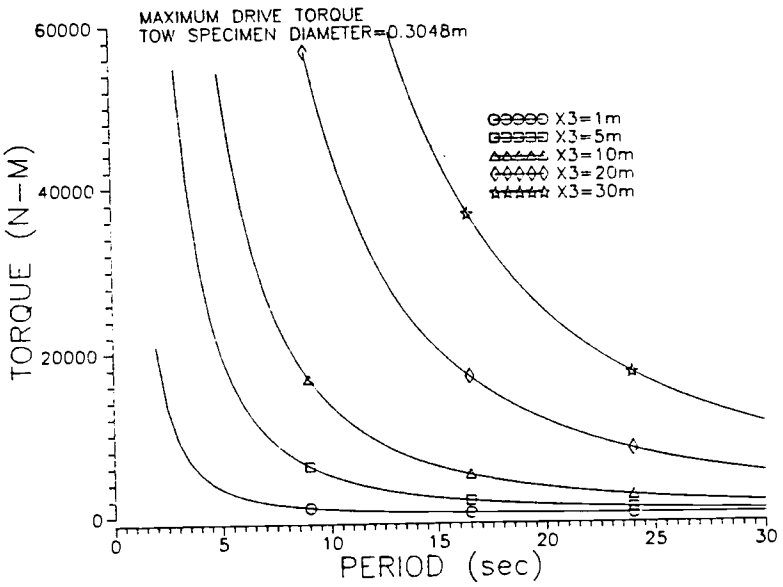

Figure 3.2.2.4e Drive torque response

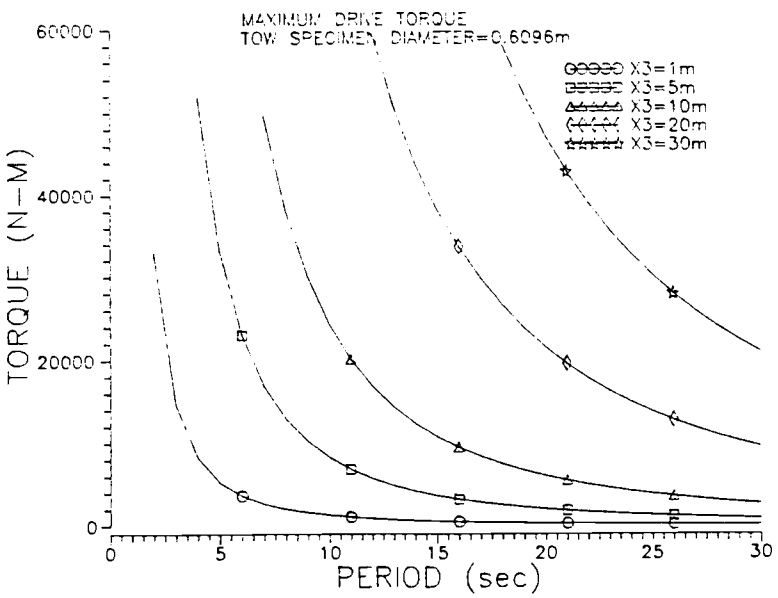

Figure 3.2.2.4f Drive torque response

With the drive torque T_D being inversely proportional to the square of the period τ the average power is inversely proportional to the cube of the period. Also note it is directly proportional to the sine of the drive torque phase angle. The strong dependence on the period can be seen in the steepness of the response curve at short periods. For simulations that are inertially dominant and hence have a drive torque phase angle near 180 degrees the average power is small due to the dependence on sine. Physically this caused by low energy dissipation. Most of the energy input to the system oscillates between potential energy stored in the springs and kinetic energy of the masses. Thus, for this nearly undamped simulation, the average power is low. As damping or drag is increased more energy is dissipated in a non-conservative manner and the torque phase angle decrease from near 180 degrees thus increasing the average power prediction.

The maximum power based on the linearized drag force can be seen in Fig. (3.2.2.7). This response was calculated from Equation (2.3.33) which can be reduced in a similar manner to the average power yielding

$$P_{max}=\pi/\tau\,|T_D|\,|\theta_1|\,[\sin(\phi_T)+1] \qquad (3.2.2.2)$$

This response is quite similar to the average power except at a torque phase angle of 180 degrees the maximum power is not zero,as is the average power. This is due to the large spring rate of the wire rope model which causes the energy to be stored at a high force and low deformation over a short time span thus yielding large power requirements.

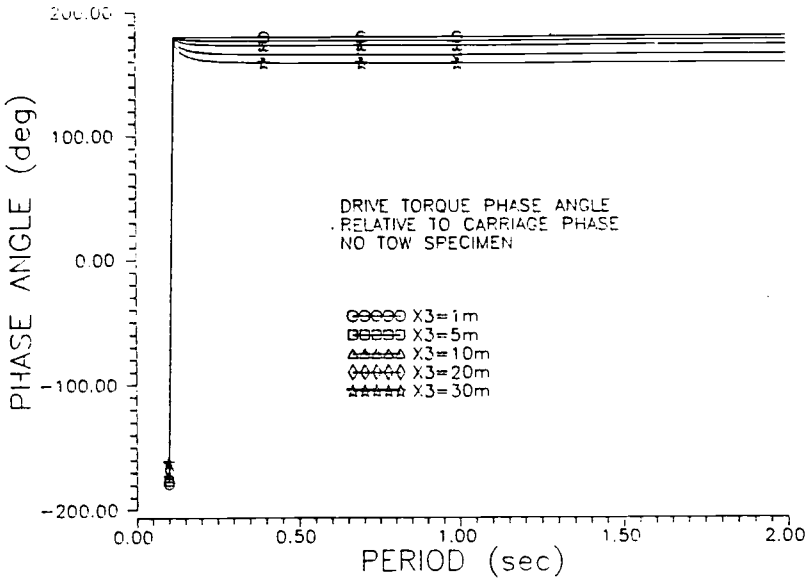

Figure 3.2.2.5a Drive torque phase response

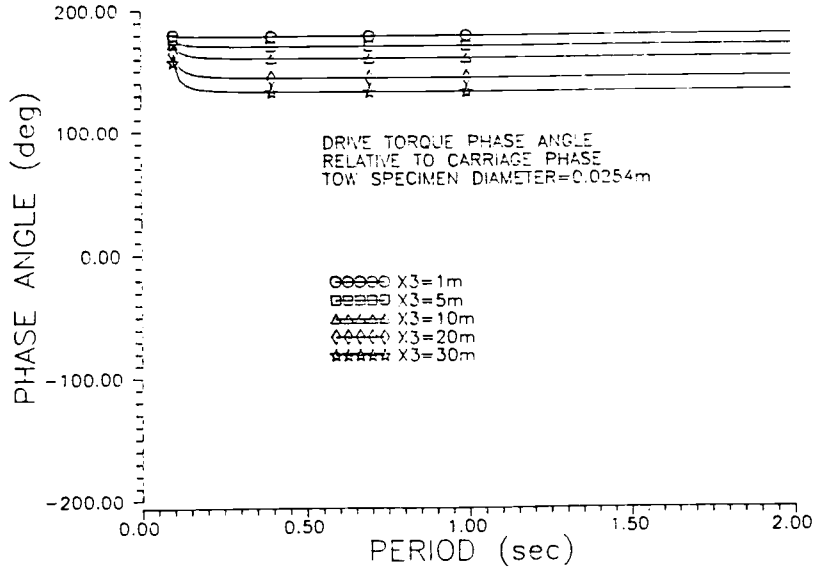

Figure 3.2.2.5b Drive torque phase response

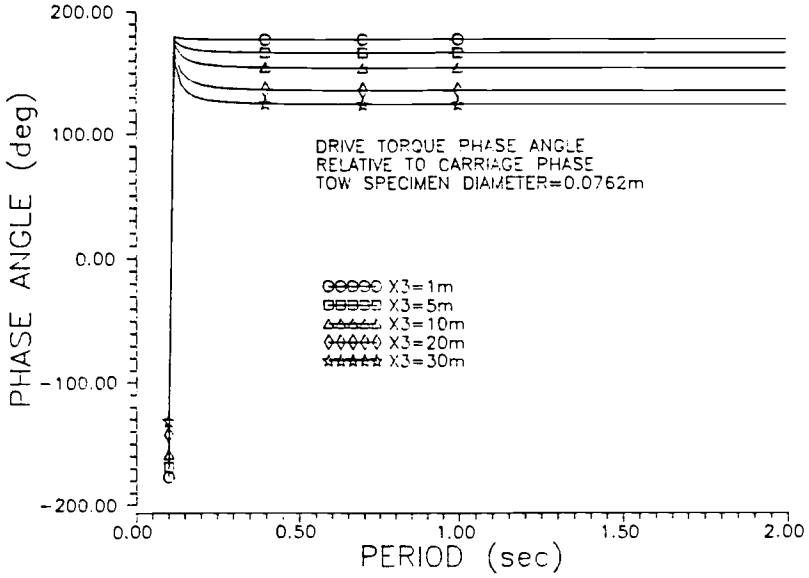

Figure 3.2.2.5c Drive torque phase response

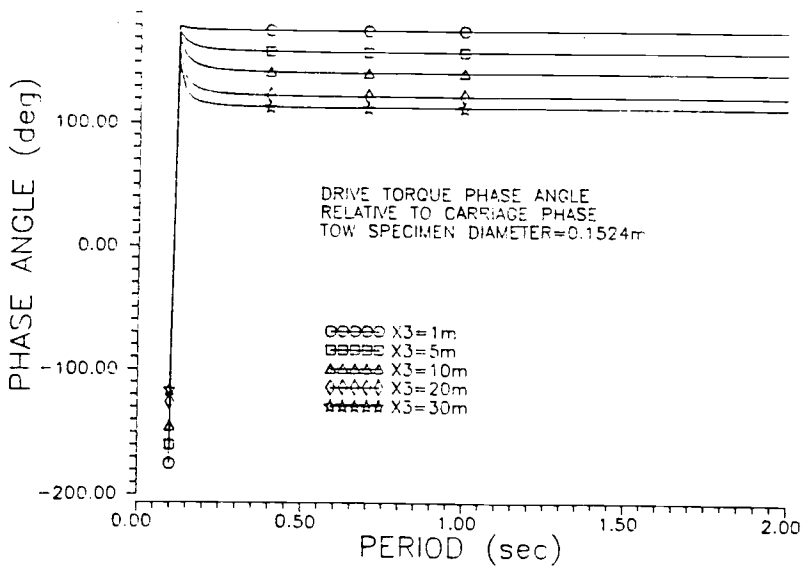

Figure 3.2.2.5d Drive torque phase response

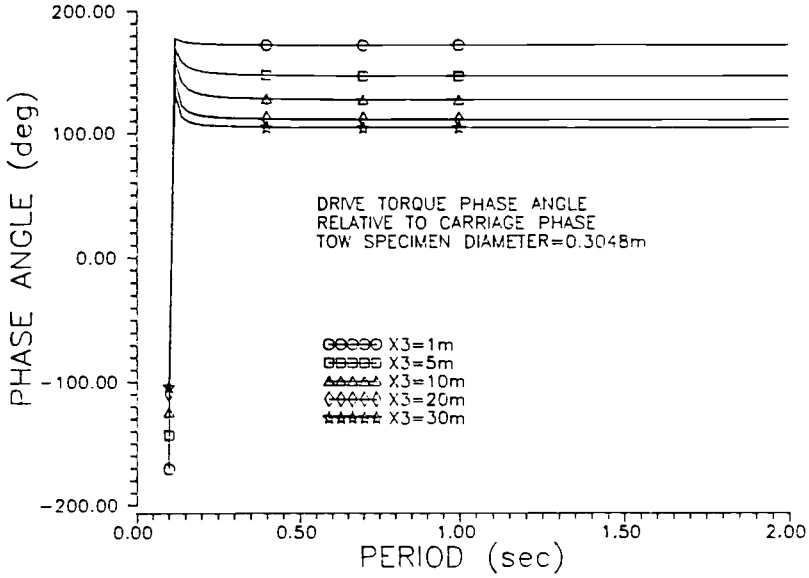

Figure 3.2.2.5e Drive torque phase response

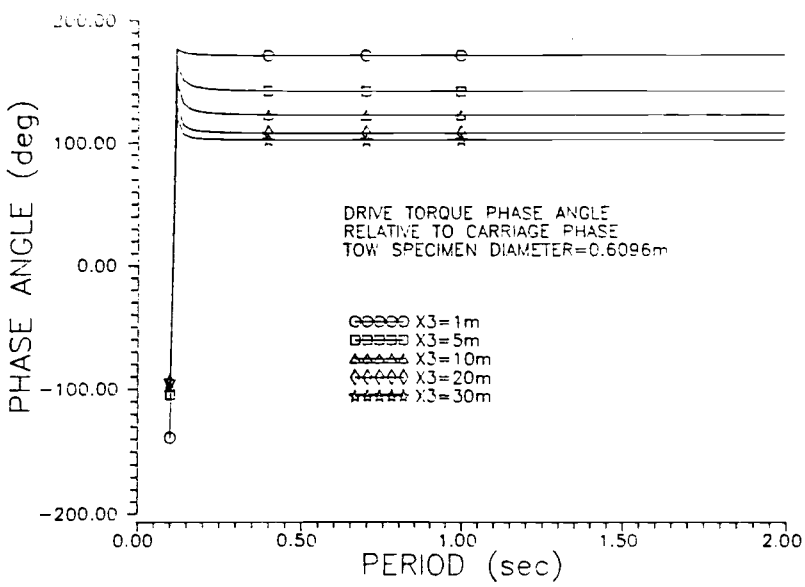

Figure 3.2.2.5f Drive torque phase response

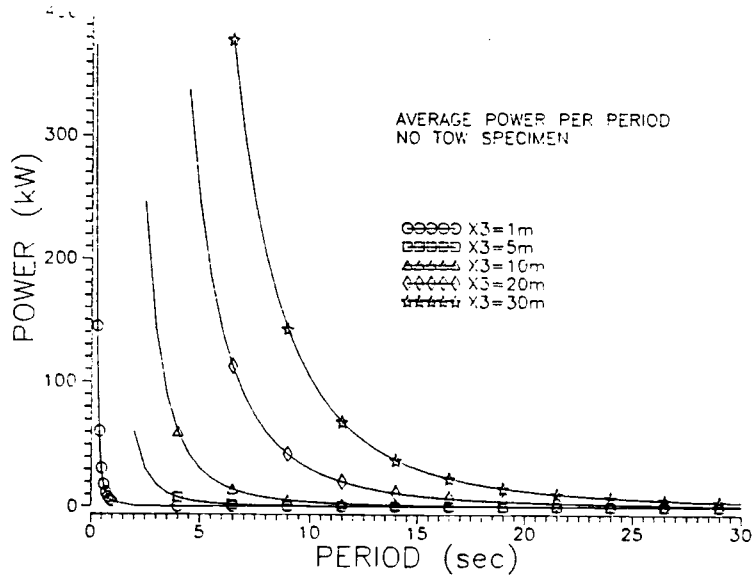

Figure 3.2.2.6a Average power response

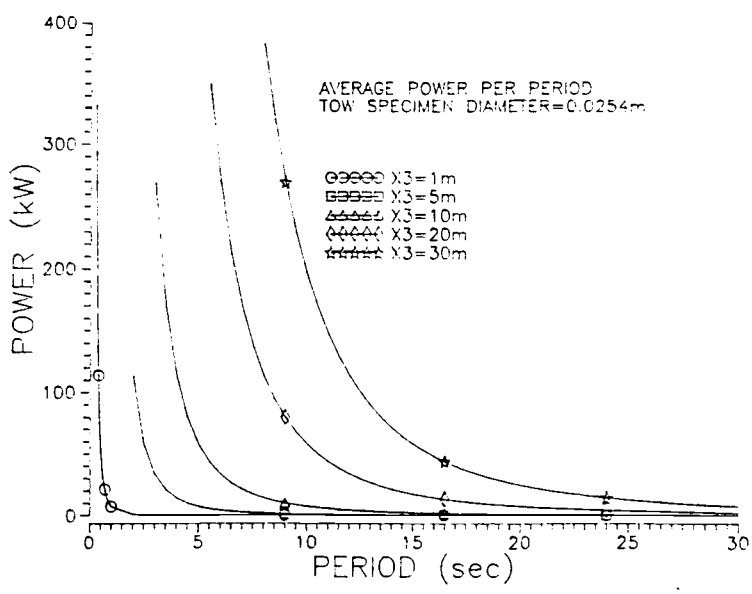

Figure 3.2.2.6b Average power response

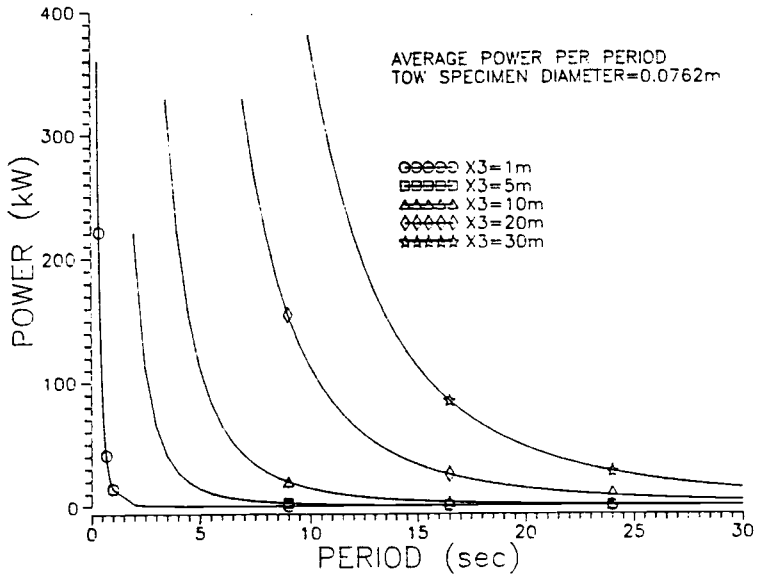

Figure 3.2.2.6c Average power response

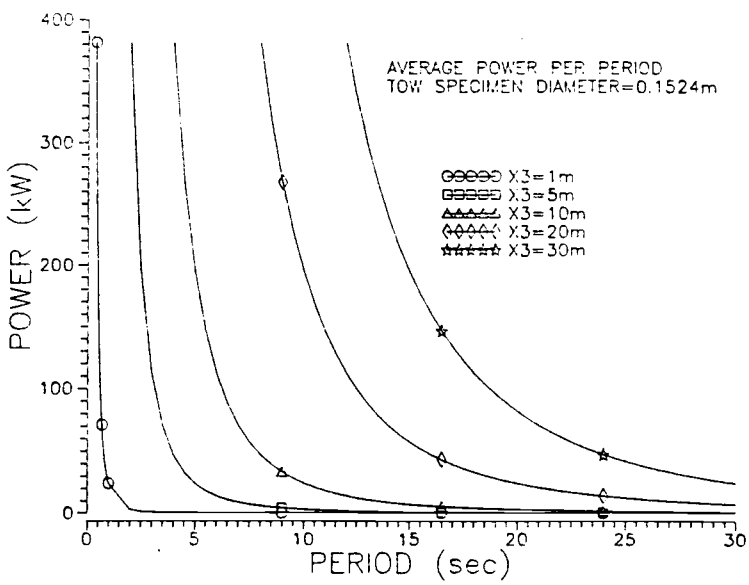

Figure 3.2.2.6d Average power response

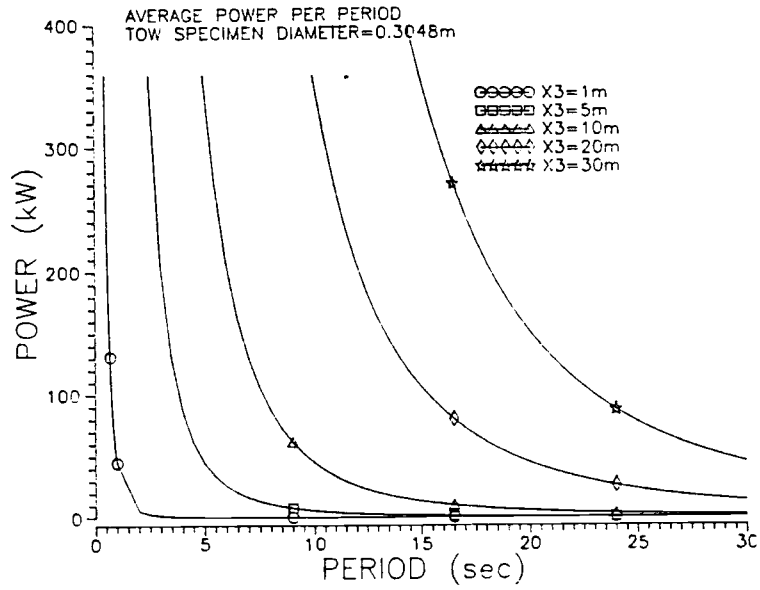

Figure 3.2.2.6e Average power response

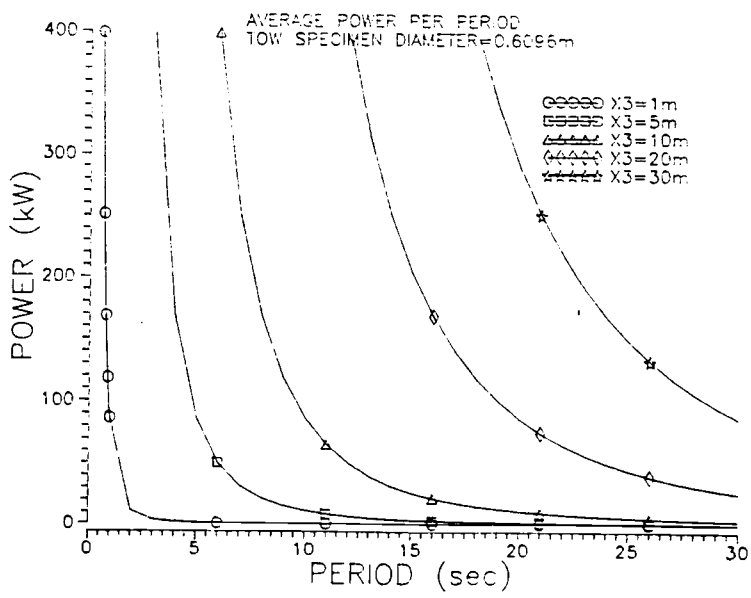

Figure 3.2.2.6f Average power response

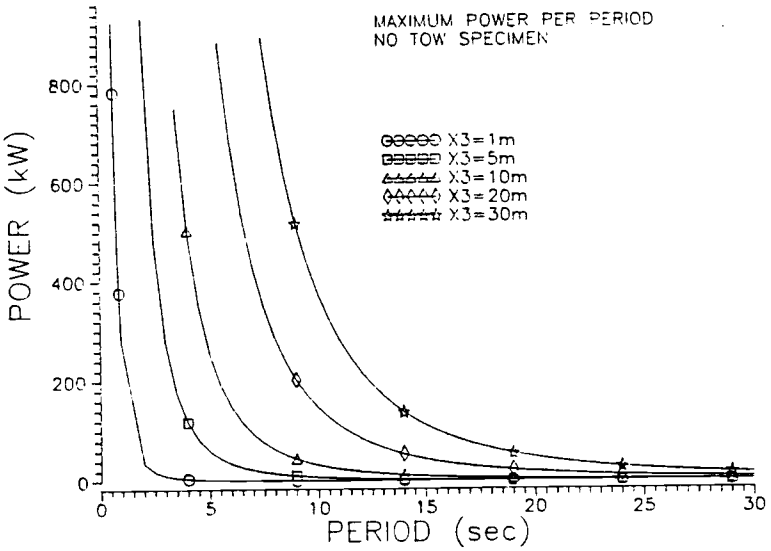

Figure 3.2.2.7a Maximum power response

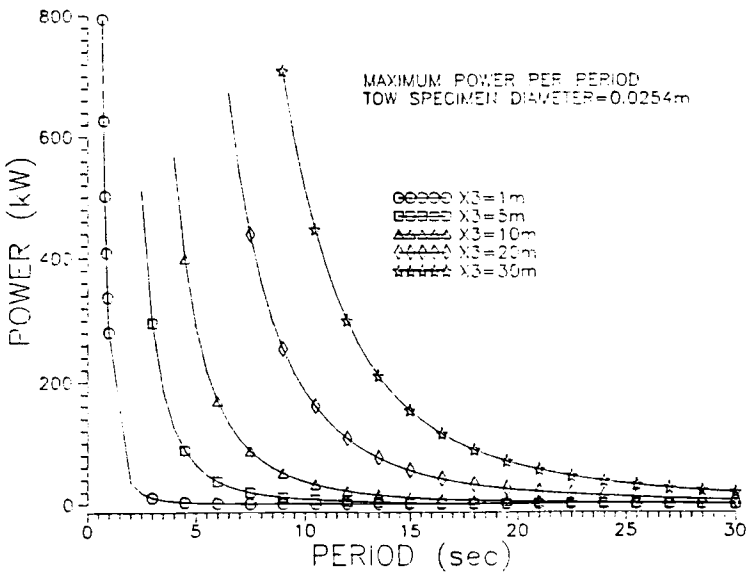

Figure 3.2.2.7b Maximum power response

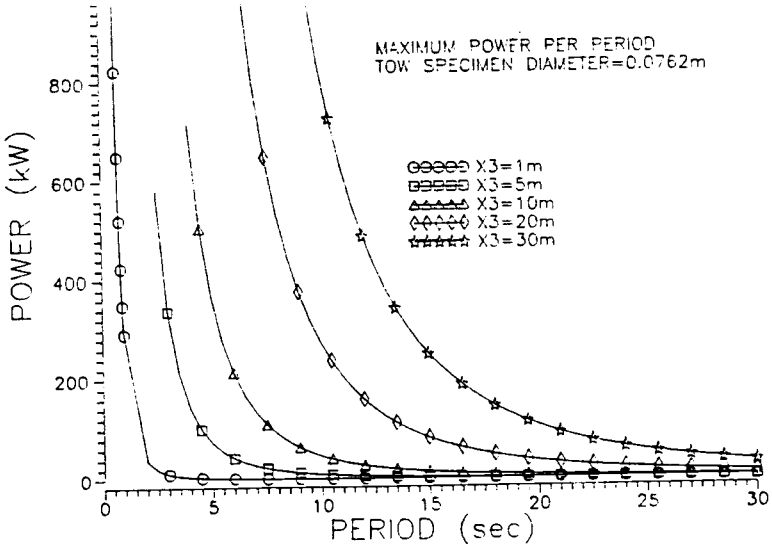

Figure 3.2.2.7c Maximum power response

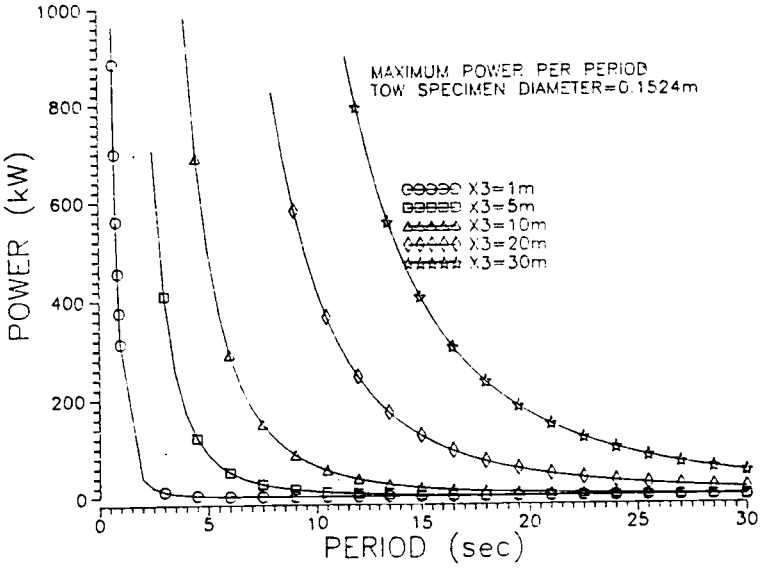

Figure 3.2.2.7d Maximum power response

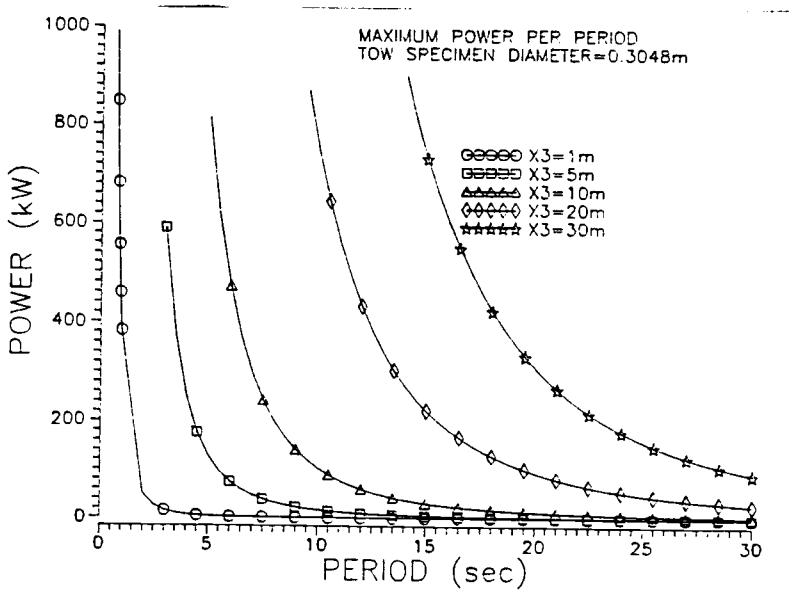

Figure 3.2.2.7e Maximum power response

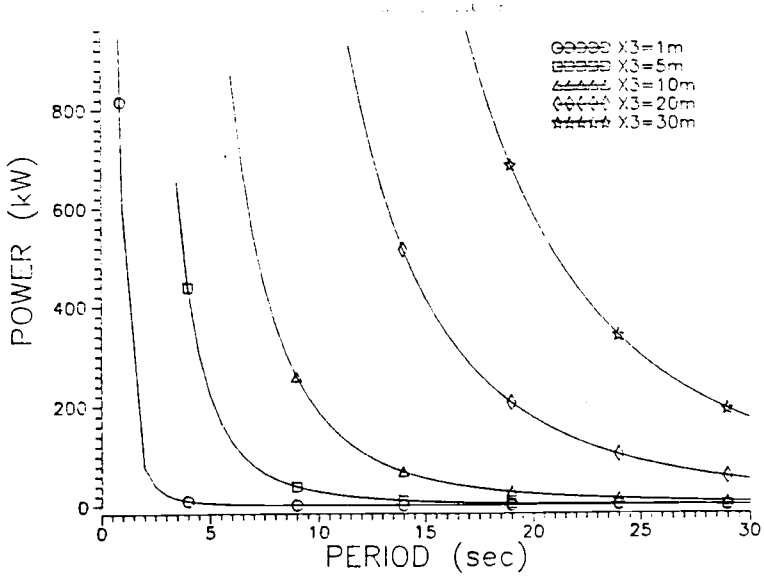

Figure 3.2.2.7f Maximum power response

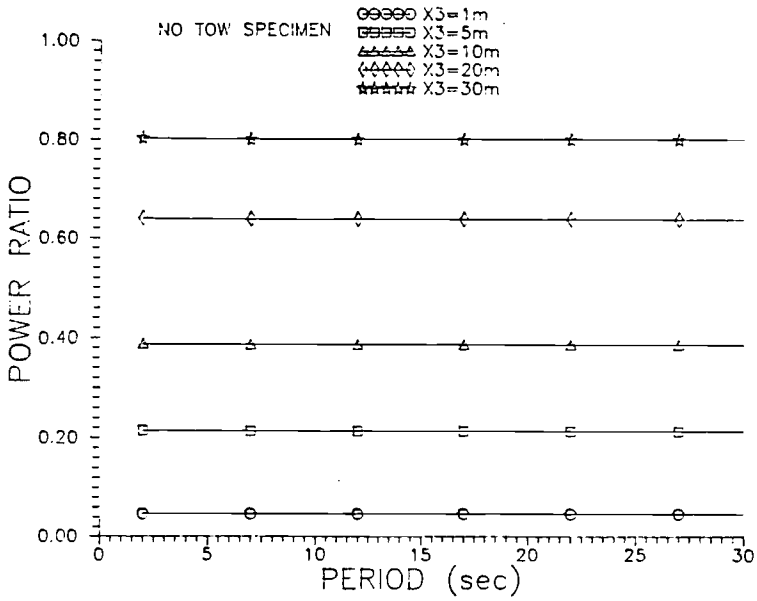

Figure 3.2.2.8a Power ratio response

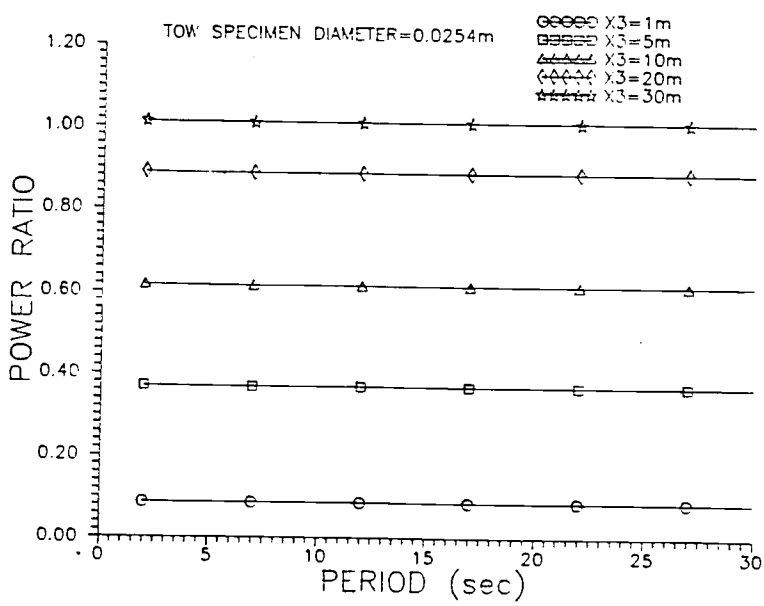

Figure 3.2.2.8b Power ratio response

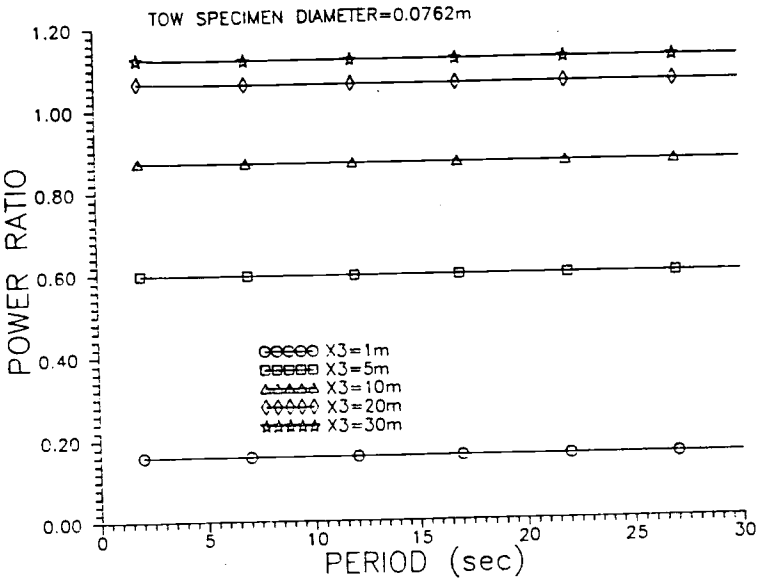

Figure 3.2.2.8c Power ratio response

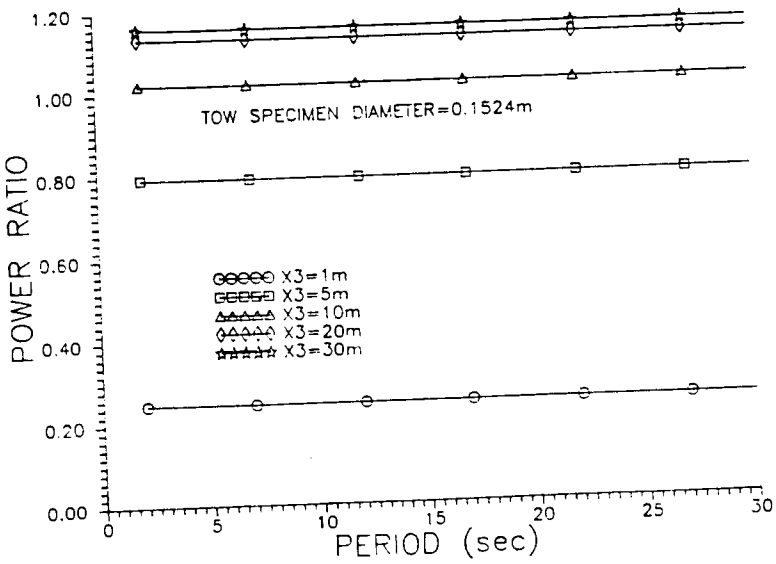

Figure 3.2.2.8d Power ratio response

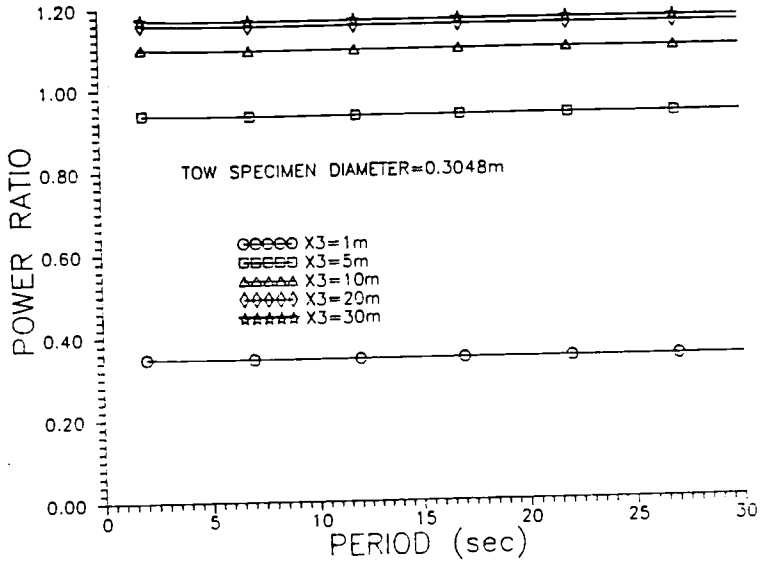

Figure 3.2.2.8e Power ratio response

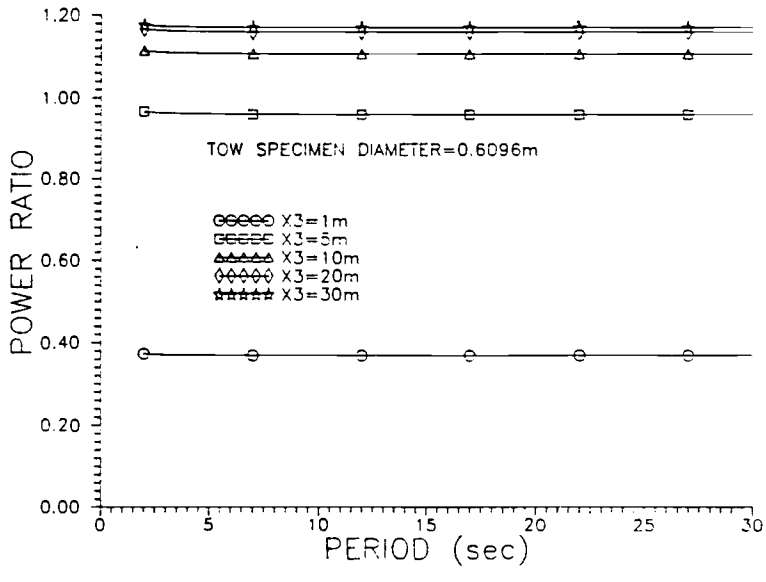

Figure 3.2.2.8f Power ratio response

The ratio of maximum power based on the linearized drag force, Equation (2.3.33), to the maximum power based on the nonlinear drag force, Equation (2.3.35), is plotted in Fig. (3.2.2.8). Equation (2.3.35) when expressed in terms of the driving period yields

$$P_D=4\pi^3\rho C_d A(|X_3|/\tau)^3 \qquad (3.2.2.3)$$

Both Equation (2.3.33) and Equation (2.3.35) have an inverse period cubed dependence and thus their ratio is a straight line. This parameter is used to give an indication as to which Equation, (2.3.33) or (2.3.35), will give the best indication of maximum power requirements. If the ratio is less than or equal to one then Equation (2.3.33) is probably the better of the two. If the ratio is significantly larger than one then Equation (2.3.35) will give better results. As can be seen in the figures the linearized power equation should work well for the applications investigated.

3.2.3 Maximum Performance Selection

Figures (3.2.1.1) through (3.2.2.8) represent various performance responses of the system model. Both the half stroke and tow cylinder diameter ranges are good representations of the anticipated use of the dynamic tow carriage. Not all of the driving periods represent real system use. For a given half stroke and cylinder diameter the force and power requirements predicted by the model may not be achievable by the real system. With this in mind a minimum period, and hence maximum

performance, must be selected for each curve in order to be consistent with the real system.

The fundamental limiting criteria is the power requirement. Section (5.3) discusses in detail the sizing of the real system power train. It was found that a maximum power of 400 kW is a reasonable upper limit. A second limiting factor is the maximum drive torque. High torque loads can exist with low power requirements when carriage/specimen acceleration is large. Thus the maximum acceleration over a particular cycle must be limited. Since most of the experimental work to be done with the carriage will be to simulate gravity waves it is reasonable to limit the carriage/specimen acceleration to 9.81 m/s^2. When selecting the minimum drive period ,or maximum performance of a particular simulation,the maximum power is limited to 400 kW as long as the peak acceleration of the carriage/specimen model is less than or equal to 1g. If the acceleration exceeds 1g then the acceleration will be the limiting parameter. Table (3.2.3.1) is a summary of this selection process. All values represent the maximum performance over one cycle.

The maximum velocity of the carriage ranges from 3.1 m/s to 17.1 m/s with maximum acceleration ranging from 0.23 to 1 g. The maximum inertial force is near 10 kN with the exception of the largest specimen at 1 and 5 m half strokes which generates 30 kN inertial forces. The maximum drag force is on the average two to three times larger then the inertial force with a peak of 56 kN for the largest tow specimen at the 20 and 30 m half strokes. Even with the imposed power limit the system shows drag dominance. The maximum power has a ceiling of 400 kW and the

Table (3.2.3.1) Summary of Maximum Performance Selection.

τ_{min} (sec)	Specimen dia. (m)	X_3 (m)	limiting parameter	$\dot{X}_3$ (m/s)	$\ddot{X}_3$ (g's)	IF_{max} (kN)	DF_{max} (kN)	Fratio	P_{max} (kw)	P_{ave} (kw)	Pratio	T_D (kN-m)	ϕ_T (deg)	R_{eD}	KC_D
2.01	0.0254	1.00	acceleration	3.1	1.0	9.91	0.68	0.07	35.8	0.90	0.08	16.7	179	6.0E4	2.5E2
4.49		5.00	acceleration	7.0	1.0	9.78	3.36	0.34	77.7	9.96	0.38	16.7	172	1.4E5	1.2E3
6.34		10.00	acceleration	9.7	1.0	9.38	6.45	0.69	132	26.5	0.62	16.4	166	1.9E5	2.4E3
8.97		20.00	acceleration	14.0	1.0	9.78	13.4	1.4	253	79.7	0.90	18.6	153	2.7E5	4.9E3
11.0		30.00	acceleration	17.1	1.0	9.82	20.7	2.1	388	147	1.02	21.1	142	3.3E5	7.4E3
2.01	0.0762	1.00	acceleration	3.1	1.0	10.2	1.32	0.13	37.2	1.76	0.16	17.0	177	1.8E5	8.2E1
4.49		5.00	acceleration	7.0	1.0	10.1	6.5	0.64	99.8	19.4	0.60	17.3	166	4.1E5	4.1E2
6.34		10.00	acceleration	9.7	1.0	9.65	12.5	1.3	167	51.4	0.88	17.9	154	5.6E5	8.1E2
8.97		20.00	acceleration	14.0	1.0	10.1	26.1	2.6	374	155	1.06	23.6	135	8.1E5	1.7E3
12.82		30.00	max power	14.7	0.74	7.45	29.0	3.9	400	181	1.14	22.26	124	8.6E5	2.5E3
2.01	0.1524	1.00	acceleration	3.1	1.0	11.2	2.3	0.21	40.1	3.00	0.24	17.7	175	3.6E5	4.1E1
4.49		5.00	acceleration	7.0	1.0	11.1	11.3	1.0	122	33.5	0.80	18.9	159	8.1E5	2.1E2
6.34		10.00	acceleration	9.7	1.0	10.6	21.6	2.0	229	88.8	1.02	21.7	141	1.1E6	4.0E2
10.48		20.00	max power	12.0	0.73	8.15	33.3	4.1	400	164	1.14	24.5	121	1.4E6	8.3E2
15.07		30.00	max power	12.5	0.53	5.91	36.3	6.1	400	193	1.16	24.9	112	1.5E6	1.2E3
2.01	0.3048	1.00	acceleration	3.1	1.0	15.1	4.2	0.28	49.0	5.60	0.34	20.8	173	7.2E5	2.0E1
4.49		5.00	acceleration	7.0	1.0	14.9	20.8	1.4	175	61.6	0.96	32.1	148	1.6E6	1.0E2
6.34		10.00	acceleration	9.7	1.0	14.3	39.9	2.8	370	164	1.10	32.1	128	2.3E6	2.0E2
12.31		20.00	max power	10.2	0.53	8.00	44.5	5.6	400	193	1.16	30.3	111	2.4E6	4.1E2
18.34		30.00	max power	10.3	0.36	5.40	45.1	8.4	400	197	1.18	29.7	104	2.4E6	6.2E2
2.01	0.6096	1.00	acceleration	3.1	1.0	30.9	8.1	0.26	78.7	10.8	0.38	32.9	171	1.4E6	1.0E1
4.49		5.00	acceleration	7.0	1.0	30.6	39.8	1.3	307	118	0.96	40.9	142	3.3E6	5.2E2
8.29		10.00	max power	7.6	0.59	18.1	47.1	2.6	400	152	1.12	35.5	122	3.5E6	1.0E2
15.23		20.00	max power	8.3	0.35	10.7	55.7	5.2	400	195	1.18	37.2	108	3.9E6	2.1E2
22.73		30.00	max power	8.3	0.23	7.19	56.2	7.8	400	198	1.19	36.6	102	3.9E6	3.1E2

average power peaks at near 200 kW. Even with the inertial forces being one-third or less of the drag forces, the maximum power is still double the average power. This demonstrates the strong effect inertial forces have on maximum power requirements. The drive torque ranges from 17 kN-m to 40 kN-m. The Reynolds number based on tow cylinder diameter has maximum values ranging from 6.0×10^4 to 3.9×10^6 and Keulegan-Carpenter parameter ranging from 1.02×10^1 to 7.41×10^3.

3.3 Free Vibration Analysis of System Model

In Section (2.2) the governing equations of motion for the system model yielded a matrix equation of the form

$$[A]\{X\}=\{B\}$$

The square matrix [A] contained the coefficients of the unknown displacement column matrix {X} which could be solved for when set equal to the given column matrix {B}. The results of this forced vibration allowed the investigation of the fundamental resonant or natural period τ_{res} by interpreting the displacement response of the driver pulley model relative to the carriage/specimen model displacement. Another means of investigating the fundamental period of the system is to perform a undamped free vibration analysis. The advantage of this method is that the fundamental period of the carriage/specimen model is solved for directly without having to interpret plots. The disadvantage is that damping is not accounted for. Equation (3.3.1) shows the natural period of a one DOF damped system τ_d in terms of the

undamped natural period τ_{ud} and the damping ratio ζ that was discussed in Section (2.4).

$$\tau_d=\tau_{ud}\ 1/\mathrm{SQRT}(1-\zeta^2) \tag{3.3.1}$$

Considering that the damping has only a second order effect on the resonant period the results should not differ much from the damped system. In general an undamped system will have a slightly shorter natural period than a damped system of equal stiffness and mass.

The governing equation of motion for a free vibration system can be arranged in the form

$$[M]\{\ddot{X}\}+[C]\{\dot{X}\}+[K]\{X\}=\{0\} \tag{3.3.2}$$

where [M],[C], and [K] are the mass, damping, and stiffness matrices of the system model respectively. Setting the damping matrix to zero for undamped free vibration yields

$$[M]\{\ddot{X}\}+[K]\{X\}=\{0\} \tag{3.3.3}$$

Since the system is linear and therefore deterministic a displacement function of the form

$$X_i=a_i\sin(\omega t-\phi) \tag{3.3.4}$$

$$i=1,2,\ldots n$$

can be chosen where a_i is the amplitude of motion of the ith coordinate and n is the number of DOF. In matrix form Equation (3.3.4) can be written

$$\{X\}=\{a\}\sin(\omega t-\phi)$$

Substituting for {X} in Equation (3.3.3) yields

$$-\omega^2[M]\{a\}\sin(\omega t-\phi)+[K]\{a\}\sin(\omega t-\phi)=\{0\}$$

rearranging terms

$$[\ [K]-\omega^2[M]\ ]\{a\}=\{0\}$$

Since both the stiffness and mass matrices are linear we have an algebraic system of linear homogeneous equations with n unknown displacements a_i and an unknown parameter ω^2. A non-trivial solution requires that the determinate of the matrix factor of {a} be equal to zero yielding

$$|\ [K]-\omega^2[M]\ |=0 \qquad (3.3.5)$$

In general the solution of this eigen problem results in a polynomial equation of degree n in ω^2. The n values of ω^2 are each unique and represent the square of the natural frequencies for the system. The natural or resonant period can be found from Equation (3.3.6).

$$\tau_{ud}=2\pi/\mathrm{SQRT}(\omega^2_{ud}) \tag{3.3.6}$$

The stiffness and mass matrices for this system can be seen in Fig.s (3.3.1) and (3.3.2) respectively. Without damping, the DOF's of the system are completely unrestrained so the first mode is that associated with rigid body motion and a natural frequency of zero. This produces a numerical instability in the solution routine used which can be avoided by applying a virtual spring constant k_v to the driver pulley affecting the θ_1 DOF. This spring constant will give the first natural period a finite value which does not apply to the real model. Therefore the first natural period is associated with the virtual spring and must be ignored. The second natural period of the solution is the first natural period of the system model. Table (3.3.1) shows the natural frequencies and periods for the system as solved for by the FORTRAN program Toweigen (see Appendix B).

Using the second natural period from each group of data the results range from 0.073 seconds for the 0.0254 m diameter specimen to 0.077 seconds for the 0.6096 m diameter specimen. The natural period can be seen to decrease slightly with increasing specimen diameter for the first two diameters listed. This is not in agreement with either the expected response or the response predicted in Section (3.2.1) for damped resonance. The solution technique used exhibited slight numerical instabilities for various combinations of mass and stiffness and may have caused this discrepancy. Nevertheless the results are reasonably close to the resonant period range of 0.15 to 0.30 seconds

predicted by the damped model. The undamped natural period is shorter than the damped period as expected.

[k]

Θ_1	X_2	X_3	X_4	X_5	X_6	X_8	X_9	X_{10}
$-2k_c - k_v/R^2$	k_c/R							
k_c/R	$-2k_c/R^2$	k_c/R^2						
	k_c/R^2	$-2k_c/R^2$	k_c/R^2					
		k_c/R^2	$-2k_c/R^2$	k_c/R	k_c/R^2			
			k_c/R	$-2k_c - k_v/R^2$		$-k_c/R$		
					$-2k_c/R^2 - k_6/R^2$	k_c/R^2		
				$-k_c/R$	k_c/R^2	$-2k_c/R^2$	k_c/R^2	
							$-2k_c/R^2$	k_c/R^2
							k_c/R^2	$-2k_c/R^2$

Figure 3.3.1 Stiffness matrix

[m]

Θ_1	X_2	X_3	X_4	X_5	X_6	X_8	X_9	X_{10}
I_1/R^2								
	m_c/R^2							
		$(m_3 + c_1\rho\forall)/R^2$						
			m_c/R^2					
				I^2/R^2				
					m_c/R^2			
						m_c/R^2		
							m_c/R^2	
								m_c/R^2

Figure 3.3.2 Mass matrix

Table 3.3.1 Natural frequencies and periods of undamped system

Tow specimen diameter (m)	Mode #	Frequency (Hz)	Period (sec)
0.00	1	2.618	0.382
	2	13.758	0.073
	3	21.945	0.046
	4	29.286	0.034
	5	35.946	0.028
	6	45.125	0.022
	7	51.175	0.020
	8	60.468	0.017
	9	106.749	0.009
0.0254	1	2.512	0.398
	2	13.758	0.073
	3	21.945	0.046
	4	29.286	0.034
	5	35.946	0.028
	6	45.125	0.022
	7	51.175	0.020
	8	60.468	0.017
	9	106.749	0.009
0.0762	1	2.627	0.381
	2	13.926	0.072
	3	22.478	0.044
	4	29.598	0.033
	5	36.877	0.027
	6	46.283	0.022
	7	52.538	0.019
	8	61.769	0.016
	9	109.593	0.009
0.1524	1	2.564	0.390
	2	13.926	0.072
	3	22.478	0.044
	4	29.598	0.033
	5	36.877	0.027
	6	46.283	0.022
	7	52.538	0.019
	8	61.769	0.016
	9	109.593	0.009
0.3048	1	2.344	0.427
	2	13.926	0.072
	3	22.478	0.044
	4	29.598	0.033
	5	36.877	0.027
	6	46.283	0.022
	7	52.538	0.019
	8	61.769	0.016
	9	109.593	0.009
0.6096	1	1.708	0.585
	2	13.926	0.072
	3	22.478	0.044
	4	29.598	0.033
	5	36.877	0.027
	6	46.283	0.022
	7	52.538	0.019
	8	61.769	0.016
	9	109.593	0.009

4.0 Tow Carriage Structural Analysis and Design

4.1 Carriage Structure Performance Requirements

The loading on the various system components has been estimated utilizing results from the system model of Chapter 2. With this loading information each component must be designed to perform under the specified conditions. The first component to be analyzed is the carriage structure which supports the tow specimen.

The function of the carriage is to rigidly support and guide the tow specimen and transfer the dynamic cable force in order to motivate the specimen through the wave channel. The major design criteria for the carriage structure are ordered as follows:

1) The structure must be light weight to minimize inertial loading of the system.

2) The structure must be rigid to minimize deflections when loaded both statically and dynamically.

3) The wetted portion of the structure must have a small drag force to minimize wasted power and provide a relatively undisturbed flow near the specimen.

4) The structure must withstand the corrosive environment of the wave channel.

5) Construction cost must be kept low relative to the overall system cost.

The above design criteria are ranked in order of importance. The weight of the structure is the most important constraint because the system model is very sensitive to the carriage mass. A large carriage mass significantly increases inertial loading which in turn increases maximum power requirements. The resonant period is also increased but to a lesser degree.

The rigidity of the structure is also an important constraint. With static loads of more than 50 kN and dynamic loads on the same order the structural integrity of the carriage is important. Since the carriage is to be instrumented, vibration is also a major concern. The stiffness to mass ratio must be kept large in order to have high natural frequencies for the various modes of vibration.

With a tow specimen being towed completely submerged a portion of the carriage structure will also be submerged or wetted. This portion of the structure must have good external flow properties in order to minimize lost power and interference with the specimen interaction with the fluid.

The structure must also withstand the corrosive environment of the wave channel for the life of the structure. The least important design criteria is cost. The performance criteria stated above are more critical because if they are not met the system will not function properly. Certainly compromises will have to be made to keep the construction costs feasible. The rest of this chapter describes a possible conceptual design of the carriage followed by the supporting analysis.

4.2 Description of the Carriage Structure Design and Model

The conceptual design of the system specifies the use of linear motion bearings that nearly span the length of the existing wave channel (see Section 5.2). These bearings when fitted to the existing facilities specify the width of the carriage structure to 3.66 m (12 ft.). The maximum depth of the structure below the bearing rail is specified by the depth of the tank to be 4.67 m (15 ft.). With these two fixed dimensions the carriage structure was designed to best meet the design criteria. A conceptual design of the carriage can be seen in Fig. (4.1.1). This design is the result of a trial and error approach constrained by the previously mentioned criteria.

The overall width is 3.66 m (12 ft.) with a length of 5.79 m (18 ft.), and a height of 5.79 m (19 ft.). The main Section of the structure is a 3.66 m by 5.49 m by 1.22 m space frame. The frame is composed of 0.13 m (5 in.) diameter main support tubes reinforced with 0.06 m (2.5 in.) diameter tubes. This part of the structure attaches to the bearing rails as indicated restricting motion to the x-direction only. This space frame also provides support for the extended tow specimen supports.

The two vertical tow specimen supports or struts, are 5.79 m (19 ft.) long tubes with a symmetric hydrofoil cross Section. The cord length is 1 m (39.4 in.) and the maximum thickness of 0.13m (5 in.) occurs at mid chord. This thickness distribution should provide similar flow characteristics for both forward and reverse towing. The single

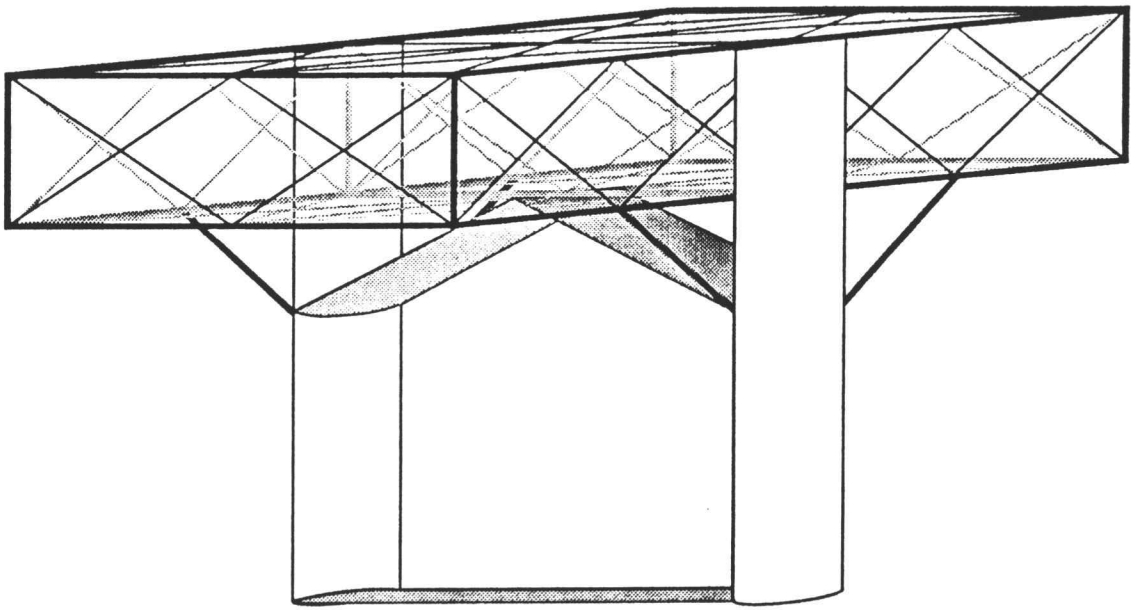

Figure 4.1.1 Conceptual design of tow carriage structure

horizontal support strut is also a symmetric hydrofoil in cross Section with a chord length of 1 m and a maximum thickness of 0.08 m (3 in.at mid chord. The tow specimen can be attached either vertically or horizontally. The specific details of how the specimen attaches to the carriage are not presented in the design nor are the details of how the specimen support struts are raised and lowered relative to the main frame.

4.3 Material Selection for the Carriage Structure

The materials were selected by considering stiffness, weight, corrosion resistance, and cost. A finite element model was developed to model the design. Using the loading predicted by the system model, a preliminary design was investigated using steel as the material. The analysis provided the required member sizes for a specified maximum deflection. The product of elastic modulus and Sectional inertia was computed for the specimen support struts, which primarily experience bending, and the product of elastic modulus and Sectional area was computed for the circular tube members of the space frame, which mainly experience axial loading. Equating similar products for various materials the overall mass of the structure was computed for each material.The stiffness product for a typical member divided by the total mass of the structure has a K/M flavor and seems appropriate for such a design where rigidity and mass are both major concerns.

Steel, aluminum, and titanium were the materials used for comparison. Alloying of these materials generally does not effect the stiffness as much as the strength. Therefore the specific alloy is not

stiffness as much as the strength. Therefore the specific alloy is not important at this point in the analysis because the structure was designed for deflections and not stresses.

Titanium had the highest stiffness to mass characteristics and steel the worst with aluminum nearly in between. Both titanium and aluminum have good to excellent corrosion properties depending on the alloy compared to steel. The cost, ease of manufacturing, and availability of these materials all rank in the opposite order of stiffness to weight. Steel is by far the cheapest and easiest material to work with, aluminum is slightly more expensive and more difficult to work with, and titanium is very expensive and difficult to work with. At this stage of the design aluminum appears to be the best compromise between performance and cost and is therefore used for the remainder of the analysis.

4.4 Description of the Finite Element Model of the Carriage Structure

In order to quantify the structural response of the tow carriage frame a finite element model was constructed. Each member of the frame was given a beginning and ending node with an element connecting the nodes. Several members may share a common node but each member has only one element. A total of 55 nodes and 137 elements are needed to model the structure. Fig. (4.4.1) shows the model of the tow carriage structure with the nodes labeled. Element numbers were left out for clarity. The global coordinates of the model are also shown. In addition to the global coordinates each node has a set of local coordinates.

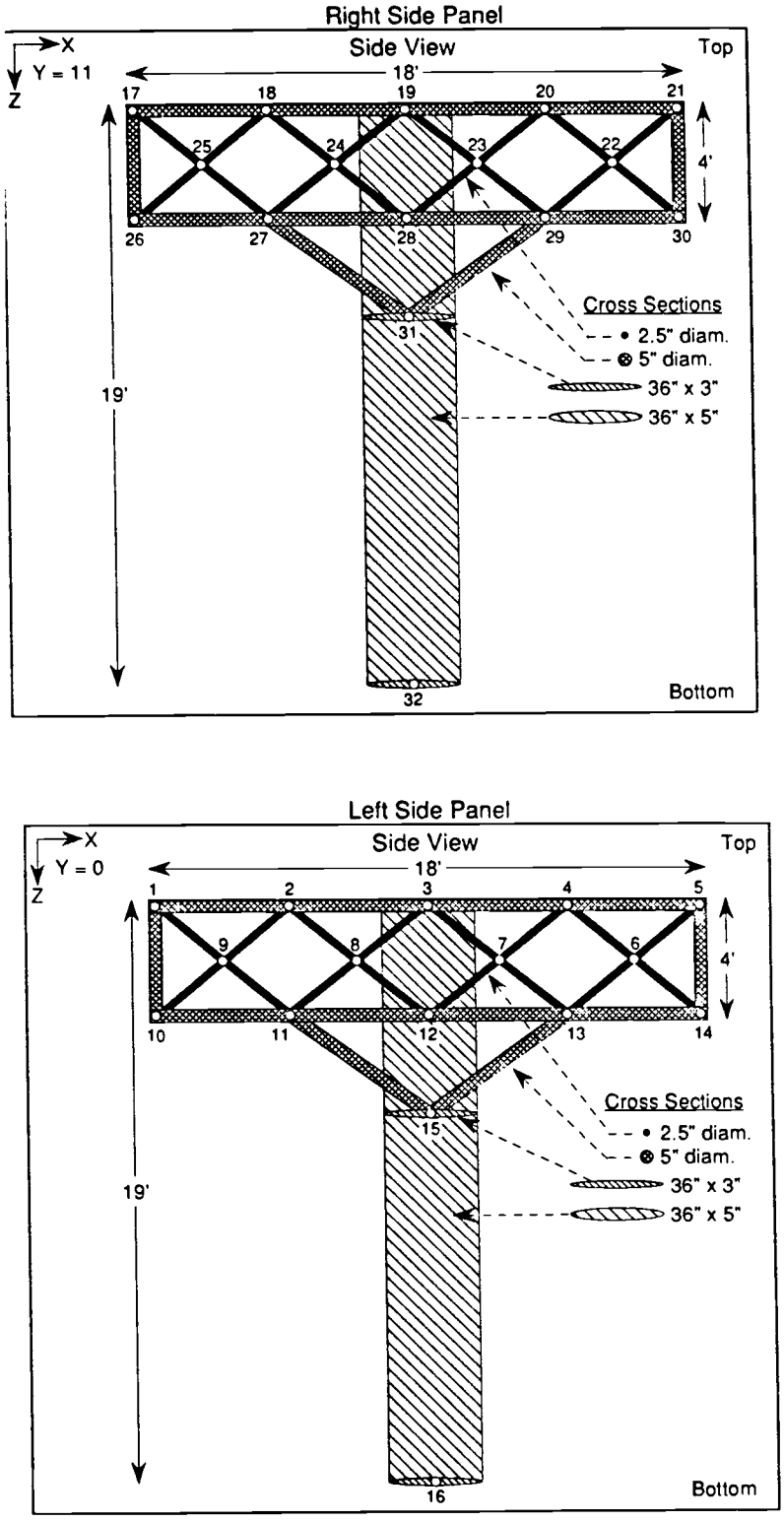

Fig. 4.4.1a Side view of finite element model

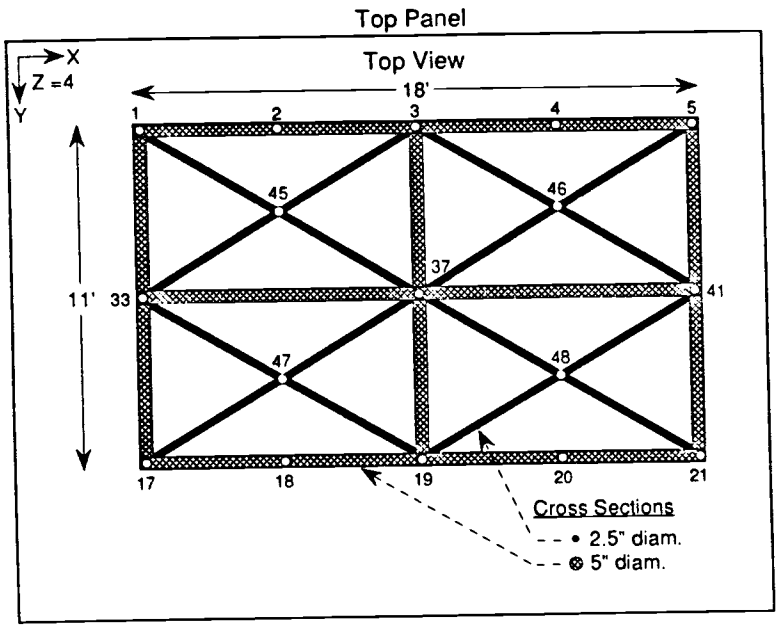

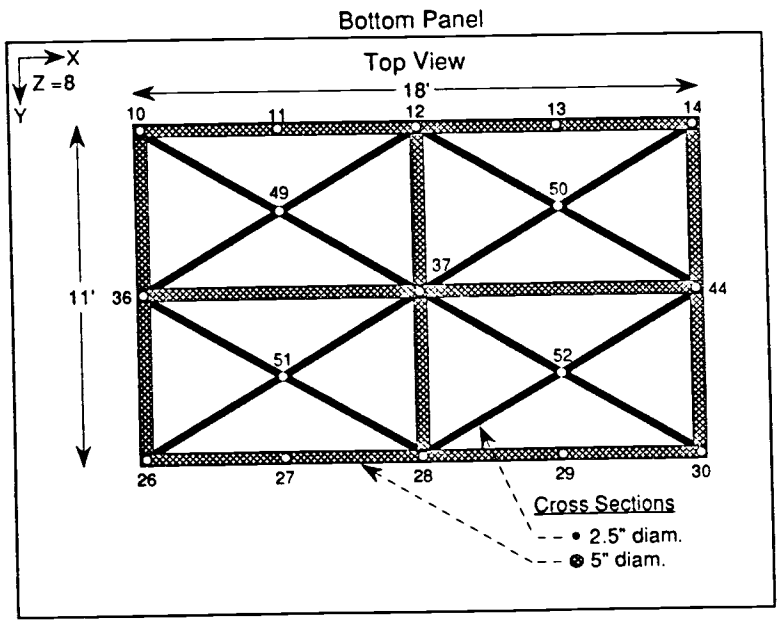

Figure 4.4.1b Top view of finite element model

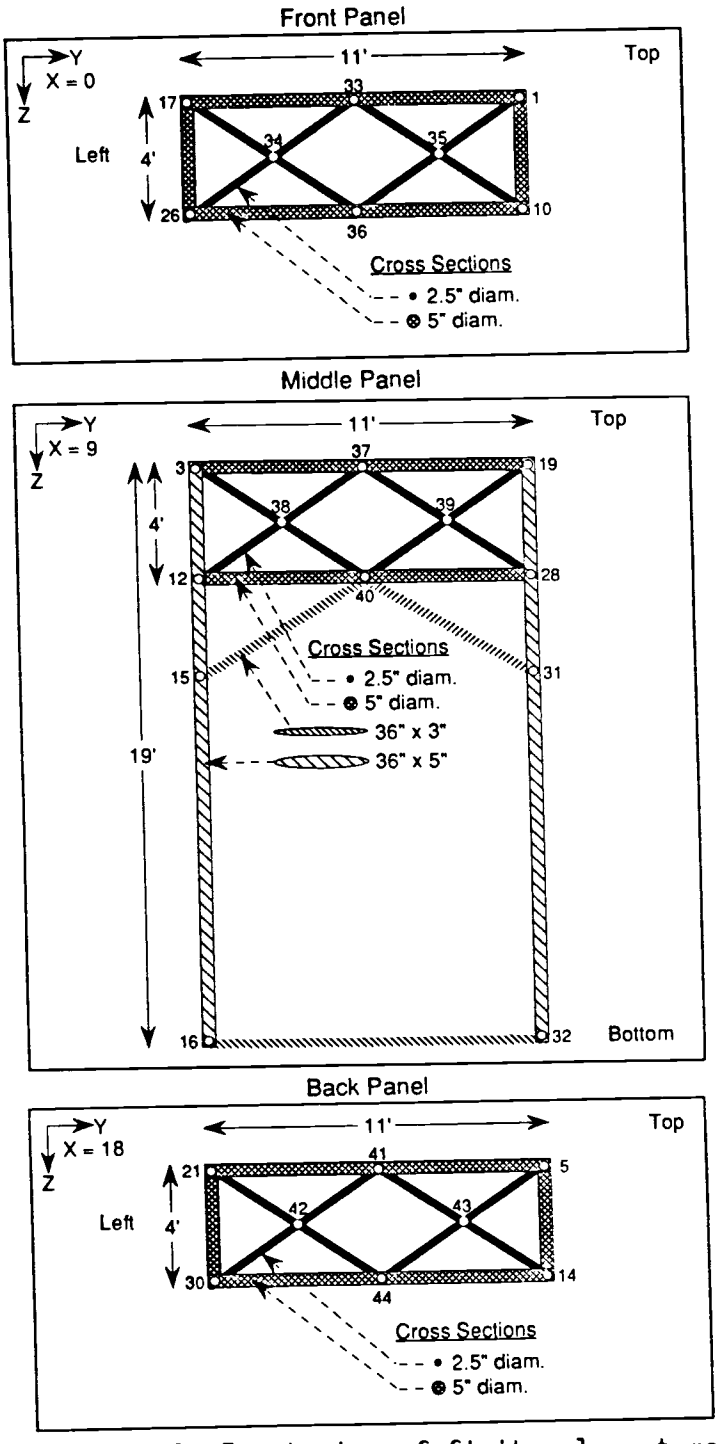

Figure 4.4.1c Front view of finite element model

The finite element program ANSYS (Swanson, 1985) was used to develop and analyze the model. Each element is modeled as a 3-D beam element. This element is a uniaxial element with compression,tension, torsion, and bending capabilities. Each element has six DOF at each of its two nodes: translation in the local x,y,and z directions and rotations about the local x,y, and z axes. Shear deflections are not considered. Each element is defined by its length, orientation, and Sectional properties. The length and orientation are computed from the geometry of the model and the Sectional properties are input directly into the program.

A total of four different Sectional properties are used for this model. Each Section can be seen in Fig. (4.4.2). The first Section is that of the main supports of the space frame which are 12.7 cm (5 in.) diameter circular aluminum tubes. A total of 40 elements are used with this cross Section. The second Section models the reinforcement members of the space frame which are 6.35 cm (2.5 in.) diameter circular aluminum tubes. A total of 87 elements are used with this cross Section. The third Section in the model is for the vertical tow specimen support struts. These elements model the hydrofoil Sectioned tubes of the conceptual design. A rectangular tube cross Section approximates this shape having a thickness of 12.7 cm. and a width of 91.4 cm (36 in.). The last Section of the model represents the horizontal tow specimen support strut. An aluminum rectangle with a thickness of 7.6 cm (3 in.) and a width of 91.4 cm approximates this hydrofoil Section.

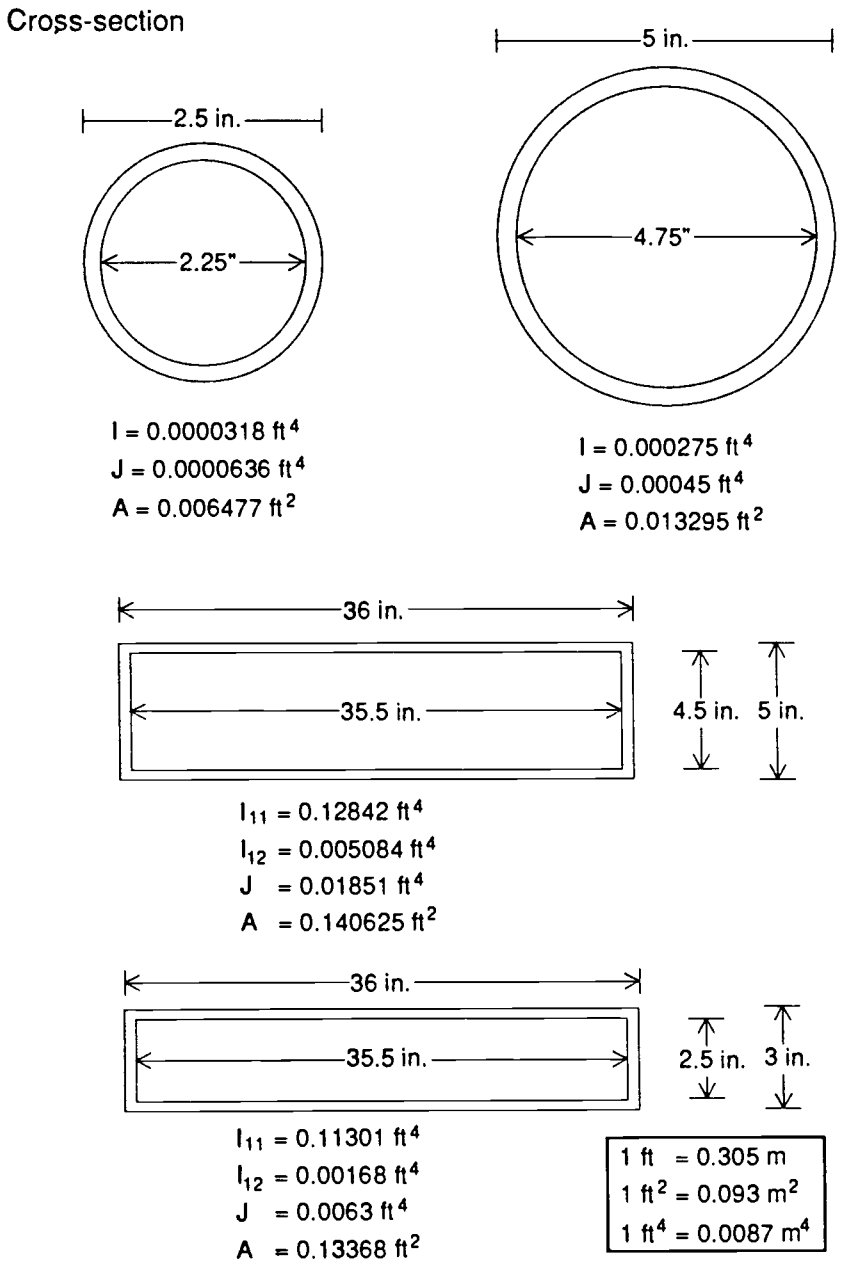

Figure 4.4.2 Cross Sectional model of element members

The interaction between the tow carriage structure and the bearing guide rails is modeled at nodes 10,26,30, and 14. Each of these nodes is only allowed one DOF in the global x-direction which is consistent with the motion of the bearings. All other translational and rotational DOF's at these four nodes are forced to have zero displacement.Thus the bearings and connection between the bearings and carriage structure are assumed infinitely rigid.

The interaction between the wire rope and the carriage structure is modeled at node 12. Here the translational DOF in the global x-direction is forced to zero. All other DOF are unrestricted from external interactions. Both a static and dynamic analysis were preformed on this model. The above description of the model and boundary conditions are common to both analyses.

4.5 Static Analysis of the Finite Element Model

The static analysis is composed of two separate load steps. The first load step is to model the maximum force imposed on the carriage structure by a horizontal tow specimen at the bottom of the support frame in the global x-direction. This force is the result of both the drag and inertial forces of the tow specimen as discussed in Section (3.2). The maximum force from this loading was found to be approximately 50 kN. This is modeled as two 25 kN forces acting in the x-direction at nodes 16 and 32.

With the above input the analysis provides the state of stresses at the end of each element, the deflection of each node, and the reaction forces of the structure. The output stresses include the net

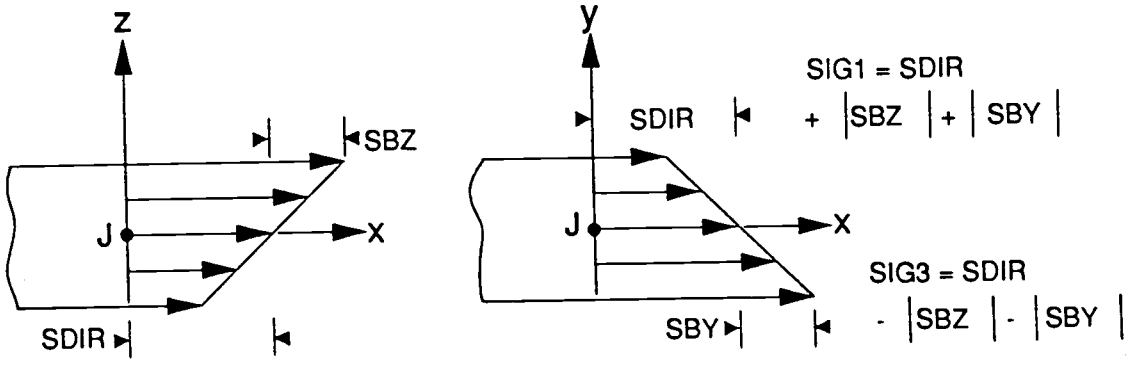

Figure 4.5.1 Stress output of finite element model

axial stresses at the ends of each element. From Fig. (4.5.1) the net stresses, sig1 and sig3, are defined as the sum of the axial stresses due to direct axial loading sdir, and axial stresses due to bending about the local y and z axes of the element sby and sbz. Shear stresses have only a small contribution to the overall maximum deflection and the overall stress level for slender elastic beams and are therefore not included in the analysis.

As stated above the stresses sig1 and sig3 are axial stresses only. Since the shear stresses are small the largest of these two stresses will closely approximate the maximum stress in a particular element. With the indicated loading stresses in all elements are less than 7000 psi. Many common alloys of aluminum have yield stresses greater then 30,000 psi resulting in a safety factor greater then four.

The maximum deflection occurs at nodes 16 and 32. Node 16 has a deflection in the global x-direction of 14.5 mm (0.57 in.) and node 32 has a similar deflection of 16.0 mm (0.63 in.). All other deflections are an order of magnitude smaller. Thus the carriage structure is quite rigid for this loading direction. The reaction forces are listed in Table (4.5.1) and are discussed later in the text.

The second load step of the static analysis considers lift forces from the tow specimen, i.e., forces that are directed normal to the relative flow field about the tow specimen. For a horizontally mounted tow specimen the lift force would act in the global z- direction. For a vertically mounted tow specimen the lift force would act in the global y-direction. Because the structure is much stiffer when loaded

Table 4.5.1 Summary of reaction forces on carriage structure

X-direction loading

Node #	F_x (N)	F_y (N)	F_z (N)	M_x (N-m)	M_y (N-m)	M_z (N-m)
10	0	-8411	-16867	-156	549	7.3
12	-49996	0	0	0	0	0
14	0	-8411	16867	156	549	7.3
26	0	-8211	-25225	-20.6	631	98
30	0	8211	25225	20.6	631	98

Y-direction loading

Node #	F_x (N)	F_y (N)	F_z (N)	M_x (N-m)	M_y (N-m)	M_z (N-m)
10	0	-1112	-2769	20	140	-13
12	0	0	0	0	0	0
14	0	-1112	-2769	20	-140	13
26	0	-1112	2769	20	-140	-13
30	0	-1112	2769	20	140	13

Sum of loading from X and Y directions plus gravity loading

Node #	F_x (N)	F_y (N)	F_z (N)	M_x (N-m)	M_y (N-m)	M_z (N-m)
10	0	9523	22248	176	689	20.3
12	49996	0	0	0	0	0
14	0	9523	22248	176	689	20.3
26	0	9323	30606	40.6	771	111

in the global z-direction compared to the y-direction,only the y-direction loading is analyzed.

For the circular cylinder tow specimen used for the system analysis lift forces are generally caused by vortex shedding. Vortex shedding and hence the lift force on these symmetric specimens is a very dynamic and complicated phenomena. This paper does not attempt to accurately quantify these forces. Instead a lift force an order of magnitude smaller than the maximum drag force is used. This is done by applying a 2.2 kN force in the global y-direction at both nodes 16 and 32.

The maximum stress from this load step is 1150 psi which implies a safety factor of 26. The maximum deflection of 8.4 mm (0.33 in.) occurs at nodes 16 and 32 in the global y-direction. All other deflections are an order of magnitude or more smaller. Thus, the structure is also quite stiff for this loading direction as well.

The reaction forces for this load step and the previous are presented in Table (4.5.1). The sum of the reaction forces from each load step is used in selecting the appropriate linear guide bearing in Section (5.2).

As mentioned above the lift force was not accurately quantified and could approach the same magnitude as the drag force. If this were to occur unacceptable deflections and stresses could result. This structure could be further stiffened for y-direction loading at the probable cost of increased mass and drag from the tow specimen supports. The above analysis and results seems sufficient for the conceptual design so the static analysis is not carried any further.

4.6 Modal Analysis of Carriage Frame

As previously discussed the lift forces on the circular cylinder tow specimen resulted from the fluid dynamic phenomena of vortex shedding. This phenomena produces harmonic fluctuating forces both normal and tangent to the specimen velocity vector. These unsteady forces can excite the structure and cause significant vibration which can interfere with instrumentation and in extreme cases cause structural damage.

Performing a modal analysis of the structure provides insight into the vibration response of the structure. The purpose of the modal analysis for this design is to find the natural frequencies and corresponding mode shape of the structure.

In terms of the carriage structure the governing equation of motion for free, undamped vibration is :

$$\mathbf{M} + \mathbf{K}\mathbf{U} = 0 \qquad (4.6.1)$$

where **M**,**K**, and **U** are the mass, stiffness, and displacement matrices of the structure respectively. As previously discussed, for linear structures the displacements are harmonic of the form:

$$U = U_o \cos \omega t \qquad (4.6.2)$$

Substituting for U and in Equation (4.6.1) gives the eigen value equation :

$$(K-\omega^2M)U_o=0 \tag{4.6.3}$$

For non-trivial solutions ($U_o \neq 0$), the determinate of $[K-\omega^2M]$ must vanish yielding:

$$|K-\omega^2M|=0 \tag{4.6.4}$$

If n is the order of the matrices, then Equation (4.6.4) results in a polynomial of order n, which has n roots: $\omega^2_1, \omega^2_2, .., \omega^2_n$. These roots are the eigen values of Equation (4.6.4). Substituting the n eigen values into Equation (4.6.3) yields n corresponding eigen vectors U_o. In a modal analysis the eigen values represent the square of the natural circular frequencies and the eigen vectors represent the corresponding mode shapes.

In order to compare the response of the structure to various natural frequencies both the participation factor (PF) and effective mass (EM) are useful parameters. The PF may be defined as a measure of the response of a structure at a given natural frequency. The PF represents how much each mode will contribute to deflections (and hence stresses) in a particular direction. The higher the PF for a given frequency and direction the more significant the mode. The actual value of the PF is only useful to compare the structural response to various frequencies and direction in the analysis. In other words the output does not represent true displacements. A PF ratio can be defined as the ratio of the PF of a particular frequency and direction to the maximum PF of the direction of interest.

The effective mass ,EM, is approximately the amount of mass that is active for a particular mode shape. The higher the EM the more significant the mode. A EM ratio can be defined as the ratio of the EM for a particular frequency and direction to the total mass of the structure.

A modal analysis of the tow carriage structure yielded the following results. In the global x-direction the first and most significant mode occurs at 19.44 Hz with a PF of 5.4 and a effective mass of 430 Kg. Fig. (4.6.1) and (4.6.2) show the frequency response for PF and EM ratios. Two other frequencies also have significant responses at 52.66 and 143.8 Hz. Figure (4.6.3) shows the mode shape for the 19.47 Hz response. This response mainly involves motion of the tow specimen support struts with minor contributions from the members of the space frame.

In the global y-direction significant modes occur at 8.08 and 40.44 Hz. The corresponding PF and EM are 4.9 and 354 Kg for the 8.08 Hz response and 5.0 and 374 Kg for the 40.44 Hz response. Figures (4.6.4) and (4.6.5) show the PF and EM ratios for the y-direction. From Fig. (4.6.6) we find the 8.08 Hz mode shape mainly excites the tow specimen support struts with minor activity in the space frame. Figure (4.6.7) shows the response to 40.44 Hz which activates the tow specimen support struts and space frame to a greater degree.

In the global z-direction the fundamental and most significant mode occurs at 31.79 Hz with a PF of 4.9 and a effective mass of 355 Kg. Figures (4.6.8) and (4.6.9) show the z-direction response of the PF and EM ratios. From the mode shape in Fig. (4.6.10) it can be seen

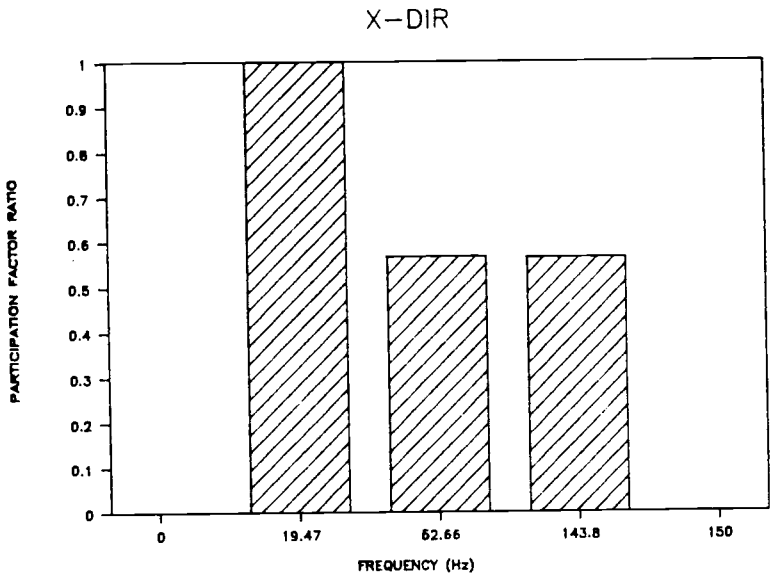

Figure 4.6.1 Participation factors in X-direction

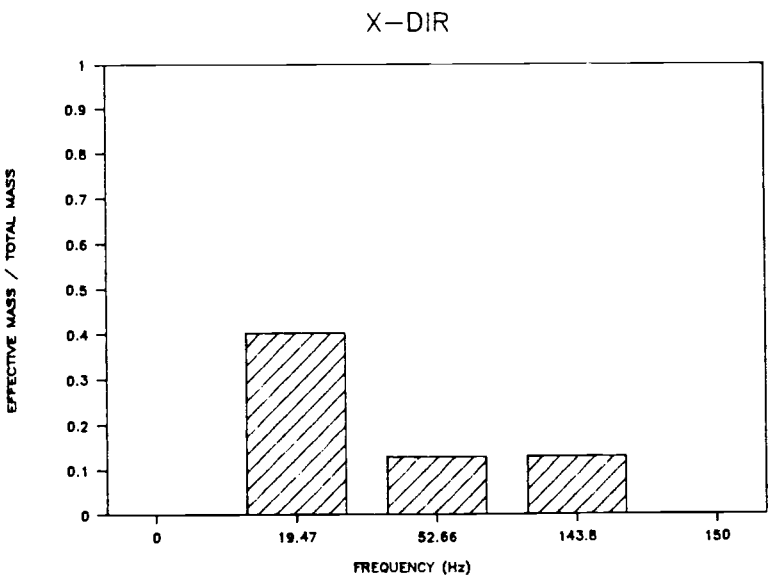

Figure 4.6.2 Effective masses in X-direction

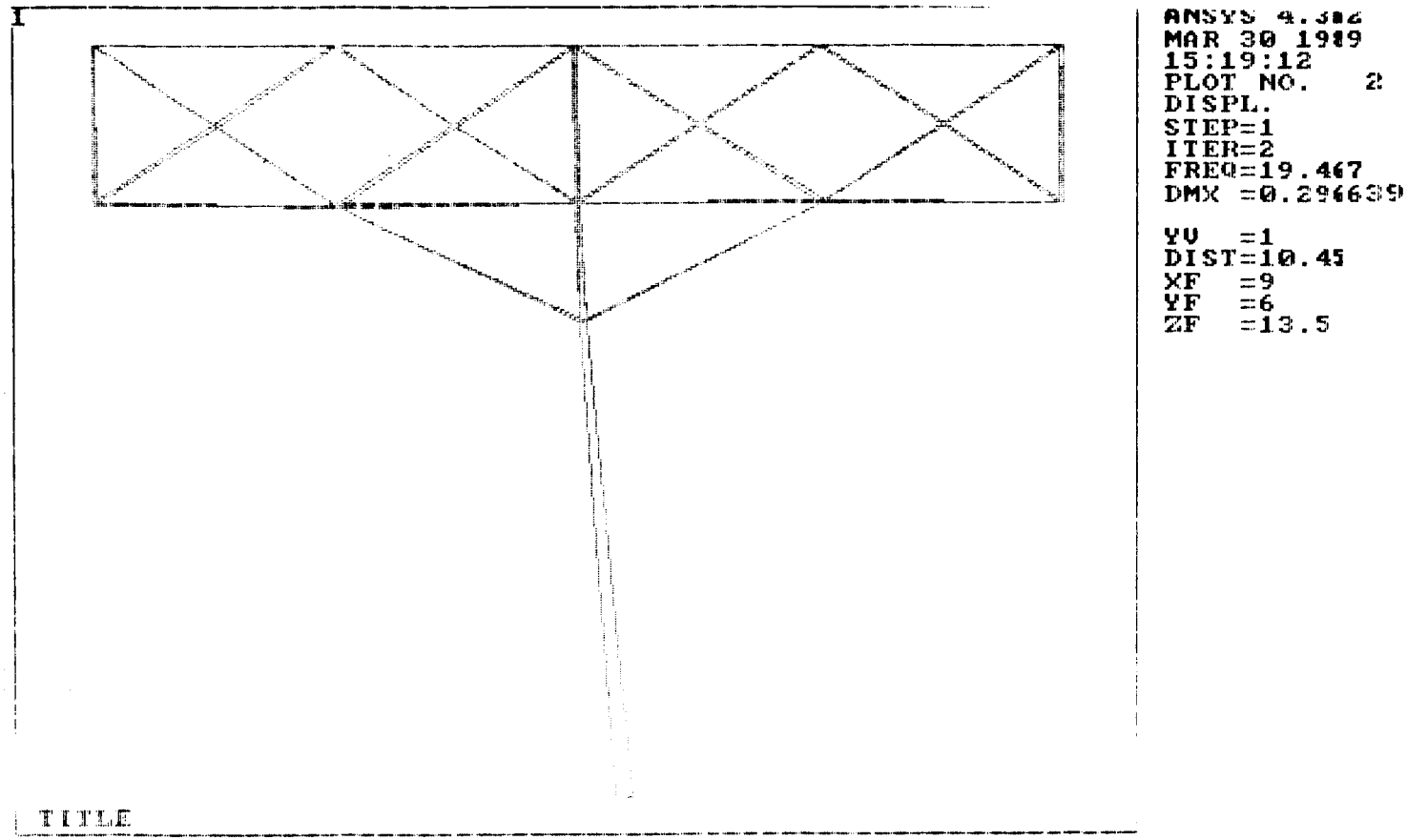

Figure 4.6.3 Mode shape for 19.467 Hz

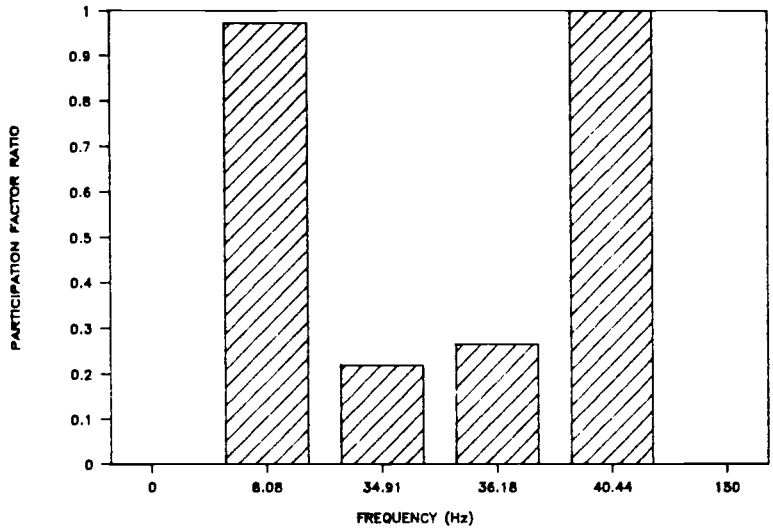

Figure 4.6.4 Participation factors for Y-direction

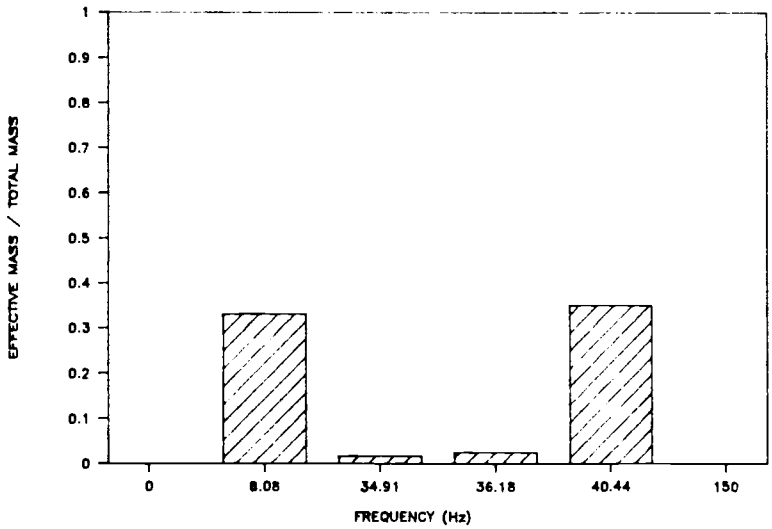

Figure 4.6.5 Effective masses for Y-direction

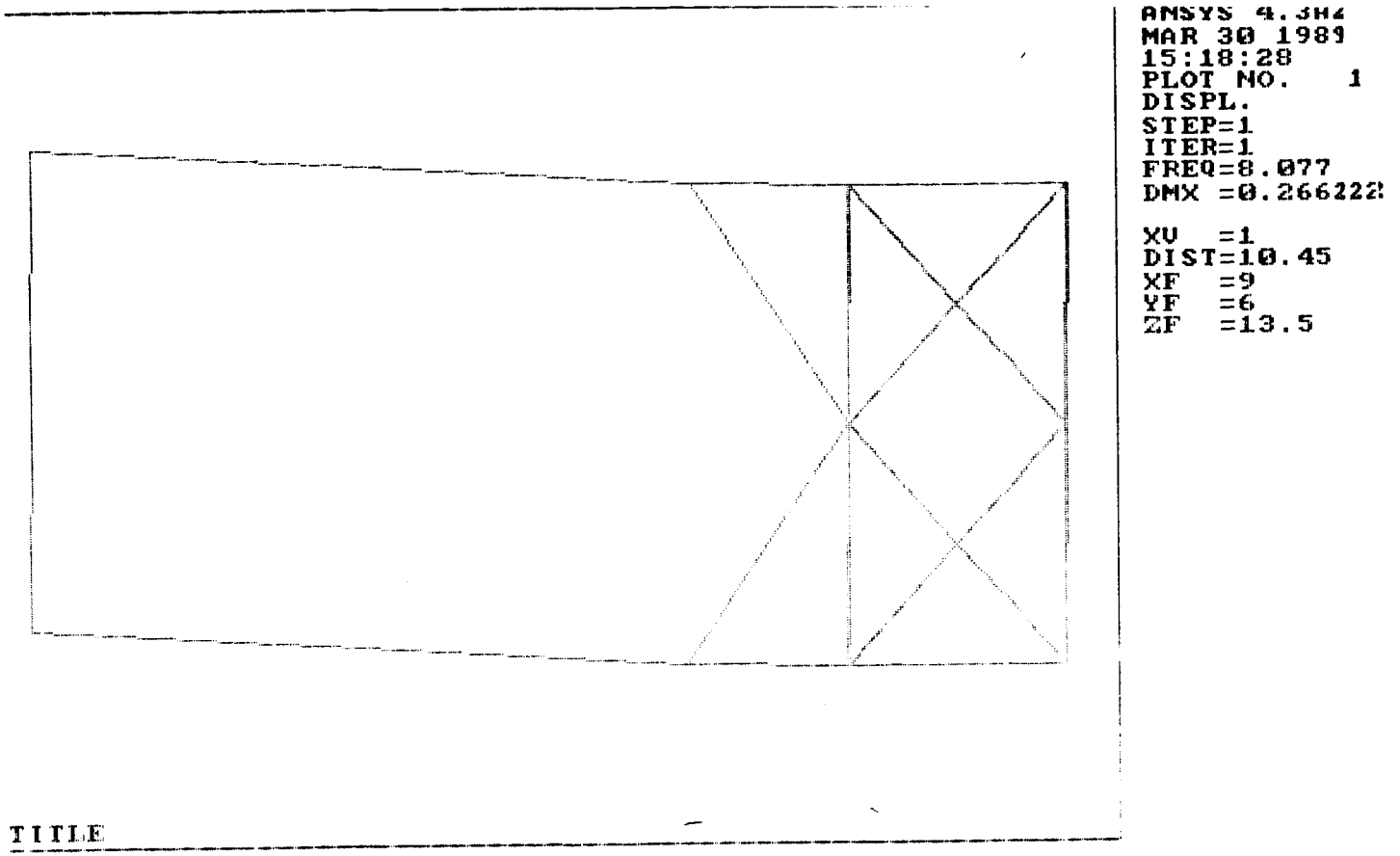

Figure 4.6.6 Mode shape at 8.077 Hz

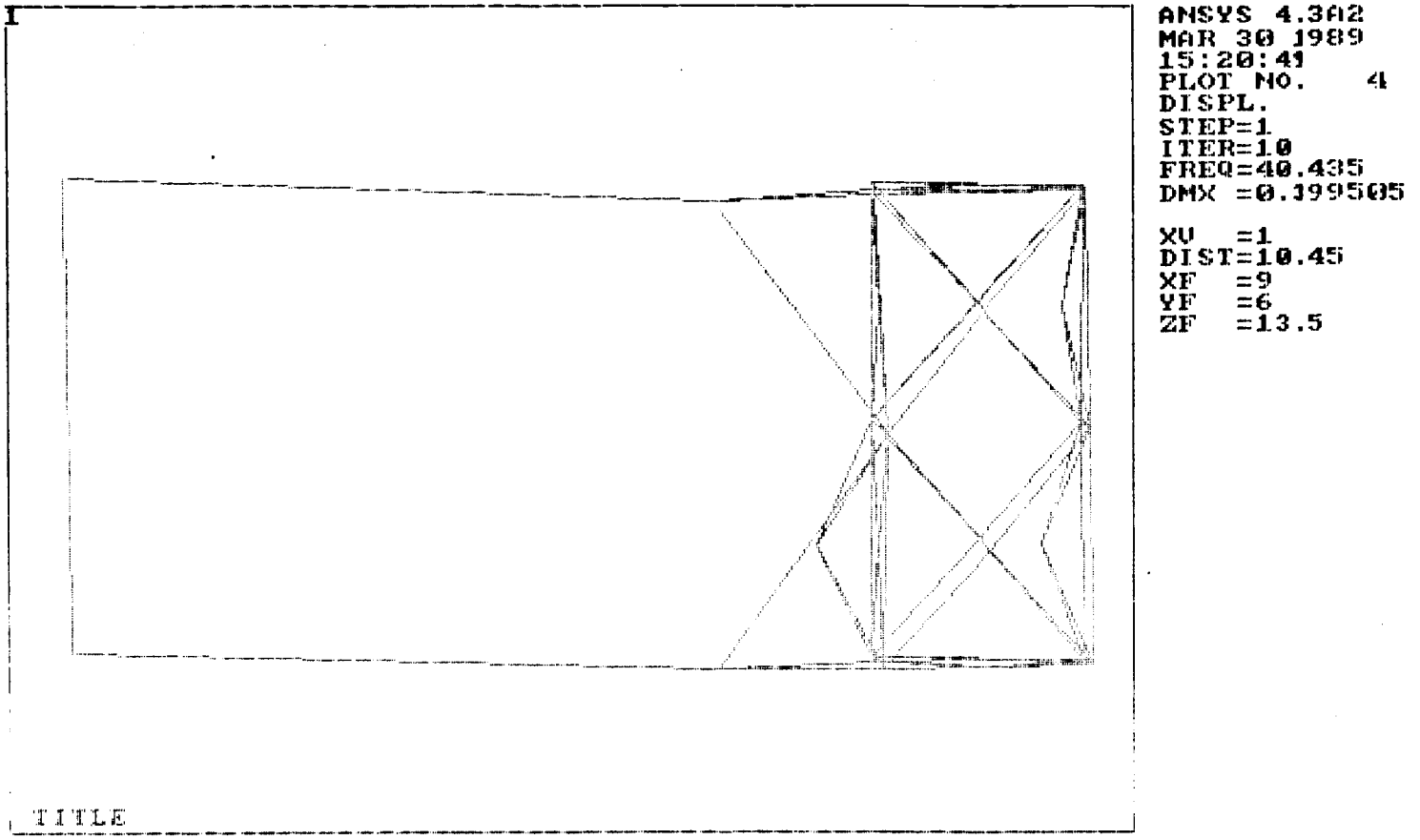

Figure 4.6.7 Mode shape at 40.44 hz

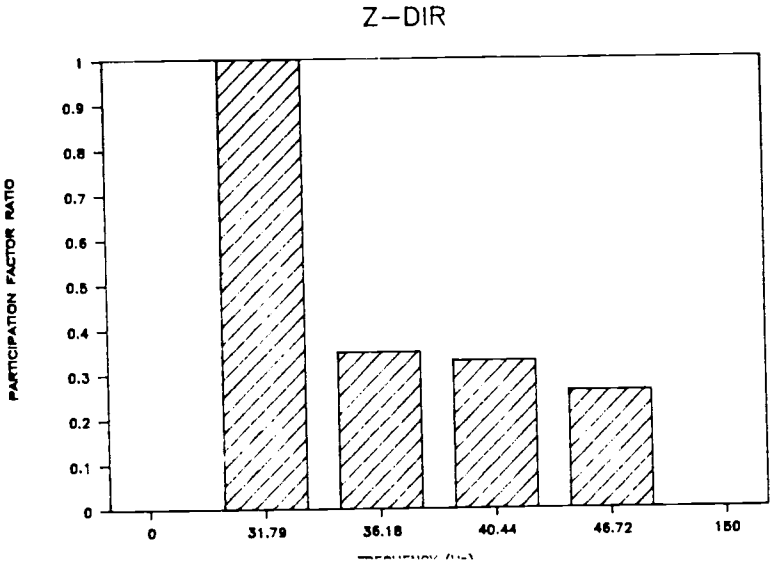

Figure 4.6.8 Participation factors for Z-direction

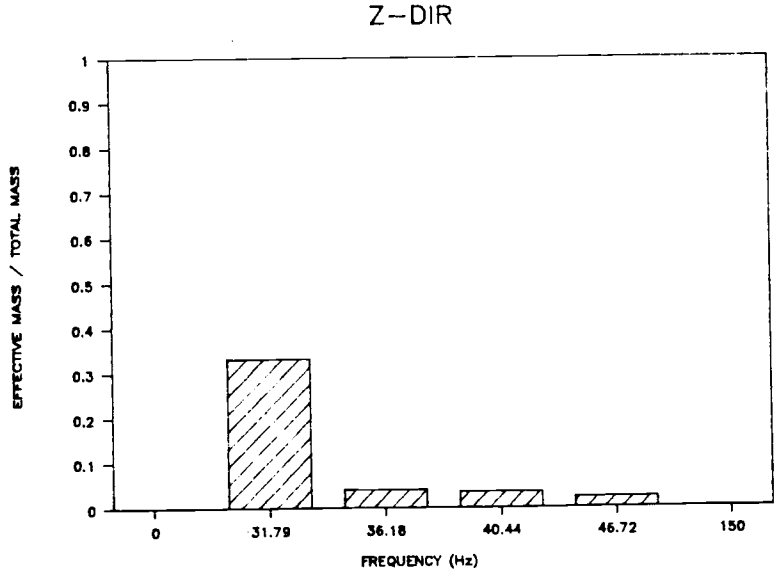

Figure 4.6.9 Effective masses for Z-direction

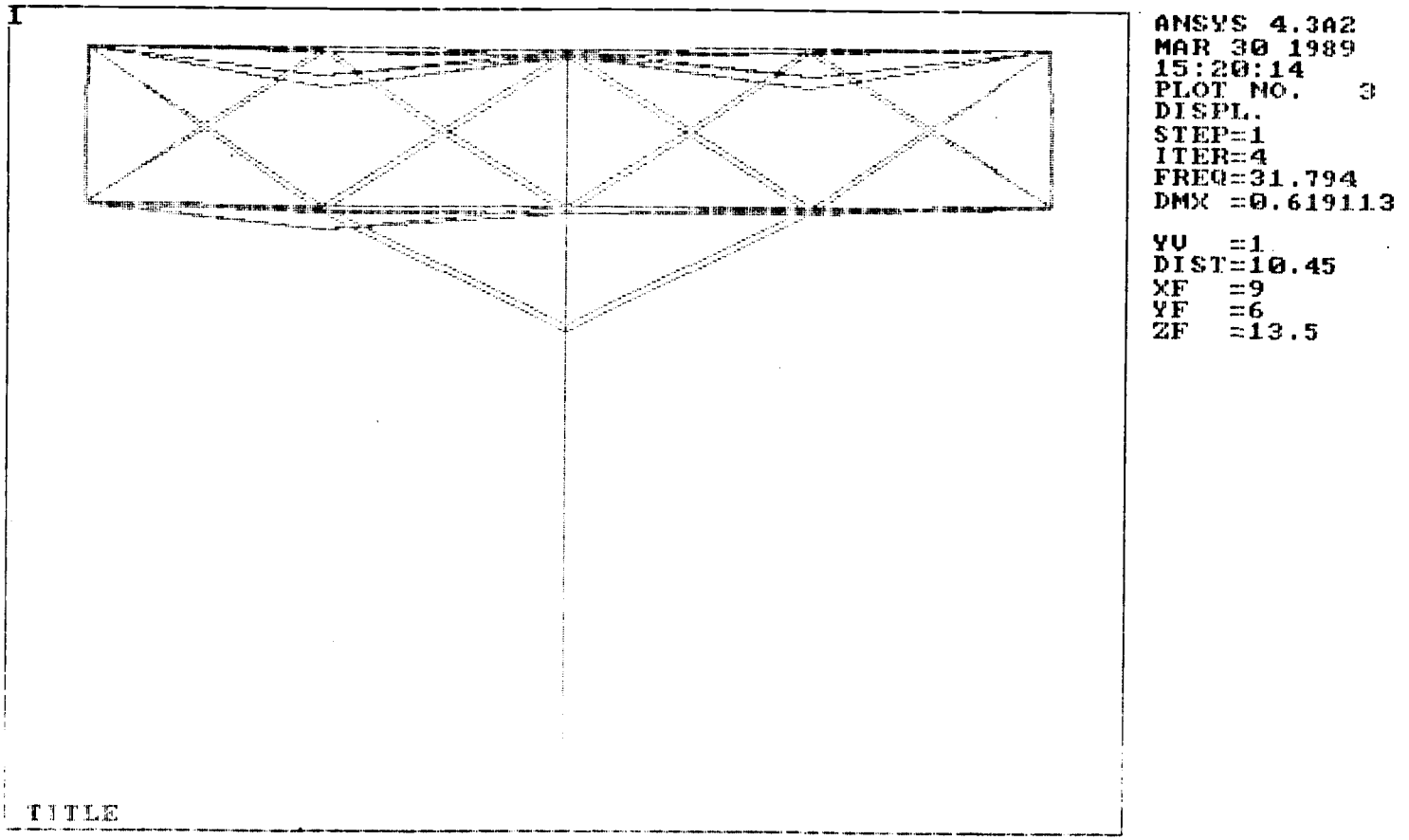

Figure 4.6.10 Mode shape at 31.75 Hz

that most of the excitation occurs in the reinforcement members of the space frame while the tow specimen support struts are relatively inactive.

The modes activating the tow specimen support struts are a worst case example. The tow carriage is modeled with the support struts extended nearly to the bottom of the wave tank. The majority of its use will probably have theses supports raised significantly. Raising the tow specimen support struts should significantly increase the natural frequency activating them and thus lower both the PF and EM.

Each of the natural frequencies discussed could cause unwanted noise in instrumentation or possible damage if adequately excited. As previously discussed, the main source of external excitement would come from vortex shedding on the tow specimen. Depending on the tow specimen orientation this fluctuating force could occur in any direction. Table (4.6.1) list the approximate value of vortex shedding frequencies for a circular cylinder using a Strouhal number of 0.2. The velocities listed are the maximum expected from Section (3.2). It can be seen that the vortex shedding frequency range and hence excitation frequency range completely covers the significant frequencies of the structure with tow specimen support struts fully extended.

The excitation frequency is a given phenomena. Either the carriage frames natural frequencies need to be increased by stiffening or the effect of the vibration on the present design needs to be further investigated. As stated, a significant increase in the natural frequencies can be obtained by raising the tow specimen support struts. In order to investigate the actual response of the present structure

Table 4.6.1 Vortex shedding frequencies of circular cylinders.

Diameter (m)	Maximum velocity (m/s)	Frequency (Hz)
0.0254	17.1	135
0.0762	14.7	38.6
0.1524	12.5	16.4
0.3048	10.3	6.76
0.6096	8.3	2.72

to harmonic loading near the natural frequencies a harmonic analysis needs to be performed. The results of such an analysis are stongly dependent on both the structural and viscous damping present. Determining the damping of this structure and its interaction with the surrounding fluid is beyond the scope of this paper. The structure is quite rigid in both x and z-directions. The harmonic loading due to vortex shedding will probably have the most significant effect in the y-direction. This could result from fluctuating lift forces on a vertically mounted tow specimen. Fortunately the damping due to the interaction of the support struts and the fluid is most significant in this direction. Until further analysis can be done it will suffice to conclude that the high rigidity of the structure and fluid damping will allow reasonable harmonic loading without damage to the structure.

5.0 Conceptual Design of the Tow Carriage System

5.1 Conceptual Layout of System

The conceptual model of the dynamic tow carriage system has five major components, 1) the carriage structure, 2) the carriage guide rail, 3) the power train, 4) the primary idler pulley, and 5) the secondary idler pulleys. A layout drawing of these components appear in Fig. (5.1.1). This chapter details the design of these various components with the exception of the carriage frame, which was discussed in Chapter 4. Each design is merely a possible conceptual layout of how these components may appear in the actual system.

5.2 Guide Rail and Support Structure

As mentioned in Chapter 3, the carriage structure is to be guided by linear motion bearings. Linear motion bearings offer the advantage over other bearing types of high rigidity, smooth operation, and low friction. For a typical bearing selection two major parameters are of concern, loading and service life. The loading for this application can be estimated from the carriage structure reaction forces in Chapter 3. Table (4.5.1) is a summary of the summation of loading magnitudes for each of the four bearings including the force contributed by gravity in the z-direction. The maximum force occurs at nodes 26 and 30 in the z-direction with a value of 3120 Kgf. From the manufactures catalog (THK) the basic static load rating C_o of the bearing must be selected by considering the maximum expected load and a safety factor. The maximum lower limit for a safety factor is between 2.5 and 5.0 as

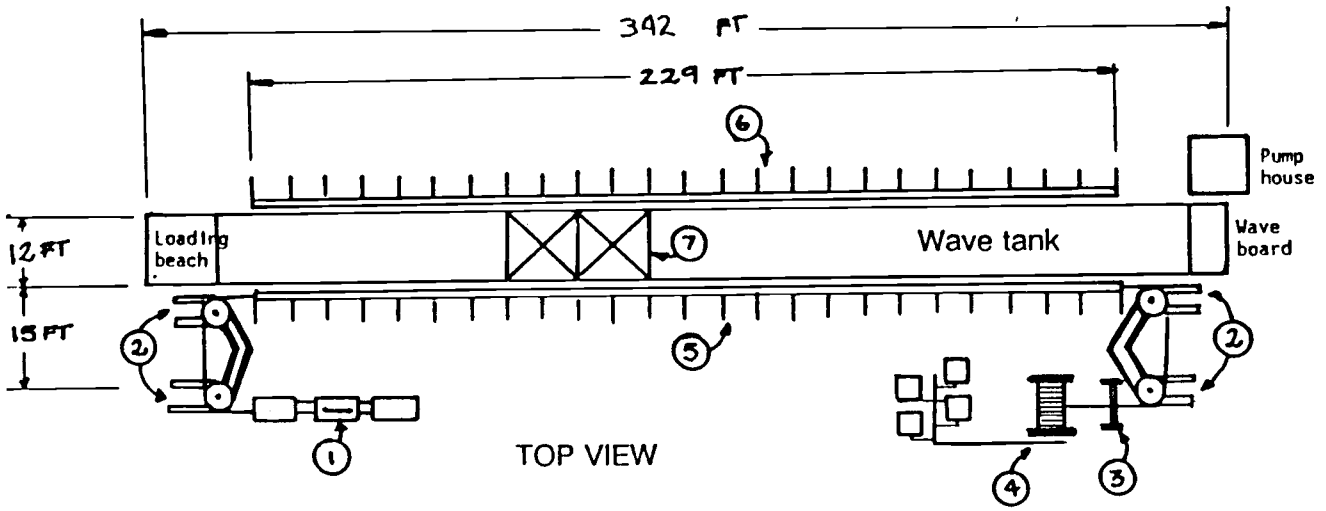

① Primary idler pulley

② Secondary idler pulley

③ Driver cable guide

④ Driver drum & drive train

⑤ Carriage bearing structure with cable way

⑥ Carriage bearing structure

⑦ Tow carriage structure

Figure 5.1.1 Layout of system components

recommended by the manufacture. Table (5.2.1) presents the pertinent parameters for selecting a linear motion bearing. The HSR 55HTA bearing has a basic static load rating of 13800 Kgf which would give a safety factor of 4.4. The maximum moment in the x,y, and z directions is found to be 17.9, 78.6, and 11.3 Kgf respectively from Table (4.5.1). The corresponding maximum moments from Table (5.2.1) M_C, M_A, and M_B are 275.7, 275.7, and 363.7 Kgf-m. This rail and bearing will easily handle the loads estimated from Chapter 3. The second consideration when selecting a bearing is the service life. The nominal life of the bearing L can be calculated from Equation (5.2.1), where C is the basic dynamic load rating and P is the maximum expected load (THK).

$$L=(C/P)^3*50 \qquad (5.2.1)$$

From Table (5.2.2) C is equal to 10600 Kgf and from Table (4.5.1) P is equal to 30606 N (3120 Kgf) yielding a nominal life of 1960 Km.

The service life time Lh can be estimated from Equation (5.2.2) where l_s is the average stroke length and n_1 is the maximum number of reciprocating operations per minute (THK).

$$Lh=(L*10^3)/(2*l_s*n_1*60) \qquad (5.2.2)$$

From Table (3.2.2) the average stroke length is 26.4 m and the average period is 8 seconds which is equal to 7.5 operations per minute, yielding a service life of 83 hours. This estimate assumes that the maximum load on the carriage structure exists for the entire cycle.

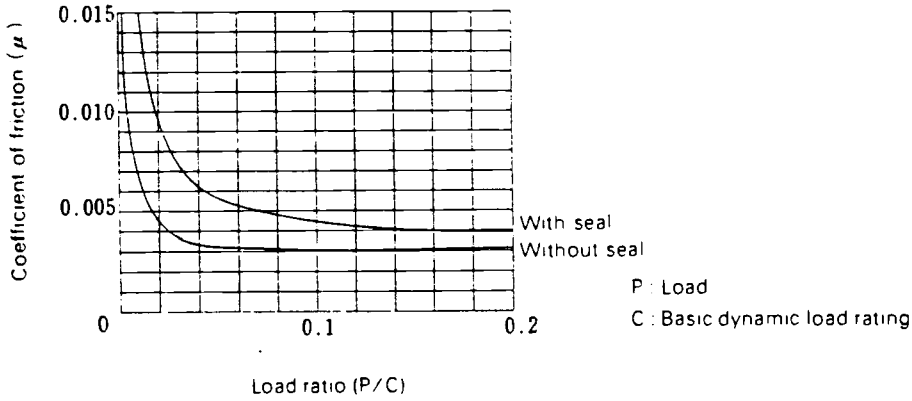

Figure 5.2.1 Load versus friction relationship for linear bearings

Best scan available for table.

Table 5.2.1 Manufactures data on THK linear motion bearing

THK type HSR-TA/HSR-HTA

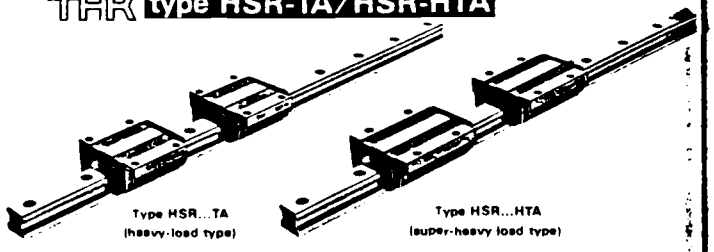

Model No	LM block dimensions mm: Width W	B	B_1	Length L	C	Height M	S×l	A	T	T_1	K	L_1	N	E	Grease nipple
HSR 15TA	47	38	4.5	53.5	30	24	M 5 × 11	12.2	7	11	19.4	40.5	4.5	5.5	Drive-in nipple
HSR 20TA	63	53	5	70	40	30	M 6 × 10	14.5	10	10	25	50	5	12	B-M6F
HSR 20HTA	63	53	5	86	40	30	M 6 × 10	14.5	10	10	25	66	5	12	B-M6F
HSR 25TA	70	57	6.5	79	45	36	M 8 × 16	18	10	16	29.5	59	6	12	B-M6F
HSR 25HTA	70	57	6.5	103	45	36	M 8 × 16	18	10	16	29.5	83	6	12	B-M6F
HSR 30TA	90	72	9	94	52	42	M10 × 16	22	10	18	35	72	7	12	B-M6F
HSR 30HTA	90	72	9	116	52	42	M10 × 18	21	10	18	35	94	7	12	B-M6F
HSR 35TA	100	82	9	107	62	48	M10 × 21	24	13	21	40	81.3	8	12	B-M6F
HSR 35HTA	100	82	9	134	62	48	M10 × 21	24	13	21	40	110	8	12	B-M6F
HSR 45TAX	120	100	10	139	80	60	M12 × 15	30	14	25	50	98	10	16	B-PT 1/8
HSR 45HTA	120	100	10	171	80	60	M12 × 15	30	14	25	50	130	10	16	B-PT 1/8
HSR 55TAX	140	116	12	163	95	70	M14 × 17	36	15	29	57	118	11	16	B-PT 1/8
HSR 55HTA	140	116	12	201	95	70	M14 × 17	36	15	29	57	156	11	16	B-PT 1/8
HSR 65TAX	170	142	14	186	110	90	M16 × 23	43	23	37	76	147	19	16	B-PT 1/8
HSR 65HTA	170	142	14	246	110	90	M16 × 23	43	23	37	76	207	19	16	B-PT 1/8
HSR 85TA	215	185	15	247	140	110	M20 × 30	51	30	55	94	179	23	16	B-PT 1/8
HSR 85HTA	215	185	15	303	140	110	M20 × 30	51	30	55	94	236	23	16	B-PT 1/8

Note: The grease nipple for the type HSR 15TA is a straight Drive-in nipple type.

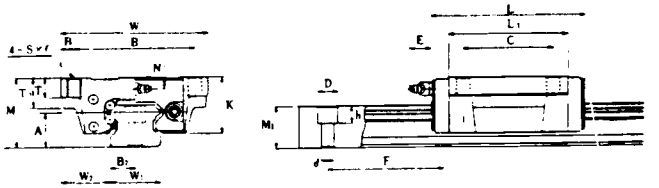

Width W	LM rail dimensions mm: W_1	B_2	Height M_1	d×D×h	Pitch F	Basic load rating: C kgf	C_0 kgf	Static permissible moment: M_A kgf·m	M_B kgf·m	M_C kgf·m	Weight: LM block kgf	LM rail kgf/m	Model No
15	16	7.5	15	4.5×7.5×5.3	60	760	1150	6.0	6.0	8.4	0.2	1.5	HSR 15TA
20	21.5	10	18	6×9.5×8.5	60	1230	1790	11.7	11.7	17.4	0.35	2.3	HSR 20TA
20	21.5	10	18	6×9.5×8.5	60	1900	2380	20.2	20.2	23.2	0.47	2.3	HSR 20HTA
23	23.5	11.5	22	7×11×9	60	1770	[illegible]	[illegible]	20.2	29.4	0.59	3.3	HSR 25TA
23	23.5	11.5	22	7×11×9	60	2420	3440	34.4	34.4	38.1	0.75	3.3	HSR 25HTA
28	31	14	26	9×14×12	80	2500	3510	32.2	32.2	48.4	1.1	4.8	HSR 30TA
28	31	14	26	9×14×12	80	3320	4680	54.7	54.7	64.5	1.3	4.8	HSR 30HTA
34	33	17	29	9×14×12	80	3320	4580	48.1	48.1	77.0	1.6	6.6	HSR 35TA
34	33	17	29	9×14×12	80	4470	6110	81.7	81.7	102.9	2.0	6.6	HSR 35HTA
45	37.5	22.5	38	14×20×17	105	5350	7170	93.8	93.8	156.8	2.8	11.0	HSR 45TAX
45	37.5	22.5	38	14×20×17	105	7170	9550	159.6	159.6	208.9	3.3	11.0	HSR 45HTA
53	43.5	26.5	44	16×23×20	120	7890	10300	162.2	162.2	[illegible]	4.3	15.1	HSR 55TAX
53	43.5	26.5	44	16×23×20	120	10600	13800	275.7	275.7	363.7	5.7	15.1	HSR 55HTA
63	53.5	31.5	53	18×26×22	150	12600	16100	316.7	316.7	497.6	8.5	22.5	HSR 65TAX
63	53.5	31.5	53	18×26×22	150	17100	21500	538.4	538.4	664.5	10.7	22.5	HSR 65HTA
85	65	42.5	65	24×35×28	180	18700	23200	762.1	762.1	942.8	17.0	35.2	HSR 85TA
85	65	42.5	65	24×35×28	180	25200	30900	930.6	930.6	1255.0	23.0	35.2	HSR 85HTA

Note: M_A, M_B, and M_C are the permissible moment values for one LM block shown at the right.

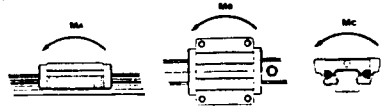

Considering that this severe loading case will not exist in actual use and that the nominal life L is a cubic function of the loading the actual service life will most likely be greater than 1000 hours of use before any measurable decay in bearing performance can be detected. If a more detailed and accurate estimate reveals that this particular bearing is under sized a larger model can be easily incorporated into the design. These bearings are offered with chrome plating to further increase service life and resistance to a corrosive environment.

The dynamic friction force F of the loaded carriage structure can be estimated from Equation (5.2.3) where μ is the friction coefficient and P is the radial load on the bearing.

$$F=\mu P \tag{5.2.3}$$

Figure (5.2.1) shows the relationship between load and friction coefficient. With a maximum load L of 3120 Kgf and a dynamic load rating C of 10600 Kgf the friction coefficient for unsealed bearings is 0.003 and the friction force per bearing is 9.4 Kgf. With four bearings the total friction force is 37 Kgf. This small force, approximately 1% of the load P, justifies neglecting friction of the bearing in Chapter 2.

The support structure for the bearing rail has two major components. The first component supports the rail on the side of the wave channel that does not involve the cable drive system. This structure is to run parallel to the east side of the wave channel and span the middle 70 m as seen in Fig. (5.1.1). A typical cross Section

of this structure can be seen in Fig. (5.2.2). The triangular support frame constructed of rectangular tubing, secures an I-beam. Each triangular support is rigidly attached to a foundation. This I-beam is attached to the support frame with bolts and shims. The shims will allow alignment of the I-beam in both the vertical and horizontal directions to help meet the precise alignment needs of the bearing rail. The bearing rail is shimmed to the I-beam for further alignment capability. Figure (5.2.3) shows a typical length of the rail and support structure. With the given spacing between supports the maximum deflection of the rail with the 3120 kgf vertical bearing load is less than 0.15 mm.

The second component of the support structure for the bearing rail is similar to the above with the exception of the cable housing. This structure which runs parallel to the west side of the wave channel must , in addition to provide support for the bearing rail, provide a housing for the drive cable that motivates the carriage structure.

Figure (5.2.4) shows a typical cross Section of the support structure and rail. This structure has the same features as the previously discussed structure with the addition of the cable housing both above and below the rail. The lower housing limits the whip of the return cable. This housing has an access plate on the left side as shown. The inside of the housing is lined with a graphite filled nylon liner to reduce cable wear and vibration as the cable whips either vertically or horizontally.

The upper cable housing performs a similar function for the upper or drive side of the cable. This housing has an opening on the right

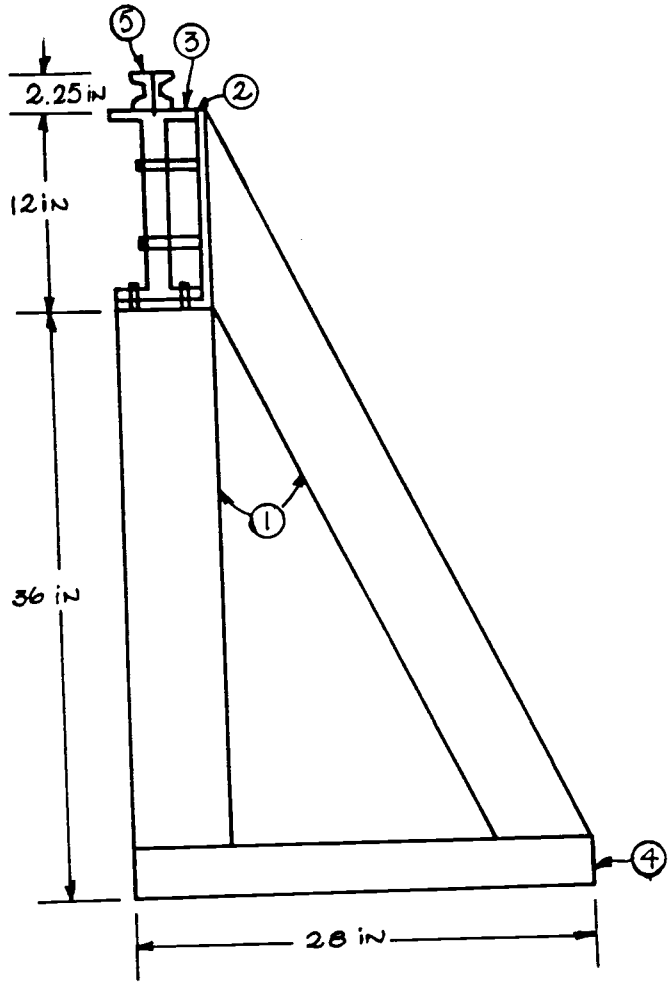

① Rectangular steel tubing 6" x 3" x 1/4"

② Angle steel L 12" x 6" x 1/2 "

③ I-beam S 12x50 12" depth - 5 1/2" width

④ Square steel tubing 3" x 3" x 1/4"

⑤ Bearing rail THK model HSR-55 HTA

Scale: 1:10 in
1 in = 2.54 cm

Figure 5.2.2 Typical cross-section of rail support

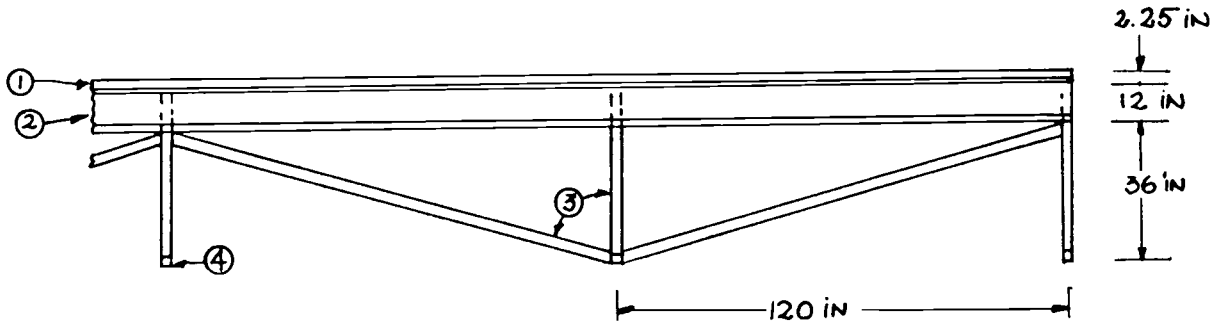

FRONT VIEW

① Bearing rail THK model HSR-55 HTA

② I-beam S12x50 12" depth - 5 1/2" thickness

③ Rectangular Steel tubing 6" x 3" x 1/4"

④ Square steel tubing 3" x 3" x 1/4"

Scale: 1:40 in
1 in = 2.54 cm

Figure 5.2.3 Typical length section of rail support

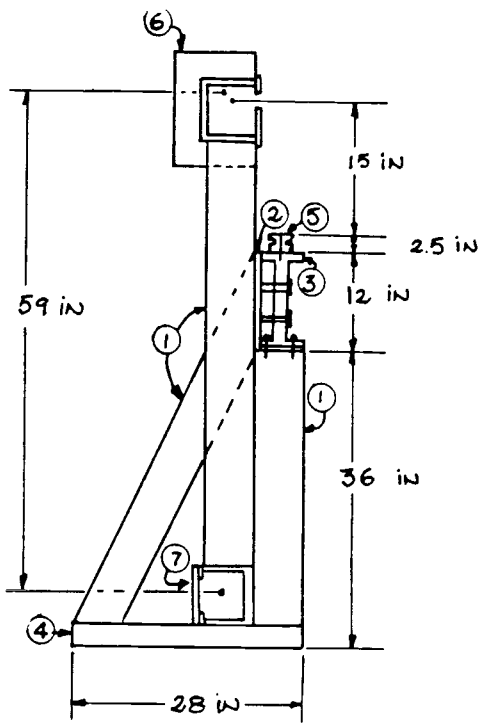

① Carbon steel rectangular tube 6" x 3" x 1/4"

② Carbon steel Angle L12" x 6" x 1/2"

③ Carbon steel I-beam S12x50

④ Carbon steel square tube 3" x 3" x 1/4"

⑤ Bearing rail THK model HSR-55 HTA

⑥ Upper wire rope housing

⑦ Lower wire rope housing with inspection plate

Scale: 1:20 in
1 in = 2.54 cm

Figure 5.2.4 Typical cross-section of cable side rail support

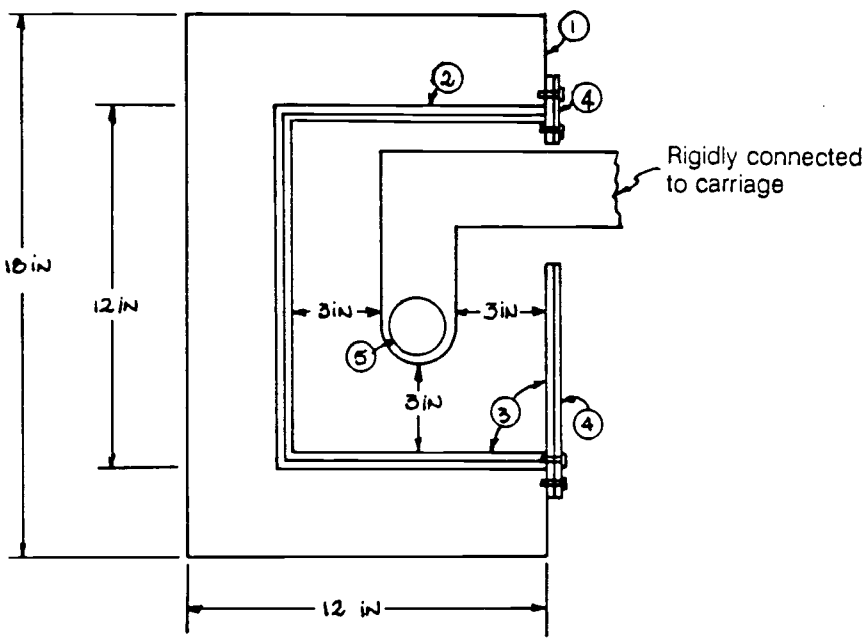

① Reinforcement webbing 1/4" thick carbon steel plate

② Carbon steel channel 12" x 8" x 3/8"

③ Graphite Filled Nylon liner

④ Revovable cover plate

⑤ 1 3/8" wire rope 6x19 Class

Figure 5.2.5 Exploded view of cable guide

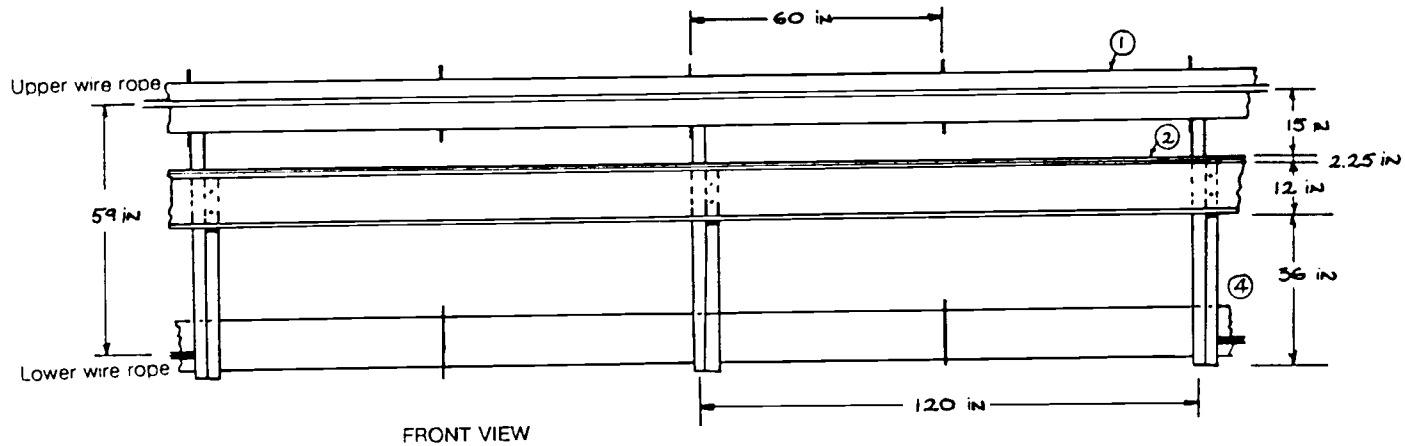

① Upper wire rope housing

② Bearing rail HSR-55 HTA

③ I-beam rail support S12 x 50

④ Lower wire rope housing

Scale: 1:30 in
1 in = 2.54 cm

Figure 5.2.6 Typical length section of cable side guide rail

side that runs the length of the guide rail. Figure (5.2.5) shows an exploded view of the upper cable housing. The open slot allows a rigid arm from the carriage structure to attach to the cable. The right face may be removed for maintenance of the polymer lining. Figure (5.2.6) shows a typical length of the support structure. Both the upper and lower cable housings has reinforcement webbing spaced every 5 ft. to add rigidity.

5.3 Power Train

The power train is composed of three major components, 1) the driver drum, 2) the cable guidance system , and 3) the power source. As mentioned in Section 3.1 the driver drum is a 1.5 m diameter drum with a width of 0.67 m . The cable is wrapped for 13 active wraps and 3 dead wraps. One span of the cable leaves the top of the drum and the other leaves the bottom. As the carriage structure is moved closer to the drum, the upper span of the cable is wrapped onto the drum and the lower span is paid out thus keeping a total of 16 wraps on the drum at all times. For reverse motion of the carriage structure the upper span pays out and the lower span takes up. The detailed design of the driver drum and bearing support is left for a manufacture such as Superior-Linderwood-Mundy Corp.[1]

A typical driver drum has helixed grooves on the cable bearing surface to aid in positioning the cable as it is wrapped and unwrapped. This works fine for the slow operating speeds typically encountered in

---

[1] Superior-Linderwood-Mundy Corp., 1101 Jolan Ave., Superior, Wisconsin, 54880

cable drum systems. However, this particular system is going to be operated at much higher speeds than a typical system, up to 245 rpm. It is unlikely that a grooved drum alone could guide the cable as it wraps and unwraps at these high speeds. In order to stabilize the cable motion as it wraps and unwraps from the drum an active cable guidance device has been conceptualized.

Figure (5.3.1) shows a front view of the active cable guide. This device has an active guide for both the upper and lower cables that allows controlled horizontal motion only. This motion is guided by a pair of linear motion bearings (THK model LBH 50). Figure (5.3.2) shows an individual guide which is composed of a front set of small rollers that limit vertical cable motion and a rear set that limits horizontal cable motion relative to the guide. Each of these two guides are attached to a pair of linear motion bearings and a hydraulic cylinder. The cylinder positions the guides such that the cable is properly fed or paid out from the driver drum via a feedback control system.

Instead of using hydraulic cylinders to position the cable guides, a mechanical system directly coupled to the drum could be used. The hydraulic approach offers the advantage of incorporating a speed dependent lag or lead in the response to system needs. This is merely a conceptual design and will need further refinement by an experienced hydraulic engineer.

A large power source is needed to drive the system. Good to excellent control of the power is required over a range of tens to hundreds of kilowatts to meet the desired performance and safe operation of the system. Internal combustion, electric, and

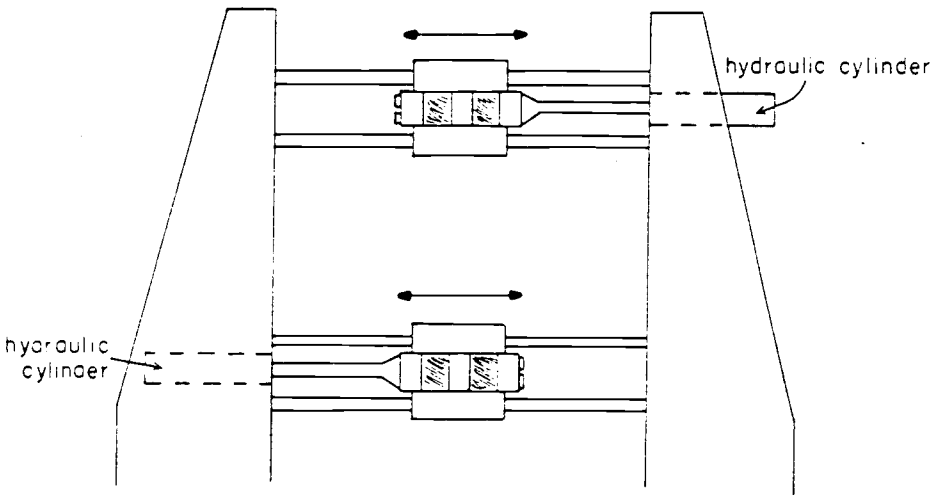

Figure 5.3.1 Cable guide frame

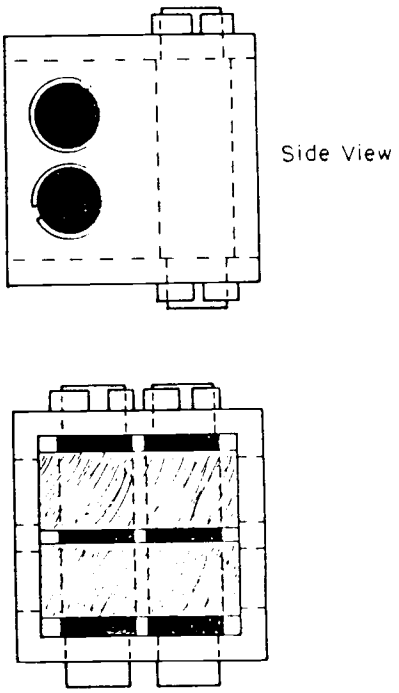

Figure 5.3.2 Individual cable guide

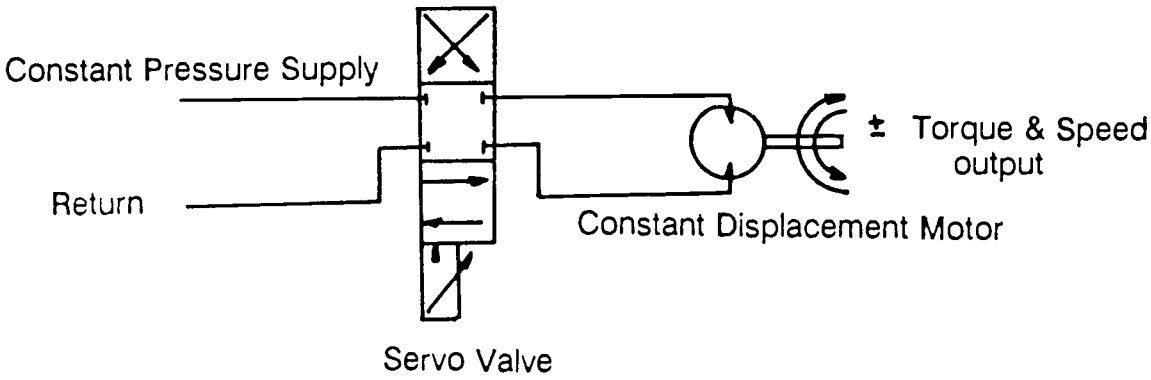

Figure 5.3.3 Simplified schematic of servovalve controlled motor

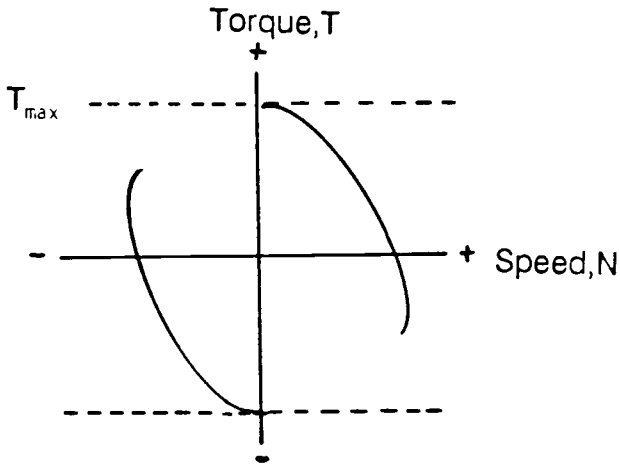

Figure 5.3.4 Torque response of servo valve controlled motor

hydraulicpower systems are all capable of delivering the needed power, although only electric and hydraulic systems are capable of providing the control response needed. This paper examines a conceptual hydraulic system.

Two common methods of hydraulic power control are servovalve controlled hydraulic motors and secondary control hydrostatic drives. Both methods use a constant pressure source,typically a fixed or variable displacement pump powered by an electric motor. Figure (5.3.3) shows a schematic diagram of a typical servovalve controlled hydraulic motor with the torque vs. speed output performance shown in Fig. (5.3.4). This system uses a servovalve to throttle the flow and hence fluid power from the pump to the motor. The servovalve causes an appreciable amount of lost power as can be seen in the sharp decrease in torque with increasing motor speed.

The secondary control hydrostatic drive uses a variable displacement motor, as opposed to the fixed displacement motor for the servovalve system, controlled by a hydraulic control cylinder as can be seen in the simplified schematic in Fig. (5.3.5). Only a small amount of flow is channeled through the pilot control valve thus decreasing flow power losses substantially. The output torque response is more linear and efficient than the servovalve controlled motor as can be seen in Fig. (5.3.6).

A summary of the advantages and disadvantages of each method can be found in Table (5.3.1). Comparing these two methods the servovalve system has a very fast response and a wide dynamic range at the cost of efficiency. The hydrostatic drive is somewhat slower in response

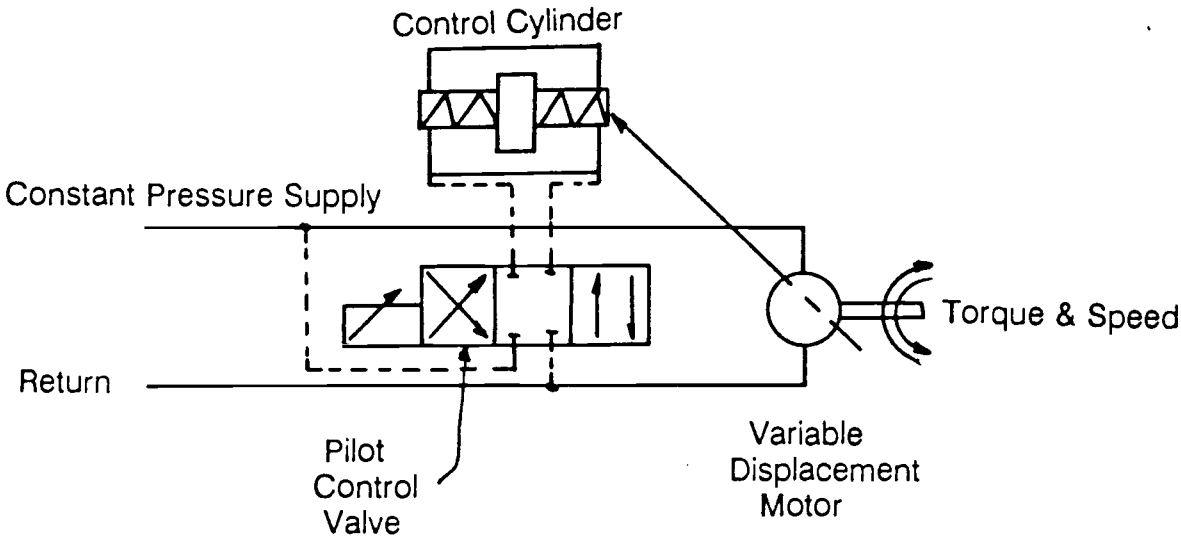

Figure 5.3.5 Simplified schematic of secondary controlled hydrostatic drive

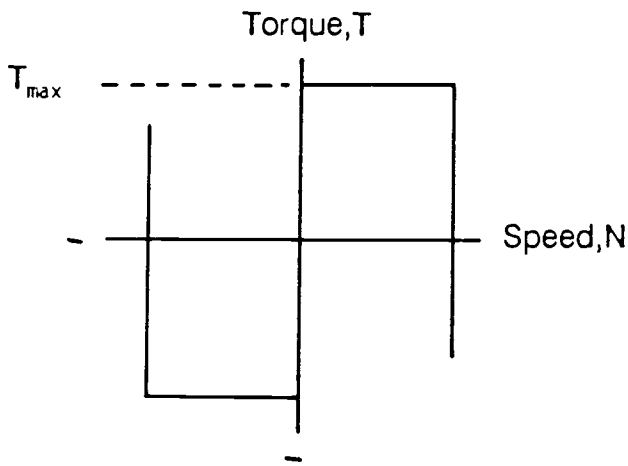

Figure 5.3.6 Torque response of secondary controlled hydrostatic drive

Table 5.3.1 Summary of performance characteristics of servovalve controlled motors and secondary control hydrostatic drives.

<u>Servovalve controlled motor</u>

Advantages: Faster response time

flow from zero to full volume in milliseconds

small signal response of valve/motor

Wide dynamic range

velocity range of > 100:1

Disadvantages: Efficiency

for damping loads approximately 40% of available peak power is dissipated in servovalve throttling thus a bigger motor and pump are required

velocity range of approximately 50:1

<u>Secondary control hydrostatic drive</u>

Advantages: Efficiency

no loss at servovalve so smaller motor and pump can be used

Disadvantages: Slower response time

zero to full volume in approximately 0.25 seconds

Narrower dynamic range

time and has a narrower dynamic range. The slower response time is not a major concern because most operating periods are greater than 2 seconds and a 0.25 second response time should prove adequate. The major tradeoff is between the wide dynamic range of the servovalve system and the high efficiency of the hydrostatic system. Due to the large power requirements of the tow carriage system and the high cost of hydraulic power systems the efficiency of the hydrostatic drive may outweigh the reduction in dynamic range.

In order to size the hydrostatic drive the operating range of the driver drum must be estimated. The tow carriage system must operate at high speed/low torque for small tow specimens and low speed/high torque for large tow specimens. Referring to Table (3.2.2) the operating range of the smallest tow specimen has a minimum speed and torque of 3.1 m/s and 16.7 kN-m and a maximum speed and torque of 17.1 m/s and 21.1 kN-m. The largest specimen has a minimum speed and torque of 3.1 m/s and 32.9 kN-m and a maximum speed and torque of 8.3 m/s and 36.6 kN-m. Table (5.3.2) summarizes these operating ranges with both carriage velocity and driver drum velocity.

With the load characteristics of the driver drum specified an appropriate hydraulic motor must be selected. One of the larger commercially available hydraulic motors is the Rexroth AA2FM. This motor and sister pump both have a 250 cm^3/rev variable displacement with a maximum speed of 2000 rpm and power capability of 255 kW. The maximum recommended operating pressure is 400 bar (5800 psi). Due to plumbing limitations an operating pressure of 293 bar (4100 psi) is a more practical limit.

The available torque at the motor shaft T_M can be estimated by Equation (5.3.1) where η is the volumetric efficiency of the motor and plumping, ΔP is the operating pressure and V is the volume displacement of the motor.

$$T_M = \eta \Delta P V \tag{5.3.1}$$

Using the recommended value of 0.85 for η (Bushey, 1988), the maximum available torque is 957 n-m (705 ft.-lbs.) per motor. With a gear reduction of 10:1 between the motors and the driver drum the small tow specimen operating range can be nearly met by running two motors in parallel at a maximum motor speed of 2000 rpm. This would require a fluid power source of 264 gal/min at 4100 psi or 471 kW (632 hp) at the pumps. Two of the above mentioned pumps running at 2000 rpm could provide this power. The maximum driver drum speed and torque is 200 rpm and 19.14 kN-m. For the large tow specimen operating range running four motors at a maximum speed of 1000 rpm will develop 38.3 kN-m at 100 rpm at the driver drum using an equivalent source. A 700 hp electric motor could be used to power the pumps, running one pump at each end of the motor output shaft.

Figure (5.3.7) shows the conceptual layout of this power train system minus the pumps and electric motor. The four hydraulic motors are connected to an idler shaft through electromagnetic clutches. The clutches will allow one to four motors to be operated at any time. This in combination with the variable displacement pumps and motors will

Table 5.3.2 Operating range of driver drum

Specimen dia. (m)	Carriage Vel. (m/s)	Drum speed (rpm)	Drive torque (kN-m)
0.0254	3.1	44	16.7
	17.1	244	21.1
0.6096	3.1	44	32.9
	8.3	118	36.6

1 - 250 cm^3/rev variable displacement hydraulic motor
2 - 1000 ft. lb. electromagnetic clutch
3 - 3" dia. - pillow block bearing
4 - 4 1/2 dia. - pillow block bearing
5 - 3/4" pitch 4" wide high velocity link chain
6 - 1" pitch 4" wide high velocity link chain
7 - 3/4" pitch 27 teeth sprocket 4" wide
8 - 3/4 " pitch 45 teeth sprocket 4" wide
9 - 1" pitch 29 teeth sprocket 4" wide
10 - 1" pitch 174 teeth sprocket 4" wide
11 - 4 1/2" solid carbon steel shaft

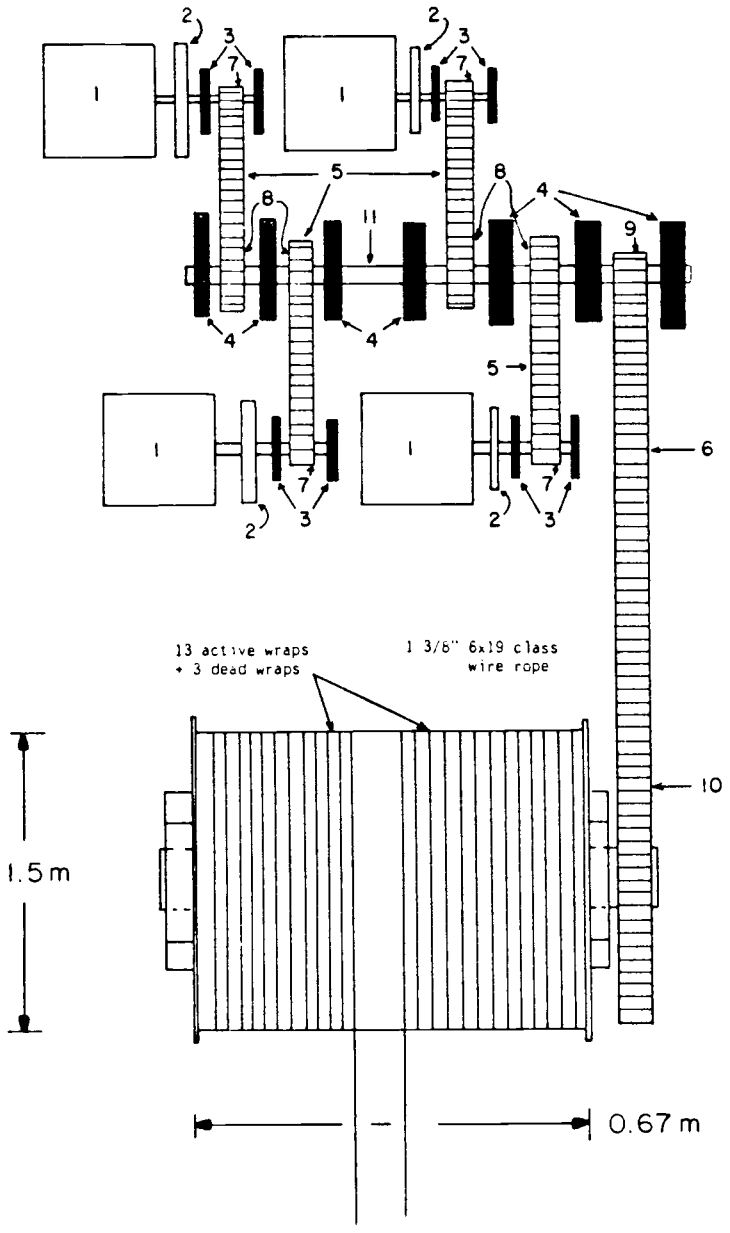

Figure 5.3.7 Top view of conceptual layout of drive train

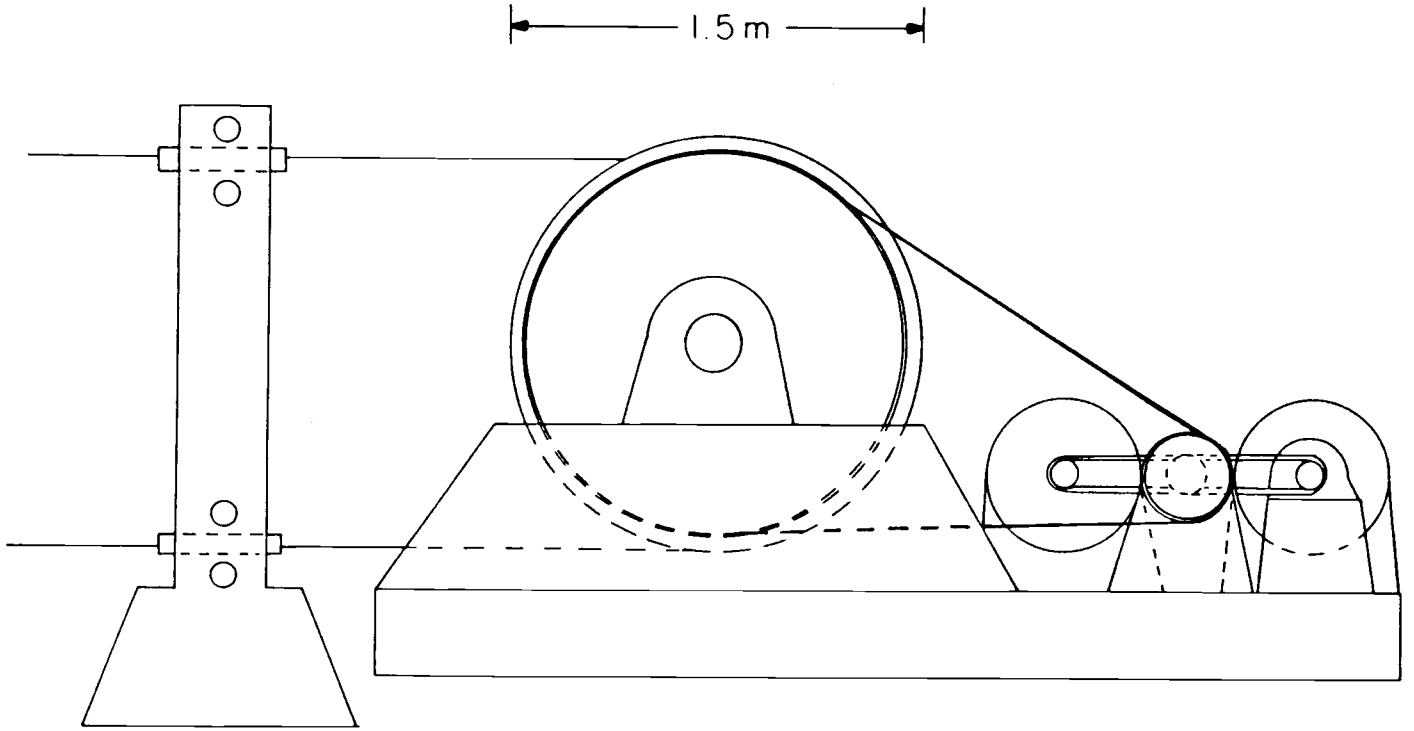

Figure 5.3.8 Side view of conceptual layout of power train

give the system a very broad and controllable operating range. The idler shaft transfers the power to the driver drum with a 10:1 gearreduction. High velocity link chain is used to efficiently transfer the large torque loads. Figure (5.3.8) shows a side view of the power train and cable guidance system.

5.4 Primary Idler Pulley

The primary idler pulley has two main functions, first it provides the bearing that returns the cable back to the driver drum and second it provides an adjustable preload tension on the cable. The first function is met by a simple pulley wheel mounted with the axis of rotation horizontal and perpendicular to the plane of the two cable spans. The wheel is 1.5 m in diameter and 7 cm thick with a groove around the circumference to stabilize the cable motion.

The preload function is provided by mounting the pulley wheel on a rigid carriage. This carriage is attached to linear motion bearings that only allow one direction of motion. As the carriage moves along the bearing the cable tension is either increased or decreased. Figure (5.4.1) shows a conceptual layout of the carriage that holds the pulley wheel. Figure (5.4.2) shows a blow up of the bearing housings. Since the motion of this carriage when the system is in use is very limited, on the order of a few millimeters, the bearings need not be very precise. In fact a loose fit would greatly reduce the possibility of jamming. The inside of the bearing housing is to be lined with a graphite filled polyamide. This material has both a substantially higher pressure-velocity rating and cost relative to the graphite

filled nylon used in the cable housing on the tow carriage guide rail supports.

Figure (5.4.3) shows an over view of the primary idler pulley. The pulley wheel carriage bears against round steel tubing which attaches to the two reinforced concrete support blocks . The support blocks are in turn fixed to the ground. Two 5 in. diameter hydraulic cylinders provide the preload on the cable with an active length of 24 in. to compensate for cable sag and stretch. These cylinders can be relaxed when the system is not in use. They will also be useful for prestretching new cable. The cable is stabilized by a roller cable guide on both top and bottom spans similar to the guides used for the cable guidance system of the driver drum.

5.5 Secondary Idler Pulley

Since the existing unidirectional wave channel is enclosed, space is limited for installing the tow carriage system. Secondary idler pulleys are used to position both the primary idler and driver drum to minimize wasted space as shown in Fig. (5.1.1). A total of four secondary idler pulleys are required, each one changing the direction of the cable by 90 degrees.

These pulleys are simple grooved pulley wheels 30 in. in diameter and 7 cm in thickness. The cable only partially wraps around these pulleys which reduces the required minimum diameter ratio.

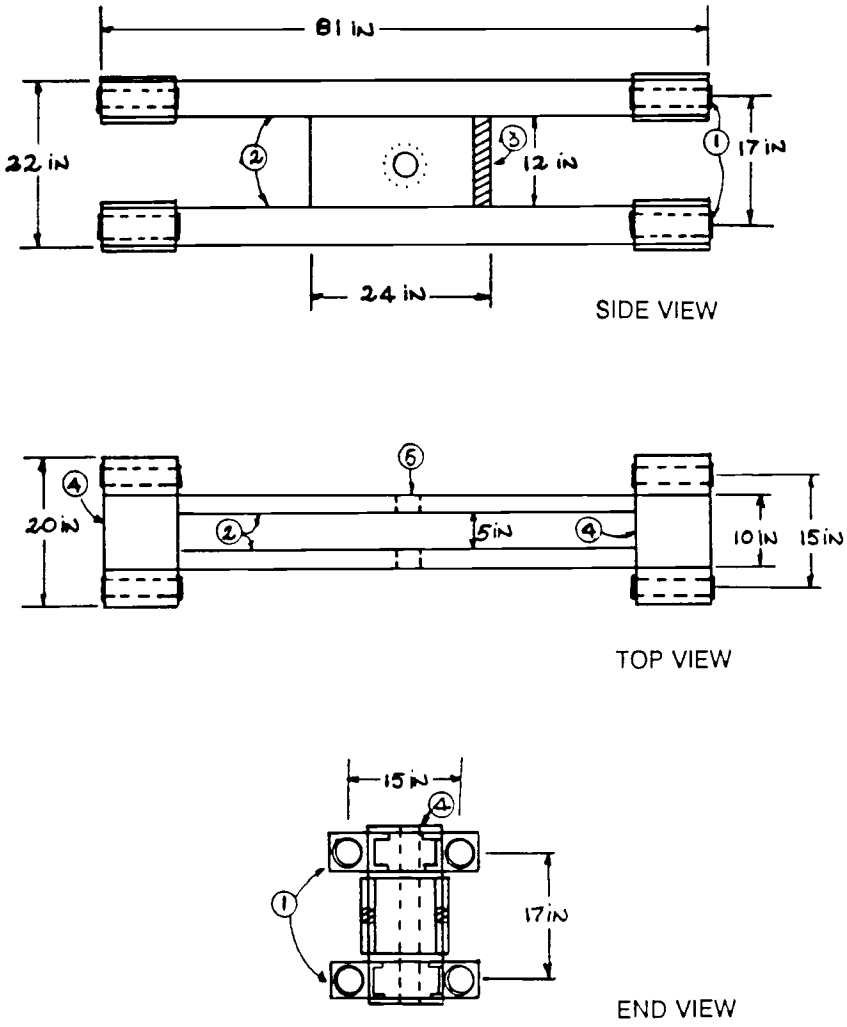

① Bearing housing

② Steel channel 5" x 2" x 1/4"

③ Pulley hub 1/2" thick steel plate with hydraulic cylinder bearing

④ 1/4" steel plate

⑤ Spindal axis for 3" axial roller bearing

Scale: 1:20 in
1 in = 2.54 cm

Figure 5.4.1 Primary idler pulley carriage design

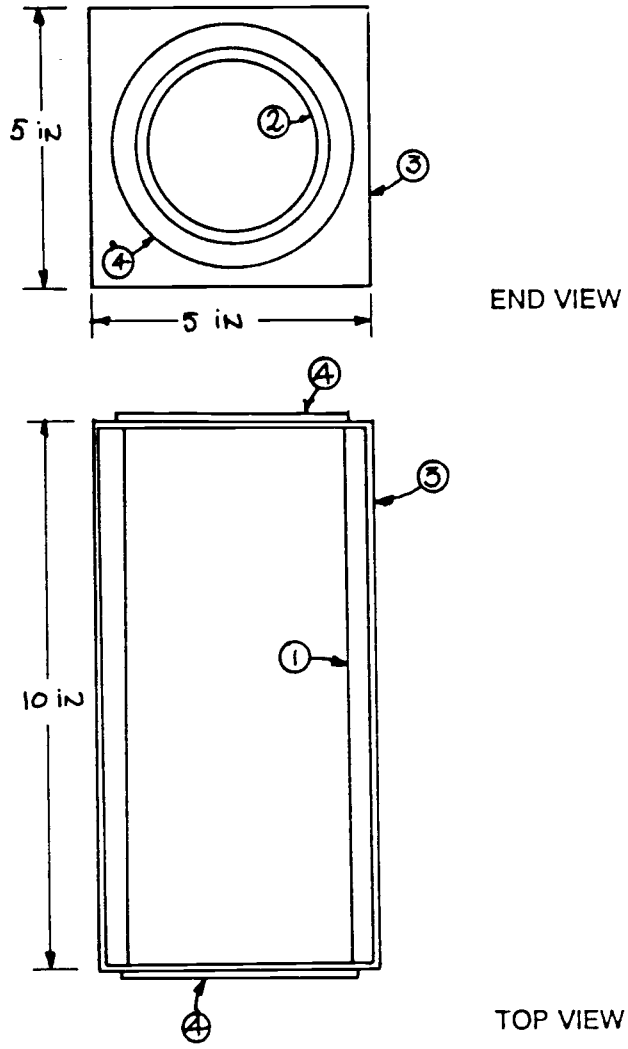

① Carbon steel Round tubing 4" O.D. 3.625 I.D.
Cold drawn seamless

② Graphite Filled Polymide bearing 3.6" O.D. 3.15" I.D.

③ Carbon steel rectangular tubing 10" x 5" x 1/4"

④ Bearing retainer thread onto tube and set with screw

Scale: 1:30 in
1 in = 2.54 cm

Figure 5.4.2 Exploded view of primary idler carriage rail bearing

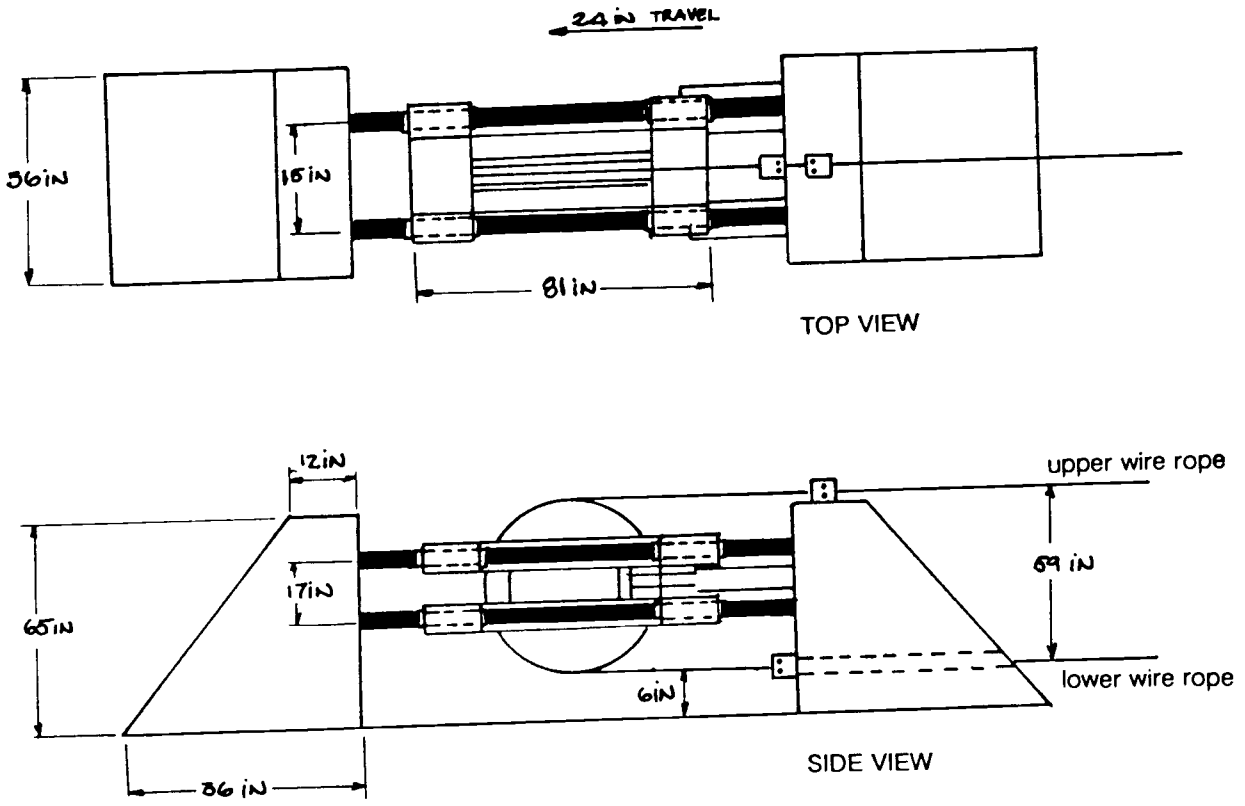

① Carbon steel Round tubing 3 1/4" O.D. 2 1/4" I.D. Cold drawn seamless

② Hydraulic cylinders 5" diameter 24" travel

③ Wire rope guide

④ Idler pulley 59" nominal diameter 3" axial with roller bearing

⑤ Reinforced concrete support block

Figure 5.4.3 Conceptual design of primary idler pulley

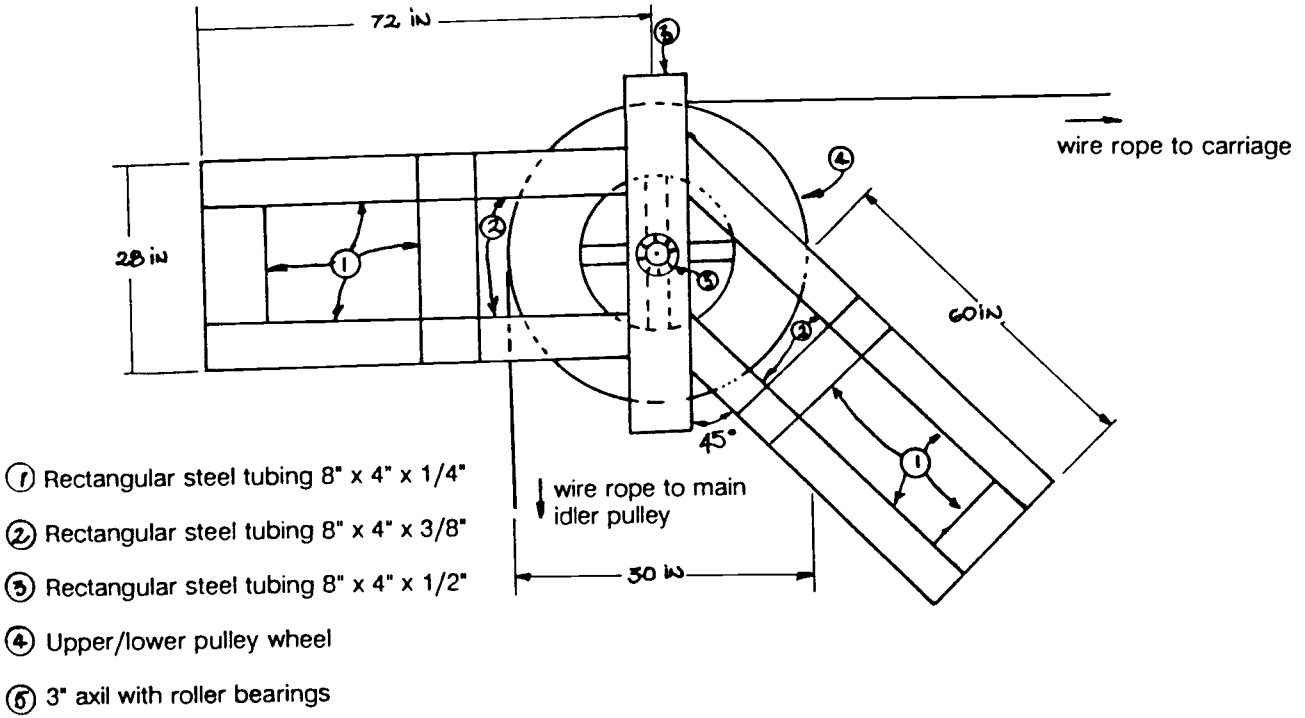

Figure 5.5.1 Top view of secondary idler pulley

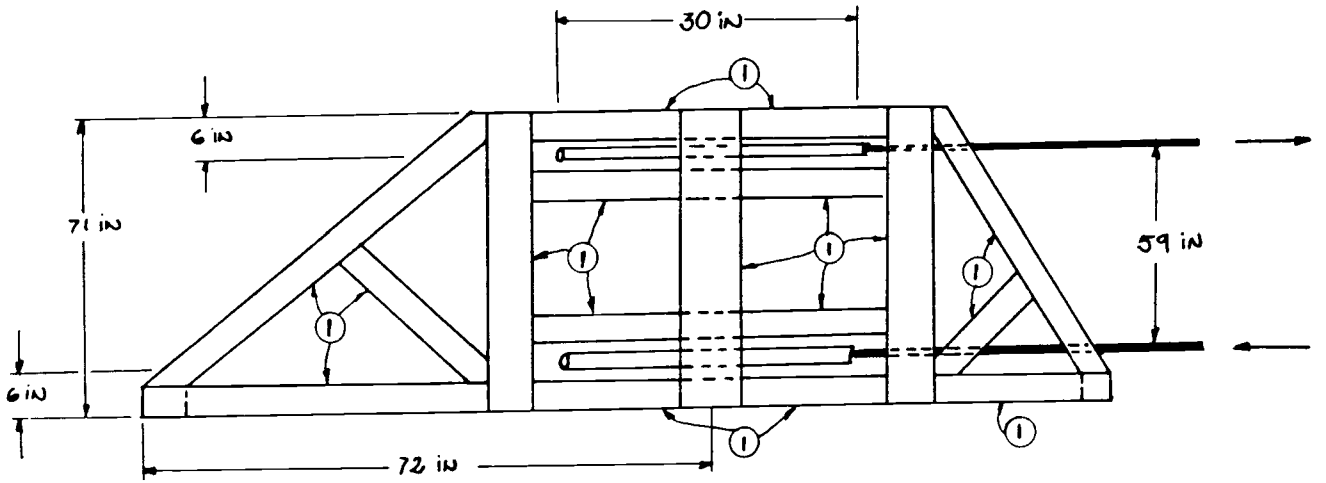

SIDE VIEW

(1) 6" x 3" x 3/8" rectangular steel tubing

Figure 5.5.2 Side view of secondary idler pulley

Each pulley has two wheels which are mounted with their axis of rotation in the vertical direction. Each wheel moves independently of the other. The upper wheel provides a bearing for the upper cable span and the lower wheel provides a bearing for the lower cable span. Each wheel is attached to a rigid support frame which in turn is secured to the ground. The secondary idler closest to the driver drum also provides stabilization of the cable motion as it traverses the width of the drum. Fig.s (5.5.1) and (5.5.2) show top and side views respectively of the conceptual layout for the secondary idler pulleys.

5.6 Total System Cost Estimation

The complete feasibility study for the dynamic tow carriage system consists of three major parts, 1) the mathematical model which quantifies system performance, 2) the conceptual design that could fulfill the desired performance, and 3) a cost estimation of the design. The first two components have been covered in detail in Chapters 2-5. The remainder of this chapter briefly covers a cost estimate of the total system.

The cost estimate is divided into five parts, 1) the drive train, 2) the carriage guidance, 3) the primary idler pulley ,4) the secondary idler pulley, and 5) the carriage structure. A summary of the cost estimate is presented seen in Table (5.6.1).

<u>Drive Train:</u> From Table (5.6.1) the drive train is divided into four components, 1) the drive drum and support, 2) the active cable guide that positions the cable on the drum, 3) the power system ,and 4) engineering and assembly. The drive drum and support cost estimate was

attained from Superior-Linderwood-Mundy Corp. The cable guide cost was estimated by the various components that make up the device by contacting suppliers of each component. Engineering and assembly costs were estimated by the author. This latter cost mainly involves coordinating the hydraulic controls of the drive train.

Carriage Guidance: The carriage guidance system is composed of the guide rail bearings and the support structure. The cost estimate for the system is composed of materials and engineering and assembly. The cost of the guide rail is an upper estimate from THK. The support structure costs were estimated by determining the needed steel from the conceptual design in Section (5.2) and then contacting a supplier for costs. Engineering and assembly costs were estimated by the author.

Primary Idler Pulley: The primary idler pulley cost estimate was developed by estimating the required materials from Section (5.4) and contacting suppliers for an upper cost estimate. Again the engineering and assembly costs were estimated by the author.

Secondary Idler pulley: The cost estimate for the secondary idler pulleys was developed by estimating the materials, engineering, and labor cost for one pulley, in a similar manner to the primary idler pulley, and then multiplying by four to get total cost.

Carriage Structure: Material costs for the carriage structure cab be divided into two components,the first being the round aluminum tubing of the space frame and the second being the aluminum hydrofoil specimen support struts. A quantity estimate of tubing was determined from the finite element model of Section (4.4) and a supplier provided a cost estimate. The hydrofoil support struts cost was estimated from an

airplane wing of similar size. Engineering and assembly costs were estimated by the author.

Table 5.6.1 Cost estimation of total system

Drive Train

A. Drive drum and support	
1-(1.5 m dia.,0.67 m width grooved for 1 3/8"cable)	$30,000
B. Cable guidance	
2-(1 1/2" dia. hydraulic cyld., 24"stroke)	$300
4-(linear motion bearings,THK LBH50)	$2,000
1-(steel support frame)	$500
C. Power	
2-(Rexroth model AA4VSG series 10 ,250 cm^3/rev pump w/control)	$19,068
4-(Rexroth model AA2FM series 10 ,250 cm^3/rev motor w/control)	$12,324
1-(Bouge electric motor 7110 CS 700 hp)	$20,000
4-(Pitts model F-49 electromagnetic clutch)	$5,416
1-(Bethlehem steel wire rope 1 3/8" dia. 6X19 Seale IWRC 1000 ft.)	$3,580
D. Engineering and assembly	$15,000
Sub-total	$108,188

Carriage Guidance

A. Materials	
1-(THK HSR 55HTA linear motion bearing 140 m)	$40,000
1-(S12X50 I-beam 460 ft.)	$10,258
1-(6"X3"X1/4" steel tube 1035 ft.)	$6,334
1-(3"X3"X1/4" steel tube 107 ft.)	$416
1-(6"X6"X1/4" steel channel 460 ft.)	$2,415
1-(12"X6"X1/4" steel channel 230 ft.)	$1,656
B. Engineering and assembly	
Labor (240 hrs @ $14.00/hr.)	$3,360
Engineering	$10,000
Sub-total	$74,440

Primary Idler Pulley

A. Materials	
1-(5"X2"X1/4" steel channel 40 ft.)	$185
2-(12"X24"X1/2" steel plate)	$100
4-(10"X10"X1/4" steel plate)	$135
1-(3"X1/2" Seamless round tubing 27 ft.)	$211
1-(1.5m dia. 7cm thick pulley wheel w/bearings)	$3,500
2-(5"dia. 24" stroke hydraulic cylinder)	$1,300
2-(reinforced concrete support blocks key into ground)	$1,800
B. Engineering and assembly	
Labor (80 hrs @ $14.00/hr.)	$1,120
Engineering	$5,000
Sub-total	$13,356

Table 5.6.1 (continued)

Secondary Idler Pulley

A. Materials	
1-(8"X4"X1/8" steel tube 72 ft.)	$487
1-(8"X4"X3/8" steel tube 20 ft.)	$254
1-(8"X4"X1/2" steel tube 24 ft.)	$427
2-(76.2cm dia. 7cm thick pulley wheel w/bearings)	$5,600
B. Engineering and assemble	
Labor (60 hrs @ $14.00/hr.)	$840
Engineering ($5,000 total or $1,250 per pulley)	$1,250
Sub-total per pulley	$8,858
Sub-total	$35,432

Carriage Structure

A. Materials	
1-(2 1/2" dia. 1/8" thick aluminum tubing 6061 T6511 400 ft)	$1,978
1-(5" dia. 1/8" thick aluminum tubing 6061 T6511 200 ft.)	$2,085
2-(Vertical specimen support aluminum 36"X5" hydrofoil 19 ft long)	$5,000
1-(Horizontal specimen support aluminum 36"X3" hydrofoil 10 ft long)	$1,500
B. Engineering and assembly	
Labor (320 hrs @ $14.00/hr)	$4,480
Engineering	$10,000
Sub-total	$25,043

Total system cost $256,460

6.0 Conclusions

6.1 Summary

The purpose of this research study is to demonstrate that a dynamic tow carriage is feasible and to develop a conceptual design. The function of the design is to illustrate the feasibility analysis and is not necessarily a final design for the optimum dynamic tow carriage.

The conceptual design consists of a lightweight yet rigid space frame used to support a hydrodynamic tow specimen. The frame or carriage is rigidly supported by high speed, low friction linear motion bearings that allow the carriage and specimen to move along the length of the wave channel. The carriage/specimen is propelled by a cable/pulley/drum reeving which in turn is powered by a hydrostatic drive system. A mathematical model of the tow carriage system predicts the carriage and specimen can be driven to speeds in excess of 55 ft/sec and accelerations of 1 g over a 200 ft stroke. With cylindrical test specimens having a length of 11 ft and diameter ranging from 1 in to 2 ft Reynolds numbers near 4×10^6
and Keulegan Carpenter parameters in excess of 8×10^3 appear feasible.

6.2 Conclusions

1) A first order mathematical model consisting of descretized mass coupled by linear springs and viscous dashpots can be used to develop design parameters for a conceptual design of the system.

2) For small diameter tow cylinder specimens, 0-8 cm diameter with a length of 3.3 m, the system is inertially dominant which causes the maximum power to be much larger than the average power consumed over one simple harmonic cycle.

3) For large diameter two cylinder specimens, 15-61 cm diameter with a length of 3.3 m ,the system is drag dominant which causes the maximum and average power per cycle to be nearly equal.

4) Tow speeds of up to 17 m/s and accelerations of 1 g are possible with a power input of less than 400 Kw yielding Reynolds numbers approaching 4×10^6 and Keulegan-Carpenter parameters approaching 8×10^3.

5) The fundamental resonant period of the system is between 0.13 and 0.40 seconds.

6) With an input power 400 Kw and accelerations limited to 1 g the maximum force on the tow carriage structure is due to viscous fluid drag with a magnitude of 50 kN.

7) The tow carriage structure when constructed of aluminum tubing and hydrofoil specimen support struts will have a mass of less than 1100 Kg.

8) The tow specimen when mounted on the carriage structure and loaded with a 50 kN fluid drag force will have a maximum deflection of less than 16 mm.

9) The lower frequency modes of vibration of the tow carriage structure corresponds with the vortex shedding frequencies of the tow specimen. Further analysis may be needed to quantify the dynamic response of the structure.

10) Linear motion rail bearings can provide a rigid guidance for the tow carriage with very low friction.

11) A cable drum-pulley system powered by hydraulic motors with an electric motor primemover can provide stable power over a broad operating range.

12) The total cost of the system is on the order of $250,000.

6.3 Recommendations for Future Studies

The following items need further investigation and/or optimization before a final design of the dynamic tow carriage system can be completed.

1) The vertical motion of the cable termed "cable whip" should be investigated in order to determine the dynamic response. This motion should be a strong function of the static preload of the system. The

analysis should determine the appropriate preload and the size and strength of the cable guides that span the guide rails.

2) the cable placement on the driver drum needs further investigation. The smooth operation of this component is essential to the safe operation of the system. The investigation should determine a safe operating speed/??? range for the driver drum and give insight to possible instabilities.

3) The dynamic structural response of the tow carriage frame needs further investigation as well as optimization. Quantification of the combined fluid/structural damping present in the system will allow the dynamic response to the model. The structures geometry may need alterations to lower noises and improve strength to weight ratio.

4) A computerized control system needs to be developed. Various sources of feedback from both the drive system and carriage frame can be used to operate the system in a stable and repeatable manner.

5) The safe operation of the dynamic tow carriage system must also be investigated. The system has the potential to cause periodic damage to both the existing equipment itself, and the operators. Both safety features and procedures must be developed to reduce the risk of damage.

REFERENCES

1. Swanson Analysis Systems, Inc., Ansys PC-Linear Software, Houston, PA, 1985.

2. Baumeister, T., Avallone, E.A., Baumeister III, T., Mark's Standard Handbook for Mechanical Engineers, McGraw-Hill Book Co., New York, 1978.

3. Bethlehem Wire Rope Catalog 3161-c, Bethlehem Steel Co., Williamsport, PA, 1985.

4. Bushey, John Personal Communication, MTS Systems Corp., Minneapolis, Minnesota, June 3, 1988.

5. Dean, R.G. and Dalrymple, R.A., Water Wave Mechanics for Engineers and Scientist's, Prentice-Hall, Inc., Englewood Cliffs, New Jersey, 1984.

6. Gerhart, P.M. and Gross, R.J., Fundamentals of Fluid Mechanics, Addison-Wesley Publishing Co., Reading, Massachusetts, 1985.

7. Hoerner, S.F., Fluid-Dynamic Drag, Published by Author, Bricktown, New Jersey, 1965.

8. Ramberg, S.E. and Owen, M.G., "Free Vibrations in Taut and Slack Marine Cables", Journal of the Structural Division, ASCE Vol.101, No. ST11, Proc. Paper 13321, Nov., 1977.

9. Sarpkaya, T. and Isaacson, M., Mechanics of Wave Forces on Offshore Structures, Van Nostrand Reinhold Co., New York, 1987.

10. THK Linear Motion Systems Catalog 75DE, THK Co., LTD., Tokyo, Japan, 1987.

APPENDICES

APPENDIX A. PROGRAM TOWPLOT

```
$DEBUG

      PROGRAM TOWPLOT

C   PROGRAM TOWPLOT DEFINES THE [A] AND {B} MATRICES FOR THE C
MATHEMATICAL MODEL OF THE DYNAMIC TOW CARRAIGE SYSTEM AS DEVELOPED C
IN CHAPTER 2. THE INDEPENDANT VARIABLE OF THE PROGRAM ARE THE C
DISPLACEMENT PHASOR OF THE CARRIAGE/SPECIMEN MODEL X3 , THE PERIOD C
OF OSCILLATION τ , AND THE DIAMETER OF THE TOW SPECIMEN CYLINDER C d.
WITH THE GIVEN INPUT THE [A] MATRIX IS INVERTED BY THE C SUBROUTINE
MATRIXC AND THE 8 UNKNOWN DISPLACEMENT PHASORS θ1 ,X2 C ,X4 ,θ2 ,X6 ,X8
,X9 ,X10 AND UNKOWN DRIVE TORQUE TD ARE SOLVED FOR C AS A FUNCTION OF
TIME.
C
C
C                OUTPUT VARIABLE AS A FUNCTION OF TIME
C
C                      DISAMP-RATIO OF X3/θ1R1
C           MAXDF-MAXIMUM NON-LINEAR DRAG FORCE PER PERIOD
C              MAXIF-MAXIMUM INERTIAL FORCE PER PERIOD
C             MAXPWR-MAXIMUM LINEARIZED POWER PER PERIOD
C        PMAX-MAXIMUM NON-LINEAR POWER PER PERIOD (DRAG ONLY)
C             AVEPWR-AVERAGE LINEARIZED POWER PER PERIOD
C               MAG(9)-MAXIMUM DRIVE TORQUE PER PERIOD
C                 PHI(1)-PHASE ANGLE OF DRIVER PULLEY
C                 PHI(9)-PHASE ANGLE OF DRIVE TORQUE
C
C
C     INITIALIZE VARIABLES

      CHARACTER*20 INFILE
      REAL*8 R,ROTI1,DENSITY,M6,K6,C,C0,C6,K,M,Ci,Cd,M3,AREA
      REAL*8  XX3R,Pi,VOL,W,PERIOD,Ceff,VAR1,VAR2,RX(9),IMX(9),PHI(9)
      REAL*8 DIAMETER
      REAL*8 XX1R,XX11R,XX5R,XX7R,DISAMP,PPD,F1,F11,F5,F7,MAXPWR
      REAL*8 AVEPWR,MAXDF,MAXIF,MAG(9),DPHI1,DPHI2,XX3I,MAGXX3
      REAL*8 OMEGA,F6,SPEED,ROTI2,acelx3,ANGLE,PMAX,PRATIO,FRATIO
      COMPLEX*16 XX3,A(9,9),B(9),X(9),SUM,BB(9),AA(9,9),BI(9),D,II
      INTEGER N,L,I,J,H,INC
      COMMON / DAT6 / A
      COMMON / DAT61 / B,X

C     DEFINE MODEL CONSTANTS

      R=0.75
      Ci=2.0
      Cd=0.7
      M3=1068.0
      Pi=4.0*DATAN(1.0)
      ROTI1=208.50
      DENSITY=1000.0
```

```
      ROTI2=55.50
      M6=196.0
      K6=38.4E6
      C=135.0
      C0=0.0
      C6=0.0
      K=3.6E6
      M=172.0
C     INPUT MODEL VARIABLES

      WRITE(*,*)'INPUT TOW CYLINDER DIAMETER M'
      READ(*,11)DIAMETER

C     START STROKE LOOP

 11   FORMAT(E13.8)

      DO 220 H=1,5

      WRITE(*,*)'INPUT REAL TOW DISPLACEMENT AMPLITUDE M'
      READ(*,11)XX3R
      WRITE(*,*)'INPUT IMAG TOW DISPLACEMENT AMPLITUDE M'
      READ(*,*)XX3I
      WRITE(*,1)
 1    FORMAT(///,1X,'INPUT DATA FILE NAME')
      READ(*,2)INFILE
 2    FORMAT(A)
      AREA= 3.658*DIAMETER
      VOL=(Pi*DIAMETER**2./4.0)*3.658
      VAR2=(M+M3+Ci*DENSITY*VOL)
      XX3=CMPLX(XX3R,XX3I)
      MAGXX3=CABS(XX3)
      N=9
      OPEN(11,FILE=INFILE,STATUS='UNKNOWN')

C     START PERIOD LOOP

      DO 150 L=10,300
      PERIOD=(DBLE(L))/10.0
      W=(20.*Pi)/(DBLE(L))
      Ceff=0.42441318*DENSITY*(Cd*AREA+0.073)*W*MAGXX3
      VAR1=(2.*C+Ceff)

C     CLEAR VARIABLE A
      D=CMPLX(0.0,0.0)

      DO 5 I=1,9
      DO 5 J=1,9
      A(I,J)=CMPLX(0.0,0.0)
 5    CONTINUE

C     DEFINE VARIABLE A
```

```
      A(1,1)=CMPLX(-K*R,-W*C*R)
      A(1,7)=CMPLX(K,W*C)
      A(1,8)=CMPLX(-2.*K+W**2*M,-2.*W*C)

      A(2,1)=CMPLX(K*R,W*C*R)
      A(2,2)=A(1,8)

      A(3,2)=A(1,7)
      A(3,3)=A(1,7)

      A(4,3)=A(1,8)
      A(4,4)=-1.*A(1,1)
      A(4,5)=A(1,7)

      A(5,3)=A(1,7)
      A(5,5)=CMPLX(-2.*K-K6+W**2*M6,-W*(2*C+C6))
      A(5,6)=A(1,7)

      A(6,3)=A(4,4)
      A(6,4)=CMPLX(-2.*K*R**2+ROTI2*W**2,-W*(2*C*R**2+C0))
      A(6,6)=A(1,1)

      A(7,4)=A(1,1)
      A(7,5)=A(1,7)
      A(7,6)=A(2,2)
      A(7,7)=A(1,7)

      A(8,6)=A(1,7)
      A(8,7)=A(2,2)
      A(8,8)=A(1,7)

      A(9,1)=CMPLX(-2.*K*R**2+ROTI1*W**2,-2.*W*C*R**2)
      A(9,2)=A(4,4)
      A(9,8)=A(1,1)
      A(9,9)=CMPLX(1.0,0.0)

      DO 19 I=1,9
      DO 19 J=1,9
      AA(I,J)=A(I,J)
 19   CONTINUE

C     CLEAR VARIABLE B AND X
      DO 20 I=1,9
      B(I)=CMPLX(0.0,0.0)
      X(I)=CMPLX(0.0,0.0)
 20   CONTINUE

C     DEFINE VARIABLE B

      B(2)=CMPLX(-K,-C*W)
      B(3)=CMPLX(2.*K-W**2*VAR2,W*VAR1)
```

```
      B(2)=B(2)*XX3
      B(3)=B(3)*XX3
      B(4)=B(2)

      DO 21 J=1,9
      BB(J)=B(J)
 21   CONTINUE


C     WRITE [A] AND {B} MATRICES AND SOLVE FOR {X}


      OPEN(3,FILE='RESULT',STATUS='UNKNOWN')
      WRITE(3,*)N
      WRITE(3,*)((A(I,J),J=1,N),I=1,N)
      WRITE(3,*)(B(I),I=1,N)
      CALL MATRIXC (N,D)
      WRITE(3,*)(X(I),I=1,N)
      CLOSE(3)

      DO 30 I=1,9
      RX(I)=DREAL(X(I))
      IMX(I)=DIMAG(X(I))
      MAG(I)=CABS(X(I))
      PHI(I)=DATAN2(IMX(I),RX(I))*180./Pi
 30   CONTINUE

C     COMPUTE OUTPUT DATA AND WRITE TO FILE

      XX1R=R*RX(1)
      XX11R=-XX1R
      XX5R=R*RX(4)+RX(5)
      XX7R=RX(5)-R*RX(4)
      DISAMP=CABS(R*X(1))/MAGXX3
      PPD=CABS(X(1)/X(4))
      MAXDF=0.5*DENSITY*(AREA*Cd+0.073)*(W*MAGXX3)**2
      MAXIF=(Ci*DENSITY*VOL+M3)*W**2*MAGXX3
      II=CMPLX(0.0,1.0)
      ANGLE=(PI/180)*(PHI(9)-PHI(1))
      MAXPWR=(MAG(1)*W*MAG(9)/2.0)*(DSIN(ANGLE)+1)/1000.0
      AVEPWR=Pi/PERIOD*(RX(1)*IMX(9)-RX(9)*IMX(1))/1000.0
      OMEGA=W*MAG(1)*60.0/(2*Pi)
      SPEED=W*MAGXX3
      PMAX=MAXDF*SPEED/1000.0
      acelx3=w**2*magxx3/9.81
      WRITE(11,140)PERIOD,DISAMP,MAXDF,MAXIF,MAXPWR,PMAX,
     & AVEPWR,MAG(9),PHI(1),phi(9)
 140  FORMAT(10E13.5)
 150  CONTINUE
 220      CONTINUE
    END
```

APPENDIX B. PROGRAM TOWEIGEN

```
$DEBUG
      PROGRAM TOWEIGEN

C     THIS PROGRAM DEFINES THE STIFFNESS MATRIX [A]
C     AND THE MASS MATRIX [B] TO INPUT INTO SUBROUTINE
C     JACOBI.THE OUTPUT IS THE NATURAL FREQUENCIES OF
C     THE DYNAMIC TOWCARRIAGE MODEL.

      DOUBLE PRECISION A,B,X,EIGV,D
      DIMENSION A(40,40),B(40,40),X(40,40),EIGV(40),D(40)
      CHARACTER*20 INFILE
      REAL*8 K,K6,M,M6,R,DENSITY,CI,DC,ROTI1,VOL,M3,Kv
      REAL*8 FREQ(9),PERIOD(9),ROTI2

      WRITE(*,10)
 10   FORMAT(///,1X,'INPUT DATA FILE NAME')
      READ(*,11)INFILE
 11   FORMAT(A)
      OPEN(2,FILE=INFILE,STATUS='UNKNOWN')


      WRITE(*,*)'INPUT CABLE STIFFNES K (N/M)'
      READ(*,*)K
      WRITE(*,*)'INPUT PULLEY STIFFNESS K6 (N/M)'
      READ(*,*)K6
      WRITE(*,*)'INPUT CABLE NODAL MASS M (Kg)'
      READ(*,*)M
      WRITE(*,*)'INPUT CARRIAGE MASS M3 (Kg)'
      READ(*,*)M3
      WRITE(*,*)'INPUT TOWSPECIMEN CYLINDER DIAMETER DC (M)'
      READ(*,*)DC
      ROTI1=208.50
      ROTI2=55.5
      R=0.7500
      DENSITY=1000.0
      N=9
      M6=196.0
      NSMAX=15
      CI=2.0
      L=3.7
      VOL=(3.1415/4.)*DC**2.*L
      DO 2 I=1,9
      DO 1 J=1,9
      A(I,J)=0.0
      B(I,J)=0.0
  1   CONTINUE
  2   CONTINUE

      A(1,1)=2.*K+Kv/R**2.
      A(1,2)=-K/R
      A(1,9)=K/R
```

```
      A(2,1)=-K/R
      A(2,2)=2.*K/R**2.
      A(2,3)=-K/R**2.
      A(3,2)=-K/R**2.
      A(3,3)=2.*K/R**2.
      A(3,4)=-K/R**2.
      A(4,3)=-K/R**2.
      A(4,4)=2.*K/R**2.
      A(4,5)=-K/R
      A(4,6)=-K/R**2.
      A(5,4)=-K/R
      A(5,5)=2.*K+Kv/R**2.
      A(5,7)=K/R
      A(6,4)=-K/R**2.
      A(6,6)=2.*K/R**2.+K6/R**2.
      A(6,7)=-K/R**2.
      A(7,5)=K/R**2.
      A(7,6)=-K/R**2.
      A(7,7)=2.*K/R**2.
      A(7,8)=-K/R**2.
      A(8,7)=-K/R**2.
      A(8,8)=2.*K/R**2.
      A(8,9)=-K/R**2.
      A(9,1)=K/R
      A(9,8)=-K/R**2.
      A(9,9)=2.*K/R**2.

      B(1,1)=ROTI1/R**2.
      B(2,2)=M/R**2.
      B(3,3)=(M3+M+CI*DENSITY*VOL)/R**2.
      B(4,4)=M/R**2.
      B(5,5)=ROTI2/R**2.
      B(6,6)=M6/R**2.
      B(7,7)=M/R**2.
      B(8,8)=M/R**2.
      B(9,9)=M/R**2.


C     DO 12 I=1,N
C     WRITE(*,7) (A(I,J),J=1,N)
C  7  FORMAT(9E9.2)
C 12  CONTINUE

C      DO 21 I=1,5
C      WRITE(*,*)
C  21  CONTINUE

C      DO 14 I=1,N
C      WRITE(*,7) (B(I,J),J=1,N)
C  14  CONTINUE
```

```
      CALL JACOBI(A,B,X,EIGV,D,N)

      DO 16 I=1,9
      FREQ(I)=DSQRT(EIGV(I))/6.28318531
      PERIOD(I)=1/FREQ(I)
      WRITE(*,15)I,FREQ(I),I,PERIOD(I)
 16   CONTINUE
 15   FORMAT(10X,'FREQ(',I1,')=',F9.3,5X,'PERIOD(',I1,')=',F9.3)
       STOP
       END


      SUBROUTINE JACOBI (A,B,X,EIGV,D,N)
      DOUBLE PRECISION A,B,X,EIGV,D,EI,NX,VV,MX,Z
      DIMENSION A(40,40),B(40,40),X(40,40),EIGV(40),D(40)
      DIMENSION EI(40),NX(40),VV(40),MX(40)
C
C     INITIALIZE EIGENVALUE AND EIGENVECTOR MATRICES
      IFPR=0
      NSMAX=15
      IF(D(40).NE.999.) WRITE(2,410)
      RTCL=1.D-12
      IOUT=5
      DO 20 I=1,N
      IF(A(I,I).GT.0. .AND. B(I,I).GT.0.)GO TO 10
      Z=0
      WRITE(2,440)
      STOP
 10   D(I)=A(I,I)/B(I,I)
 20   EIGV(I)=D(I)
      DO 40 I=1,N
      DO 30 J=1,N
 30   X(I,J)=0.
 40   X(I,I)=1.
      IF(N.EQ.1) RETURN
C
C     INITIALIZE SWEEP COUNTER AND BEGIN ITERATION
C
      NSWEEP=0
      NR=N-1
 50   NSWEEP=NSWEEP+1
      IF(IFPR.EQ.1) WRITE(2,420)NSWEEP
C
C     CHECK IF PRESENT OFF-DIAGONAL ELEMENT IS LARGE
C
      EPS=(.01**NSWEEP)**2
      DO 220 J=1,NR
      JJ=J+1
      DO 220 K=JJ,N
```

```
      EPTOLA=(A(J,K)*A(J,K))/(A(J,J)*A(K,K))
      EPTOLB=(B(J,K)*B(J,K))/(B(J,J)*B(K,K))
      IF((EPTOLA.LT.EPS).AND.(EPTOLB.LT.EPS)) GO TO 220
C
C     IF ZEROING IS REQUIRED,CALCULATE THE ROTATION MATRIX
C
      AKK=A(K,K)*B(J,K)-B(K,K)*A(J,K)
      AJJ=A(J,J)*B(J,K)-B(J,J)*A(J,K)
      AB=A(J,J)*B(K,K)-A(K,K)*B(J,J)
      CHECK=(AB*AB+4.*AKK*AJJ)/4.
      IF(CHECK)60,60,70
      Z=0
 60   WRITE(2,440)
      STOP
 70   SQCH=DSQRT(CHECK)
      D1=AB/2.+SQCH
      D2=AB/2.-SQCH
      DEN=D1
      IF(DABS(D2).GT.DABS(D1))DEN=D2
      IF(DEN)90,80,90
 80   CA=0.
      CG=-A(J,K)/A(K,K)
      CG=-A(J,K)/A(K,K)
      GO TO 100
 90   CA=AKK/DEN
      CG=-AJJ/DEN
CC
CC    GENERALIZED ROTATION TO ZERO OFF-DIAGONAL ELEMENT
CC
 100  IF(N-2)110,200,110
 110  JP1=J+1
      JM1=J-1
      KP1=K+1
      KM1=K-1
      IF(JM1-1)140,120,120
 120  DO 130 I=1,JM1
      AJ=A(I,J)
      BJ=B(I,J)
      AK=A(I,K)
      BK=B(I,K)
      A(I,J)=AJ+CG*AK
      B(I,J)=BJ+CG*BK
 130  B(I,K)=BK+CA*BJ
 140  IF(KP1-N)150,150,170
 150  DO 160 I=KP1,N
      AJ=A(J,I)
      BJ=B(J,I)
      AK=A(K,I)
      BK=B(K,I)
      A(J,I)=AJ+CG*AK
      B(J,I)=BJ+CG*BK
      A(K,I)=AK+CA*AJ
```

```
 160  B(K,I)=BK+CA*BJ
 170  IF(JP1-KM1)180,180,200
 180  DO 190 I=JP1,KM1
      AJ=A(J,I)
      BJ=B(J,I)
      AK=A(I,K)
      BK=B(I,K)
      A(J,I)=AJ+CG*AK
      B(J,I)=BJ+CG*BK
      A(I,K)=AK+CA*AJ
 190  B(I,K)=BK+CA*BJ
 200  AK=A(K,K)
      BK=B(K,K)
      A(K,K)=AK+2.*CA*A(J,K)+CA*CA*A(J,J)
      B(K,K)=BK+2.*CA*B(J,K)+CA*CA*B(J,J)
      A(J,J)=A(J,J)+2.*CG*A(J,K)+CG*CG*AK
      B(J,J)=B(J,J)+2.*CG*B(J,K)+CG*CG*BK
      A(J,K)=0.
      B(J,K)=0.
CC
CC    UPDATE THE EIGENVECTOR MATRIX AFTER EACH ROTATION
CC
      DO 210 I=1,N
      XJ=X(I,J)
      XK=X(I,K)
      X(I,J)=XJ+CG*XK
 210  X(I,K)=XK+CA*XJ
 220  CONTINUE
CC
CC    UPDATE THE EIGENVALUES AFTER EACH SWEEP
CC
      DO 230 I=1,N
      IF (A(I,I).GT.0. .AND. B(I,I).GT.0.) GO TO 230
      Z=0
      WRITE(2,440)
      STOP
 230  EIGV(I)=A(I,I)/B(I,I)
      IF(IFPR.EQ.0) GO TO 240
      WRITE(2,430) (EIGV(I),I=1,N)
CC
CC    CHECK FOR CONVERGENCE
CC
 240  DO 250 I=1,N
      TOL=RTCL*D(I)
      DIF=DABS(EIGV(I)-D(I))
      IF(DIF.GT.TOL) GO TO 390
 250  CONTINUE
CC
CC    CHECK ALL OFF-DIAGONAL ELEMENTS TO SE IF ANOTHER
CC    SWEEP IS REQUIRED
CC
      EPS=RTCL**2
```

```
      DO 260 J=1,NR
      JJ=J+1
      DO 260 K=JJ,N
      EPSA=(A(J,K)*A(J,K))/(A(J,J)*A(K,K))
      EPSB=(B(J,K)*B(J,K))/(B(J,J)*B(K,K))
      IF((EPSA.LT.EPS).AND.(EPSB.LT.EPS)) GO TO 260
      GO TO 390
 260  CONTINUE
CC
CC    FILL OUT BOTTOM TRIANGLE OF RESULTANT MATRICES
CC    AND SCALE EIGENVECTORS
CC
 270  DO 280 I=1,N
      DO 280 J=1,N
      A(J,I)=A(I,J)
 280  B(J,I)=B(I,J)
      DO 290 J=1,N
      BB=DSQRT(B(J,J))
      DO 290 K=1,N
 290  X(K,J)=X(K,J)/BB
CC
CC    UPDATE MATRIX AND START NEW SWEEP IF ALLOWED
CC
      DO 300 I=1,N
 300  EI(I)=EIGV(I)
      KX=0
      DO 320 J=1,N
      SMALL=1.0E20
      DO 310 I=1,N
      IF(EI(I).GT.SMALL) GO TO 310
      KKK=I
      SMALL=EI(I)
 310  CONTINUE
      KX=KX+1
      NX(KX)=KKK
      EIGV(J)=EI(KKK)
      EI(KKK)=1.E20
 320  CONTINUE
      DO 330 I=1,N
      II=NX(I)
 330  MX(II)=I
      DO 360 J=1,N
      DO 350 JT=1,N
      JJ=NX(J)
      VV(JT)=X(JT,J)
 340  FORMAT(6I5,6E15.4)
      X(JT,J)=X(JT,JJ)
      X(JT,JJ)=VV(JT)
 350  CONTINUE
      KJ=MX(J)
      NX(KJ)=JJ
      MX(JJ)=MX(J)
```

```
360  CONTINUE
     IF(D(40).EQ.999.) RETURN
     WRITE(2,430) (EIGV(IL),IL=1,N)
     WRITE(2,380)
     DO 370 LI=1,N
370  WRITE(2,430) (X(LI,LJ),LJ=1,N)
380  FORMAT(/,10X,'EIGENVECTORS',/)
     RETURN
390  DO 400 I=1,N
400  D(I)=EIGV(I)
     IF(NSWEEP.LT.NSMAX) GO TO 50
     GO TO 270
410  FORMAT (//,10X,'EIGENVALUES',/)
420  FORMAT(/,'27HOSWEEP NUMBER IN *JACOBI*= ',I4)
430  FORMAT(6E8.2/)
440  FORMAT('***ERROR MATRICES NOT POSITIVE DEFINITE STOP***')
     END
```

APPENDIX C

ANSYS Input/Output Files

All input/output data are in English units

Force-lbs.
Length-ft.
Mass-slugs

```
***** INPUT SWITCHED FROM FILE 5 TO FILE38  NAME=STATIC8.PRP

NEW TITLE= STATICX









ELEMENT TYPE  1 USES STIF  4
 KEYOPT(1-9)=   0   0   0     0   0   0      0   0   0
 INOTPR= 0  NUMBER OF NODES=   3



ELASTIC BEAM, 3-D

CURRENT NODAL DOF SET IS  UX    UY    UZ    ROTX  ROTY  ROTZ
 THREE-DIMENSIONAL STRUCTURE



 MATERIAL   1          COEFFICIENTS OF EX   VS. TEMP EQUATION
  C0 =  0.1440000E+10

PROPERTY TABLE EX    MAT=   1  NUM. POINTS=  2
       TEMPERATURE     DATA        TEMPERATURE     DATA
     0.00000E+00 0.14400E+10  2300.0     0.14400E+10


 MATERIAL   1          COEFFICIENTS OF DENS VS. TEMP EQUATION
  C0 =   5.237000

PROPERTY TABLE DENS  MAT=   1  NUM. POINTS=  2
       TEMPERATURE     DATA        TEMPERATURE     DATA
     0.00000E+00  5.2370      2300.0      5.2370

ELEMENT TYPE  2 USES STIF  4
 KEYOPT(1-9)=   0   0   0     0   0   0      0   0   0
 INOTPR= 0  NUMBER OF NODES=   3

ELASTIC BEAM, 3-D

CURRENT NODAL DOF SET IS  UX    UY    UZ    ROTX  ROTY  ROTZ
 THREE-DIMENSIONAL STRUCTURE
```

```
 MATERIAL   2          COEFFICIENTS OF EX   VS. TEMP EQUATION
  C0 =  0.1440000E+10

PROPERTY TABLE EX    MAT=   2  NUM. POINTS=  2
       TEMPERATURE     DATA        TEMPERATURE     DATA
     0.00000E+00 0.14400E+10  2300.0     0.14400E+10

 MATERIAL   2          COEFFICIENTS OF DENS VS. TEMP EQUATION
  C0 =   5.237000

PROPERTY TABLE DENS  MAT=   2  NUM. POINTS=  2
       TEMPERATURE     DATA        TEMPERATURE     DATA
     0.00000E+00  5.2370      2300.0      5.2370

ELEMENT TYPE  3 USES STIF  4
 KEYOPT(1-9)=   0   0   0     0   0   0      0   0   0
 INOTPR= 0  NUMBER OF NODES=   3

ELASTIC BEAM, 3-D

CURRENT NODAL DOF SET IS  UX    UY    UZ    ROTX  ROTY  ROTZ
 THREE-DIMENSIONAL STRUCTURE

 MATERIAL   3          COEFFICIENTS OF EX   VS. TEMP EQUATION
  C0 =  0.1440000E+10

PROPERTY TABLE EX    MAT=   3  NUM. POINTS=  2
       TEMPERATURE     DATA        TEMPERATURE     DATA
     0.00000E+00 0.14400E+10  2300.0     0.14400E+10

 MATERIAL   3          COEFFICIENTS OF DENS VS. TEMP EQUATION
  C0 =   5.237000

PROPERTY TABLE DENS  MAT=   3  NUM. POINTS=  2
       TEMPERATURE     DATA        TEMPERATURE     DATA
     0.00000E+00  5.2370      2300.0      5.2370

ELEMENT TYPE  4 USES STIF  4
 KEYOPT(1-9)=   0   0   0     0   0   0      0   0   0
 INOTPR= 0  NUMBER OF NODES=   3

ELASTIC BEAM, 3-D

CURRENT NODAL DOF SET IS  UX    UY    UZ    ROTX  ROTY  ROTZ
 THREE-DIMENSIONAL STRUCTURE

 MATERIAL   4          COEFFICIENTS OF EX   VS. TEMP EQUATION
  C0 =  0.1440000E+10

PROPERTY TABLE EX    MAT=   4  NUM. POINTS=  2
       TEMPERATURE     DATA        TEMPERATURE     DATA
```

```
     0.00000E+00 0.14400E+10  2300.0     0.14400E+10

  MATERIAL   4          COEFFICIENTS OF DENS VS. TEMP EQUATION
   C0 =   5.237000

 PROPERTY TABLE DENS  MAT=   4  NUM. POINTS=  2
        TEMPERATURE     DATA        TEMPERATURE     DATA
     0.00000E+00  5.2370      2300.0      5.2370

  REAL CONSTANT SET   1  ITEMS   1 TO   6
   0.13318E-01  0.27500E-03  0.27500E-03  0.41670       0.41670
0.00000E+00

  REAL CONSTANT SET   2  ITEMS   1 TO   6
   0.64760E-02  0.31800E-04  0.31800E-04  0.20830       0.20830
0.00000E+00

  REAL CONSTANT SET   3  ITEMS   1 TO   6
   0.14062      0.50840E-02  0.12842       3.0000       0.41670
0.00000E+00

  REAL CONSTANT SET   3  ITEMS   7 TO  10
   0.00000E+00  0.18510E-01  0.00000E+00  0.00000E+00

  REAL CONSTANT SET   4  ITEMS   1 TO   6
   0.13368      0.16800E-02  0.11301       3.0000       0.25000
0.00000E+00

  REAL CONSTANT SET   4  ITEMS   7 TO  10
   0.00000E+00  0.63000E-02  0.00000E+00  0.00000E+00

 ANALYSIS TYPE=  0   (STATIC ANALYSIS)

 NODE    1  KCS= 0  X,Y,Z= 0.00000E+00 0.00000E+00  4.0000

 NODE    2  KCS= 0  X,Y,Z=  4.5000     0.00000E+00  4.0000

 NODE    3  KCS= 0  X,Y,Z=  9.0000     0.00000E+00  4.0000

 NODE    4  KCS= 0  X,Y,Z=  13.500     0.00000E+00  4.0000

 NODE    5  KCS= 0  X,Y,Z=  18.000     0.00000E+00  4.0000

 NODE    6  KCS= 0  X,Y,Z=  15.750     0.00000E+00  6.0000

 NODE    7  KCS= 0  X,Y,Z=  11.250     0.00000E+00  6.0000

 NODE    8  KCS= 0  X,Y,Z=  6.7500     0.00000E+00  6.0000

 NODE    9  KCS= 0  X,Y,Z=  2.2500     0.00000E+00  6.0000

 NODE   10  KCS= 0  X,Y,Z= 0.00000E+00 0.00000E+00  8.0000
```

```
NODE   11  KCS= 0  X,Y,Z=  4.5000      0.00000E+00  8.0000
NODE   12  KCS= 0  X,Y,Z=  9.0000      0.00000E+00  8.0000
NODE   13  KCS= 0  X,Y,Z=  13.500      0.00000E+00  8.0000
NODE   14  KCS= 0  X,Y,Z=  18.000      0.00000E+00  8.0000
NODE   15  KCS= 0  X,Y,Z=  9.0000      0.00000E+00  11.000
NODE   16  KCS= 0  X,Y,Z=  9.0000      0.00000E+00  23.000
NODE   17  KCS= 0  X,Y,Z= 0.00000E+00  12.000       4.0000
NODE   18  KCS= 0  X,Y,Z=  4.5000      12.000       4.0000
NODE   19  KCS= 0  X,Y,Z=  9.0000      12.000       4.0000
NODE   20  KCS= 0  X,Y,Z=  13.500      12.000       4.0000
NODE   21  KCS= 0  X,Y,Z=  18.000      12.000       4.0000
NODE   22  KCS= 0  X,Y,Z=  15.750      12.000       6.0000
NODE   23  KCS= 0  X,Y,Z=  11.250      12.000       6.0000
NODE   24  KCS= 0  X,Y,Z=  6.7500      12.000       6.0000
NODE   25  KCS= 0  X,Y,Z=  2.2500      12.000       6.0000
NODE   26  KCS= 0  X,Y,Z= 0.00000E+00  12.000       8.0000
NODE   27  KCS= 0  X,Y,Z=  4.5000      12.000       8.0000
NODE   28  KCS= 0  X,Y,Z=  9.0000      12.000       8.0000
NODE   29  KCS= 0  X,Y,Z=  13.500      12.000       8.0000
NODE   30  KCS= 0  X,Y,Z=  18.000      12.000       8.0000
NODE   31  KCS= 0  X,Y,Z=  9.0000      12.000       11.000
NODE   32  KCS= 0  X,Y,Z=  9.0000      12.000       23.000
NODE   33  KCS= 0  X,Y,Z= 0.00000E+00  6.0000       4.0000
NODE   34  KCS= 0  X,Y,Z= 0.00000E+00  9.0000       6.0000
NODE   35  KCS= 0  X,Y,Z= 0.00000E+00  3.0000       6.0000
NODE   36  KCS= 0  X,Y,Z= 0.00000E+00  6.0000       8.0000
```

```
NODE   37  KCS= 0  X,Y,Z=  9.0000      6.0000      4.0000

NODE   38  KCS= 0  X,Y,Z=  9.0000      3.0000      6.0000

NODE   39  KCS= 0  X,Y,Z=  9.0000      9.0000      6.0000

NODE   40  KCS= 0  X,Y,Z=  9.0000      6.0000      8.0000

NODE   41  KCS= 0  X,Y,Z=  18.000      6.0000      4.0000

NODE   42  KCS= 0  X,Y,Z=  18.000      9.0000      6.0000

NODE   43  KCS= 0  X,Y,Z=  18.000      3.0000      6.0000

NODE   44  KCS= 0  X,Y,Z=  18.000      6.0000      8.0000

NODE   45  KCS= 0  X,Y,Z=  4.5000      3.0000      4.0000

NODE   46  KCS= 0  X,Y,Z=  13.500      3.0000      4.0000

NODE   47  KCS= 0  X,Y,Z=  4.5000      9.0000      4.0000

NODE   48  KCS= 0  X,Y,Z=  13.500      9.0000      4.0000

NODE   49  KCS= 0  X,Y,Z=  4.5000      3.0000      8.0000

NODE   50  KCS= 0  X,Y,Z=  13.500      3.0000      8.0000

NODE   51  KCS= 0  X,Y,Z=  4.5000      9.0000      8.0000

NODE   52  KCS= 0  X,Y,Z=  13.500      9.0000      8.0000

NODE   53  KCS= 0  X,Y,Z=  18.000      12.000      11.000

NODE   54  KCS= 0  X,Y,Z=  18.000     0.00000E+00  11.000

NODE   55  KCS= 0  X,Y,Z=  18.000     0.00000E+00  23.000

REAL CONSTANT NUMBER=  1
ELEMENT     1      17    18     0
ELEMENT     2      18    19     0
ELEMENT     3      19    20     0
ELEMENT     4      20    21     0
ELEMENT     5      21    30     0
ELEMENT     6      30    29     0
ELEMENT     7      29    28     0
ELEMENT     8      28    27     0
ELEMENT     9      27    26     0
ELEMENT    10      26    17     0
ELEMENT    11       1     2     0
ELEMENT    12       2     3     0
```

ELEMENT	13	3	4	0
ELEMENT	14	4	5	0
ELEMENT	15	5	14	0
ELEMENT	16	14	13	0
ELEMENT	17	13	12	0
ELEMENT	18	12	11	0
ELEMENT	19	11	10	0
ELEMENT	20	10	1	0
ELEMENT	21	17	33	0
ELEMENT	22	33	1	0
ELEMENT	23	10	36	0
ELEMENT	24	36	26	0
ELEMENT	25	21	41	0
ELEMENT	26	41	5	0
ELEMENT	27	14	44	0
ELEMENT	28	44	30	0
ELEMENT	29	3	37	0
ELEMENT	30	37	19	0
ELEMENT	31	28	40	0
ELEMENT	32	40	12	0
ELEMENT	33	36	40	0
ELEMENT	34	40	44	0
ELEMENT	35	33	37	0
ELEMENT	36	37	41	0
ELEMENT	37	13	15	0
ELEMENT	38	11	15	0
ELEMENT	39	29	31	0
ELEMENT	40	27	31	0

REAL CONSTANT NUMBER= 2

ELEMENT	41	17	25	0
ELEMENT	42	25	27	0
ELEMENT	43	26	25	0
ELEMENT	44	25	18	0
ELEMENT	45	18	24	0
ELEMENT	46	27	24	0
ELEMENT	47	24	19	0
ELEMENT	48	24	28	0
ELEMENT	49	28	23	0
ELEMENT	50	19	23	0
ELEMENT	51	23	29	0
ELEMENT	52	23	20	0
ELEMENT	53	20	22	0
ELEMENT	54	29	22	0
ELEMENT	55	22	21	0
ELEMENT	56	22	30	0
ELEMENT	57	1	9	0
ELEMENT	58	10	9	0
ELEMENT	59	9	2	0
ELEMENT	60	9	11	0
ELEMENT	61	11	8	0
ELEMENT	62	2	8	0

ELEMENT	63	8	3	0
ELEMENT	64	8	12	0
ELEMENT	65	12	7	0
ELEMENT	66	3	7	0
ELEMENT	67	7	4	0
ELEMENT	68	7	13	0
ELEMENT	69	13	6	0
ELEMENT	70	4	6	0
ELEMENT	71	6	5	0
ELEMENT	72	6	14	0
ELEMENT	73	17	34	0
ELEMENT	74	26	34	0
ELEMENT	75	34	33	0
ELEMENT	76	34	36	0
ELEMENT	77	36	35	0
ELEMENT	78	33	35	0
ELEMENT	79	35	1	0
ELEMENT	80	35	10	0
ELEMENT	81	21	42	0
ELEMENT	82	30	42	0
ELEMENT	83	42	41	0
ELEMENT	84	42	44	0
ELEMENT	85	44	43	0
ELEMENT	86	41	43	0
ELEMENT	87	43	5	0
ELEMENT	88	43	14	0
ELEMENT	89	3	38	0
ELEMENT	90	38	40	0
ELEMENT	91	12	38	0
ELEMENT	92	38	37	0
ELEMENT	93	37	39	0
ELEMENT	94	39	28	0
ELEMENT	95	40	39	0
ELEMENT	96	39	19	0
ELEMENT	97	1	45	0
ELEMENT	98	45	37	0
ELEMENT	99	33	45	0
ELEMENT	100	45	3	0
ELEMENT	101	3	46	0
ELEMENT	102	46	41	0
ELEMENT	103	37	46	0
ELEMENT	104	46	5	0
ELEMENT	105	37	48	0
ELEMENT	106	48	21	0
ELEMENT	107	19	48	0
ELEMENT	108	48	41	0
ELEMENT	109	33	47	0
ELEMENT	110	47	19	0
ELEMENT	111	17	47	0
ELEMENT	112	47	37	0
ELEMENT	113	10	49	0
ELEMENT	114	49	40	0

```
 ELEMENT   115      36    49     0
 ELEMENT   116      49    12     0
 ELEMENT   117      12    50     0
 ELEMENT   118      50    44     0
 ELEMENT   119      40    50     0
 ELEMENT   120      50    14     0
 ELEMENT   121      40    52     0
 ELEMENT   122      52    30     0
 ELEMENT   123      28    52     0
 ELEMENT   124      52    44     0
 ELEMENT   125      36    51     0
 ELEMENT   126      51    28     0
 ELEMENT   127      26    51     0
 ELEMENT   128      51    40     0

 REAL CONSTANT NUMBER=  3
 ELEMENT   129      19    28    21
 ELEMENT   130      28    31    30
 ELEMENT   131      31    32    53
 ELEMENT   132       3    12     5
 ELEMENT   133      12    15    14
 ELEMENT   134      15    16    54

 REAL CONSTANT NUMBER=  4
 ELEMENT   135      16    32    55
 ELEMENT   136      40    15    44
 ELEMENT   137      40    31    44

 SPECIFIED DISP UY   FOR SELECTED NODES IN RANGE    10 TO    10 BY
1
  VALUES= 0.00000E+00 0.00000E+00  ADDITIONAL DOFS=  UZ    ROTX  ROTY
ROTZ

 SPECIFIED DISP UY   FOR SELECTED NODES IN RANGE    14 TO    14 BY
1
  VALUES= 0.00000E+00 0.00000E+00  ADDITIONAL DOFS=  UZ    ROTX  ROTY
ROTZ

 SPECIFIED DISP UY   FOR SELECTED NODES IN RANGE    26 TO    26 BY
1
  VALUES= 0.00000E+00 0.00000E+00  ADDITIONAL DOFS=  UZ    ROTX  ROTY
ROTZ

 SPECIFIED DISP UY   FOR SELECTED NODES IN RANGE    30 TO    30 BY
1
  VALUES= 0.00000E+00 0.00000E+00  ADDITIONAL DOFS=  UZ    ROTX  ROTY
ROTZ

 SPECIFIED DISP UX   FOR SELECTED NODES IN RANGE    12 TO    12 BY
1
  VALUES= 0.00000E+00 0.00000E+00  ADDITIONAL DOFS=
```

```
MASTER DOF      FOR ALL SELECTED NODES
ADDITIONAL DOFS=

SPECIFIED FORCE FX   FOR SELECTED NODES IN RANGE    16 TO    16 BY
1
 VALUES=  5620.0     0.00000E+00

SPECIFIED FORCE FX   FOR SELECTED NODES IN RANGE    32 TO    32 BY
1


 VALUES=  5620.0     0.00000E+00



***  NOTE  ***
NPRINT IS ZERO OR GREATER THAN NITTER. SOLUTION PRINTOUT
WILL BE SUPPRESSED UNLESS OTHER PRINT CONTROLS HAVE BEEN DEFINED.

***  NOTE  ***
DATA CHECKED - NO ERRORS FOUND

*** PREP7 GLOBAL STATUS ***

TITLE= STATICX

ANALYSIS TYPE=     0
NUMBER OF ELEMENT TYPES=     4
   137 ELEMENTS CURRENTLY SELECTED.  MAX ELEMENT NUMBER =    137
    55 NODES CURRENTLY SELECTED.     MAX NODE NUMBER =        55
MAXIMUM LINEAR PROPERTY NUMBER=     4
MAXIMUM REAL CONSTANT SET NUMBER=     4
ACTIVE COORDINATE SYSTEM=     0  (CARTESIAN)
NUMBER OF IMPOSED DISPLACEMENTS=    21
NUMBER OF NODAL FORCES=     2

ANALYSIS DATA WRITTEN ON FILE27

ENTER  FINISH  TO LEAVE PREP7



ALL CURRENT PREP7 DATA WRITTEN TO FILE16   NAME= FILE16.DAT
 FOR POSSIBLE RESUME FROM THIS POINT


***** ROUTINE COMPLETED *****  CP=       59.3200   TIME=   10.8411

STORE SG1I  FOR ELEMENT TYPE STIF  4  FROM ITEM    19

STORE SG3I  FOR ELEMENT TYPE STIF  4  FROM ITEM    20
```

```
STORE SG1J  FOR ELEMENT TYPE STIF  4  FROM ITEM    21

STORE SG3J  FOR ELEMENT TYPE STIF  4  FROM ITEM    22

USE LOAD STEP     1  ITERATION     1  SECTION   1  FOR LOAD CASE
1


GEOMETRY STORED FOR     55  NODES    137  ELEMENTS
 TITLE= STATICX8


DISPLACEMENT STORED FOR   55 NODES

STRESSES STORED FOR    4  SELECTED ITEMS

ITERATION SUMMARY INFORMATION STORED

NODAL FORCES STORED FOR  137 ELEMENTS

REACTIONS STORED FOR   21 REACTIONS

FOR LOAD STEP=     1  ITERATION=     1  SECTION=   1
 TIME=  0.000000E+00   LOAD CASE=  1
 TITLE= STATICX8


PRINT ELEMENT STRESS ITEMS PER ELEMENT

         ***** POST1 ELEMENT STRESS LISTING *****

 LOAD STEP     1  ITERATION=     1  SECTION=  1
 TIME=   0.00000E+00     LOAD CASE=  1
```

ELEM	SG1I	SG3I	SG1J	SG3J
1	-157811.93	-269128.31	-193237.42	-233702.82
2	-412776.40	-502794.56	-304013.53	-611557.43
3	611557.43	304013.53	502794.56	412776.40
4	233702.82	193237.42	269128.31	157811.93
5	312968.16	221963.51	377253.07	157678.59
6	188607.93	-557306.53	187214.94	-555913.54
7	175117.10	-226036.01	17963.359	-68882.261

8	68882.261	-17963.359	226036.01	-175117.10
9	555913.54	-187214.94	557306.53	-188607.93
10	-157678.59	-377253.07	-221963.51	-312968.16
11	-229884.99	-254192.98	-197338.17	-286739.80
12	-371772.34	-504186.04	-276970.01	-598988.36
13	598988.36	276970.01	504186.04	371772.34
14	286739.80	197338.17	254192.98	229884.99

***** POST1 ELEMENT STRESS LISTING *****

LOAD STEP 1 ITERATION= 1 SECTION= 1
TIME= 0.00000E+00 LOAD CASE= 1

ELEM	SG1I	SG3I	SG1J	SG3J
15	254826.50	141758.33	299556.68	97028.141
16	316525.34	-400786.51	302778.97	-387040.14
17	292316.85	-104473.48	177713.91	10129.455
18	-10129.455	-177713.91	104473.48	-292316.85
19	387040.14	-302778.97	400786.51	-316525.34
20	-97028.141	-299556.68	-141758.33	-254826.50
21	82026.626	-17744.896	109811.55	-45529.817
22	71729.258	-40860.833	51137.027	-20268.602
23	138716.39	-13311.453	118199.40	7205.5367
24	-22365.840	-103039.10	-825.05161	-124579.88
25	17744.896	-82026.626	45529.817	-109811.55
26	40860.833	-71729.258	20268.602	-51137.027
27	13311.453	-138716.39	-7205.5367	-118199.40
28	103039.10	22365.840	124579.88	825.05161

***** POST1 ELEMENT STRESS LISTING *****

LOAD STEP 1 ITERATION= 1 SECTION= 1
TIME= 0.00000E+00 LOAD CASE= 1

ELEM	SG1I	SG3I	SG1J	SG3J
29	34100.358	-34100.358	61082.735	-61082.735
30	28318.219	-28318.219	19735.998	-19735.998
31	48134.433	-48134.433	23656.312	-23656.312
32	28156.904	-28156.904	38675.469	-38675.469
33	86473.590	-103230.66	229087.71	-245844.78
34	245844.78	-229087.71	103230.66	-86473.590
35	114291.14	23433.851	106659.01	31065.980
36	-31065.980	-106659.01	-23433.851	-114291.14
37	-324272.46	-561439.65	-272903.87	-612808.24
38	561439.65	324272.46	612808.24	272903.87
39	-384880.57	-678737.86	-427750.61	-635867.82
40	678737.86	384880.57	635867.82	427750.61
41	818780.23	767988.03	834062.95	752705.31
42	969853.78	640495.24	975629.41	634719.62

***** POST1 ELEMENT STRESS LISTING *****

LOAD STEP 1 ITERATION= 1 SECTION= 1
TIME= 0.00000E+00 LOAD CASE= 1

ELEM	SG1I	SG3I	SG1J	SG3J
43	-202977.86	-501623.90	-215998.21	-488603.55
44	-88786.676	-608144.40	-91858.358	-605072.71
45	473439.13	169811.87	538066.81	105184.20
46	296898.28	-245673.04	230162.59	-178937.34
47	23174.199	19805.337	30818.574	12160.962

48	326264.92	303124.20	368372.19	261016.93
49	-261016.93	-368372.19	-303124.20	-326264.92
50	-12160.962	-30818.574	-19805.337	-23174.199
51	178937.34	-230162.59	245673.04	-296898.28
52	-105184.20	-538066.81	-169811.87	-473439.13
53	605072.71	91858.358	608144.40	88786.676
54	-634719.62	-975629.41	-640495.24	-969853.78
55	-752705.31	-834062.95	-767988.03	-818780.23
56	488603.55	215998.21	501623.90	202977.86

***** POST1 ELEMENT STRESS LISTING *****

LOAD STEP 1 ITERATION= 1 SECTION= 1
TIME= 0.00000E+00 LOAD CASE= 1

ELEM	SG1I	SG3I	SG1J	SG3J
57	680365.18	624811.13	677710.36	627465.95
58	-152248.20	-421480.14	-178587.06	-395141.28
59	-35108.226	-530545.14	-28106.735	-537546.63
60	834272.01	491622.54	836696.74	489197.81
61	294171.66	-242674.75	252103.99	-200607.08
62	411785.86	97352.874	468671.00	40467.736
63	35152.647	8778.2573	39250.218	4680.6857
64	257832.52	237547.29	326876.67	168503.14
65	-168503.14	-326876.67	-237547.29	-257832.52
66	-4680.6857	-39250.218	-8778.2573	-35152.647
67	-40467.736	-468671.00	-97352.874	-411785.86
68	200607.08	-252103.99	242674.75	-294171.66
69	-489197.81	-836696.74	-491622.54	-834272.01

70	537546.63	28106.735	530545.14	35108.226

***** POST1 ELEMENT STRESS LISTING *****

LOAD STEP 1 ITERATION= 1 SECTION= 1
TIME= 0.00000E+00 LOAD CASE= 1

ELEM	SG1I	SG3I	SG1J	SG3J
71	-627465.95	-677710.36	-624811.13	-680365.18
72	395141.28	178587.06	421480.14	152248.20
73	59601.451	24517.202	73710.077	10408.576
74	-51432.930	-137431.55	-73037.241	-115827.24
75	-27939.486	-158862.91	3699.0006	-190501.39
76	106085.54	-21319.961	131663.98	-46898.402
77	53049.538	-132227.76	16712.005	-95890.228
78	160192.31	10200.477	149988.26	20404.523
79	-4100.2207	-77113.403	-3260.1417	-77953.482
80	128939.90	40423.661	123838.07	45525.497
81	-24517.202	-59601.451	-10408.576	-73710.077
82	137431.55	51432.930	115827.24	73037.241
83	158862.91	27939.486	190501.39	-3699.0006
84	21319.961	-106085.54	46898.402	-131663.98

***** POST1 ELEMENT STRESS LISTING *****

LOAD STEP 1 ITERATION= 1 SECTION= 1
TIME= 0.00000E+00 LOAD CASE= 1

ELEM	SG1I	SG3I	SG1J	SG3J
85	132227.76	-53049.538	95890.228	-16712.005
86	-10200.477	-160192.31	-20404.523	-149988.26
87	77113.403	4100.2207	77953.482	3260.1417

88	-40423.661	-128939.90	-45525.497	-123838.07
89	3418.8858	-3418.8858	5844.4931	-5844.4931
90	21113.459	-21113.459	78777.193	-78777.193
91	3751.8288	-3751.8288	17426.909	-17426.909
92	46829.623	-46829.623	34307.899	-34307.899
93	10160.456	-10160.456	48580.694	-48580.694
94	21028.756	-21028.756	9625.9535	-9625.9535
95	66528.054	-66528.054	23881.794	-23881.794
96	8524.5319	-8524.5319	9538.5215	-9538.5215
97	41917.546	-23781.022	43134.733	-24998.208
98	42902.885	-21990.226	37638.166	-16725.507

***** POST1 ELEMENT STRESS LISTING *****

LOAD STEP 1 ITERATION= 1 SECTION= 1
TIME= 0.00000E+00 LOAD CASE= 1

ELEM	SG1I	SG3I	SG1J	SG3J
99	-142553.02	-241514.96	-159130.42	-224937.56
100	-160091.19	-226761.55	-150288.25	-236564.49
101	236564.49	150288.25	226761.55	160091.19
102	224937.56	159130.42	241514.96	142553.02
103	16725.507	-37638.166	21990.226	-42902.885
104	24998.208	-43134.733	23781.022	-41917.546
105	215568.26	155086.52	215810.78	154844.00
106	230940.71	142595.74	233655.66	139880.79
107	69343.519	-90374.900	29487.364	-50518.745
108	12216.611	-36199.750	21291.712	-45274.851
109	45274.851	-21291.712	36199.750	-12216.611

110	50518.745	-29487.364	90374.900	-69343.519
111	-139880.79	-233655.66	-142595.74	-230940.71
112	-154844.00	-215810.78	-155086.52	-215568.26

***** POST1 ELEMENT STRESS LISTING *****

LOAD STEP 1 ITERATION= 1 SECTION= 1
TIME= 0.00000E+00 LOAD CASE= 1

ELEM	SG1I	SG3I	SG1J	SG3J
113	201858.50	102208.58	185889.89	118177.19
114	166174.05	136907.27	252139.53	50941.791
115	-143805.31	-169121.41	-130331.39	-182595.32
116	-135598.50	-176363.75	-84316.925	-227645.33
117	227645.33	84316.925	176363.75	135598.50
118	182595.32	130331.39	169121.41	143805.31
119	-50941.791	-252139.53	-136907.27	-166174.05
120	-118177.19	-185889.89	-102208.58	-201858.50
121	228319.05	40849.753	149907.64	119261.16
122	172640.24	95554.072	184688.37	83505.943
123	-115404.23	-248502.18	-155468.92	-208437.49
124	-154318.21	-209268.57	-158654.10	-204932.68
125	204932.68	158654.10	209268.57	154318.21
126	208437.49	155468.92	248502.18	115404.23

***** POST1 ELEMENT STRESS LISTING *****

LOAD STEP 1 ITERATION= 1 SECTION= 1
TIME= 0.00000E+00 LOAD CASE= 1

ELEM	SG1I	SG3I	SG1J	SG3J
127	-83505.943	-184688.37	-95554.072	-172640.24

128	-119261.16	-149907.64	-40849.753	-228319.05
129	5194.8480	-5194.8480	560537.11	-560537.11
130	560037.96	-560037.96	776787.19	-776787.19
131	784992.17	-784992.17	303.80719	-303.80719
132	4226.8567	-4226.8567	637905.13	-637905.13
133	637339.07	-637339.07	780939.12	-780939.12
134	790463.36	-790463.36	303.80719	-303.80719
135	945.54457	-945.54457	3708.9315	-3708.9315
136	1674.0020	-1674.0020	8460.2739	-8460.2739
137	4495.0498	-4495.0498	5493.0574	-5493.0574

PRINT NODAL DISPLACEMENTS

***** POST1 NODAL DISPLACEMENT LISTING *****

LOAD STEP 1 ITERATION= 1 SECTION= 1
TIME= 0.00000E+00 LOAD CASE= 1

THE FOLLOWING X,Y,Z DISPLACEMENTS ARE IN NODAL COORDINATES

NODE	UX	UY	UZ	ROTX	ROTY	ROTZ
1	-0.66186323E-03	0.47391427E-03	0.55081225E-03	0.54937587E-04	0.24323979E-03	0.94007025E-04
2	-0.14182351E-02	0.77876682E-03	0.15054490E-04	0.44471573E-04	-0.54707842E-04	-0.13267782E-05
3	-0.27869200E-02	-0.26802637E-18	0.13495330E-17	-0.90430693E-19	0.49723654E-03	-0.39779721E-03
4	-0.14182351E-02	-0.77876682E-03	-0.15054490E-04	-0.44471573E-04	-0.54707842E-04	-0.13267782E-05
5	-0.66186323E-03	-0.47391427E-03	-0.55081225E-03	-0.54937587E-04	0.24323979E-03	0.94007025E-04
6	0.50627483E-03	-0.42788451E-03	-0.12901570E-02	-0.12630593E-03	-0.97456569E-04	0.11101580E-03
7	-0.17705822E-02	-0.57014414E-03	-0.12124988E-02	-0.14460355E-04	0.52156504E-03	-0.12934191E-03
8	-0.17705822E-02	0.57014414E-03	0.12124988E-02	0.14460355E-04	0.52156504E-03	-0.12934191E-03
9	0.50627483E-03	0.42788451E-03	0.12901570E-02	0.12630593E-03	-0.97456569E-04	0.11101580E-03
10	0.16184718E-03	0.00000000E+00	0.00000000E+00	0.00000000E+00	0.00000000E+00	0.00000000E+00

```
     11         0.29350526E-03      0.57357080E-03      0.36156199E-02
-0.33807227E-04 -0.24202419E-04  0.78887096E-04
     12         0.00000000E+00      0.22361681E-18      0.13250516E-17
-0.18032434E-18  0.10918032E-02 -0.41932489E-03

          ***** POST1 NODAL DISPLACEMENT LISTING *****

  LOAD STEP     1  ITERATION=     1  SECTION=  1
  TIME=   0.00000E+00     LOAD CASE=  1

  THE FOLLOWING X,Y,Z DISPLACEMENTS ARE IN NODAL COORDINATES

    NODE      UX              UY              UZ              ROTX
        ROTY            ROTZ
     13           0.29350526E-03    -0.57357080E-03    -0.36156199E-02
0.33807227E-04 -0.24202419E-04  0.78887096E-04
     14         0.16184718E-03      0.00000000E+00      0.00000000E+00
0.00000000E+00  0.00000000E+00  0.00000000E+00
     15         0.47029215E-02      0.93682210E-18      0.13145000E-17
-0.26087886E-18  0.20767186E-02 -0.49913620E-03
     16         0.47192773E-01      0.39452175E-17      0.13146223E-17
-0.23968496E-18  0.42732941E-02 -0.41575017E-03
     17         0.18699056E-02      0.67214376E-03      0.74296065E-03
0.21096789E-03  0.21756394E-03 -0.30897528E-03
     18         0.12028114E-02      0.55285467E-04      0.47020117E-03
0.77476950E-04 -0.65470593E-04 -0.22873681E-04
     19        -0.22776820E-03     -0.29273767E-18     -0.13301297E-17
-0.18383641E-18  0.73087968E-03 -0.42179674E-04
     20           0.12028114E-02    -0.55285467E-04    -0.47020117E-03
-0.77476950E-04 -0.65470593E-04 -0.22873681E-04
     21           0.18699056E-02    -0.67214376E-03    -0.74296065E-03
-0.21096789E-03  0.21756394E-03 -0.30897528E-03
     22           0.32545005E-02    -0.39420981E-04    -0.16818343E-02
-0.42284441E-04 -0.13182321E-03 -0.39121484E-04
     23           0.11162499E-02    -0.37297978E-04    -0.15796423E-02
0.15548746E-04  0.66443079E-03  0.31867075E-05
     24         0.11162499E-02      0.37297978E-04      0.15796423E-02
-0.15548746E-04  0.66443079E-03  0.31867075E-05

          ***** POST1 NODAL DISPLACEMENT LISTING *****

  LOAD STEP     1  ITERATION=     1  SECTION=  1
  TIME=   0.00000E+00     LOAD CASE=  1

  THE FOLLOWING X,Y,Z DISPLACEMENTS ARE IN NODAL COORDINATES

    NODE      UX              UY              UZ              ROTX
        ROTY            ROTZ
     25         0.32545005E-02      0.39420981E-04      0.16818343E-02
0.42284441E-04 -0.13182321E-03 -0.39121484E-04
     26         0.27449461E-02      0.00000000E+00      0.00000000E+00
0.00000000E+00  0.00000000E+00  0.00000000E+00
```

```
     27          0.33210377E-02      0.70479469E-04      0.41406237E-02
-0.14395115E-04  0.33493799E-05  0.13796019E-04
     28          0.34005984E-02      0.44921368E-18     -0.13515660E-17
-0.19606280E-18  0.12547056E-02 -0.69386025E-04
     29          0.33210377E-02     -0.70479469E-04     -0.41406237E-02
0.14395115E-04  0.33493799E-05  0.13796019E-04
     30          0.27449461E-02      0.00000000E+00      0.00000000E+00
0.00000000E+00  0.00000000E+00  0.00000000E+00
     31          0.84819812E-02      0.10817206E-17     -0.13767102E-17
-0.24873321E-18  0.21830564E-02 -0.75736461E-04
     32          0.52119552E-01      0.39452334E-17     -0.13768324E-17
-0.22935432E-18  0.43627463E-02 -0.40282107E-03
     33         -0.68817913E-03      0.53822349E-03      0.40524020E-04
-0.33077571E-04  0.12967395E-03 -0.19991397E-03
     34          0.15934630E-02      0.16722017E-03      0.17542638E-03
0.50003453E-04  0.47000971E-03 -0.33024599E-03
     35          0.94138562E-04      0.48687773E-03      0.34807243E-03
0.41011653E-04  0.42028253E-03 -0.15719350E-03
     36          0.15845132E-02      0.26126028E-03      0.50779775E-03
-0.51185821E-05 -0.36361206E-03 -0.21027207E-03

          ***** POST1 NODAL DISPLACEMENT LISTING *****

  LOAD STEP     1  ITERATION=     1  SECTION=  1
  TIME=   0.00000E+00     LOAD CASE=  1

  THE FOLLOWING X,Y,Z DISPLACEMENTS ARE IN NODAL COORDINATES

    NODE      UX              UY              UZ              ROTX
        ROTY            ROTZ
     37         -0.25778854E-03    -0.21361349E-18      0.14937877E-18
-0.22835027E-18  0.87120118E-04 -0.12799502E-03
     38         -0.78227291E-03     0.17485726E-19      0.75663315E-18
-0.18147944E-18  0.52983436E-03 -0.24223955E-03
     39          0.70869893E-03     0.74676863E-19     -0.53774978E-18
-0.22705065E-18  0.69393287E-03 -0.27850099E-03
     40          0.15321474E-02     0.34109116E-18      0.10575628E-18
-0.20699244E-18  0.16715530E-02 -0.31414766E-03
     41         -0.68817913E-03    -0.53822349E-03     -0.40524020E-04
0.33077571E-04  0.12967395E-03 -0.19991397E-03
     42          0.15934630E-02    -0.16722017E-03     -0.17542638E-03
-0.50003453E-04  0.47000971E-03 -0.33024599E-03
     43          0.94138562E-04    -0.48687773E-03     -0.34807243E-03
-0.41011653E-04  0.42028253E-03 -0.15719350E-03
     44          0.15845132E-02    -0.26126028E-03     -0.50779775E-03
0.51185821E-05 -0.36361206E-03 -0.21027207E-03
     45         -0.11094011E-02     0.12066207E-02      0.29977639E-03
-0.98515890E-04 -0.36639136E-04 -0.75692304E-04
     46         -0.11094011E-02    -0.12066207E-02     -0.29977639E-03
0.98515890E-04 -0.36639136E-04 -0.75692304E-04
     47          0.15176192E-03    -0.64049517E-03      0.36915770E-03
0.15992514E-03 -0.77040513E-04 -0.84488388E-04
```

```
     48          0.15176192E-03      0.64049517E-03   -0.36915770E-03
-0.15992514E-03 -0.77040513E-04 -0.84488388E-04

          ***** POST1 NODAL DISPLACEMENT LISTING *****

  LOAD STEP     1  ITERATION=     1  SECTION=  1
  TIME=   0.00000E+00     LOAD CASE=  1

  THE FOLLOWING X,Y,Z DISPLACEMENTS ARE IN NODAL COORDINATES

    NODE      UX              UY              UZ              ROTX
        ROTY            ROTZ
     49         0.77609558E-03      0.10802115E-03      0.18877886E-02
0.21530940E-03 -0.18958086E-03 -0.10751301E-04
     50           0.77609558E-03    -0.10802115E-03    -0.18877886E-02
-0.21530940E-03 -0.18958086E-03 -0.10751301E-04
     51         0.23594642E-02      0.32972661E-03      0.19755822E-02
-0.18566994E-03 -0.20622175E-03 -0.57342526E-04
     52           0.23594642E-02    -0.32972661E-03    -0.19755822E-02
0.18566994E-03 -0.20622175E-03 -0.57342526E-04

 MAXIMUMS
 NODE         32              46              29              50
        32              15
 VALUE            0.52119552E-01   -0.12066207E-02   -0.41406237E-02
-0.21530940E-03  0.43627463E-02 -0.49913620E-03

 PRINT REACTION FORCES PER NODE

          ***** POST1 REACTION FORCE LISTING *****

  LOAD STEP     1  ITERATION=     1  SECTION=  1
  TIME=   0.00000E+00     LOAD CASE=  1

  THE FOLLOWING X,Y,Z FORCES ARE IN NODAL COORDINATES

    NODE      FX              FY              FZ              MX
        MY              MZ
     10                  -1891.2690      -3792.5339      -115.24699
     405.15921       5.3397273
     12   -11240.000

     14                   1891.2690       3792.5339       115.24699
     405.15921       5.3397273
     26                  -1846.7694      -5670.9463      -15.222790
     466.16236       72.314572
     30                   1846.7694       5670.9463       15.222790
     466.16236       72.314572

 TOTAL        -11240.000            0.11368684E-11    0.54569682E-11
0.18118840E-12   1742.6431       155.30860
```

```
***** ROUTINE COMPLETED *****  CP=      130.1200   TIME=   10.4555

***UNKNOWN OR NON-UNIQUE COMMAND(PREP7)= INPU

***** INPUT SWITCHED FROM FILE 5 TO FILE38  NAME=STATIC8.PRP

NEW TITLE= STATICY



ELEMENT TYPE  1 USES STIF  4
 KEYOPT(1-9)=   0   0   0     0   0   0      0   0   0
 INOTPR= 0  NUMBER OF NODES=   3

ELASTIC BEAM, 3-D

CURRENT NODAL DOF SET IS  UX    UY    UZ    ROTX  ROTY  ROTZ
 THREE-DIMENSIONAL STRUCTURE

 MATERIAL   1          COEFFICIENTS OF EX   VS. TEMP EQUATION
  C0 =  0.1440000E+10

PROPERTY TABLE EX    MAT=   1  NUM. POINTS=  2
       TEMPERATURE     DATA        TEMPERATURE     DATA
     0.00000E+00 0.14400E+10  2300.0     0.14400E+10

 MATERIAL   1          COEFFICIENTS OF DENS VS. TEMP EQUATION
  C0 =   5.237000

PROPERTY TABLE DENS  MAT=   1  NUM. POINTS=  2
       TEMPERATURE     DATA        TEMPERATURE     DATA
     0.00000E+00  5.2370      2300.0      5.2370

ELEMENT TYPE  2 USES STIF  4
 KEYOPT(1-9)=   0   0   0     0   0   0      0   0   0
 INOTPR= 0  NUMBER OF NODES=   3

ELASTIC BEAM, 3-D

CURRENT NODAL DOF SET IS  UX    UY    UZ    ROTX  ROTY  ROTZ
 THREE-DIMENSIONAL STRUCTURE

 MATERIAL   2          COEFFICIENTS OF EX   VS. TEMP EQUATION
  C0 =  0.1440000E+10

PROPERTY TABLE EX    MAT=   2  NUM. POINTS=  2
       TEMPERATURE     DATA        TEMPERATURE     DATA
     0.00000E+00 0.14400E+10  2300.0     0.14400E+10

 MATERIAL   2          COEFFICIENTS OF DENS VS. TEMP EQUATION
  C0 =   5.237000
```

```
PROPERTY TABLE DENS  MAT=   2  NUM. POINTS=  2
       TEMPERATURE     DATA        TEMPERATURE     DATA
     0.00000E+00  5.2370      2300.0      5.2370

ELEMENT TYPE  3 USES STIF  4
 KEYOPT(1-9)=   0   0   0     0   0   0      0   0   0
 INOTPR= 0  NUMBER OF NODES=   3

ELASTIC BEAM, 3-D

CURRENT NODAL DOF SET IS  UX    UY    UZ    ROTX  ROTY  ROTZ
 THREE-DIMENSIONAL STRUCTURE

 MATERIAL   3          COEFFICIENTS OF EX   VS. TEMP EQUATION
  C0 =  0.1440000E+10

PROPERTY TABLE EX    MAT=   3  NUM. POINTS=  2
       TEMPERATURE     DATA        TEMPERATURE     DATA
     0.00000E+00 0.14400E+10  2300.0     0.14400E+10

 MATERIAL   3          COEFFICIENTS OF DENS VS. TEMP EQUATION
  C0 =   5.237000

PROPERTY TABLE DENS  MAT=   3  NUM. POINTS=  2
       TEMPERATURE     DATA        TEMPERATURE     DATA
     0.00000E+00  5.2370      2300.0      5.2370

ELEMENT TYPE  4 USES STIF  4
 KEYOPT(1-9)=   0   0   0     0   0   0      0   0   0
 INOTPR= 0  NUMBER OF NODES=   3

ELASTIC BEAM, 3-D

CURRENT NODAL DOF SET IS  UX    UY    UZ    ROTX  ROTY  ROTZ
 THREE-DIMENSIONAL STRUCTURE

 MATERIAL   4          COEFFICIENTS OF EX   VS. TEMP EQUATION
  C0 =  0.1440000E+10

PROPERTY TABLE EX    MAT=   4  NUM. POINTS=  2
       TEMPERATURE     DATA        TEMPERATURE     DATA
     0.00000E+00 0.14400E+10  2300.0     0.14400E+10

 MATERIAL   4          COEFFICIENTS OF DENS VS. TEMP EQUATION
  C0 =   5.237000

PROPERTY TABLE DENS  MAT=   4  NUM. POINTS=  2
       TEMPERATURE     DATA        TEMPERATURE     DATA
     0.00000E+00  5.2370      2300.0      5.2370

 REAL CONSTANT SET   1  ITEMS   1 TO   6
```

```
   0.13318E-01   0.27500E-03   0.27500E-03   0.41670        0.41670
0.00000E+00

  REAL CONSTANT SET   2  ITEMS   1 TO   6
   0.64760E-02   0.31800E-04   0.31800E-04   0.20830        0.20830
0.00000E+00

  REAL CONSTANT SET   3  ITEMS   1 TO   6
   0.14062       0.50840E-02   0.12842        3.0000        0.41670
0.00000E+00

  REAL CONSTANT SET   3  ITEMS   7 TO  10
   0.00000E+00   0.18510E-01   0.00000E+00   0.00000E+00

  REAL CONSTANT SET   4  ITEMS   1 TO   6
   0.13368       0.16800E-02   0.11301        3.0000        0.25000
0.00000E+00

  REAL CONSTANT SET   4  ITEMS   7 TO  10
   0.00000E+00   0.63000E-02   0.00000E+00   0.00000E+00

 ANALYSIS TYPE=  0   (STATIC ANALYSIS)

 NODE    1  KCS= 0  X,Y,Z= 0.00000E+00 0.00000E+00  4.0000

 NODE    2  KCS= 0  X,Y,Z=  4.5000     0.00000E+00  4.0000

 NODE    3  KCS= 0  X,Y,Z=  9.0000     0.00000E+00  4.0000

 NODE    4  KCS= 0  X,Y,Z=  13.500     0.00000E+00  4.0000

 NODE    5  KCS= 0  X,Y,Z=  18.000     0.00000E+00  4.0000

 NODE    6  KCS= 0  X,Y,Z=  15.750     0.00000E+00  6.0000

 NODE    7  KCS= 0  X,Y,Z=  11.250     0.00000E+00  6.0000

 NODE    8  KCS= 0  X,Y,Z=  6.7500     0.00000E+00  6.0000

 NODE    9  KCS= 0  X,Y,Z=  2.2500     0.00000E+00  6.0000

 NODE   10  KCS= 0  X,Y,Z= 0.00000E+00 0.00000E+00  8.0000

 NODE   11  KCS= 0  X,Y,Z=  4.5000     0.00000E+00  8.0000

 NODE   12  KCS= 0  X,Y,Z=  9.0000     0.00000E+00  8.0000

 NODE   13  KCS= 0  X,Y,Z=  13.500     0.00000E+00  8.0000

 NODE   14  KCS= 0  X,Y,Z=  18.000     0.00000E+00  8.0000

 NODE   15  KCS= 0  X,Y,Z=  9.0000     0.00000E+00  11.000
```

```
NODE   16  KCS= 0  X,Y,Z=  9.0000      0.00000E+00  23.000
NODE   17  KCS= 0  X,Y,Z= 0.00000E+00  12.000       4.0000
NODE   18  KCS= 0  X,Y,Z=  4.5000      12.000       4.0000
NODE   19  KCS= 0  X,Y,Z=  9.0000      12.000       4.0000
NODE   20  KCS= 0  X,Y,Z=  13.500      12.000       4.0000
NODE   21  KCS= 0  X,Y,Z=  18.000      12.000       4.0000
NODE   22  KCS= 0  X,Y,Z=  15.750      12.000       6.0000
NODE   23  KCS= 0  X,Y,Z=  11.250      12.000       6.0000
NODE   24  KCS= 0  X,Y,Z=  6.7500      12.000       6.0000
NODE   25  KCS= 0  X,Y,Z=  2.2500      12.000       6.0000
NODE   26  KCS= 0  X,Y,Z= 0.00000E+00  12.000       8.0000
NODE   27  KCS= 0  X,Y,Z=  4.5000      12.000       8.0000
NODE   28  KCS= 0  X,Y,Z=  9.0000      12.000       8.0000
NODE   29  KCS= 0  X,Y,Z=  13.500      12.000       8.0000
NODE   30  KCS= 0  X,Y,Z=  18.000      12.000       8.0000
NODE   31  KCS= 0  X,Y,Z=  9.0000      12.000       11.000
NODE   32  KCS= 0  X,Y,Z=  9.0000      12.000       23.000
NODE   33  KCS= 0  X,Y,Z= 0.00000E+00  6.0000       4.0000
NODE   34  KCS= 0  X,Y,Z= 0.00000E+00  9.0000       6.0000
NODE   35  KCS= 0  X,Y,Z= 0.00000E+00  3.0000       6.0000
NODE   36  KCS= 0  X,Y,Z= 0.00000E+00  6.0000       8.0000
NODE   37  KCS= 0  X,Y,Z=  9.0000      6.0000       4.0000
NODE   38  KCS= 0  X,Y,Z=  9.0000      3.0000       6.0000
NODE   39  KCS= 0  X,Y,Z=  9.0000      9.0000       6.0000
NODE   40  KCS= 0  X,Y,Z=  9.0000      6.0000       8.0000
NODE   41  KCS= 0  X,Y,Z=  18.000      6.0000       4.0000
```

NODE	42	KCS= 0	X,Y,Z=	18.000	9.0000	6.0000
NODE	43	KCS= 0	X,Y,Z=	18.000	3.0000	6.0000
NODE	44	KCS= 0	X,Y,Z=	18.000	6.0000	8.0000
NODE	45	KCS= 0	X,Y,Z=	4.5000	3.0000	4.0000
NODE	46	KCS= 0	X,Y,Z=	13.500	3.0000	4.0000
NODE	47	KCS= 0	X,Y,Z=	4.5000	9.0000	4.0000
NODE	48	KCS= 0	X,Y,Z=	13.500	9.0000	4.0000
NODE	49	KCS= 0	X,Y,Z=	4.5000	3.0000	8.0000
NODE	50	KCS= 0	X,Y,Z=	13.500	3.0000	8.0000
NODE	51	KCS= 0	X,Y,Z=	4.5000	9.0000	8.0000
NODE	52	KCS= 0	X,Y,Z=	13.500	9.0000	8.0000
NODE	53	KCS= 0	X,Y,Z=	18.000	12.000	11.000
NODE	54	KCS= 0	X,Y,Z=	18.000	0.00000E+00	11.000
NODE	55	KCS= 0	X,Y,Z=	18.000	0.00000E+00	23.000

REAL CONSTANT NUMBER= 1

ELEMENT	1	17	18	0
ELEMENT	2	18	19	0
ELEMENT	3	19	20	0
ELEMENT	4	20	21	0
ELEMENT	5	21	30	0
ELEMENT	6	30	29	0
ELEMENT	7	29	28	0
ELEMENT	8	28	27	0
ELEMENT	9	27	26	0
ELEMENT	10	26	17	0
ELEMENT	11	1	2	0
ELEMENT	12	2	3	0
ELEMENT	13	3	4	0
ELEMENT	14	4	5	0
ELEMENT	15	5	14	0
ELEMENT	16	14	13	0
ELEMENT	17	13	12	0
ELEMENT	18	12	11	0
ELEMENT	19	11	10	0
ELEMENT	20	10	1	0
ELEMENT	21	17	33	0
ELEMENT	22	33	1	0

ELEMENT	23	10	36	0
ELEMENT	24	36	26	0
ELEMENT	25	21	41	0
ELEMENT	26	41	5	0
ELEMENT	27	14	44	0
ELEMENT	28	44	30	0
ELEMENT	29	3	37	0
ELEMENT	30	37	19	0
ELEMENT	31	28	40	0
ELEMENT	32	40	12	0
ELEMENT	33	36	40	0
ELEMENT	34	40	44	0
ELEMENT	35	33	37	0
ELEMENT	36	37	41	0
ELEMENT	37	13	15	0
ELEMENT	38	11	15	0
ELEMENT	39	29	31	0
ELEMENT	40	27	31	0

REAL CONSTANT NUMBER= 2

ELEMENT	41	17	25	0
ELEMENT	42	25	27	0
ELEMENT	43	26	25	0
ELEMENT	44	25	18	0
ELEMENT	45	18	24	0
ELEMENT	46	27	24	0
ELEMENT	47	24	19	0
ELEMENT	48	24	28	0
ELEMENT	49	28	23	0
ELEMENT	50	19	23	0
ELEMENT	51	23	29	0
ELEMENT	52	23	20	0
ELEMENT	53	20	22	0
ELEMENT	54	29	22	0
ELEMENT	55	22	21	0
ELEMENT	56	22	30	0
ELEMENT	57	1	9	0
ELEMENT	58	10	9	0
ELEMENT	59	9	2	0
ELEMENT	60	9	11	0
ELEMENT	61	11	8	0
ELEMENT	62	2	8	0
ELEMENT	63	8	3	0
ELEMENT	64	8	12	0
ELEMENT	65	12	7	0
ELEMENT	66	3	7	0
ELEMENT	67	7	4	0
ELEMENT	68	7	13	0
ELEMENT	69	13	6	0
ELEMENT	70	4	6	0
ELEMENT	71	6	5	0
ELEMENT	72	6	14	0

ELEMENT	73	17	34	0
ELEMENT	74	26	34	0
ELEMENT	75	34	33	0
ELEMENT	76	34	36	0
ELEMENT	77	36	35	0
ELEMENT	78	33	35	0
ELEMENT	79	35	1	0
ELEMENT	80	35	10	0
ELEMENT	81	21	42	0
ELEMENT	82	30	42	0
ELEMENT	83	42	41	0
ELEMENT	84	42	44	0
ELEMENT	85	44	43	0
ELEMENT	86	41	43	0
ELEMENT	87	43	5	0
ELEMENT	88	43	14	0
ELEMENT	89	3	38	0
ELEMENT	90	38	40	0
ELEMENT	91	12	38	0
ELEMENT	92	38	37	0
ELEMENT	93	37	39	0
ELEMENT	94	39	28	0
ELEMENT	95	40	39	0
ELEMENT	96	39	19	0
ELEMENT	97	1	45	0
ELEMENT	98	45	37	0
ELEMENT	99	33	45	0
ELEMENT	100	45	3	0
ELEMENT	101	3	46	0
ELEMENT	102	46	41	0
ELEMENT	103	37	46	0
ELEMENT	104	46	5	0
ELEMENT	105	37	48	0
ELEMENT	106	48	21	0
ELEMENT	107	19	48	0
ELEMENT	108	48	41	0
ELEMENT	109	33	47	0
ELEMENT	110	47	19	0
ELEMENT	111	17	47	0
ELEMENT	112	47	37	0
ELEMENT	113	10	49	0
ELEMENT	114	49	40	0
ELEMENT	115	36	49	0
ELEMENT	116	49	12	0
ELEMENT	117	12	50	0
ELEMENT	118	50	44	0
ELEMENT	119	40	50	0
ELEMENT	120	50	14	0
ELEMENT	121	40	52	0
ELEMENT	122	52	30	0
ELEMENT	123	28	52	0
ELEMENT	124	52	44	0

```
 ELEMENT   125      36    51     0
 ELEMENT   126      51    28     0
 ELEMENT   127      26    51     0
 ELEMENT   128      51    40     0

 REAL CONSTANT NUMBER=  3
 ELEMENT   129      19    28    21
 ELEMENT   130      28    31    30
 ELEMENT   131      31    32    53
 ELEMENT   132       3    12     5
 ELEMENT   133      12    15    14
 ELEMENT   134      15    16    54

 REAL CONSTANT NUMBER=  4
 ELEMENT   135      16    32    55
 ELEMENT   136      40    15    44
 ELEMENT   137      40    31    44

 SPECIFIED DISP UY   FOR SELECTED NODES IN RANGE    10 TO    10 BY
1
  VALUES= 0.00000E+00 0.00000E+00  ADDITIONAL DOFS=  UZ    ROTX  ROTY
ROTZ

 SPECIFIED DISP UY   FOR SELECTED NODES IN RANGE    14 TO    14 BY
1
  VALUES= 0.00000E+00 0.00000E+00  ADDITIONAL DOFS=  UZ    ROTX  ROTY
ROTZ

 SPECIFIED DISP UY   FOR SELECTED NODES IN RANGE    26 TO    26 BY
1
  VALUES= 0.00000E+00 0.00000E+00  ADDITIONAL DOFS=  UZ    ROTX  ROTY
ROTZ

 SPECIFIED DISP UY   FOR SELECTED NODES IN RANGE    30 TO    30 BY
1
  VALUES= 0.00000E+00 0.00000E+00  ADDITIONAL DOFS=  UZ    ROTX  ROTY
ROTZ

 SPECIFIED DISP UX   FOR SELECTED NODES IN RANGE    12 TO    12 BY
1
  VALUES= 0.00000E+00 0.00000E+00  ADDITIONAL DOFS=


 MASTER DOF      FOR ALL SELECTED NODES
 ADDITIONAL DOFS=

 SPECIFIED FORCE FY   FOR SELECTED NODES IN RANGE    16 TO    16 BY
 1
  VALUES=  500.00     0.00000E+00

 SPECIFIED FORCE FY   FOR SELECTED NODES IN RANGE    32 TO    32 BY
 1
```

```
 VALUES=  500.00     0.00000E+00

*** NOTE ***
NPRINT IS ZERO OR GREATER THAN NITTER. SOLUTION PRINTOUT
WILL BE SUPPRESSED UNLESS OTHER PRINT CONTROLS HAVE BEEN DEFINED.

*** NOTE ***
DATA CHECKED - NO ERRORS FOUND

*** PREP7 GLOBAL STATUS ***

TITLE= STATICY

ANALYSIS TYPE=     0
NUMBER OF ELEMENT TYPES=     4
   137 ELEMENTS CURRENTLY SELECTED.  MAX ELEMENT NUMBER =    137
    55 NODES CURRENTLY SELECTED.     MAX NODE NUMBER =        55
MAXIMUM LINEAR PROPERTY NUMBER=     4
MAXIMUM REAL CONSTANT SET NUMBER=     4
ACTIVE COORDINATE SYSTEM=     0  (CARTESIAN)
NUMBER OF IMPOSED DISPLACEMENTS=    21
NUMBER OF NODAL FORCES=     2

ANALYSIS DATA WRITTEN ON FILE27

ENTER  FINISH  TO LEAVE PREP7



ALL CURRENT PREP7 DATA WRITTEN TO FILE16   NAME= FILE16.DAT
 FOR POSSIBLE RESUME FROM THIS POINT


***** ROUTINE COMPLETED *****  CP=       72.7800   TIME=   10.7388

STORE SG1I  FOR ELEMENT TYPE STIF  4  FROM ITEM    19

STORE SG3I  FOR ELEMENT TYPE STIF  4  FROM ITEM    20

STORE SG1J  FOR ELEMENT TYPE STIF  4  FROM ITEM    21

STORE SG3J  FOR ELEMENT TYPE STIF  4  FROM ITEM    22

USE LOAD STEP     1  ITERATION     1  SECTION   1  FOR LOAD CASE
1



GEOMETRY STORED FOR     55  NODES    137  ELEMENTS
 TITLE= STATICX8
```

DISPLACEMENT STORED FOR 55 NODES

STRESSES STORED FOR 4 SELECTED ITEMS

ITERATION SUMMARY INFORMATION STORED

NODAL FORCES STORED FOR 137 ELEMENTS

REACTIONS STORED FOR 21 REACTIONS

FOR LOAD STEP= 1 ITERATION= 1 SECTION= 1
TIME= 0.000000E+00 LOAD CASE= 1
TITLE= STATICX8

PRINT ELEMENT STRESS ITEMS PER ELEMENT

***** POST1 ELEMENT STRESS LISTING *****

LOAD STEP 1 ITERATION= 1 SECTION= 1
TIME= 0.00000E+00 LOAD CASE= 1

ELEM	SG1I	SG3I	SG1J	SG3J
1	22374.724	13479.104	24190.585	11663.243
2	63738.523	45231.208	81880.846	27088.885
3	81880.846	27088.885	63738.523	45231.208
4	24190.585	11663.243	22374.724	13479.104
5	27846.759	23356.163	42589.530	8613.3911
6	68998.228	-59736.034	45445.504	-36183.311
7	22229.206	-31727.786	12385.607	-21884.187
8	12385.607	-21884.187	22229.206	-31727.786
9	45445.504	-36183.311	68998.228	-59736.034
10	42589.530	8613.3911	27846.759	23356.163
11	-13479.104	-22374.724	-11663.243	-24190.585
12	-45231.208	-63738.523	-27088.885	-81880.846
13	-27088.885	-81880.846	-45231.208	-63738.523
14	-11663.243	-24190.585	-13479.104	-22374.724

***** POST1 ELEMENT STRESS LISTING *****

LOAD STEP 1 ITERATION= 1 SECTION= 1
TIME= 0.00000E+00 LOAD CASE= 1

ELEM	SG1I	SG3I	SG1J	SG3J
15	-23356.163	-27846.759	-8613.3911	-42589.530
16	59736.034	-68998.228	36183.311	-45445.504
17	31727.786	-22229.206	21884.187	-12385.607
18	21884.187	-12385.607	31727.786	-22229.206
19	36183.311	-45445.504	59736.034	-68998.228
20	-8613.3911	-42589.530	-23356.163	-27846.759
21	2242.4201	-9445.5443	867.14352	-8070.2677
22	8070.2677	-867.14352	9445.5443	-2242.4201
23	9086.5431	3008.0758	12107.308	-12.688670
24	12.688670	-12107.308	-3008.0758	-9086.5431
25	2242.4201	-9445.5443	867.14352	-8070.2677
26	8070.2677	-867.14352	9445.5443	-2242.4201
27	9086.5431	3008.0758	12107.308	-12.688670
28	12.688670	-12107.308	-3008.0758	-9086.5431

***** POST1 ELEMENT STRESS LISTING *****

LOAD STEP 1 ITERATION= 1 SECTION= 1
TIME= 0.00000E+00 LOAD CASE= 1

ELEM	SG1I	SG3I	SG1J	SG3J
29	7163.5281	-14584.159	187.86971	-7608.5005
30	7608.5005	-187.86971	14584.159	-7163.5281
31	-46189.257	-113525.77	-31828.314	-127886.71
32	127886.71	31828.314	113525.77	46189.257

33	12505.606	-12505.606	14486.094	-14486.094
34	14486.094	-14486.094	12505.606	-12505.606
35	3960.8808	-3960.8808	1628.4760	-1628.4760
36	1628.4760	-1628.4760	3960.8808	-3960.8808
37	53506.387	14348.366	68840.543	-985.79018
38	53506.387	14348.366	68840.543	-985.79018
39	-14348.366	-53506.387	985.79018	-68840.543
40	-14348.366	-53506.387	985.79018	-68840.543
41	-70528.500	-78994.424	-68793.932	-80728.992
42	-64189.033	-88170.514	-53536.690	-98822.857

***** POST1 ELEMENT STRESS LISTING *****

LOAD STEP 1 ITERATION= 1 SECTION= 1
TIME= 0.00000E+00 LOAD CASE= 1

ELEM	SG1I	SG3I	SG1J	SG3J
43	80462.674	24369.816	69144.892	35687.597
44	78670.010	25621.286	83055.538	21235.758
45	-36699.706	-59611.520	-23197.789	-73113.437
46	65315.721	-10041.162	50997.679	4276.8794
47	32325.927	23637.142	36323.315	19639.753
48	-40967.216	-53897.442	-38210.927	-56653.731
49	-38210.927	-56653.731	-40967.216	-53897.442
50	36323.315	19639.753	32325.927	23637.142
51	50997.679	4276.8794	65315.721	-10041.162
52	-23197.789	-73113.437	-36699.706	-59611.520
53	83055.538	21235.758	78670.010	25621.286
54	-53536.690	-98822.857	-64189.033	-88170.514

55	-68793.932	-80728.992	-70528.500	-78994.424
56	69144.892	35687.597	80462.674	24369.816

***** POST1 ELEMENT STRESS LISTING *****

LOAD STEP 1 ITERATION= 1 SECTION= 1
TIME= 0.00000E+00 LOAD CASE= 1

ELEM	SG1I	SG3I	SG1J	SG3J
57	78994.424	70528.500	80728.992	68793.932
58	-24369.816	-80462.674	-35687.597	-69144.892
59	-25621.286	-78670.010	-21235.758	-83055.538
60	88170.514	64189.033	98822.857	53536.690
61	10041.162	-65315.721	-4276.8794	-50997.679
62	59611.520	36699.706	73113.437	23197.789
63	-23637.142	-32325.927	-19639.753	-36323.315
64	53897.442	40967.216	56653.731	38210.927
65	56653.731	38210.927	53897.442	40967.216
66	-19639.753	-36323.315	-23637.142	-32325.927
67	73113.437	23197.789	59611.520	36699.706
68	-4276.8794	-50997.679	10041.162	-65315.721
69	98822.857	53536.690	88170.514	64189.033
70	-21235.758	-83055.538	-25621.286	-78670.010

***** POST1 ELEMENT STRESS LISTING *****

LOAD STEP 1 ITERATION= 1 SECTION= 1
TIME= 0.00000E+00 LOAD CASE= 1

ELEM	SG1I	SG3I	SG1J	SG3J
71	80728.992	68793.932	78994.424	70528.500
72	-35687.597	-69144.892	-24369.816	-80462.674

73	-4497.7174	-6489.2534	-485.73721	-10501.234
74	11568.741	1834.0696	11713.181	1689.6296
75	9488.8738	3936.6372	8686.1556	4739.3554
76	-2438.1579	-8613.6551	-1583.9341	-9467.8790
77	9467.8790	1583.9341	8613.6551	2438.1579
78	-4739.3554	-8686.1556	-3936.6372	-9488.8738
79	10501.234	485.73721	6489.2534	4497.7174
80	-1689.6296	-11713.181	-1834.0696	-11568.741
81	-4497.7174	-6489.2534	-485.73721	-10501.234
82	11568.741	1834.0696	11713.181	1689.6296
83	9488.8738	3936.6372	8686.1556	4739.3554
84	-2438.1579	-8613.6551	-1583.9341	-9467.8790

***** POST1 ELEMENT STRESS LISTING *****

LOAD STEP 1 ITERATION= 1 SECTION= 1
TIME= 0.00000E+00 LOAD CASE= 1

ELEM	SG1I	SG3I	SG1J	SG3J
85	9467.8790	1583.9341	8613.6551	2438.1579
86	-4739.3554	-8686.1556	-3936.6372	-9488.8738
87	10501.234	485.73721	6489.2534	4497.7174
88	-1689.6296	-11713.181	-1834.0696	-11568.741
89	15919.557	12098.478	23537.543	4480.4918
90	39159.352	-9583.5549	59068.659	-29492.862
91	46463.535	32384.184	54426.683	24421.035
92	38317.439	37997.647	40132.720	36182.367
93	-36182.367	-40132.720	-37997.647	-38317.439
94	-24421.035	-54426.683	-32384.184	-46463.535

95	29492.862	-59068.659	9583.5549	-39159.352
96	-4480.4918	-23537.543	-12098.478	-15919.557
97	-16366.139	-26960.405	-12618.154	-30708.390
98	-14717.184	-28429.953	-19897.943	-23249.194

***** POST1 ELEMENT STRESS LISTING *****

LOAD STEP 1 ITERATION= 1 SECTION= 1
TIME= 0.00000E+00 LOAD CASE= 1

ELEM	SG1I	SG3I	SG1J	SG3J
99	168.70965	-7013.3198	467.93984	-7312.5499
100	3631.2749	-10709.298	6426.5514	-13504.575
101	6426.5514	-13504.575	3631.2749	-10709.298
102	467.93984	-7312.5499	168.70965	-7013.3198
103	-19897.943	-23249.194	-14717.184	-28429.953
104	-12618.154	-30708.390	-16366.139	-26960.405
105	23249.194	19897.943	28429.953	14717.184
106	30708.390	12618.154	26960.405	16366.139
107	13504.575	-6426.5514	10709.298	-3631.2749
108	7312.5499	-467.93984	7013.3198	-168.70965
109	7013.3198	-168.70965	7312.5499	-467.93984
110	10709.298	-3631.2749	13504.575	-6426.5514
111	26960.405	16366.139	30708.390	12618.154
112	28429.953	14717.184	23249.194	19897.943

***** POST1 ELEMENT STRESS LISTING *****

LOAD STEP 1 ITERATION= 1 SECTION= 1
TIME= 0.00000E+00 LOAD CASE= 1

ELEM	SG1I	SG3I	SG1J	SG3J

113	65971.524	47243.158	62518.202	50696.480
114	69889.047	43364.118	74454.529	38798.637
115	-28435.922	-31935.783	-24468.725	-35902.979
116	-14728.866	-45474.612	-15916.416	-44287.062
117	-15916.416	-44287.062	-14728.866	-45474.612
118	-24468.725	-35902.979	-28435.922	-31935.783
119	74454.529	38798.637	69889.047	43364.118
120	62518.202	50696.480	65971.524	47243.158
121	-38798.637	-74454.529	-43364.118	-69889.047
122	-50696.480	-62518.202	-47243.158	-65971.524
123	44287.062	15916.416	45474.612	14728.866
124	35902.979	24468.725	31935.783	28435.922
125	31935.783	28435.922	35902.979	24468.725
126	45474.612	14728.866	44287.062	15916.416

***** POST1 ELEMENT STRESS LISTING *****

LOAD STEP 1 ITERATION= 1 SECTION= 1
TIME= 0.00000E+00 LOAD CASE= 1

ELEM	SG1I	SG3I	SG1J	SG3J
127	-47243.158	-65971.524	-50696.480	-62518.202
128	-43364.118	-69889.047	-38798.637	-74454.529
129	-1243.7575	-1823.3890	-1200.9895	-1866.1570
130	-2873.7748	-8148.8186	120073.42	-131096.01
131	152484.58	-157735.25	88153.814	-93404.480
132	1823.3890	1243.7575	1866.1570	1200.9895
133	8148.8186	2873.7748	131096.01	-120073.42
134	157735.25	-152484.58	93404.480	-88153.814

135	164815.81	-164815.81	164815.81	-164815.81
136	-7277.2574	-19588.143	33416.572	-60281.972
137	19588.143	7277.2574	60281.972	-33416.572

PRINT NODAL DISPLACEMENTS

```
          ***** POST1 NODAL DISPLACEMENT LISTING *****

  LOAD STEP     1  ITERATION=     1  SECTION=  1
  TIME=   0.00000E+00     LOAD CASE=  1

  THE FOLLOWING X,Y,Z DISPLACEMENTS ARE IN NODAL COORDINATES

    NODE      UX              UY              UZ              ROTX
        ROTY            ROTZ
      1         0.22628681E-03   -0.55373197E-04      0.71115169E-04
-0.18774209E-04 -0.79503074E-04  0.20573878E-04
      2         0.17026520E-03   -0.17422574E-04      0.52098893E-03
-0.50857114E-04 -0.12972883E-03  0.63277062E-05
      3        0.60628106E-19      0.67672269E-05      0.10090641E-02
-0.10868376E-03 -0.19139101E-19 -0.54445500E-19
      4       -0.17026520E-03   -0.17422574E-04       0.52098893E-03
-0.50857114E-04  0.12972883E-03 -0.63277062E-05
      5       -0.22628681E-03   -0.55373197E-04       0.71115169E-04
-0.18774209E-04  0.79503074E-04 -0.20573878E-04
      6       -0.17581601E-03   -0.91572185E-05       0.36314681E-03
-0.14831293E-04  0.10991383E-03 -0.66823725E-05
      7        0.25309296E-04      0.13623351E-03      0.89254158E-03
-0.77273837E-04  0.46798107E-04 -0.53193350E-04
      8      -0.25309296E-04      0.13623351E-03      0.89254158E-03
-0.77273837E-04 -0.46798107E-04  0.53193350E-04
      9         0.17581601E-03   -0.91572185E-05      0.36314681E-03
-0.14831293E-04 -0.10991383E-03  0.66823725E-05
     10      -0.36935416E-06      0.00000000E+00      0.00000000E+00
0.00000000E+00  0.00000000E+00  0.00000000E+00
     11      -0.14841531E-04      0.17166769E-03      0.81735155E-03
-0.16637825E-03 -0.12793724E-03  0.48694051E-04
     12        0.00000000E+00      0.43339435E-03      0.10133240E-02
-0.10453477E-03 -0.62508092E-20 -0.57442244E-19

          ***** POST1 NODAL DISPLACEMENT LISTING *****

  LOAD STEP     1  ITERATION=     1  SECTION=  1
  TIME=   0.00000E+00     LOAD CASE=  1

  THE FOLLOWING X,Y,Z DISPLACEMENTS ARE IN NODAL COORDINATES

    NODE      UX              UY              UZ              ROTX
        ROTY            ROTZ
```

```
     13          0.14841531E-04      0.17166769E-03      0.81735155E-03
-0.16637825E-03  0.12793724E-03 -0.48694051E-04
     14          0.36935416E-06      0.00000000E+00      0.00000000E+00
0.00000000E+00  0.00000000E+00  0.00000000E+00
     15       -0.31449606E-21      0.13484989E-02      0.10248059E-02
-0.71922157E-03  0.27779439E-20 -0.66562389E-19
     16          0.24674952E-19      0.27533008E-01      0.10466836E-02
-0.20057340E-02  0.16737847E-20 -0.53157776E-19
     17         -0.22628681E-03     -0.55373197E-04     -0.71115169E-04
-0.18774209E-04  0.79503074E-04  0.20573878E-04
     18         -0.17026520E-03     -0.17422574E-04     -0.52098893E-03
-0.50857114E-04  0.12972883E-03  0.63277062E-05
     19          0.86794573E-18      0.67672269E-05     -0.10090641E-02
-0.10868376E-03 -0.60956532E-20 -0.52409914E-19
     20          0.17026520E-03     -0.17422574E-04     -0.52098893E-03
-0.50857114E-04 -0.12972883E-03 -0.63277062E-05
     21          0.22628681E-03     -0.55373197E-04     -0.71115169E-04
-0.18774209E-04 -0.79503074E-04 -0.20573878E-04
     22          0.17581601E-03     -0.91572185E-05     -0.36314681E-03
-0.14831293E-04 -0.10991383E-03 -0.66823725E-05
     23        -0.25309296E-04      0.13623351E-03     -0.89254158E-03
-0.77273837E-04 -0.46798107E-04 -0.53193350E-04
     24          0.25309296E-04      0.13623351E-03     -0.89254158E-03
-0.77273837E-04  0.46798107E-04  0.53193350E-04

          ***** POST1 NODAL DISPLACEMENT LISTING *****

  LOAD STEP     1  ITERATION=     1  SECTION=  1
  TIME=   0.00000E+00     LOAD CASE=  1

  THE FOLLOWING X,Y,Z DISPLACEMENTS ARE IN NODAL COORDINATES

    NODE      UX              UY              UZ              ROTX
       ROTY            ROTZ
     25         -0.17581601E-03     -0.91572185E-05     -0.36314681E-03
-0.14831293E-04  0.10991383E-03  0.66823725E-05
     26          0.36935416E-06      0.00000000E+00      0.00000000E+00
0.00000000E+00  0.00000000E+00  0.00000000E+00
     27          0.14841531E-04      0.17166769E-03     -0.81735155E-03
-0.16637825E-03  0.12793724E-03  0.48694051E-04
     28          0.83742457E-18      0.43339435E-03     -0.10133240E-02
-0.10453477E-03 -0.10774486E-19 -0.57793766E-19
     29        -0.14841531E-04      0.17166769E-03     -0.81735155E-03
-0.16637825E-03 -0.12793724E-03 -0.48694051E-04
     30       -0.36935416E-06      0.00000000E+00      0.00000000E+00
0.00000000E+00  0.00000000E+00  0.00000000E+00
     31          0.80121914E-18      0.13484989E-02     -0.10248059E-02
-0.71922157E-03 -0.12346020E-19 -0.70929342E-19
     32          0.66141278E-18      0.27533008E-01     -0.10466836E-02
-0.20057340E-02 -0.11241860E-19 -0.53291127E-19
     33          0.63504531E-18     -0.40366688E-04      0.15129185E-19
-0.19431940E-04 -0.30511449E-18  0.34983275E-04
```

```
     34         -0.53146470E-04    -0.57990146E-05    -0.21550878E-04
-0.82930271E-05  0.25957619E-04  0.94247912E-05
     35          0.53146470E-04   -0.57990146E-05     0.21550878E-04
-0.82930271E-05 -0.25957619E-04  0.94247912E-05
     36         0.34683123E-18     0.25197123E-04     0.58857675E-19
-0.50029367E-06  0.64592052E-19  0.29704935E-04

          ***** POST1 NODAL DISPLACEMENT LISTING *****

  LOAD STEP     1  ITERATION=     1  SECTION=  1
  TIME=   0.00000E+00     LOAD CASE=  1

  THE FOLLOWING X,Y,Z DISPLACEMENTS ARE IN NODAL COORDINATES

    NODE      UX              UY              UZ              ROTX
       ROTY             ROTZ
     37          0.50461657E-18   -0.86924205E-05     0.20625802E-17
-0.17843477E-03  0.20592139E-20 -0.42801666E-19
     38         0.23780041E-18     0.29905751E-03     0.63386380E-03
-0.20025521E-03 -0.25763420E-19 -0.76937216E-19
     39          0.65277003E-18     0.29905751E-03    -0.63386380E-03
-0.20025521E-03 -0.14514875E-19 -0.72082019E-19
     40          0.39643996E-18     0.76613399E-03    -0.61277540E-18
0.39063169E-04  0.21323682E-20 -0.67433767E-19
     41          0.34966690E-18   -0.40366688E-04     0.14320952E-19
-0.19431940E-04  0.27277676E-18 -0.34983275E-04
     42           0.53146470E-04    -0.57990146E-05    -0.21550878E-04
-0.82930271E-05 -0.25957619E-04 -0.94247912E-05
     43        -0.53146470E-04    -0.57990146E-05     0.21550878E-04
-0.82930271E-05  0.25957619E-04 -0.94247912E-05
     44         0.41931936E-18     0.25197123E-04     0.48733311E-20
-0.50029367E-06 -0.57874745E-19 -0.29704935E-04
     45         0.51524482E-04     0.60091891E-04     0.34116856E-03
-0.10482950E-03 -0.71762096E-04  0.71710809E-05
     46       -0.51524482E-04     0.60091891E-04     0.34116856E-03
-0.10482950E-03  0.71762096E-04 -0.71710809E-05
     47        -0.51524482E-04     0.60091891E-04    -0.34116856E-03
-0.10482950E-03  0.71762096E-04  0.71710809E-05
     48          0.51524482E-04     0.60091891E-04    -0.34116856E-03
-0.10482950E-03 -0.71762096E-04 -0.71710809E-05

          ***** POST1 NODAL DISPLACEMENT LISTING *****

  LOAD STEP     1  ITERATION=     1  SECTION=  1
  TIME=   0.00000E+00     LOAD CASE=  1

  THE FOLLOWING X,Y,Z DISPLACEMENTS ARE IN NODAL COORDINATES

    NODE      UX              UY              UZ              ROTX
       ROTY             ROTZ
     49         0.51048114E-04     0.30615267E-03     0.19966938E-03
-0.87635981E-04 -0.62477030E-04  0.64022556E-04
```

```
     50       -0.51048114E-04       0.30615267E-03       0.19966938E-03
-0.87635981E-04  0.62477030E-04 -0.64022556E-04
     51       -0.51048114E-04       0.30615267E-03    -0.19966938E-03
-0.87635981E-04  0.62477030E-04  0.64022556E-04
     52        0.51048114E-04       0.30615267E-03    -0.19966938E-03
-0.87635981E-04 -0.62477030E-04 -0.64022556E-04

 MAXIMUMS
 NODE          1              16              16              32
        4              50
 VALUE          0.22628681E-03     0.27533008E-01     0.10466836E-02
-0.20057340E-02  0.12972883E-03 -0.64022556E-04

 PRINT REACTION FORCES PER NODE

          ***** POST1 REACTION FORCE LISTING *****

  LOAD STEP     1  ITERATION=     1  SECTION=  1
  TIME=   0.00000E+00     LOAD CASE=  1

  THE FOLLOWING X,Y,Z FORCES ARE IN NODAL COORDINATES

    NODE      FX              FY              FZ              MX
        MY              MZ
     10                  -250.00000      -622.50387       14.976753
     102.39078      -9.6007942
     12  -0.16248444E-11

     14                  -250.00000      -622.50387       14.976753
    -102.39078       9.6007942
     26                  -250.00000       622.50387       14.976753
    -102.39078      -9.6007942
     30                  -250.00000       622.50387       14.976753
     102.39078       9.6007942

 TOTAL   -0.16248444E-11 -1000.00000     -0.54569682E-11   59.907013
    0.00000000E+00  0.46185278E-13


 ***** ROUTINE COMPLETED *****  CP=      149.4500   TIME=   10.6642

 ***** INPUT SWITCHED FROM FILE 5 TO FILE38  NAME=MODE8.PRP

 ELEMENT TYPE  1 USES STIF  4
  KEYOPT(1-9)=   0   0   0     0   0   0      0   0   0
  INOTPR= 0  NUMBER OF NODES=   3

 ELASTIC BEAM, 3-D

 CURRENT NODAL DOF SET IS  UX    UY    UZ    ROTX  ROTY  ROTZ
  THREE-DIMENSIONAL STRUCTURE
```

```
 MATERIAL   1          COEFFICIENTS OF EX   VS. TEMP EQUATION
  C0 =  0.1440000E+10

PROPERTY TABLE EX    MAT=   1  NUM. POINTS=  2
       TEMPERATURE     DATA        TEMPERATURE     DATA
     0.00000E+00 0.14400E+10  2300.0     0.14400E+10

 MATERIAL   1          COEFFICIENTS OF DENS VS. TEMP EQUATION
  C0 =   5.237000

PROPERTY TABLE DENS  MAT=   1  NUM. POINTS=  2
       TEMPERATURE     DATA        TEMPERATURE     DATA
     0.00000E+00  5.2370      2300.0      5.2370

ELEMENT TYPE  2 USES STIF  4
 KEYOPT(1-9)=   0   0   0     0   0   0      0   0   0
 INOTPR= 0  NUMBER OF NODES=   3

ELASTIC BEAM, 3-D

CURRENT NODAL DOF SET IS  UX    UY    UZ    ROTX  ROTY  ROTZ
 THREE-DIMENSIONAL STRUCTURE

 MATERIAL   2          COEFFICIENTS OF EX   VS. TEMP EQUATION
  C0 =  0.1440000E+10

PROPERTY TABLE EX    MAT=   2  NUM. POINTS=  2
       TEMPERATURE     DATA        TEMPERATURE     DATA
     0.00000E+00 0.14400E+10  2300.0     0.14400E+10

 MATERIAL   2          COEFFICIENTS OF DENS VS. TEMP EQUATION
  C0 =   5.237000

PROPERTY TABLE DENS  MAT=   2  NUM. POINTS=  2
       TEMPERATURE     DATA        TEMPERATURE     DATA
     0.00000E+00  5.2370      2300.0      5.2370

ELEMENT TYPE  3 USES STIF  4
 KEYOPT(1-9)=   0   0   0     0   0   0      0   0   0
 INOTPR= 0  NUMBER OF NODES=   3

ELASTIC BEAM, 3-D

CURRENT NODAL DOF SET IS  UX    UY    UZ    ROTX  ROTY  ROTZ
 THREE-DIMENSIONAL STRUCTURE

 MATERIAL   3          COEFFICIENTS OF EX   VS. TEMP EQUATION
  C0 =  0.1440000E+10

PROPERTY TABLE EX    MAT=   3  NUM. POINTS=  2
       TEMPERATURE     DATA        TEMPERATURE     DATA
     0.00000E+00 0.14400E+10  2300.0     0.14400E+10
```

```
 MATERIAL   3          COEFFICIENTS OF DENS VS. TEMP EQUATION
  C0 =   5.237000

PROPERTY TABLE DENS  MAT=   3  NUM. POINTS=  2
       TEMPERATURE     DATA        TEMPERATURE     DATA
     0.00000E+00  5.2370      2300.0      5.2370

ELEMENT TYPE  4 USES STIF  4
 KEYOPT(1-9)=   0   0   0     0   0   0      0   0   0
 INOTPR= 0  NUMBER OF NODES=   3

ELASTIC BEAM, 3-D

CURRENT NODAL DOF SET IS  UX    UY    UZ    ROTX  ROTY  ROTZ
 THREE-DIMENSIONAL STRUCTURE

 MATERIAL   4          COEFFICIENTS OF EX   VS. TEMP EQUATION
  C0 =  0.1440000E+10

PROPERTY TABLE EX    MAT=   4  NUM. POINTS=  2
       TEMPERATURE     DATA        TEMPERATURE     DATA
     0.00000E+00 0.14400E+10  2300.0     0.14400E+10

 MATERIAL   4          COEFFICIENTS OF DENS VS. TEMP EQUATION
  C0 =   5.237000

PROPERTY TABLE DENS  MAT=   4  NUM. POINTS=  2
       TEMPERATURE     DATA        TEMPERATURE     DATA
     0.00000E+00  5.2370      2300.0      5.2370

 REAL CONSTANT SET   1  ITEMS   1 TO   6
  0.13318E-01  0.27500E-03  0.27500E-03  0.41670       0.41670
0.00000E+00

 REAL CONSTANT SET   2  ITEMS   1 TO   6
  0.64760E-02  0.31800E-04  0.31800E-04  0.20830       0.20830
0.00000E+00

 REAL CONSTANT SET   3  ITEMS   1 TO   6
  0.14062      0.50840E-02  0.12842       3.0000       0.41670
0.00000E+00

 REAL CONSTANT SET   3  ITEMS   7 TO  10
  0.00000E+00  0.18510E-01  0.00000E+00  0.00000E+00

 REAL CONSTANT SET   4  ITEMS   1 TO   6
  0.13368      0.16800E-02  0.11301       3.0000       0.25000
0.00000E+00

 REAL CONSTANT SET   4  ITEMS   7 TO  10
  0.00000E+00  0.63000E-02  0.00000E+00  0.00000E+00
```

```
ANALYSIS TYPE=  2   (MODE-FREQUENCY ANALYSIS)
KAY( 3)=   0
KAY( 2)=   4
NODE    1  KCS= 0  X,Y,Z= 0.00000E+00 0.00000E+00  4.0000
NODE    2  KCS= 0  X,Y,Z=  4.5000     0.00000E+00  4.0000
NODE    3  KCS= 0  X,Y,Z=  9.0000     0.00000E+00  4.0000
NODE    4  KCS= 0  X,Y,Z=  13.500     0.00000E+00  4.0000
NODE    5  KCS= 0  X,Y,Z=  18.000     0.00000E+00  4.0000
NODE    6  KCS= 0  X,Y,Z=  15.750     0.00000E+00  6.0000
NODE    7  KCS= 0  X,Y,Z=  11.250     0.00000E+00  6.0000
NODE    8  KCS= 0  X,Y,Z=  6.7500     0.00000E+00  6.0000
NODE    9  KCS= 0  X,Y,Z=  2.2500     0.00000E+00  6.0000
NODE   10  KCS= 0  X,Y,Z= 0.00000E+00 0.00000E+00  8.0000
NODE   11  KCS= 0  X,Y,Z=  4.5000     0.00000E+00  8.0000
NODE   12  KCS= 0  X,Y,Z=  9.0000     0.00000E+00  8.0000
NODE   13  KCS= 0  X,Y,Z=  13.500     0.00000E+00  8.0000
NODE   14  KCS= 0  X,Y,Z=  18.000     0.00000E+00  8.0000
NODE   15  KCS= 0  X,Y,Z=  9.0000     0.00000E+00  11.000
NODE   16  KCS= 0  X,Y,Z=  9.0000     0.00000E+00  23.000
NODE   17  KCS= 0  X,Y,Z= 0.00000E+00  12.000      4.0000
NODE   18  KCS= 0  X,Y,Z=  4.5000      12.000      4.0000
NODE   19  KCS= 0  X,Y,Z=  9.0000      12.000      4.0000
NODE   20  KCS= 0  X,Y,Z=  13.500      12.000      4.0000
NODE   21  KCS= 0  X,Y,Z=  18.000      12.000      4.0000
NODE   22  KCS= 0  X,Y,Z=  15.750      12.000      6.0000
NODE   23  KCS= 0  X,Y,Z=  11.250      12.000      6.0000
```

NODE	24	KCS= 0	X,Y,Z=	6.7500	12.000	6.0000
NODE	25	KCS= 0	X,Y,Z=	2.2500	12.000	6.0000
NODE	26	KCS= 0	X,Y,Z=	0.00000E+00	12.000	8.0000
NODE	27	KCS= 0	X,Y,Z=	4.5000	12.000	8.0000
NODE	28	KCS= 0	X,Y,Z=	9.0000	12.000	8.0000
NODE	29	KCS= 0	X,Y,Z=	13.500	12.000	8.0000
NODE	30	KCS= 0	X,Y,Z=	18.000	12.000	8.0000
NODE	31	KCS= 0	X,Y,Z=	9.0000	12.000	11.000
NODE	32	KCS= 0	X,Y,Z=	9.0000	12.000	23.000
NODE	33	KCS= 0	X,Y,Z=	0.00000E+00	6.0000	4.0000
NODE	34	KCS= 0	X,Y,Z=	0.00000E+00	9.0000	6.0000
NODE	35	KCS= 0	X,Y,Z=	0.00000E+00	3.0000	6.0000
NODE	36	KCS= 0	X,Y,Z=	0.00000E+00	6.0000	8.0000
NODE	37	KCS= 0	X,Y,Z=	9.0000	6.0000	4.0000
NODE	38	KCS= 0	X,Y,Z=	9.0000	3.0000	6.0000
NODE	39	KCS= 0	X,Y,Z=	9.0000	9.0000	6.0000
NODE	40	KCS= 0	X,Y,Z=	9.0000	6.0000	8.0000
NODE	41	KCS= 0	X,Y,Z=	18.000	6.0000	4.0000
NODE	42	KCS= 0	X,Y,Z=	18.000	9.0000	6.0000
NODE	43	KCS= 0	X,Y,Z=	18.000	3.0000	6.0000
NODE	44	KCS= 0	X,Y,Z=	18.000	6.0000	8.0000
NODE	45	KCS= 0	X,Y,Z=	4.5000	3.0000	4.0000
NODE	46	KCS= 0	X,Y,Z=	13.500	3.0000	4.0000
NODE	47	KCS= 0	X,Y,Z=	4.5000	9.0000	4.0000
NODE	48	KCS= 0	X,Y,Z=	13.500	9.0000	4.0000
NODE	49	KCS= 0	X,Y,Z=	4.5000	3.0000	8.0000

```
NODE    50  KCS= 0  X,Y,Z=  13.500      3.0000      8.0000

NODE    51  KCS= 0  X,Y,Z=  4.5000      9.0000      8.0000

NODE    52  KCS= 0  X,Y,Z=  13.500      9.0000      8.0000

NODE    53  KCS= 0  X,Y,Z=  18.000      12.000      11.000

NODE    54  KCS= 0  X,Y,Z=  18.000     0.00000E+00  11.000

NODE    55  KCS= 0  X,Y,Z=  18.000     0.00000E+00  23.000

REAL CONSTANT NUMBER=  1
ELEMENT      1      17     18      0
ELEMENT      2      18     19      0
ELEMENT      3      19     20      0
ELEMENT      4      20     21      0
ELEMENT      5      21     30      0
ELEMENT      6      30     29      0
ELEMENT      7      29     28      0
ELEMENT      8      28     27      0
ELEMENT      9      27     26      0
ELEMENT     10      26     17      0
ELEMENT     11       1      2      0
ELEMENT     12       2      3      0
ELEMENT     13       3      4      0
ELEMENT     14       4      5      0
ELEMENT     15       5     14      0
ELEMENT     16      14     13      0
ELEMENT     17      13     12      0
ELEMENT     18      12     11      0
ELEMENT     19      11     10      0
ELEMENT     20      10      1      0
ELEMENT     21      17     33      0
ELEMENT     22      33      1      0
ELEMENT     23      10     36      0
ELEMENT     24      36     26      0
ELEMENT     25      21     41      0
ELEMENT     26      41      5      0
ELEMENT     27      14     44      0
ELEMENT     28      44     30      0
ELEMENT     29       3     37      0
ELEMENT     30      37     19      0
ELEMENT     31      28     40      0
ELEMENT     32      40     12      0
ELEMENT     33      36     40      0
ELEMENT     34      40     44      0
ELEMENT     35      33     37      0
ELEMENT     36      37     41      0
ELEMENT     37      13     15      0
ELEMENT     38      11     15      0
```

```
ELEMENT    39      29    31     0
ELEMENT    40      27    31     0

REAL CONSTANT NUMBER=  2
ELEMENT    41      17    25     0
ELEMENT    42      25    27     0
ELEMENT    43      26    25     0
ELEMENT    44      25    18     0
ELEMENT    45      18    24     0
ELEMENT    46      27    24     0
ELEMENT    47      24    19     0
ELEMENT    48      24    28     0
ELEMENT    49      28    23     0
ELEMENT    50      19    23     0
ELEMENT    51      23    29     0
ELEMENT    52      23    20     0
ELEMENT    53      20    22     0
ELEMENT    54      29    22     0
ELEMENT    55      22    21     0
ELEMENT    56      22    30     0
ELEMENT    57       1     9     0
ELEMENT    58      10     9     0
ELEMENT    59       9     2     0
ELEMENT    60       9    11     0
ELEMENT    61      11     8     0
ELEMENT    62       2     8     0
ELEMENT    63       8     3     0
ELEMENT    64       8    12     0
ELEMENT    65      12     7     0
ELEMENT    66       3     7     0
ELEMENT    67       7     4     0
ELEMENT    68       7    13     0
ELEMENT    69      13     6     0
ELEMENT    70       4     6     0
ELEMENT    71       6     5     0
ELEMENT    72       6    14     0
ELEMENT    73      17    34     0
ELEMENT    74      26    34     0
ELEMENT    75      34    33     0
ELEMENT    76      34    36     0
ELEMENT    77      36    35     0
ELEMENT    78      33    35     0
ELEMENT    79      35     1     0
ELEMENT    80      35    10     0
ELEMENT    81      21    42     0
ELEMENT    82      30    42     0
ELEMENT    83      42    41     0
ELEMENT    84      42    44     0
ELEMENT    85      44    43     0
ELEMENT    86      41    43     0
ELEMENT    87      43     5     0
ELEMENT    88      43    14     0
```

ELEMENT	89	3	38	0
ELEMENT	90	38	40	0
ELEMENT	91	12	38	0
ELEMENT	92	38	37	0
ELEMENT	93	37	39	0
ELEMENT	94	39	28	0
ELEMENT	95	40	39	0
ELEMENT	96	39	19	0
ELEMENT	97	1	45	0
ELEMENT	98	45	37	0
ELEMENT	99	33	45	0
ELEMENT	100	45	3	0
ELEMENT	101	3	46	0
ELEMENT	102	46	41	0
ELEMENT	103	37	46	0
ELEMENT	104	46	5	0
ELEMENT	105	37	48	0
ELEMENT	106	48	21	0
ELEMENT	107	19	48	0
ELEMENT	108	48	41	0
ELEMENT	109	33	47	0
ELEMENT	110	47	19	0
ELEMENT	111	17	47	0
ELEMENT	112	47	37	0
ELEMENT	113	10	49	0
ELEMENT	114	49	40	0
ELEMENT	115	36	49	0
ELEMENT	116	49	12	0
ELEMENT	117	12	50	0
ELEMENT	118	50	44	0
ELEMENT	119	40	50	0
ELEMENT	120	50	14	0
ELEMENT	121	40	52	0
ELEMENT	122	52	30	0
ELEMENT	123	28	52	0
ELEMENT	124	52	44	0
ELEMENT	125	36	51	0
ELEMENT	126	51	28	0
ELEMENT	127	26	51	0
ELEMENT	128	51	40	0

REAL CONSTANT NUMBER= 3

ELEMENT	129	19	28	21
ELEMENT	130	28	31	30
ELEMENT	131	31	32	53
ELEMENT	132	3	12	5
ELEMENT	133	12	15	14
ELEMENT	134	15	16	54

REAL CONSTANT NUMBER= 4

ELEMENT	135	16	32	55
ELEMENT	136	40	15	44

```
 ELEMENT   137      40    31    44

 SPECIFIED DISP UY   FOR SELECTED NODES IN RANGE    10 TO    10 BY
1
  VALUES= 0.00000E+00 0.00000E+00  ADDITIONAL DOFS=  UZ    ROTX  ROTY
ROTZ

 SPECIFIED DISP UY   FOR SELECTED NODES IN RANGE    14 TO    14 BY
1
  VALUES= 0.00000E+00 0.00000E+00  ADDITIONAL DOFS=  UZ    ROTX  ROTY
ROTZ

 SPECIFIED DISP UY   FOR SELECTED NODES IN RANGE    26 TO    26 BY
1
  VALUES= 0.00000E+00 0.00000E+00  ADDITIONAL DOFS=  UZ    ROTX  ROTY
ROTZ

 SPECIFIED DISP UY   FOR SELECTED NODES IN RANGE    30 TO    30 BY
1
  VALUES= 0.00000E+00 0.00000E+00  ADDITIONAL DOFS=  UZ    ROTX  ROTY
ROTZ

 SPECIFIED DISP UX   FOR SELECTED NODES IN RANGE    12 TO    12 BY
1
  VALUES= 0.00000E+00 0.00000E+00  ADDITIONAL DOFS=


 MASTER DOF UX   FOR SELECTED NODES IN RANGE    16 TO    16 IN STEPS
OF    1
 ADDITIONAL DOFS=  UY    ROTY  ROTZ
 NUMBER OF MASTER DOF=     4

 MASTER DOF UX   FOR SELECTED NODES IN RANGE    15 TO    15 IN STEPS
OF    1
 ADDITIONAL DOFS=  UY    ROTZ
 NUMBER OF MASTER DOF=     7

 MASTER DOF UX   FOR SELECTED NODES IN RANGE    31 TO    31 IN STEPS
OF    1
 ADDITIONAL DOFS=  UY    ROTZ
 NUMBER OF MASTER DOF=    10

 MASTER DOF UX   FOR SELECTED NODES IN RANGE    32 TO    32 IN STEPS
OF    1
 ADDITIONAL DOFS=  UY    ROTY  ROTZ
 NUMBER OF MASTER DOF=    14

 TOTAL MASTER D.O.F.=    20
 NO ROTATIONAL MASTER KEY=  1

 NITTER=      1  NPRINT=     1  NPOST=     1
```

```
ALL PRINT CONTROLS RESET TO     1
 ALL POST DATA FILE CONTROLS RESET TO     1

***  NOTE  ***
NO TITLE DEFINED FOR ANALYSIS

***  NOTE  ***
DATA CHECKED - NO ERRORS FOUND

*** PREP7 GLOBAL STATUS ***

TITLE=  TITLE

ANALYSIS TYPE=     2
NUMBER OF ELEMENT TYPES=     4
   137 ELEMENTS CURRENTLY SELECTED.  MAX ELEMENT NUMBER =    137
    55 NODES CURRENTLY SELECTED.     MAX NODE NUMBER =        55
MAXIMUM LINEAR PROPERTY NUMBER=     4
MAXIMUM REAL CONSTANT SET NUMBER=     4
ACTIVE COORDINATE SYSTEM=     0  (CARTESIAN)
NUMBER OF MASTER D.O.F.=    14
TOTAL MASTER D.O.F. REQUESTED=    20
NUMBER OF IMPOSED DISPLACEMENTS=    21

ANALYSIS DATA WRITTEN ON FILE27

ENTER  FINISH  TO LEAVE PREP7



ALL CURRENT PREP7 DATA WRITTEN TO FILE16   NAME= FILE16.DAT
 FOR POSSIBLE RESUME FROM THIS POINT


***** ROUTINE COMPLETED *****  CP=       49.0500   TIME=    9.2783

***** INPUT SWITCHED FROM FILE 5 TO FILE27  NAME=FILE27.DAT

NEW TITLE=  TITLE



  *** ANSYS REV 4.3  OREGON STATE U   CP=     21.03 ***
  FOR SUPPORT CALL HAROLD LAURSEN    PHONE (503) 754-3322    TWX


 TITLE

**UNIVERSITY VERSION FOR EDUCATIONAL PURPOSES ONLY**

NUMBER OF ELEMENT TYPES=   4
```

```
VIRTUAL MEMORY DRIVER SIZE=   1.4 MB

NUMBER OF REAL CONSTANT SETS=   4

NUMBER OF ELEMENTS =   137  MAXIMUM NODE NUMBER USED =    55

SWITCHED TO FIXED FORMAT INPUT

 XMIN= 0.0000E+00  XMAX=  18.00      YMIN= 0.0000E+00  YMAX=  12.00
   ZMIN=  4.000      ZMAX=  23.00

MAXIMUM MATERIAL NUMBER=   4

M.D.O.F. PRINTOUT SUPPRESSED

NUMBER OF SPECIFIED MASTER D.O.F.=    14
TOTAL NUMBER OF MASTER D.O.F.    =    20
NO ROTATION MASTER KEY=  1


***** LOAD SUMMARY -      21 DISPLACEMENTS        0 FORCES        0
PRESSURES     *****



          ***** CENTROID, MASS, AND MASS MOMENTS OF INERTIA *****

 CALCULATIONS ASSUME ELEMENT MASS AT ELEMENT CENTROID

 TOTAL MASS =   73.029

                              MOM. OF INERTIA         MOM. OF INERTIA
    CENTROID                   ABOUT ORIGIN           ABOUT CENTROID

 XC =   9.0000            IXX =   0.1641E+05      IXX =    4371.
 YC =   6.0000            IYY =   0.1901E+05      IYY =    3683.
 ZC =   11.352            IZZ =   0.1111E+05      IZZ =    2570.
                          IXY =   -3944.          IXY =  -0.2425E-11
                          IYZ =   -4974.          IYZ =  -0.7921E-11
                          IZX =   -7461.          IZX =  -0.8677E-11


 *** MASS SUMMARY BY ELEMENT TYPE ***

 TYPE      MASS
    1   73.0293

 RANGE OF ELEMENT MAXIMUM STIFFNESS IN GLOBAL COORDINATES
MAXIMUM= 0.246566E+09  AT ELEMENT    133.
```

```
MINIMUM= 0.119480E+07  AT ELEMENT    128.

  *** ELEMENT STIFFNESS FORMULATION TIMES
 TYPE  NUMBER  STIF  TOTAL CP   AVE CP

   1     137     4     9.310    0.068
TIME AT END OF ELEMENT STIFFNESS FORMULATION  CP=      53.220
MAXIMUM WAVE FRONT ALLOWED=  200.
EQUATION SOLUTION    ELEM=    55 L.S.=    1 ITER=     1  CP=    68.380

EQUATION SOLUTION    ELEM=   112 L.S.=    1 ITER=     1  CP=    98.970

EQUATION SOLUTION    ELEM=   133 L.S.=    1 ITER=     1  CP=   131.980

MAXIMUM IN-CORE WAVE FRONT=    156.
     MATRIX SOLUTION TIMES
 READ IN ELEMENT STIFFNESSES   CP=          5.400
 NODAL COORD. TRANSFORMATION   CP=          0.000
 MATRIX TRIANGULARIZATION      CP=         74.850
TIME AT END OF MATRIX TRIANGULARIZATION  CP=        143.570
EQUATION SOLVER MAXIMUM PIVOT= 0.29474E+09 AT NODE    12. ROTY
EQUATION SOLVER MINIMUM PIVOT=  13654.     AT NODE    51. UZ
TIME AT START OF EIGENVALUE EXTRACTION  CP=     144.120
NUMBER OF MODES AVAILABLE FROM REDUCED MATRICES=   20.
EIGENVALUE EXTRACTION TIME  CP=       6.920


    ***** EIGENVALUE (NATURAL FREQUENCY) SOLUTION *****

 MODE    FREQUENCY (CYCLES/TIME)

   1      8.07730662
   2      19.4672341
   3      26.2835498
   4      31.7942612
   5      33.4105539
   6      34.9126175
   7      35.2081983
   8      35.5266613
   9      36.1842309
  10      40.4346625
  11      46.7161086
  12      52.6619061
  13      143.792751
  14      156.406671
  15      223.487564
  16      270.222585
  17      353.737232
  18      409.856718
  19      463.415868
  20      618.267512
```

***** REDUCED MASS DISTRIBUTION *****

ROW	NODE	DIR	VALUE
1	48	UZ	0.37665
3	45	UZ	0.43393
4	46	UZ	0.42353
6	32	UX	7.9528
7	15	UY	18.279
8	49	UZ	0.42678
9	16	UX	9.6827
10	31	UX	17.537
11	31	UY	27.831
12	31	UZ	38.414
13	32	UY	9.3026
18	15	UX	14.759
19	16	UY	7.6691
20	47	UZ	0.37051

MASS(X,Y,Z) = 49.93 63.08 40.45

***** PARTICIPATION FACTOR CALCULATION ***** X DIRECTION

MODE	FREQUENCY	PERIOD	PARTIC.FACTOR	RATIO	EFFECTIVE MASS	CUMULATIVE MASS FRACTION
1	8.07731	0.12380	0.41833E-03	0.000077	0.175003E-06	0.349947E-08
2	19.4672	0.51368E-01	-5.4191	1.000000	29.3669	0.587239
3	26.2835	0.38047E-01	-0.39173	0.072287	0.153453	0.590308
4	31.7943	0.31452E-01	0.11541E-01	0.002130	0.133196E-03	0.590310
5	33.4106	0.29931E-01	0.19402E-01	0.003580	0.376440E-03	0.590318
6	34.9126	0.28643E-01	0.32857E-02	0.000606	0.107959E-04	0.590318
7	35.2082	0.28402E-01	0.18103E-01	0.003341	0.327709E-03	0.590324
8	35.5267	0.28148E-01	0.19343E-01	0.003569	0.374147E-03	0.590332
9	36.1842	0.27636E-01	0.39737E-02	0.000733	0.157903E-04	0.590332
10	40.4347	0.24731E-01	-0.53170E-02	0.000981	0.282702E-04	0.590333

```
  11      46.7161        0.21406E-01   0.42504E-02       0.000784
0.180658E-04          0.590333
  12      52.6619        0.18989E-01    3.0758           0.567590
 9.46077              0.779517
  13      143.793        0.69545E-02   -3.0671           0.565976
 9.40704              0.967626
  14      156.407        0.63936E-02  -0.28127           0.051903
0.791123E-01          0.969208
  15      223.488        0.44745E-02   0.78443           0.144753
0.615336              0.981513
  16      270.223        0.37007E-02   0.52572           0.097012
0.276383              0.987040
  17      353.737        0.28270E-02   0.44066           0.081315
0.194179              0.990923
  18      409.857        0.24399E-02  -0.67373           0.124325
0.453912              0.999999
  19      463.416        0.21579E-02  -0.19849E-02       0.000366
0.393971E-05          0.999999
  20      618.268        0.16174E-02  -0.52029E-02       0.000960
0.270705E-04           1.00000
                                          SUM OF EFFECTIVE MASSES=
 50.0084


          ***** PARTICIPATION FACTOR CALCULATION *****  Y  DIRECTION

                      CUMULATIVE
 MODE      FREQUENCY        PERIOD   PARTIC.FACTOR       RATIO
EFFECTIVE MASS        MASS FRACTION

   1      8.07731        0.12380       -4.9167           0.972935
 24.1740              0.443302
   2      19.4672        0.51368E-01   0.17172E-03       0.000034
0.294878E-07          0.443302
   3      26.2835        0.38047E-01  -0.13970E-02       0.000276
0.195169E-05          0.443302
   4      31.7943        0.31452E-01  -0.38739           0.076659
0.150074              0.446054
   5      33.4106        0.29931E-01   0.21476E-02       0.000425
0.461202E-05          0.446055
   6      34.9126        0.28643E-01   -1.1264           0.222898
 1.26880              0.469322
   7      35.2082        0.28402E-01  -0.27130           0.053686
0.736050E-01          0.470672
   8      35.5267        0.28148E-01  -0.22343E-03       0.000044
0.499195E-07          0.470672
   9      36.1842        0.27636E-01   -1.3432           0.265801
 1.80423              0.503758
  10      40.4347        0.24731E-01    5.0535           1.000000
 25.5376              0.972066
```

```
  11      46.7161        0.21406E-01    1.2342          0.244230
 1.52327              1.000000
  12      52.6619        0.18989E-01  -0.14561E-02      0.000288
0.212030E-05          1.000000
  13      143.793        0.69545E-02  -0.10416E-02      0.000206
0.108491E-05          1.000000
  14      156.407        0.63936E-02   0.50773E-03      0.000100
0.257790E-06          1.000000
  15      223.488        0.44745E-02   0.21581E-03      0.000043
0.465726E-07          1.000000
  16      270.223        0.37007E-02   0.12639E-03      0.000025
0.159753E-07          1.000000
  17      353.737        0.28270E-02   0.51062E-04      0.000010
0.260735E-08          1.000000
  18      409.857        0.24399E-02  -0.10033E-03      0.000020
0.100669E-07          1.000000
  19      463.416        0.21579E-02  -0.78395E-03      0.000155
0.614585E-06          1.000000
  20      618.268        0.16174E-02  -0.15096E-05      0.000000
0.227894E-11          1.000000
                                          SUM OF EFFECTIVE MASSES=
 54.5316


         ***** PARTICIPATION FACTOR CALCULATION *****  Z  DIRECTION

                      CUMULATIVE
 MODE      FREQUENCY        PERIOD   PARTIC.FACTOR       RATIO
EFFECTIVE MASS        MASS FRACTION

   1      8.07731        0.12380       0.13671          0.027749
0.186885E-01          0.586144E-03
   2      19.4672        0.51368E-01  -0.44144E-02      0.000896
0.194872E-04          0.586755E-03
   3      26.2835        0.38047E-01  -0.93711E-02      0.001902
0.878170E-04          0.589510E-03
   4      31.7943        0.31452E-01   -4.9266          1.000000
 24.2711              0.761827
   5      33.4106        0.29931E-01  -0.61112E-02      0.001240
0.373470E-04          0.761828
   6      34.9126        0.28643E-01   0.23839          0.048389
0.568318E-01          0.763611
   7      35.2082        0.28402E-01  -0.49371          0.100214
0.243751              0.771256
   8      35.5267        0.28148E-01  -0.11528E-02      0.000234
0.132900E-05          0.771256
   9      36.1842        0.27636E-01    1.7265          0.350443
 2.98075              0.864744
  10      40.4347        0.24731E-01    1.6261          0.330062
 2.64412              0.947674
```

```
  11      46.7161        0.21406E-01    1.2916          0.262180
 1.66836              1.000000
  12      52.6619        0.18989E-01   0.71594E-03      0.000145
0.512568E-06          1.000000
  13      143.793        0.69545E-02   0.42799E-03      0.000087
0.183177E-06          1.000000
  14      156.407        0.63936E-02  -0.21218E-03      0.000043
0.450195E-07          1.000000
  15      223.488        0.44745E-02  -0.94711E-04      0.000019
0.897017E-08          1.000000
  16      270.223        0.37007E-02  -0.56509E-04      0.000011
0.319327E-08          1.000000
  17      353.737        0.28270E-02  -0.23611E-04      0.000005
0.557469E-09          1.000000
  18      409.857        0.24399E-02   0.49140E-04      0.000010
0.241475E-08          1.000000
  19      463.416        0.21579E-02  -0.11490E-02      0.000233
0.132009E-05          1.000000
  20      618.268        0.16174E-02   0.64327E-06      0.000000
0.413797E-12           1.00000
                                          SUM OF EFFECTIVE MASSES=
 31.8838


  ***** EXPANDED MODE SHAPE FOR MODE    1    LOAD STEP   1   *****
FREQUENCY =    8.07731      (CYCLES/TIME)

   NODE       UX                UY                UZ                ROTX
       ROTY              ROTZ
    1    0.239289E-02   -0.429395E-03    0.723758E-03   -0.161072E-03
-0.810242E-03    0.235251E-03
    2    0.178904E-02    0.178993E-03    0.532874E-02   -0.552750E-03
-0.134309E-02    0.123212E-03
    3   -0.394282E-07    0.582412E-03    0.104161E-01   -0.119805E-02
 0.889348E-08    0.228293E-08
    4   -0.178911E-02    0.178977E-03    0.532869E-02   -0.552759E-03
 0.134309E-02   -0.123225E-03
    5   -0.239296E-02   -0.429527E-03    0.723690E-03   -0.161092E-03
 0.810259E-03   -0.235292E-03
    6   -0.187543E-02    0.103079E-03    0.372223E-02   -0.139457E-03
 0.112734E-02   -0.165601E-03
    7    0.253358E-03    0.203633E-02    0.919732E-02   -0.890014E-03
 0.487476E-03   -0.597788E-03
    8   -0.253407E-03    0.203632E-02    0.919736E-02   -0.890012E-03
-0.487462E-03    0.597788E-03
    9    0.187538E-02    0.103100E-03    0.372229E-02   -0.139440E-03
-0.112735E-02    0.165588E-03
   10    0.890067E-04    0.000000E+00    0.000000E+00    0.000000E+00
 0.000000E+00    0.000000E+00
```

```
   11   -0.118027E-03    0.233059E-02    0.842725E-02   -0.175414E-02
-0.132261E-02    0.669797E-03
   12    0.000000E+00    0.538049E-02    0.104593E-01   -0.121598E-02
 0.117453E-07    0.391177E-08
   13    0.117988E-03    0.233060E-02    0.842719E-02   -0.175414E-02
 0.132261E-02   -0.669798E-03
   14   -0.890924E-04    0.000000E+00    0.000000E+00    0.000000E+00
 0.000000E+00    0.000000E+00
   15    0.109350E-07    0.148053E-01    0.105750E-01   -0.707393E-02
 0.185288E-08    0.142432E-08
   16    0.582435E-07    0.265991        0.107829E-01   -0.192324E-01
 0.401014E-08    0.189239E-08
   17   -0.246065E-02   -0.437417E-03   -0.744791E-03   -0.165810E-03
 0.842589E-03    0.244404E-03
   18   -0.183930E-02    0.185036E-03   -0.550929E-02   -0.554344E-03
 0.138325E-02    0.122421E-03
   19   -0.604311E-07    0.583285E-03   -0.107382E-01   -0.119864E-02
 0.666600E-08   -0.111461E-08
   20    0.183919E-02    0.185058E-03   -0.550932E-02   -0.554330E-03
-0.138325E-02   -0.122408E-03
   21    0.246055E-02   -0.437272E-03   -0.744859E-03   -0.165778E-03
-0.842570E-03   -0.244360E-03
   22    0.191745E-02    0.107473E-03   -0.384702E-02   -0.138023E-03
-0.116603E-02   -0.166823E-03
   23   -0.262908E-03    0.203919E-02   -0.948848E-02   -0.889313E-03
-0.501413E-03   -0.596879E-03
   24    0.262806E-03    0.203920E-02   -0.948845E-02   -0.889316E-03
 0.501426E-03    0.596879E-03
   25   -0.191753E-02    0.107453E-03   -0.384696E-02   -0.138042E-03
 0.116602E-02    0.166835E-03
   26   -0.620667E-04    0.000000E+00    0.000000E+00    0.000000E+00
 0.000000E+00    0.000000E+00
   27    0.132826E-03    0.233155E-02   -0.869228E-02   -0.175318E-02
 0.136266E-02    0.669835E-03
   28   -0.291863E-07    0.538117E-02   -0.107827E-01   -0.121536E-02
 0.100665E-07   -0.296470E-08
   29   -0.132906E-03    0.233154E-02   -0.869236E-02   -0.175318E-02
-0.136266E-02   -0.669834E-03
   30    0.619455E-04    0.000000E+00    0.000000E+00    0.000000E+00
 0.000000E+00    0.000000E+00
   31    0.399578E-08    0.148032E-01   -0.109009E-01   -0.707303E-02
 0.106552E-07   -0.930756E-09
   32    0.353169E-07    0.265990       -0.111089E-01   -0.192330E-01
 0.273824E-08    0.189328E-08
   33   -0.345096E-06   -0.283827E-03   -0.296794E-06   -0.219388E-03
 0.162859E-04    0.385481E-03
   34   -0.602240E-03    0.302409E-04   -0.258054E-03   -0.751193E-04
 0.266043E-03    0.108180E-03
   35    0.606993E-03    0.274888E-04    0.253576E-03   -0.741936E-04
-0.256129E-03    0.106330E-03
   36    0.268713E-06    0.343991E-03   -0.412423E-05   -0.180600E-04
 0.933222E-05    0.349394E-03
```

```
   37   -0.102458E-07    0.450738E-03   -0.158152E-03   -0.185978E-02
-0.296334E-07    0.147614E-08
   38   -0.112223E-06    0.377531E-02    0.641175E-02   -0.208269E-02
-0.217940E-07    0.388820E-07
   39   -0.126611E-06    0.377766E-02   -0.673458E-02   -0.208266E-02
-0.229958E-07   -0.338816E-07
   40   -0.200768E-06    0.870697E-02   -0.164668E-03    0.234498E-03
 0.161667E-06    0.185285E-08
   41    0.312270E-06   -0.283817E-03   -0.325101E-06   -0.219371E-03
-0.161191E-04   -0.385479E-03
   42    0.603606E-03    0.304636E-04   -0.258380E-03   -0.752754E-04
-0.266021E-03   -0.107567E-03
   43   -0.605607E-03    0.272796E-04    0.253223E-03   -0.745350E-04
 0.256152E-03   -0.106937E-03
   44   -0.556728E-06    0.343989E-03   -0.517868E-05   -0.160836E-04
-0.150983E-04   -0.349392E-03
   45    0.552216E-03    0.973883E-03    0.386933E-02   -0.109516E-02
-0.720321E-03    0.115207E-03
   46   -0.552242E-03    0.973845E-03    0.386933E-02   -0.109511E-02
 0.720319E-03   -0.115214E-03
   47   -0.567870E-03    0.997087E-03   -0.388880E-02   -0.109733E-02
 0.761920E-03    0.117159E-03
   48    0.567823E-03    0.997137E-03   -0.388879E-02   -0.109738E-02
-0.761924E-03   -0.117149E-03
   49    0.518286E-03    0.364213E-02    0.228839E-02   -0.917212E-03
-0.635460E-03    0.752638E-03
   50   -0.518481E-03    0.364220E-02    0.202589E-02   -0.918426E-03
 0.636268E-03   -0.752617E-03
   51   -0.511411E-03    0.363260E-02   -0.220609E-02   -0.912645E-03
 0.683181E-03    0.751649E-03
   52    0.511194E-03    0.363254E-02   -0.220905E-02   -0.911477E-03
-0.682793E-03   -0.751669E-03

 MAXIMUMS
 NODE          17              16              32              32
        18              49
 VALUE   -0.246065E-02    0.265991       -0.111089E-01   -0.192330E-01
  0.138325E-02    0.752638E-03


   ***** EXPANDED MODE SHAPE FOR MODE    2    LOAD STEP   1   *****
FREQUENCY =    19.4672     (CYCLES/TIME)

    NODE      UX              UY              UZ              ROTX
        ROTY            ROTZ
     1   -0.162618E-02    0.423433E-02    0.227088E-02    0.722175E-03
  0.124444E-02    0.157521E-03
     2   -0.530217E-02    0.544285E-02   -0.815985E-03    0.424646E-03
-0.252141E-03   -0.221502E-04
     3   -0.116338E-01    0.514867E-06    0.226226E-04   -0.129704E-05
  0.193178E-02   -0.283599E-02
```

4	-0.530886E-02	-0.544136E-02	0.841405E-03	-0.425921E-03	-0.246633E-03	-0.221539E-04
5	-0.163488E-02	-0.423416E-02	-0.226664E-02	-0.722565E-03	0.124868E-02	0.156802E-03
6	0.355712E-02	-0.299037E-02	-0.525798E-02	-0.905123E-03	-0.352919E-03	0.725539E-03
7	-0.740159E-02	-0.404169E-02	-0.495924E-02	-0.543354E-04	0.218325E-02	-0.892281E-03
8	-0.740302E-02	0.404560E-02	0.500002E-02	0.543141E-04	0.218129E-02	-0.891698E-03
9	0.356292E-02	0.299207E-02	0.527569E-02	0.905425E-03	-0.358212E-03	0.726158E-03
10	0.237815E-02	0.000000E+00	0.000000E+00	0.000000E+00	0.000000E+00	0.000000E+00
11	0.207598E-02	0.416339E-02	0.159350E-01	-0.275436E-03	-0.160257E-03	0.579711E-03
12	0.000000E+00	0.449358E-06	0.226532E-04	0.272334E-05	0.484483E-02	-0.306980E-02
13	0.207817E-02	-0.416317E-02	-0.158979E-01	0.278000E-03	-0.154682E-03	0.579590E-03
14	0.238210E-02	0.000000E+00	0.000000E+00	0.000000E+00	0.000000E+00	0.000000E+00
15	0.212496E-01	-0.412788E-05	0.225481E-04	0.141901E-05	0.939014E-02	-0.367329E-02
16	0.207778	-0.266026E-05	0.225337E-04	-0.125296E-05	0.183800E-01	-0.853117E-02
17	0.197417E-01	0.526745E-02	0.450117E-02	0.152383E-02	0.118805E-02	-0.197881E-02
18	0.159701E-01	0.144492E-02	0.332213E-02	0.592818E-03	-0.391147E-03	-0.166950E-03
19	0.759316E-02	-0.437438E-05	0.102351E-04	-0.105332E-05	0.451924E-02	-0.820331E-03
20	0.159670E-01	-0.145153E-02	-0.331078E-02	-0.594385E-03	-0.388703E-03	-0.166191E-03
21	0.197376E-01	-0.527082E-02	-0.449885E-02	-0.152465E-02	0.118992E-02	-0.197833E-02
22	0.279609E-01	-0.864719E-03	-0.102064E-01	-0.468447E-03	-0.808352E-03	-0.117732E-03
23	0.158157E-01	-0.103009E-02	-0.959689E-02	0.875324E-04	0.401481E-02	-0.155744E-03
24	0.158150E-01	0.102654E-02	0.961528E-02	-0.903306E-04	0.401392E-02	-0.156083E-03
25	0.279638E-01	0.862484E-03	0.102145E-01	0.467006E-03	-0.810720E-03	-0.118142E-03
26	0.248126E-01	0.000000E+00	0.000000E+00	0.000000E+00	0.000000E+00	0.000000E+00
27	0.287120E-01	0.127180E-02	0.245558E-01	-0.151417E-03	0.705330E-04	0.202502E-03
28	0.296805E-01	0.155588E-05	0.101612E-04	-0.238039E-05	0.749844E-02	-0.104441E-02
29	0.287130E-01	-0.126920E-02	-0.245389E-01	0.147995E-03	0.730287E-04	0.201775E-03

```
   30    0.248142E-01    0.000000E+00    0.000000E+00    0.000000E+00
 0.000000E+00    0.000000E+00
   31    0.594082E-01    0.929052E-05    0.101525E-04   -0.187229E-05
 0.125189E-01   -0.121839E-02
   32    0.296639       -0.260717E-05    0.101669E-04    0.159311E-05
 0.229549E-01   -0.615756E-02
   33    0.227982E-02    0.437156E-02    0.221765E-03   -0.215163E-03
 0.632540E-03   -0.170393E-02
   34    0.168632E-01    0.180424E-02    0.698102E-03    0.414833E-03
 0.264664E-02   -0.251836E-02
   35    0.399703E-02    0.348068E-02    0.205670E-02    0.370603E-03
 0.214891E-02   -0.168075E-02
   36    0.145741E-01    0.219239E-02    0.267411E-02   -0.790774E-04
-0.196692E-02   -0.177965E-02
   37    0.453935E-02   -0.185478E-05    0.172027E-04   -0.921747E-06
 0.536419E-03   -0.903816E-03
   38   -0.204583E-03    0.191531E-05    0.239383E-04    0.116951E-05
 0.227584E-02   -0.203047E-02
   39    0.121239E-01   -0.349061E-05    0.186350E-04   -0.116334E-05
 0.430945E-02   -0.208074E-02
   40    0.144981E-01   -0.291493E-06    0.306235E-04   -0.878627E-05
 0.863990E-02   -0.313897E-02
   41    0.228058E-02   -0.437304E-02   -0.220932E-03    0.214692E-03
 0.634214E-03   -0.170420E-02
   42    0.168357E-01   -0.180918E-02   -0.691656E-03   -0.411832E-03
 0.264577E-02   -0.253002E-02
   43    0.396961E-02   -0.347705E-02   -0.204940E-02   -0.364284E-03
 0.214907E-02   -0.166907E-02
   44    0.145743E-01   -0.219235E-02   -0.265337E-02    0.407600E-04
-0.185406E-02   -0.177942E-02
   45   -0.163331E-02    0.672937E-02    0.195695E-02   -0.327153E-03
-0.126859E-03   -0.608068E-03
   46   -0.163479E-02   -0.672684E-02   -0.192255E-02    0.325507E-03
-0.121787E-03   -0.608228E-03
   47    0.838899E-02   -0.296678E-02    0.343841E-02    0.978471E-03
-0.480879E-03   -0.669658E-03
   48    0.838868E-02    0.296064E-02   -0.341212E-02   -0.979462E-03
-0.477254E-03   -0.669059E-03
   49    0.749611E-02    0.142207E-02    0.142870E-01    0.127912E-02
-0.891245E-03   -0.154616E-03
   50    0.749741E-02   -0.142336E-02   -0.928906E-02   -0.125488E-02
-0.897059E-03   -0.154518E-03
   51    0.212602E-01    0.239911E-02    0.108309E-01   -0.797300E-03
-0.115854E-02   -0.358759E-03
   52    0.212600E-01   -0.239796E-02   -0.107610E-01    0.772180E-03
-0.116193E-02   -0.358985E-03

MAXIMUMS
NODE          32              45              27              21
       32              16
VALUE    0.296639        0.672937E-02    0.245558E-01   -0.152465E-02
 0.229549E-01   -0.853117E-02
```

```
  ***** EXPANDED MODE SHAPE FOR MODE    3    LOAD STEP   1   *****
FREQUENCY =    26.2835      (CYCLES/TIME)

    NODE       UX                UY                UZ                ROTX
        ROTY              ROTZ
      1   -0.129880E-01   -0.664888E-02    0.575584E-02   -0.183470E-02
  0.100814E-02    0.172294E-02
      2   -0.183674E-01   -0.435458E-02    0.522015E-02   -0.743580E-03
 -0.440555E-03    0.281589E-04
      3   -0.296511E-01    0.249663E-04    0.773892E-04    0.347320E-06
  0.600768E-02    0.254030E-02
      4   -0.183919E-01    0.439110E-02   -0.513475E-02    0.746112E-03
 -0.422137E-03    0.228009E-04
      5   -0.130214E-01    0.665811E-02   -0.574344E-02    0.183755E-02
  0.102624E-02    0.171697E-02
      6   -0.277995E-02    0.242099E-02   -0.142554E-01    0.743544E-03
 -0.134532E-02   -0.460170E-03
      7   -0.186720E-01    0.365976E-02   -0.132700E-01   -0.198989E-03
  0.544443E-02    0.698251E-03
      8   -0.186766E-01   -0.362177E-02    0.134089E-01    0.207854E-03
  0.543748E-02    0.702642E-03
      9   -0.275808E-02   -0.240587E-02    0.143150E-01   -0.738017E-03
 -0.136315E-02   -0.454311E-03
     10   -0.787828E-02    0.000000E+00    0.000000E+00    0.000000E+00
  0.000000E+00    0.000000E+00
     11   -0.174660E-02   -0.426846E-02    0.335448E-01    0.469601E-03
  0.138558E-03   -0.616814E-03
     12    0.000000E+00    0.588889E-05    0.771644E-04    0.143116E-04
  0.101877E-01    0.320176E-02
     13   -0.174016E-02    0.427165E-02   -0.334185E-01   -0.451944E-03
  0.157600E-03   -0.618096E-03
     14   -0.786763E-02    0.000000E+00    0.000000E+00    0.000000E+00
  0.000000E+00    0.000000E+00
     15    0.402533E-01   -0.321668E-04    0.767129E-04    0.118151E-04
  0.167670E-01    0.409156E-02
     16    0.352570       -0.487480E-05    0.767101E-04   -0.793993E-05
  0.295737E-01    0.487884E-01
     17   -0.459092E-01   -0.632946E-02   -0.360009E-02   -0.161480E-02
 -0.419103E-03    0.112789E-02
     18   -0.428878E-01   -0.495932E-02   -0.411546E-02   -0.711172E-03
  0.251703E-03    0.879067E-04
     19   -0.362061E-01   -0.150204E-05    0.869992E-04   -0.216841E-05
 -0.395916E-02    0.266253E-02
     20   -0.429132E-01    0.495478E-02    0.421447E-02    0.708668E-03
  0.272293E-03    0.879798E-04
     21   -0.459423E-01    0.633368E-02    0.361484E-02    0.161480E-02
 -0.398866E-03    0.113223E-02
     22   -0.520743E-01    0.274757E-02    0.927160E-02    0.886876E-03
  0.943775E-03   -0.535030E-03
```

23 -0.432831E-01 0.383133E-02 0.870634E-02 -0.112849E-03
-0.345936E-02 0.786588E-03
24 -0.432888E-01 -0.382455E-02 -0.854912E-02 0.104611E-03
-0.346681E-02 0.787692E-03
25 -0.520535E-01 -0.274825E-02 -0.920299E-02 -0.888964E-03
0.923313E-03 -0.534943E-03
26 -0.485594E-01 0.000000E+00 0.000000E+00 0.000000E+00
0.000000E+00 0.000000E+00
27 -0.532809E-01 -0.428860E-02 -0.205209E-01 0.402743E-03
-0.186313E-03 -0.609475E-03
28 -0.552265E-01 0.165247E-04 0.868444E-04 -0.947450E-05
-0.632484E-02 0.319095E-02
29 -0.532717E-01 0.430992E-02 0.206641E-01 -0.417225E-03
-0.164937E-03 -0.615654E-03
30 -0.485418E-01 0.000000E+00 0.000000E+00 0.000000E+00
0.000000E+00 0.000000E+00
31 -0.793239E-01 0.508436E-04 0.871952E-04 -0.971087E-05
-0.968555E-02 0.403878E-02
32 -0.245417 -0.443634E-05 0.871980E-04 0.101549E-04
-0.151188E-01 0.496854E-01
33 -0.315914E-01 -0.507420E-02 0.896965E-04 -0.327518E-03
0.163877E-04 0.279294E-02
34 -0.401774E-01 -0.319742E-02 0.101755E-02 -0.618288E-03
-0.130623E-03 0.346408E-02
35 -0.182996E-01 -0.265376E-02 -0.106202E-03 -0.625598E-03
0.138481E-02 0.382470E-02
36 -0.284977E-01 -0.325035E-02 0.893599E-03 -0.475538E-04
-0.938161E-03 0.279303E-02
37 -0.308882E-01 0.112644E-04 0.921143E-04 0.871253E-06
0.314942E-03 -0.341028E-03
38 -0.227866E-01 0.253080E-04 0.109929E-03 0.100903E-04
0.556853E-02 0.188747E-02
39 -0.391309E-01 -0.249653E-05 0.113997E-03 -0.464161E-05
-0.384813E-02 0.167173E-02
40 -0.289837E-01 0.114938E-04 0.163829E-03 -0.173599E-04
0.291266E-02 0.951925E-02
41 -0.315864E-01 0.508040E-02 -0.854645E-04 0.326178E-03
0.427390E-04 0.279251E-02
42 -0.402389E-01 0.318992E-02 -0.100015E-02 0.626712E-03
-0.129334E-03 0.343586E-02
43 -0.183642E-01 0.266848E-02 0.126574E-03 0.641685E-03
0.138459E-02 0.385238E-02
44 -0.284987E-01 0.325324E-02 -0.839597E-03 -0.451304E-04
-0.647610E-03 0.279160E-02
45 -0.265456E-01 0.355670E-02 0.104177E-01 -0.131955E-02
-0.425848E-03 0.602120E-03
46 -0.265486E-01 -0.352041E-02 -0.100510E-01 0.132286E-02
-0.405899E-03 0.598156E-03
47 -0.359408E-01 0.510320E-03 -0.392796E-02 -0.995133E-03
0.239635E-03 0.633395E-03
48 -0.359439E-01 -0.517067E-03 0.427078E-02 0.994096E-03
0.262020E-03 0.633850E-03

```
   49   -0.157889E-01   -0.396079E-02    0.200695E-01   -0.106218E-02
-0.110937E-02    0.157082E-03
   50   -0.157879E-01    0.396587E-02   -0.785410E-02    0.113583E-02
-0.110737E-02    0.155869E-03
   51   -0.408661E-01   -0.314473E-02   -0.112636E-02   -0.192772E-02
 0.460480E-03    0.321732E-04
   52   -0.408641E-01    0.316640E-02    0.138796E-02    0.185864E-02
 0.475260E-03    0.285691E-04

MAXIMUMS
NODE         16               5               11               51
       16               32
VALUE    0.352570        0.665811E-02    0.335448E-01   -0.192772E-02
 0.295737E-01    0.496854E-01


  ***** EXPANDED MODE SHAPE FOR MODE    4    LOAD STEP   1   *****
FREQUENCY =   31.7943     (CYCLES/TIME)

   NODE      UX              UY              UZ              ROTX
       ROTY             ROTZ
    1    0.777033E-02    0.558568E-02    0.158556E-02    0.408922E-02
-0.932570E-02    0.253594E-02
    2    0.526259E-02    0.178435E-01    0.184747E-01    0.636932E-02
-0.271793E-02    0.242316E-02
    3   -0.174774E-04    0.243613E-01    0.315885E-01    0.877243E-02
 0.502039E-05    0.223616E-04
    4   -0.531940E-02    0.178741E-01    0.184115E-01    0.636126E-02
 0.271823E-02   -0.244859E-02
    5   -0.784699E-02    0.540249E-02    0.151539E-02    0.407467E-02
 0.936500E-02   -0.260003E-02
    6   -0.397158E-02    0.388451E-02    0.126616E-01    0.353000E-02
 0.352997E-02   -0.115203E-02
    7    0.850904E-03    0.625044E-02    0.288178E-01    0.879521E-02
 0.148489E-02   -0.455923E-03
    8   -0.868857E-03    0.618410E-02    0.288372E-01    0.880127E-02
-0.148269E-02    0.466521E-03
    9    0.388541E-02    0.389180E-02    0.126975E-01    0.355528E-02
-0.353657E-02    0.111940E-02
   10   -0.355903E-02    0.000000E+00    0.000000E+00    0.000000E+00
 0.000000E+00    0.000000E+00
   11   -0.184466E-02   -0.942794E-02    0.260033E-01    0.888759E-02
-0.381758E-02   -0.267557E-02
   12    0.000000E+00   -0.139203E-01    0.312766E-01    0.124760E-01
 0.287555E-05    0.292888E-04
   13    0.177998E-02   -0.935125E-02    0.260365E-01    0.888050E-02
 0.382419E-02    0.266466E-02
   14    0.343510E-02    0.000000E+00    0.000000E+00    0.000000E+00
 0.000000E+00    0.000000E+00
```

15	-0.627714E-04	-0.525011E-01	0.310166E-01	0.104365E-01	-0.456937E-04	0.332067E-04
16	-0.144380E-02	0.155074E-01	0.311564E-01	-0.719083E-02	-0.144774E-03	-0.131607E-03
17	0.277431E-01	0.883458E-02	0.990123E-02	-0.127299E-02	-0.202220E-01	-0.335140E-02
18	0.208677E-01	0.658124E-02	0.773281E-01	0.160371E-02	-0.155842E-01	0.129545E-02
19	-0.433428E-04	0.119789E-01	0.137043	0.390649E-02	0.142353E-04	-0.187456E-04
20	-0.209232E-01	0.655957E-02	0.772623E-01	0.161476E-02	0.155838E-01	-0.127240E-02
21	-0.277854E-01	0.900562E-02	0.980623E-02	-0.125082E-02	0.202679E-01	0.340952E-02
22	-0.175876E-01	0.243311E-02	0.531528E-01	0.183986E-02	0.156434E-01	0.711746E-03
23	0.400658E-02	0.258458E-02	0.123719	0.386745E-02	0.606175E-02	-0.380182E-03
24	-0.404919E-02	0.264194E-02	0.123796	0.386155E-02	-0.603440E-02	0.370942E-03
25	0.175875E-01	0.242646E-02	0.532573E-01	0.181626E-02	-0.156591E-01	-0.683344E-03
26	-0.114730E-01	0.000000E+00	0.000000E+00	0.000000E+00	0.000000E+00	0.000000E+00
27	-0.631956E-02	-0.325974E-02	0.112669	0.202537E-02	-0.170247E-01	-0.962493E-03
28	0.236397E-04	-0.525343E-02	0.137394	0.358130E-02	0.215008E-04	-0.254485E-04
29	0.632480E-02	-0.332660E-02	0.112511	0.203153E-02	0.170299E-01	0.971944E-03
30	0.114008E-01	0.000000E+00	0.000000E+00	0.000000E+00	0.000000E+00	0.000000E+00
31	0.954755E-04	-0.113466E-01	0.138392	0.463815E-04	0.237458E-04	-0.288656E-04
32	0.260252E-03	0.158778E-01	0.138252	0.164273E-02	0.599005E-05	-0.148387E-03
33	-0.112269E-02	0.641142E-02	0.395954E-02	0.204968E-02	-0.337646E-01	-0.119676E-02
34	-0.608316E-02	0.211893E-02	0.364358E-02	0.110574E-02	-0.376660E-02	-0.108757E-02
35	-0.660966E-02	0.346050E-02	0.240987E-02	0.760783E-03	0.212969E-03	0.107295E-02
36	0.533602E-03	0.326148E-03	0.474646E-02	-0.190903E-02	-0.179167E-01	0.474520E-03
37	0.148223E-04	0.166728E-01	0.996463E-01	0.107363E-01	-0.114602E-03	0.165707E-05
38	-0.177218E-03	0.930167E-02	0.773003E-01	0.121492E-01	-0.429443E-04	0.605755E-04
39	-0.169569E-03	0.541325E-03	0.126349	0.325845E-02	-0.317998E-04	-0.580545E-04
40	-0.293235E-03	-0.579371E-02	0.123295	0.968127E-02	0.207526E-03	-0.120068E-04

```
   41    0.114008E-02    0.641394E-02    0.394140E-02    0.207013E-02
 0.341062E-01    0.119427E-02
   42    0.792521E-02    0.239882E-02    0.323500E-02    0.904805E-03
 0.378068E-02    0.186794E-02
   43    0.842694E-02    0.318620E-02    0.196609E-02    0.322926E-03
-0.202217E-03   -0.186238E-02
   44   -0.925507E-03    0.316340E-03    0.340467E-02    0.616153E-03
 0.105419E-01   -0.477151E-03
   45    0.242237E-03    0.165878E-01    0.442891        0.102507E-01
-0.509945E-02    0.184561E-02
   46   -0.227494E-03    0.165540E-01    0.444933        0.103533E-01
 0.509451E-02   -0.185982E-02
   47    0.546289E-02    0.182013E-03    0.617059        0.116939E-02
-0.123159E-01    0.236076E-03
   48   -0.545534E-02    0.246190E-03    0.619089        0.106190E-02
 0.123069E-01   -0.221976E-03
   49    0.467098E-03   -0.647926E-02    0.381502        0.114885E-01
-0.990600E-02   -0.136377E-02
   50   -0.744395E-03   -0.636292E-02    0.461225E-01    0.993120E-02
 0.109414E-01    0.139207E-02
   51   -0.265881E-02    0.191282E-02    0.781373E-01   -0.259774E-02
-0.188118E-01   -0.261178E-03
   52    0.240959E-02    0.179311E-02    0.743428E-01   -0.110653E-02
 0.193067E-01    0.233634E-03

MAXIMUMS
NODE          21              15              48              12
       41              21
VALUE   -0.277854E-01   -0.525011E-01    0.619089        0.124760E-01
 0.341062E-01    0.340952E-02


 *** STORAGE REQUIREMENT SUMMARY
MAXIMUM FIXED MEMORY USED    =       0
MAXIMUM TEMPORARY MEMORY USED=       0
MAXIMUM TOTAL MEMORY USED    =       0
MAXIMUM TEMPORARY AVAILABLE  =       0


  *** PROBLEM STATISTICS
 NO. OF ACTIVE DEGREES OF FREEDOM =    271
 R.M.S. WAVEFRONT SIZE =   102.1
 NUMBER OF MASTER DEGREES OF FREEDOM =    20



 *** ANSYS BINARY FILE STATISTICS
BUFFER SIZE USED= 1024
POST DATA WRITTEN ON FILE12

***** END OF INPUT ENCOUNTERED ON FILE27.  FILE27 REWOUND
```

```
***** INPUT FILE SWITCHED FROM FILE27 TO FILE 5

ENTER   HELP   FOR ANSYS DOCUMENTATION
ENTER   /EOF   TO EXIT

/EOF ENCOUNTERED ON FILE 5


***** ROUTINE COMPLETED *****  CP=      220.2500   TIME=    9.3464
```

APPENDIX D CALCULATION OF K6

Calculation of the linear spring rate k_6

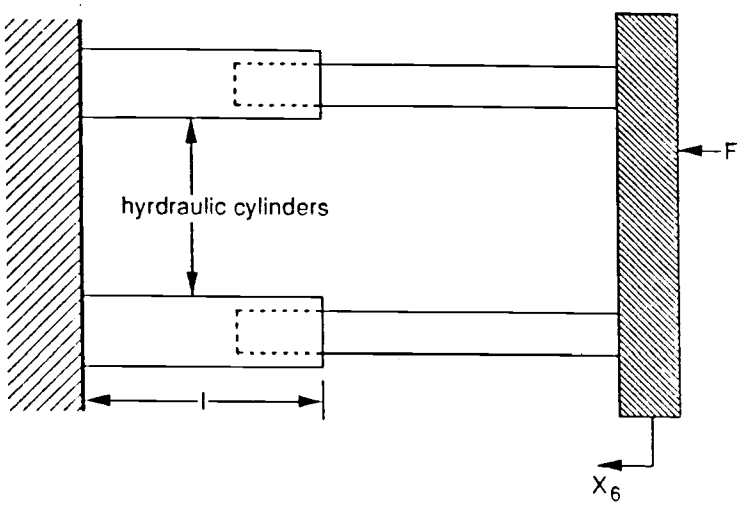

Figure D.1 FBD of hydrualic cylinders

Bulk modulus of hydraulic oil , $E_v=\sigma/(\Delta V/V)$

$$\Delta V/V=(X_6\ A)/(l\ A)= X_6/l$$

where $A=\pi\ d^2$

$$E_v=\sigma/(X_6/l)$$

$$X_6=\sigma l/E_v$$

$$F_6=k_6X_6=k_6\sigma l/E_v$$

$$k_6=F_6E_v/(\sigma l)$$